Thermodynamic Properties at Infinite Dilution of Deep Eutectic Solvents with Organic Solutes at Different Temperatures

LINDOKUHLE MANYONI

(Student Number: 21410397)

Submitted in the Fulfilment of the Academic Requirements of the Degree of

Master of Applied Sciences in Chemistry

Department of Chemistry, Faculty of Applied Sciences at Durban University of Technology

Durban, KwaZulu Natal, South Africa

January 2023

DEDICATION

In loving memory of my family,

Nomvula Bongekile Mnguni (Mom);

Mziwakhe Nicholas Manyoni (Dad);

Khethelo Fisokuhle Manyoni (Brother);

Ziningi Lethukuthula Manyoni (Sister);

and Kwanele Khwezi Manyoni (Sister).

PREFACE

I, Manyoni Lindokuhle, pronounce that:

- The research assessment detailed in the present thesis, unless or otherwise indicated, is my original study.
- This thesis/dissertation has never been submitted for any degree or examination at some other institution.
- Lastly, the present dissertation does not consist other people's writings, data, pictures, graphs, or any other information, unless it is explicitly indicated.

Mr. Lindokuhle Manyoni

Date 29/09/2022

Prof. G. Gan Redhi

Date 19/01/2023

ACKNOWLEDGEMENTS

I convey my utmost gratitude to:

- My Ancestors for everything
- Prof G. G Redhi for his enthusiastic supervision and mentorship throughout the study.
- Thanks to Department of Chemistry, Durban University of Technology, Durban, South Africa, for providing the facilities to conduct this study.

For the last time, I would like to express my appreciations to:

- My family especially my mom, Nomvula Bongekile Mnguni Manyoni for the support and encouragement they have given me since my day one at university.
- My friends, Bonga Furtune Mondli Msomi and Senzo Mpangase for their support throughout the study.

ABSTRACT

Many industrial processes in the chemical industry require surge amounts of energy to separate organic mixtures. While numerous separating substances used for this purpose are volatile and have closely related boiling points to the mixtures, they are environmentally harmful. As a result, new separation substances in the space of these solvents should be researched.

The latest group of solvents known as deep eutectic solvents (DESs), classified as Type (III), were studied in the space of conventional organic solvents, which are currently used in industrial processes for extraction or separation purposes. In the forecast, deep eutectic solvents have gained significant interest as part of the low melting temperature solvents with many other attractive and unique properties. This includes their physical, thermophysical, and thermodynamic properties. These properties were investigated in this study in order to better understand the intermolecular interactions of 1-ethyl-1-methylpyrrolidinium bromide + glycerol [(EMPYR) Br + Gly] or 1-ethyl-1-methylpyrrolidinium bromide + ethylene glycol [(EMPYR) Br + EG], with methanol or ethanol. Hence, the first section of the study investigated the physical properties, including density and sound velocity, of deep eutectic solvents and their binary mixtures, as a function of temperature. The obtained physical properties were used to compute the thermophysical properties, i.e., excess molar volume (V_m^E), intermolecular free length (L_f), variation in isentropic compressibility (ΔK_s), and isentropic compressibility (K_s), to advance the study of the intermolecular interactions of the selected deep eutectic solvents and their binary mixtures.

Furthermore, the second section of this study investigated the infinite dilution activity coefficients of five different deep eutectic solvents, including (1) 1-ethyl-1-methylpyrrolidinium bromide + glycerol [(EMPYR) Br + Gly], (2) 1-ethyl-1-methylpyrrolidinium bromide + ethylene glycol [(EMPYR) Br + EG], (3) 1-ethyl-1-methylpyrrolidinium bromide + 1-pentanediol [(EMPYR) Br + 1.5-PDO], (4) 1-ethyl-1-methylpyrrolidinium bromide + 1-hexanediol [(EMPYR) Br + 1.6-HDO], and (5) trihexyltetradecylphosphonium decanoate + ethylene glycol [(THTDP) Dc + EG], with various solutes at different temperatures. The obtained infinite dilution activity coefficients (γ_{13}^{∞}) were utilized to compute the other thermodynamic properties, viz., enthalpy ($\Delta H_1^{E,\infty}$), entropy ($\Delta S_1^{E,\infty}$), and Gibbs free energy ($\Delta G_1^{E,\infty}$) as well as the selectivity (S_{ij}^{∞}) and capacity (k_j^{∞}), of the selected organic solutes. The separation was possible with the investigated solvents. As is known, the accurate and precise analysis of the thermodynamic properties of liquid substances such as deep eutectic solvents is of significant interest to the chemical industry as it would help ascertain the implementation of these solvents on a large scale for industrial separation processes.

Table of Contents

LIST OF TABLES

Table 5-8: Standard deviations (σ) and constant coefficients (A_i) for {[(EMPYR) Br + Gly] (x_1) + ethanol (x_2)}, binary systems at different temperatures and the atmospheric pressure

Table 5-9: Averages of infinite dilution activity coefficients for the chosen organic solutes in the [(EMPYR) Br + Gly], DES at a molar ratio of 1:2 and at four different temperatures: With the standard state of the solute's hypothetical liquid at zero pressure.

Table 5-10: Partial molar excess properties such as enthalpies ($\Delta H_1^{E,\infty}$), Gibbs free energies ($\Delta G_1^{E,\infty}$), and entropies ($T_{ref}\,\Delta S_1^{E,\infty}$) for the organic solutes in the [(EMPYR) Br + Gly], DES at the reference temperature $T_{ref} = 313.15$ K.

Table 5-11: Averages of infinite dilution activity coefficients for the chosen organic solutes in the [(EMPYR) Br + EG], DES at a molar ratio of 1:4 and at four different temperatures: With the standard state of the solute's hypothetical liquid at zero pressure

Table 5-12: Partial molar properties such as enthalpies ($\Delta H_1^{E,\infty}$), Gibbs free energies ($\Delta G_1^{E,\infty}$), and entropies ($T_{ref}\,\Delta S_1^{E,\infty}$) for the organic solutes in the [(EMPYR) Br + EG], DES at the reference temperature, $T_{ref} = 313.15$ K.

Table 5-13: Averages of infinite dilution activity coefficients for the chosen organic solutes in the [(EMPYR) Br + 1.5-PDO], DES at a molar ratio of 1:2 and at four different temperatures: With the standard state of the solute's hypothetical liquid at zero pressure

Table 5-14: Partial molar properties such as enthalpies ($\Delta H_1^{E,\infty}$), Gibbs free energies ($\Delta G_1^{E,\infty}$), and entropies ($T_{ref}\,\Delta S_1^{E,\infty}$) for the organic solutes in the [(EMPYR) Br + 1.5-PDO], DES at the reference temperature $T_{ref} = 313.15$ K

Table 5-15: Averages of infinite dilution activity coefficients for the chosen organic solutes in the [(EMPYR) Br + 1.6-HDO], DES at a molar ratio of 1:2 and at four different temperatures: With the standard state of the solute's hypothetical liquid at zero pressure

Table 5-16: Partial molar properties such as enthalpies ($\Delta H_1^{E,\infty}$), Gibbs free energies ($\Delta G_1^{E,\infty}$), and entropies ($T_{ref}\,\Delta S_1^{E,\infty}$) for the organic solutes in the [(EMPYR) Br + 1.6-HDO], DES at the reference temperature $T_{ref} = 313.15$ K

LIST OF FIGURES

Figure 5-2: Variation in isentropic compressibilities (ΔK_s) of {[(EMPYR) Br + EG] (x_1) + methanol (x_2)}, binary systems as a function of mole fraction $x_1 =$ (0-1) at T = (293.15; 298.15; 303.15; 308.15; and 313.15) K

Figure 5-3: Isentropic compressibilities (K_s) of {[(EMPYR) Br + EG] (x_1) + methanol (x_2)}, binary systems as a function of mole fraction of $x_1 =$ (0-1) at T = (293.15; 298.15; 303.15; 308.15; and 313.15) K

Figure 5-4: Intermolecular free length values (L_f) of {[(EMPYR) Br + EG] (x_1) + methanol (x_2)}, binary systems as a function of mole fraction of $x_1 =$ (0-1) at T = (293.15; 298.15; 303.15; 308.15; and 313.15) K

Figure 5-5: Excess molar volumes (V_m^E) of {[(EMPYR) Br + EG] (x_1) + ethanol (x_2)}, binary systems as a function of mole fraction of x_1= (0-1) at T = (293.15; 298.15; 303.15; 308.15; and 313.15) K

Figure 5-6: Variation in isentropic compressibilities (ΔK_s) of {[(EMPYR) Br + EG] (x_1) + ethanol (x_2)}, binary systems as a function of mole fraction of x_1= (0-1) at T = (293.15; 298.15; 303.15; 308.15; and 313.15) K

Figure 5-7: Isentropic compressibilities (K_s) of {[(EMPYR) Br + EG] (x_1) + ethanol (x_2)}, binary systems as a function of mole fraction of $x_1 =$ (0-1) at T = (293.15; 298.15; 303.15; 308.15; and 313.15) K

Figure 5-8: Intermolecular free length values (L_f) of {[(EMPYR) Br + EG] (x_1) + ethanol (x_2)}, binary systems as a function of mole fraction of $x_1 =$ (0-1) at T = (293.15; 298.15; 303.15; 308.15; and 313.15) K

Figure 5-9: Excess molar volumes (V_m^E) of {[(EMPYR) Br + Gly] (x_1) + methanol (x_2)}, binary systems as a function of mole fraction of $x_1 =$ (0-1) at T = (293.15; 298.15; 303.15; 308.15; and 313.15) K

Figure 5-10: Variation in isentropic compressibilities (ΔK_s) of {[(EMPYR) Br + Gly] (x_1) + methanol (x_2)}, binary systems as a function of mole fraction of $x_1 =$ (0-1) at T = (293.15; 298.15; 303.15; 308.15; and 313.15) K

NOMENCLATURE

British Symbols

A	Regressed parameter of Antione absolute vapour pressure for the correlation
B	Regressed parameter of Antione absolute vapour pressure for the correlation
C	Regressed parameter of Antione absolute vapour pressure for the correlation
C_L	Concentration of a solute in liquid
C_M	Concentration in gas phase
a_i	Activity
a_t	Polar contribution parameter for correlation of Tsonopolus
b_t	Polar contribution parameter for correlation of Tsonopolus
c	Constant elasticity
A_i	Correlation coefficient
B^o	Parameter for the Antione Vapour Pressure Equation
B^1	Parameter for the Antione Vapour Pressure Equation
B_{ij}	Second virial coefficient, interaction $(cm^3.mol^{-1})$
B_{virial}	Second virial coefficient, density expansion $(cm^3.mol^{-1})$
E_i	Ionization potential of component (i) $(kj.mol^{-1})$
G^E	Excess Gibbs free energy per mole $(kj.mol^{-1})$
$\Delta G_1^{E,\infty}$	Change in partial molar excess Gibbs free energy of a component (i) in a solution $(kj.mol^{-1})$
f_i	Fugacity of the pure component (i) (kPa)

$\widehat{f_i}$	Fugacity of the component (i) in a solution (kPa)
f^o	Correlation term of the Tsonopolus, defined in Eq. (3-22)
f^1	Correlation term of the Tsonopolus, defined in Eq. (3-23)
f^2	Correlation term of Tsonopolus, defined in Eq. (3-24)
f^3	Correlation term of Tsonopolus, defined in Eq. (3-25)
H	Solubility constant of Henry's Law
H^E	Excess enthalpy $(kj.mol^{-1})$
H_i	Partial molar excess enthalpy of a component (i) in a solution $(kj.mol^{-1})$
$\Delta H_1^{E,\infty}$	Change in partial excess molar enthalpy of a component (i) in a solution $(kj.mol^{-1})$
I_c	Critical ionization energy $(kj.mol^{-1})$
J_2^3	Factor for the pressure correction term
K	Constant in a Parachor equation
$K_{a,w}$	Air-water partitioning constant
K_L	Partition coefficient
k	Number of coefficients in Redlich-Kister Equation
k_i	Capacity
k_j^∞	Capacity of a solute at infinite dilution
k_{12}	Parameter of empirical binary interaction
K_s	Isentropic compressibility (Pa^{-1})
$K_{s,m}$	Molar isentropic compressibility (Pa^{-1})

ΔK_s	Variation in isentropic compressibility (Pa^{-1})
L_f	Intermolecular free length (m)
M	Composition of the contents in an oscillator
M_o	Composition of the unfilled oscillator
M_w	Molecular mass of the constant
M_1	Molar mass of the component (i), solvent 1 $(g.mol^{-1})$
M_2	Molar mass of component (j), solvent 2 $(g.mol^{-1})$
n	Moles (mmols)
n	Number of experiments
N	Degree of polynomial
P	Parachor
P	Pressure (Pa)
P_1^* or P_1^{sat}	Saturated vapour pressure of a solute (Pa)
P_c	Critical pressure (Pa)
P_w	Saturated vapour pressure of water (Pa)
P_i	Column inlet pressure (Pa)
P_o	Column outlet pressure (Pa)
R	Ideal gas constant
S_{ij}^{∞} or S_{13}^{∞}	Selectivity of component (i) in the excess of component (j)
S^E	Excess entropy $(kj.mol^{-1})$

$\Delta S_1^{E,\infty}$	Change in partial molar excess entropy of a component (i) in a solution (kj.mol^{-1})
T	Absolute temperature (K)
T_c	Critical temperature (K)
T_f	Ambient temperature (K)
t_R	Retention time of solute (s)
t_M or t_G	Retention time of the carrier gar (s)
U	Instrumental (GLC) outlet volumetric flow rate $(\text{m}^3.\text{s}^{-1})$
U_o	Corrected instrumental outlet volumetric flow rate $(\text{m}^3.\text{s}^{-1})$
u	Speed of sound/ sound velocity (m.s^{-1})
V	Volume (m^3)
V_c	Critical molar volume of a solute $(\text{cm}^3.\text{mol}^{-1})$
V_G	Vapour phase volume (m^3)
V_L	Liquid phase volume (m^3)
V_m	Molar volume $(\text{cm}^3.\text{mol}^{-1})$
V_1^{∞}	Partial molar volume of a solute $(\text{m}^3.\text{mol}^{-1})$
V_1^*	Molar volume of a solute $(\text{m}^3.\text{mol}^{-1})$
V_N	Net retention volume of a solute (m^3)
V_m^E	Excess molar volume $(\text{cm}^3.\text{mol}^{-1})$
x	Mole fraction of components
Z	Compressibility factor

Greek Symbols

Γ or γ	Activity coefficient of a component
α	Separation factor
ρ	Density
σ	Standard deviation
ω	Acentric factor
τ	Correspondence periods of the pure components for known density
ϕ	Volume fraction

Notation

Δ	Change or difference

Subscripts

o	Initial value
1	Component of interest
2	Carrier gas
2	Second component in a binary mixture
3	Solvent in a stationary phase
c	Critical property
G	Gas phase
f	Babble flow meter
L	Liquid phase

m	Molar
s	Isentropic
w	Water

Superscripts

o	Initial value
E	Excess property
Exp	Experimental value
∞	Infinite dilution
∗	Represents saturation
Sat	Represents saturation
Lit	Literature value

ABBREVIATION

Acronyms

COS	Conventional Organic Solvent
DES	Deep Eutectic Solvent
HBA	Hydrogen Bond Acceptor
HBD	Hydrogen Bond Donor
LDF	London Dispersive Forces
OH	Hydroxyl Group
VOC	Volatile Organic Compound

Solvent Components

ChCl	Choline chloride
Gly	Glycerol
EG	Ethylene glycol
1.5-PDO	1.5-pentanediol
1.6-HDO	1.6-hexanediol
MEK	Methyl ethyl ketone
HxD	Hexadecane
2-PYR	2-pyrrolidone
NMP	N-methyl-2-pyrrolidone
NMF	N-methylformamide
(EMPYR) Br	1-ethyl-1-methylphyrrolidinium bromide

(THTDP) Dc	Trihexyltetradecylphosphonium decanoate
[BMPYR][$B(CN)_4$]	1-butyl-1-methylpyrrolidinium tetracynoborate
[HMPYR][Tf_2N]	1-hexyl-1-methylpyrrolidinium bis(trifloromethylsulfonyl)imide
[$P_{6,6,6,14}$] [DCA]	Trihexyltetradecylphosphonium dicynamide
[$(OH)_2C_3$MPyrr][Cl]	2.3-dihydroxypropyl-N-methyl-2-oxopyrrolidinium chloride
[$P_{14,6,6,6}$][$(C_8H_{17})_2PO_2$]	Trihexyltetradecylphosphonium bis(2,4,4-trimethylpentyl)phosphinate
[HMPYR] [BTI]	1-hexyl-1-methylpyrrolidinium bis(trifloromethylsulfonyl)imide
[OMPYR] [BTI]	1-octyl-1-methylpyrrolidinium bis(trifloromethylsulfonyl)imide
[OMIM] [NO_3]	1-methyl-3-octylimidazolium nitrate

Approaches and Methods

LLE	Liquid-Liquid Extraction
VLE	Vapour-Liquid Equilibrium
R. D	Relative Deviation
IDAC	Infinite Dilution Activity Coefficient
COSMO-RS	Conductor-like Screening Model for Solvents Methods
GMC	Group Contribution Methods
QSPR	Quantitative Structure Property Relationships
SPACE	Solvatochromic Parameters for Activity Coefficient Estimations
LSR	Linear Solvation Relationships
UNIFAC	Universal Quasi-Chemical Functional Group Activity Coefficients

Instrumentation

DEM	Differential Ebulliometry Method
DSC	Differential Static Cell
DPM	Dew Points Method
FID	Flame Ionization Detector
GC	Gas Chromatography
GLC	Gas Liquid Chromatography
HSC	Head Space Chromatography
TCD	Thermal Conductivity Detector
IGS	Inert Gas Stripping
RDM	Rayleigh Distillation Method
TGA	Thermogravimetric Analysis

LIST OF PUBLICATIONS

- **L. Manyoni**, B. Kabane, G. G. Redhi, Deep eutectic solvents as a possible entrainer for industrial separation problems: Pre-screening tool for solvent selection. *Fluid Phase Equilibria,* 553 (2022) 113266.

- **L. Manyoni**, G. G. Redhi, Measurements of limiting activity coefficients for aromatic and aliphatic hydrocarbons in Deep Eutectic Solvent, 1-ethyl-1-methylpyrrolidinium bromide + ethylene glycol at different temperatures and a stated molar ratio. *Journal of Chemical Thermodynamics and Thermal Analysis,* 7 (2022) 100057-100064.

- **L. Manyoni**, B. Kabane, G. G. Redhi, Excess thermodynamic functions of phosphonium based deep eutectic solvent for various organic solutes at different temperatures. *Journal of the Taiwan Institute of Chemical Engineers*, 132 (2022) 104463.

- **L. Manyoni,** G. G. Redhi, 1,6-hexanediol based deep eutectic solvent and their excess data at infinite dilution. *Journal of Chemical Thermodynamics and Thermal Analysis* (reference number: CTTA 100088).

- **L. Manyoni**, G. G. Redhi, Physicochemical properties of binary systems containing deep eutectic solvent and common alcohols (*under review*).

- **L. Manyoni**, G. G. Redhi, Separation potential of 1.5-pentanediol based deep eutectic solvent: Excess thermodynamic data (*under review*).

CHAPTER ONE

INTRODUCTION

1.1 Background

The chemical industry is a diverse industry with many service and product offerings, that supply various industries, including the food, manufacturing, pharmaceutical, and petroleum industries, to mention a few (Martins *et al.*, 2017; Cseri *et al.*, 2018; Grundtvig *et al.*, 2018; Murador *et al.*, 2019). Lately, the chemical industry has come under critical observation and scrutiny, as world leaders investigate and debate the role that chemical processes and substances contribute to global climate change (Pena-Pereira *et al.*, 2015; Tobiszewski and Namiesnik, 2017; Joshi and Adhikari, 2019). This has initiated a search for alternative methods and substances for facilitating the production of chemical products in an environmentally friendly manner (Armenta *et al.*, 2019; Choi and Verpoorte, 2019; Pacheco-Fernández and Pino, 2019). The key to the search for a more environmentally friendly approach to chemical production is finding innovative methods to improve chemical processes.

Chemical substances used in industrial separation processes consume a significant amount of energy, finance, and toxic by-products (Lee *et al.*, 2012; Wang *et al.*, 2017; Cheng *et al.*, 2018; Torres-Valenzuela *et al.*, 2020). A key contributor to these constraints is the volatile nature of the organic solvents used in most chemical separation processes (Jakobsen *et al.*, 2005; Cvetanovic, 2019; Thompson *et al.*, 2019; Albuquerque *et al.*, 2021). The most common of these volatile organic compounds (VOCs), also known as conventional organic solvents, are N-methyl-2-pyrrolidone (NMP); N-methyl formamide (NMF); glycerol; diethylene glycol (DEG); and triethylene glycol (TEG). These solvents have various shortcomings, such as being highly volatile, non-recyclable, having low yields in production due to the closely related boiling points, and are also expensive (Vanda *et al.*, 2018; Gullón *et al.*, 2020; Jalili *et al.*, 2020; Makos *et al.*, 2020). Ionic liquids were seen as a relatively new class of environmentally friendly organic solvents that could possibly replace the predominantly organic solvents used and mentioned above. However, the main disadvantage is that their production is energy intensive, and some are highly toxic, viscous, and costly (Singh and Savoy, 2020; Uddin *et al.*, 2020; Paucar *et al.*, 2021). As a result, for chemical organic separation operations in diverse sectors, new technologies, procedures, and substances should be investigated.

Deep eutectic solvents (DESs) have emerged as an alternative environmentally friendly solvent to both conventional organic solvents as well as conventional ionic liquids for liquid-liquid extraction (LLE) and azeotropic distillation (Shishov *et al.*, 2017; Hansen *et al.*, 2020; Shekaari *et al.*, 2020a; Smink *et al.*, 2020; Zante *et al.*, 2020). These deep eutectic solvents are combinations made from a eutectic component mixture of Bronsted or Lewis acids and bases, which consist of various cationic or anionic components (Lee *et al.*, 2020; Wang *et al.*, 2020). They have more potential applications for the purposes of chemical separation, and in addition, they are less expensive compared to recently used solvents, and favour the green approach to chemical processing since they are mostly derived from non-toxic and renewable bio-resources, as well as share many virtuous characteristics with conventional ionic liquids (Hansen *et al.*, 2020; Perna *et al.*, 2020; Ramon and Guillena, 2020).

Moreover, most deep eutectic solvents have the extremely desirable attribute of being liquids that release only a small amount of vapour into the atmosphere, making them ideal solvents in this regard. A second intriguing feature of a deep eutectic solvent is that it is a designer solvent, meaning it can be "designed" to be exactly what is needed. In other ways, a deep eutectic solvent can be designed and adjusted to have the specific characteristics required for a given task. This is due to the fact that a deep eutectic solvent is a product of the eutectic mixing of two or more components, namely a hydrogen bond acceptor (HBA) and a hydrogen bond donor (HBD) (El Achkar *et al.*, 2021; Haghbakhsh *et al.*, 2021). Since their potential applications as new separating solvents were discovered a decade ago, research on these solvents has accelerated significantly. However, if the chemical and petrochemical industries want to use deep eutectic solvents in industrial processes as an innovation or a novel strategy, a complete study of these solvents' intermolecular interactions is required (Alkhatib *et al.*, 2020; Santana-Mayor *et al.*, 2020).

The intermolecular interactions between deep eutectic solvents and a list of organic solutes, icluding 2,2-dimethybutane, pentane, hexane, heptane, octane, n-nonane, n-decane, 1-pentene, 1-hexane, 1-heptene, 1-pentyne, 1-hexyne, 1-heptyne, cyclopentane, cyclohexane, methylcyclohexane, cyclopentene, cyclohexene, o-xylene, m-xylene, p-xylene, benzene, ethylbenzene, toluene, methanol, ethanol, 2-propanol, butan-1-ol, acetone, methyl ethyl ketone, thiophene, and water, were measured using density and sound velocity meter, as well as gas-liquid chromatography.

To justify the chemical and petrochemical industries' interest, the experimental data obtained were computed in this work and compared to the ones obtained from the literature. Table 1-1 and Figures 1-1 to 1-5 provided a list and structures of the solvent systems that were investigated:

Table 1-1: List of the investigated deep eutectic solvents

Deep eutectic solvents (DESs)	*Mole Ratio*
1-ethyl-1-methylpyrrolidinium bromide + glycerol	1:2
1-ethyl-1-methylpyrrolidinium bromide + ethylene glycol	1:4
1-ethyl-1-methylpyrrolidinium bromide + 1.5-pentanediol	1:2
1-ethyl-1-methylpyrrolidinium bromide + 1.6-hexanediol	1:2
Trihexyltetradecylphosphonium decanoate + ethylene glycol	1:4

The structures of the compounds used for the preparation of the systems are given in the figures below.

Figure 1-1: 1-ethyl-1-methypyrrolidinium bromide + glycerol, [(EMPYR) Br + Gly]

Figure 1-2: 1-ethyl-1-methylpyrrolidinium bromide + ethylene glycol, [(EMPYR) Br + EG]

Figure 1-3: 1-ethyl-1-methylpyrrolidinium bromide + 1.5-pentanediol, [(EMPYR)Br + 1.5-PDO]

Figure 1-4: 1-ethyl-1-methylpyrrolidinium bromide + 1.6-hexanediol, [(EMPYR) Br + 1.6-HDO]

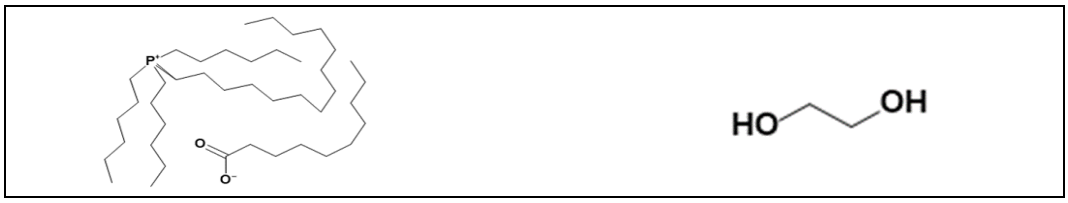

Figure 1-5: Trihexyltetradecylphosphonium decanoate + ethylene glycol, [(THTDP) Dc + EG]

1.2 Problem Statement

The conventionally used organic solvents in liquid-liquid extraction and azeotropic distillation have many drawbacks. A number of these conventional organic solvents are toxic to human beings and the environment, are flammable, and are non-recyclable due to their inherent volatility as well as closely interrelated boiling points. This has started a quest in the scientific community to develop green methods based on the principles of green chemistry, methods substantively yield chemical products in industrial processes and are proven to be harmless to the environment as well as human and animal health.

Attempts have been made to investigate and research alternative environmentally friendly methods and substances that are cost-effective, environmentally friendly, and improve the efficiency of the existing extraction processes (Verma *et al.*, 2019; Alizadehdakhel and Golzary, 2020; Singh and Savoy, 2020; Reeves *et al.*, 2021). Ionic liquids (ILs) are widely known as new low-volatile solvents with chemical and thermal stability, low vapour pressure, and high solvation properties (Vekariya, 2017; Singh and Savoy, 2020), have recently received significant attention as an alternative to the conventional organic solvents used in different chemical industries (Soleimani, 2020). However, the synthesis and purification of ionic liquids is costly and difficult to attain, hence, this could limit their potential application in industrial processes (Hassanshahi *et al.*, 2020; Paucar *et al.*, 2021). Furthermore, companies are apprehensive about using new substances in general, especially those that might lead to changes in established industrial processes. Deep eutectic solvents, on the other hand, have shown to have some advantages over ionic liquids in terms of physiognomies, and they are deserving of further exploration because they appear to be

superior to ionic liquids. Beside choline chloride-based deep eutectic solvents, studies regarding deep eutectic solvents are still limited, particularly those containing unpopular organic salts, such as phosphonium, pyrrolidinium, and more. Thus, the present study aims to cover this gap.

1.3 Aim and the Objectives of the Study

Aim

The aim of the study was to analyse and evaluate pyrrolidinium and phosphonium based-DESs as future solvents in the separation of azeotropic mixtures with their closely related boiling points.

Objectives

- To determine the molecular interactions of the selected organic solutes using density, sound velocity, as well as other thermophysical properties,
- To determine the infinite dilution activity coefficients and thermodynamic properties of pyrrolidinium and phosphonium-based DESs,
- To ascertain the performance of pyrrolidinium and phosphonium based-DESs as organic solvents in the chemical separation of binary mixtures by calculating selectivities and capacities,
- And to compare deep eutectic solvents' characteristics to the recently used conventional organic solvents as well as ionic liquids.

1.4 Context of the Study:

This assessment completely describes the preparation of pyrrolidinium and phosphonium based DESs as well as their industrial applications, in terms of the molecular interactions through the experimental thermophysical properties, i.e., excess molar volume (V_m^E), variation in isentropic compressibility (ΔK_s), isentropic compressibility (k_s), intermolecular free length (L_f), and infinite dilution activity coefficients (γ_{13}^{∞}), the partial molar properties, i.e., $\Delta H_1^{E,\infty}$, $\Delta G_1^{E,\infty}$, and $\Delta S_1^{E,\infty}$ as well as selectivity (S_{ij}^{∞}) and capacity (k_j^{∞}), for the selected organic solutes. Five deep eutectic solvents were prepared successfully, according to the mole ratios listed. The first four deep eutectic solvents were prepared based on the ionic liquid, 1-ethyl-1-methylpyrrolidinium bromide, combined with various conventional organic solvents, such as glycerol, ethylene glycol, 1.5-

pentanediol, and 1.6-hexanediol. One deep eutectic solvent was prepared from trihexyltetradecylphosphonium decanoate combined with ethylene glycol. The mole ratios of all the prepared deep eutectic solvents were stated early on in this chapter in the classification of deep eutectic solvents (Table 1-1). Normally, deep eutectic solvents are divided into four classes: Type (I), Type (II), Type (III), and Type (IV). This study discusses Type (III), which are the most attractive when compared to the others mentioned, due to its melting point, which depends on the intermolecular interactions between the hydrogen bond acceptors (HBAs) and hydrogen bond donors (HBDs). While the other deep eutectic solvents are prepared from metal-based compounds, in this study Type (III) deep eutectic solvents were prepared by combining hydrogen bond acceptors based on pyrrolidinium and/or phosphonium materials together with various types of hydrogen bond donors such as glycerol, ethylene glycol, 1.5-pentanediol, and 1.6-hexanediol. The hydrogen bond acceptors were ionic liquids, and the hydrogen bond donors were organic solvents that are commonly used for extraction purposes, as mentioned above. Based on the literature survey, this is the first work to evaluate thermophysical properties and infinite dilution activity coefficients as well as the other thermodynamic properties by an application of pyrrrolidinium and phosphonium based-DESs with the chosen solvents.

The investigated systems, listed in Table 1-1 and displayed in the Figures 1-1 to 1-5 have not been studied previously. The thermophysical properties and infinite dilution activity coefficients of organic mixtures were studied for different solutes at different temperatures under atmospheric pressure. Furthermore, the obtained thermodynamic data was computed from instrumental data. The interactions between the deep eutectic solvent and organic solutes were described in terms of hydrogen-bonds, dispersive, repulsive, and dipole-dipole interactions. The comparison of the capacities and selectivities of the investigated deep eutectic solvents as well as their corresponding mixtures were studied in detail regarding the interactions amongst the organic molecules and dipole-dipole interactions.

In this study, a digital vibrating analysis tube (U-tube) fitted Anton Paar Densitometer was used during the experimental study at various temperatures. Ethanol and acetone were used to clean and dry the cell by the application of the automatic X sampler 452 module. A built-in thermostat controller had the ability to record an accurate temperature while measuring the physical properties, that is, density and sound velocity. The separation of binary mixtures was conducted by a density and sound velocity meter (Anton Paar DSA 5000 M) with a built-in thermostat.

In the second part of this study, a stainless-steel column packed with solid support material, chromosorb W HP 80-100 mesh, was utilised and then coated with the deep eutectic solvent. The

support material used was known to be non-reactive to both the carrier gas (helium) and the injected solutes. In addition, the thermal conductivity detector (TCD), a widely used detector in various chemical industries for the separation of organic mixtures because of its advantages, such as simplicity and robustness. The separation of mixtures was then conducted by gas-liquid chromatography (GC-Shimadzu 2014) coupled with the TCD.

1.5 Structure of the Thesis:

Chapter one

Introduces and contextualizes the research. It also provides the rationale, aims, objectives, and outline of the research project and dissertation.

Chapter two

The literature review fully describes the techniques and extracting solvents that have been used in previous studies by many scientific researchers for the evaluation of the thermodynamic functions and limiting activity coefficients.

Chapter three

Details the theoretical background for thermodynamic properties.

Chapter four

Details of the experimental procedures used in this research study

Chapter five

It presents the calculations of the experimental data for the test systems and the investigated deep eutectic solvent systems.

Chapter six

It gives a discussion of the results presented and a comparison with the previous studies.

Chapter seven

Conclusion of the study and recommendations based on the study findings

CHAPTER TWO

LITERATURE REVIEW

2.1 Introduction

Scientific researchers have increased their efforts in the last few decades to find more environmentally friendly organic solvents for chemical separation in industrial processes (Turosung and Ghosh, 2017; Cunha and Fernandes, 2018; Nkosi *et al.*, 2018b; Koshekov, 2020; Verma *et al.*, 2020). A key step in this direction has been to investigate the thermodynamic and physicochemical properties of new 'green' solvents to improve the environmental and sustainability factors affecting the chemical and petrochemical industries. Existing literature reveals that key areas to look at when investigating new potential organic solvents are:

- Organic solvents in industrial extraction processes: properties, preparations, and applications.
- Generalization on physical, thermophysical, and infinite dilution activity coefficients as well as other thermodynamic properties.
- Advancement of density and sound velocity meter method
- Advancement of the gas-liquid chromatography (GLC) technique

To address the above-mentioned points, the present study begins by discussing organic solvents in general, conventional organic solvents (COSs), and ionic liquids (ILs), as well as deep eutectic solvents (DESs), which are the solvents of interest.

2.2 Organic Solvents

Organic solvents are carbon-based substances with the ability to dissolve one or more substances. These substances can be utilized to develop millions of commercial products, with specific uses depending on a particular solvent's general properties, such as boiling point, volatility, colour, and molecular weight (Joshi and Adhikari, 2019).

In the chemical industry, some organic solvents can be used as a result of chemical separation of mixtures to produce other solvents (Cheremisinoff, 2003; Calvo-Flores *et al.*, 2018). The solvents that are used for such extractions are conventional organic solvents, also known as industrial solvents (Obst and König, 2018; Mukhamatdinov *et al.*, 2020).

2.3 Conventional Organic Solvents

Conventional organic solvents have received a lot of criticism because many are highly toxic to people and the environment, volatile; costly; have a low yield in production; and are highly flammable (Obst and König, 2018; Abdussalam-Mohammed *et al.*, 2020; Garcia-Vaquero *et al.*, 2020). This group of solvents includes N-methyl-2-pyrrolidone; glycerol; diethylene glycol; triethylene glycol; acetonitrile; diethyl ether; and toluene. These are used in the chemical industry for the separation of other solvents from solvent mixtures (Joshi and Adhikari, 2019; Brouwer and Schuur, 2020; Fan *et al.*, 2020; Torres-Valenzuela *et al.*, 2020).

2.4 Ionic Liquids

2.4.1 Definition and Structures of Ionic Liquids

Ionic liquids (ILs) are a relatively new class of organic solvents that have been investigated as replacements for the older conventional organic solvents (Paucar *et al.*, 2021; Zhou *et al.*, 2021). They are known to be interesting liquid substances with distinctive properties such as negligible vapor pressure, good thermal stability, and wide-spread electrochemical stability that most conventional organic solvents generally lack (Ren *et al.*, 2020; Singh and Savoy, 2020). A list of a few ionic liquids is displayed in Figure 2-1.

Structures

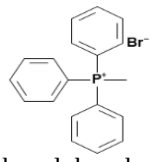 Triphenylphosphonium bromide	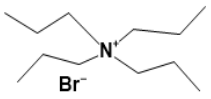 Tetrapropylammonium bromide	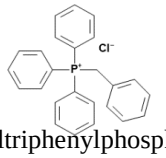 Benzyltriphenylphosphonium bromide
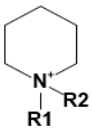 Dialkylpiperidinium	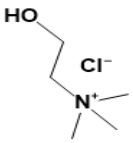 Choline chloride	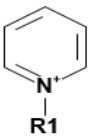 N-alkylpyridinium

Figure 2-1: Chemical structures of ionic liquids

2.4.2 Brief History of Ionic Liquids

The first ionic liquid was discovered in 1914, from the synthesis of ethylammonium nitrate salt in ambient temperature by Walden (1914). Then, Charles (1934) presented the first copyright for the ionic liquids, alkylpyridinium chloride and dialkylimidizolium chloride, which were used individually with aluminium chloride, but the resulting mixture was unstable in the presence of water. Research on ionic liquids stopped until, Wilkes and Zaworotko (1992) described 1-ethyl-3-methylimidizolium-based ionic liquids as new air and water stable materials. This led to a resurgence of investigations into ionic liquids as alternatives to the solvents used at that time and currently (Wishart and Castner, 2007; Skoronski *et al.*, 2020; Zhang *et al.*, 2020b).

2.4.3 Challenges Facing Ionic Liquids

A number of conventional ionic liquids have been prepared from bio-incompatible precursors such as imidazolium, pyridinium, morpholinium, ammonium, and phosphonium salts, which are vastly superior to conventional organic solvents, though they too are known to be abstemiously toxic and non-biodegradable themselves (Wang *et al.*, 2018a; Kravchyk *et al.*, 2020; Szalaty *et al.*, 2020; Uddin *et al.*, 2020). And it is for these reasons that the need to develop biocompatible substances has arisen for the benefit of the chemical separation industry.

Deep eutectic solvents have presented promising characteristics to even better those of ionic liquids because they share the superior qualities of ionic liquids without the drawbacks of high costs of the starting materials, toxicity, non-biodegradability, and complex preparation requiring purification (Perna *et al.*, 2020; Santana-Mayor *et al.*, 2020; Shishov *et al.*, 2020). Deep eutectic solvents are an innovative class of solvent mixtures with a relatively low melting temperature (Abranches and Coutinho, 2022; Jiao *et al.*, 2022). The section that follows provide more information on the definition, background, properties, preparation or synthesis, and classification of these solvents.

2.5 Deep Eutectic Solvents

2.5.1 Definition and Background of Deep Eutectic Solvents

Deep eutectic solvents (DESs) are organic mixtures with low melting points (less than 100 Degrees Celsius) that are created by mixing two or more organic components (Hansen *et al.*, 2020; Santana-Mayor *et al.*, 2020; Shishov *et al.*, 2020). As illustrated in Figure 2-2, these mixtures are homogeneous and liquidate or solidify at temperatures lower than the melting points of all their constituents.

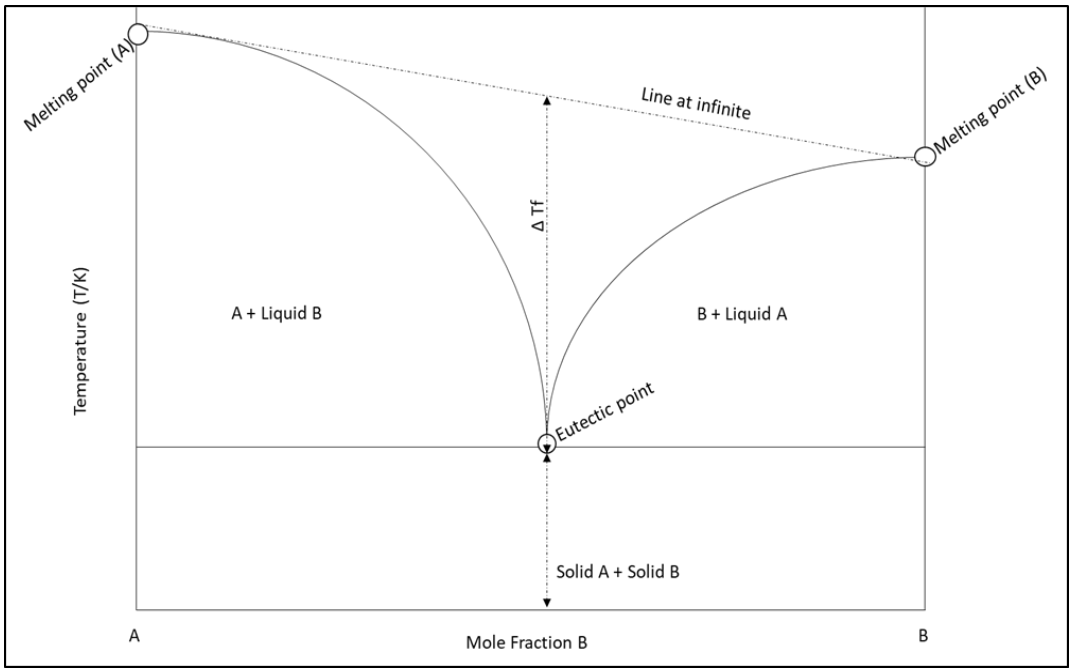

Figure 2-2: Schematic diagram of deep eutectic solvent forming eutectic mixture

The points, melting point (A) and melting point (B) represent the maximum melting temperature for each component, and A (solid) and B (liquid) are contributing components in a mixture. The difference in the freezing point at the eutectic composition of a mixture of A and B compared to a theoretical ideal mixture, ΔT_f, is a change related to the magnitude of the interaction between A and B, according to this diagram. The larger the ΔT_f, the stronger the interaction. Contributing components melt or solidify at the eutectic point. Furthermore, the temperature is lower than the melting point of each component at this moment. Furthermore, the temperature is a dependent variable, while mole fraction B is an independent variable.

2.5.2 History

Deep eutectic solvents (DESs) were formally introduced in 2003 as a new, more environmentally friendly class of solvents that are alternatives to ionic liquids and conventional organic solvents (Abbott *et al.*, 2003). Their development was propagated by the reported drawbacks of conventional ILs, such as high costs of the starting materials, complex preparation requiring purification, high toxicity, and non-biodegradability (Jhong *et al.*, 2009; Hayyan *et al.*, 2012; Płotka-Wasylka *et al.*, 2020). Deep eutectic solvents were disclosed to have a number of advantages over ionic liquids, including: (I) their relatively simple preparation since the quaternary ammonium salt (e.g., hydrogen bond accepter) and hydrogen bond donor (HBD) or metal salt hydrates can be simply mixed and turned into deep eutectic solvent with no further purification; (II) they have low preparation cost due to the relatively low costs of raw materials needed to produce them; and (III) they are predicted to have a high degree of bio-compatibility when utilizing quaternary ammonium salts like choline chloride (Zhao and Baker, 2013; Vanda *et al.*, 2018; Murador *et al.*, 2019).

In a number of instances, deep eutectic solvents are formed by combining quaternary ammonium salts, i.e., hydrogen bond acceptors (HBAs), together with a hydrogen bond donors (HBDs), which have the potential to form a complex with the halide anion of the hydrogen bond acceptor (Abbott *et al.*, 2004; Kohli *et al.*, 2020). Deep eutectic solvents are classified into four groups with the following general formulas. Given in Table 2-1 and 2-2 below:

Table 2-1: Deep eutectic solvent general formulae and their terms (Smith *et al.*, 2014)

Groups Classification	*General Formulae*	*Terms*
Type (I)	$Cat^+X^- zMCl_x$	M = Zn, Sn, Fe, Ga, In, Al
Type (II)	$Cat^+X^- zMCl_x \cdot yH_2O$	M = Cr, Co, Cu, Fe, Ni
Type (III)	$Cat^+X^- zRZ$	Z = OH, COOH, $CONH_2$
Type (IV)	$MCl_x + RZ = MCl_{x-1}^+ \cdot RZ + MCl_{x+1}^-$	Z = OH, $CONH_2$ and M = Al, Zn

Table 2-2: Deep eutectic solvent groups classification (Abbott *et al.*, 2014)

Groups classification	*Deep eutectic solvent*
Type (I)	Quaternary ammonium salt + Metal chloride
Type (II)	Quaternary ammonium salt + Metal chloride hydrate
Type (III)	Quaternary ammonium salt + HBD
Type (IV)	Metal chloride hydrate + HBD

Of all the mentioned classes of deep eutectic solvents, Type (III) has shown the most promise in acting as a new superior class of organic solvents in chemical separation (Zhekenov *et al.*, 2017; Zaib *et al.*, 2020). This type (Type III) is naturally formed through hydrogen bonds, where the charge delocalization taking place through hydrogen bonds amongst the hydrogen bond donor and the halide results in a decrease in the freezing point of the mixture (Shang *et al.*, 2022; Sosa *et al.*, 2022). Type (III) DESs are made by combining a quaternary ammonium salt, i.e., a hydrogen bond accepters (HBAs) such as choline chloride, pyrrolidinium, phosphonium or sulfonium salts with a hydrogen bond donors (HBDs) such as alcohol, a polyol, a carboxylic acid, an amine or an amide (Rodriguez *et al.*, 2017; Zhekenov *et al.*, 2017). This forms an eutectic mixture at a melting temperature that is lower than that of the individual component materials used (Hansen *et al.*, 2020; Ramon and Guillena, 2020).

Abbott *et al.* (2003) reported the first application of a Type (III) deep eutectic solvent as a combination of choline chloride and urea (134 °C and 304 °C melting points, respectively) at a mole ratio of 1:2, which exhibited a melting temperature of 12 °C as a DES solvent. Several scientific researchers have started to focus on Type (III) deep eutectic solvents, especially choline chloride-based deep eutectic solvents in combination with various types of hydrogen bond donors (Zhekenov *et al.*, 2017; Ruggeri *et al.*, 2019; Xue *et al.*, 2020). For reasons unknown, research on the other hydrogen bond acceptors (quaternary ammonium salts), such as ammonium, pyrrolidinium, phosphonium, piperidinium, and imidazolium, has been largely neglected. As a result, the present study aims to contribute to the literature of deep eutectic solvents prepared based on these quaternary ammonium salts.

The list of different component materials commonly used for the preparation of deep eutectic solvents are given in Figures 2-3 and 2-4 for hydrogen bond acceptors and donors, respectively.

Hydrogen Bond Acceptors

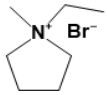 1-ethyl-methylpyrrolidinium bromide	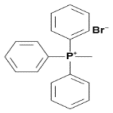 Methyltriphenylphosphonium bromide	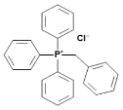 Benzyltriphenylphosphonium chloride
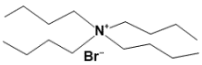 Tetrabutylammonium bromide	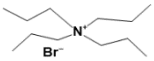 Tetrapropylammonium bromide	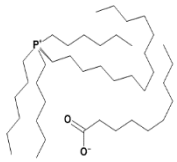 Trihexyltetradecylphosphonium decanoate
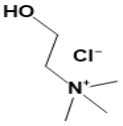 Choline chloride	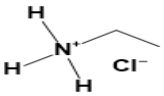 Ethyl ammonium chloride	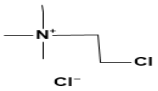 2-chloro-N, N, N-trimethylethyl ammonium chloride

Figure 2-3: Some of the hydrogen bond acceptors commonly used in the synthesis of deep eutectic solvents

Hydrogen Bond Donors

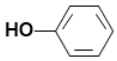 Phenol	 O-cresol	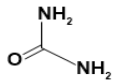 Urea	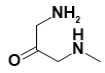 1-methyl urea
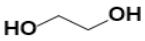 Ethylene glycol	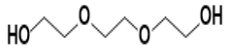 Triethylene glycol	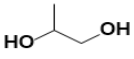 1.2-propylene glycol	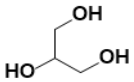 Glycerol
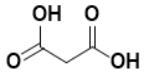 Malonic acid	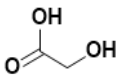 Glycolic acid	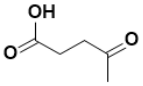 Levulinic acid	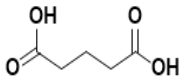 Adipic acid
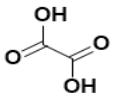 Oxalic acid	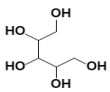 Xylitol	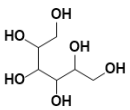 Sorbitol	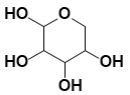 Xylose

Figure 2-4: Some of the hydrogen bond donors commonly used in the synthesis of deep eutectic solvents

2.5.3 Potential Applications of Deep Eutectic Solvents in Chemical Industries

The applications of deep eutectic solvents are determined by their unique properties. These properties are the result of the combination of organic materials used to form a specific deep eutectic solvent. This allows a wide range of applications, as illustrated in Table 2-3. In the present section, deep eutectic solvent applications are divided based on the collective state of their application areas, such as: chemical engineering, biochemistry, analytical chemistry, electrochemistry, synthesis, and catalysis, as given in Table 2-3.

Table 2-3 Fields and application areas of DESs in chemical industry (Obeten *et al.*, 2017)

Chemical Engineering	*Application area*
	Plasticizers
	Coatings
	Dispersing agent
	Robotics
	Separation technology
Biochemistry/Biology	*Application area*
	Sample preparation
	Analytical separation
	Detection system
Electrochemistry	*Application areas*
	Metal plating
	Electrolyte batteries
	Fuel cells
	Cells panels
Synthesis and Catalysis	*Application area*
	Organic synthesis
	Inorganic synthesis
	Nano chemistry
	Catalysis

2.6 Deep Eutectic Solvents in Separations

Deep eutectic solvents are potential solvent mixtures that can increase the efficiency and environmental friendliness of existing separation methods. In the chemical process sector, distillation is the most often used separation method. Separation becomes difficult and costly when the components to be separated have comparative volatilities, because a large number of trays and a high reflux ratio are required. Hence, liquid-liquid extraction and extractive distillation is required.

2.6.1 Extractive Distillation

Extractive distillation (ED) is a prominent separation process for separating azeotropic mixtures. In extractive distillation, choosing the right entrainer is crucial to getting the best extraction efficiency (Shen *et al.*, 2022). Deep eutectic solvents (DESs), which are less expensive and more environmentally friendly, have non-toxicity, biodegradability, and high recyclability (Bryant *et al.*, 2022; Ijardar *et al.*, 2022). As a new trend in extractive distillation, common organic solvents are being substituted by novel extractants.

The high boiling point entrainer is introduced into the extractive distillation column at the top, causing the volatiles to change to the point where the separation factor surpasses 1.00 (Ijardar *et al.*, 2022). The extractive agent flows to the bottom of the distillation column, where it is separated from the extracted component by a second distillation. As a result, the no extracted components are refined to the highest point of the extractive tower. As depicted in Figure 2-5,

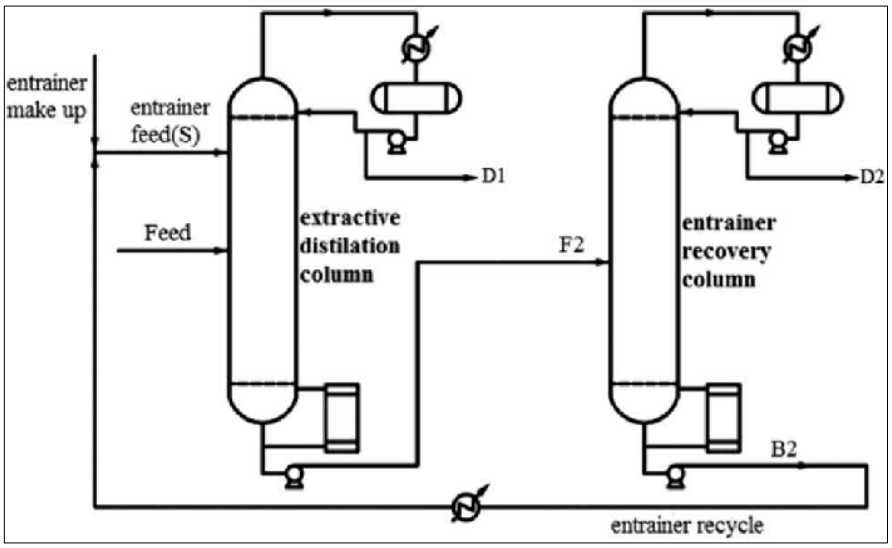

Figure 2-5: Schematic diagram of extractive distillation (Wang *et al.*, 2018a)

2.6.2 Liquid-Liquid Extraction

Liquid-liquid extraction (LLE) is a typical sample preparation technique that is more selective than traditional solvent extraction methods (Hammad *et al.*, 2022; Khatibi *et al.*, 2022). Analytes are transferred from an aqueous sample to a water-insoluble solvent in the LLE method (Khatibi *et al.*, 2022). Using selective solvents, aromatic compounds are separated from aliphatic chemicals in the feed stream in this method (Coto *et al.*, 2022).

In industry, this separation technique is utilized for the various separation processes, including:

- Separation of systems with comparable boiling temperatures,
- Separation of high-boiling-point systems,
- Separation of azeotropes,
- For separation of temperature sensitive solutes,
- Used for extraction of solutions.

2.6.3 Application of Deep Eutectic Solvents for Liquid-Liquid Extraction

Deep eutectic solvents are harmless and biodegradable, as well as immiscible with most aliphatic compounds. As a result, many deep eutectic solvents are extremely miscible with aromatic compounds, allowing aliphatic and aromatic mixtures to be separated (Alimoradi *et al.*, 2022; Chabib *et al.*, 2022). The LLE separation performance is determined by the selectivity and capacity of a solvent. A selectivity and capacity study is necessary to determine the economic viability of using deep eutectic solvents for aliphatic-aromatic separations. Deep eutectic solvents make it easier to regenerate extraction solvent due to their low vapour pressure. Separation should be used to prevent solvent loss in the raffinate. To regenerate deep eutectic solvent from the final extract, distillation is utilized, which requires heating and cooling (Figure 2-6).

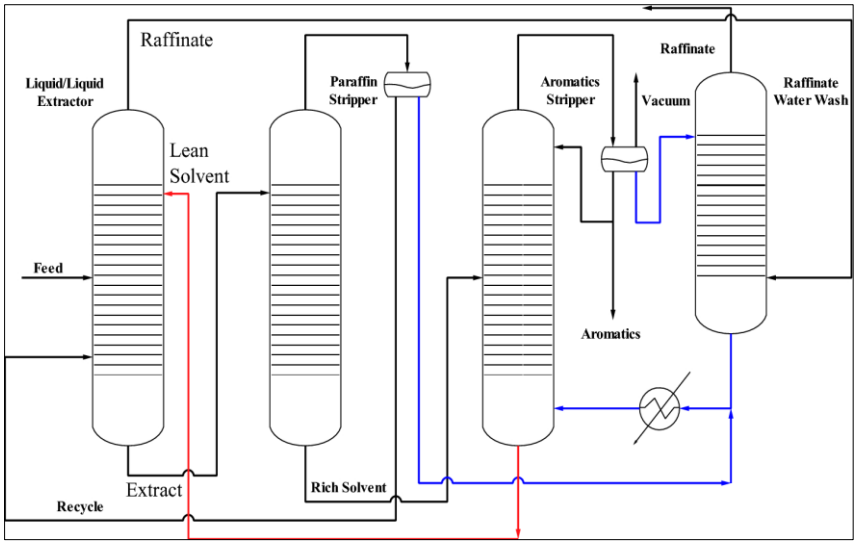

Figure 2-6: A typical liquid-liquid extraction (Addouni *et al.*, 2020)

2.6.4 Solvent Selection Criteria

Although deep eutectic solvents are essentially known to have low toxicity and biodegradability, a few of them do appear to be toxic and non-biodegradable (Marciniak and Wlozlo, 2018; Płotka-Wasylka *et al.*, 2020). However, as mentioned in the paragraphs above, this depends on the materials used for forming a specific deep eutectic solvent (Jangir *et al.*, 2020; Xu *et al.*, 2021). Furthermore, others have low thermal stability because of the component materials (Ghaedi *et al.*, 2018). For that reason, there are quite a few principles that should be considered when selecting a solvent for certain purposes. Nevertheless, it is still hard to choose a suitable environmentally friendly solvent that can serve as an alternative for both conventional organic solvents and ionic liquids. Table 2-4 gives criteria for choosing or selecting greener solvents for extraction or separation processes:

Table 2-4 Primary selection procedure for green solvents (Curzons *et al.*, 1999)

Criteria	*Details*
Distribution coefficient	A solvent should be easily distributed
Selectivity	A solvent should be highly selective to the chemical process
Recoverability	The solvent should be recovered easily in a chemical process
Stability	A solvent should be chemically and thermally stable
Synthesis	Preparation of a solvent should use minimal preparation energy

Price	A solvent should be relatively cheap
Toxicity	Solvents should not be toxic to humans and the environment
Biodegradability	A solvent should be easily decomposed by bacteria or any other living organisms.
Availability	Solvents should be easily accessible in large amounts
Flammability	Solvent should be non-flammable
Purity	A solvent must be of a high purity to prevent excessive energy consumption

2.7 Thermodynamic Studies

2.7.1 Thermophysical Properties of Deep Eutectic Solvent Mixtures

Haghbakhsh and Raeissi (2018c) investigated the volumetric properties of ethyl alcohol and reline, deep eutectic solvent. The densities of reline/ethanol systems were determined experimentally at various temperatures, T = (293.15-333.15) K and an atmospheric pressure of 100 kPa, covering the complete concentration range. For all the investigated systems and temperatures, the volumetric properties of interest were determined in order to calculate other derivative thermodynamic properties. This comprised excess molar volumes, partial molar volumes, partial molar volumes at infinite dilution, excess partial molar volumes, excess partial molar volumes at infinite dilution, and isobaric volume expansions, as well as the correlation of the density to temperature. At all concentrations and temperatures, the excess molar volumes were negative. This indicates the molecular arrangement of the hydrogen bond network, with reline primarily in central places and a tendency to be surrounded by ethanol molecules. Moreover, the obtained data was correlated by the use of Redlich-Kister Equation.

Haghbakhsh and Raeissi (2020) investigated volumetric properties as part of the thermophysical properties of systems of ethaline with methanol in a temperature range of T = 283.15-323.15 K. The Redlich-Kister model was used to compute and model the excess volumes of the investigated systems. All of the excess measurements were negative, indicating that the mixtures have greater hydrogen bond contributions and better interstitial accommodations than the pure states. Other volumetric parameters, such as partial molar volumes and excess partial molar volumes, were also computed for each mixture and at infinite dilution. When comparing the predicted volumetric properties of ethaline with methanol, it was discovered that ethaline had a higher tendency for

solvation in the mixture. As a result, it's suggested that the hydrogen bond networks in the mixture are formed in a pattern in which ethaline molecules occupy central locations and are surrounded by methanol molecules.

Haghbakhsh and Raeissi (2018b) studied the excess volumes of mixtures of 12 different systems containing deep eutectic solvents such as reline, glycine, ethaline, maline, tegaline, and glucoline with methanol, ethanol, isopropanol, water, and DMSO by the Prigogine-Flory-Patterson theory. The obtained data revealed that the excess molar volume and temperature are linear for all the studied systems. Furthermore, the excess molar volume data revealed a negative deviation for all the studied systems from the ideal mixture. Hence, the obtained data was in good agreement with the ones computed from the Redlich-Kister Equation.

Moghimi and Roosta (2019) measured the density and viscosity data of a (choline chloride + glucose) deep eutectic solvent with water at different temperatures and the mole fraction of (0-1). The thermodynamic parameters, such as excess molar volumes, dynamic viscosity, and activity coefficients, were computed from the measured density and viscosity data for intermolecular interactions that arise in a mixture. Negative excess molar volume, positive dynamic viscosity deviation, and activity coefficients less than unity found indicate a higher interaction between water and deep eutectic solvent when compared to solute-solute and solvent-solvent pairs, or, in other words, a negative deviation from the ideality of the system examined. Furthermore, the data was compared to previous work and found to be consistent with the relative deviation (1%).

Kuddushi *et al.* (2019) studied the peculiar effect of water on the physicochemical properties of choline chloride-based deep eutectic solvents theoretically and practically at different temperatures T = (293.15-323.15) K. The density and speed of sound were measured to compute the physicochemical properties such as excess molar volume and excess molar isentropic compressibilities. The obtained data revealed negative values for both properties. In terms of deep eutectic solvent composition and temperature, the creation of hydrogen bonds, ion-water and hydrogen bond donor-water interactions were interpreted. Thus, they indicated intermolecular interactions' dominance over intra-molecular interactions. The Redlich-Kister Equation was used to correlate the excess molar volume and excess molar isentropic compressibility data, and satisfactory agreement was found.

Patyar *et al.* (2021) studied experimentally and theoretically the excess molar properties of aqueous choline chloride-based deep eutectic solvents. The list of the studied deep eutectic solvents was as follows: (I) choline chloride/ethylene glycol, (II) choline chloride/glycerol, and

(III) choline chloride/1.4-butenediol, all with a mole ratio of 1:2. The density values of the systems were measured at temperatures T = (293.15-323.15) K and atmospheric pressures. Intermolecular interactions resulted in negative excess molar volume data for all of the studied systems. By comparing the values of excess molar volumes with the Prigogine-Flory-Patterson (PFP) theory and the extended real associated solution model (ERAS), the non-ideal behaviour of the investigated systems was determined. Thus, a good agreement was obtained.

Shekaari *et al.* (2021) reported the measurements of the density and speed of sound data of the deep eutectic solvents (viz., choline chloride + ethylene glycol and choline chloride + glycerol) solutions as the innovative class of solvents at temperatures ranging from T = (288.15-318.15) K. The obtained density and speed of sound data were used to compute thermophysical properties such as apparent molar volume and isentropic compressibility. Furthermore, the obtained thermophysical properties were positive, indicating strong intermolecular interaction over intra-molecular interaction. The Redlich-Meyer Equation was used to calculate a number of qualities, including standard partial molar volume and partial molar isentropic compressibility, in order to correlate the apparent molar volume and isentropic compressibility values.

Similarly, Shekaari *et al.* (2020c) reported the density and speed of sound data of the ionic liquid, 1-ethyl-3-methylimidazolium ethyl sulfate [EMIM] [ES] in the deep eutectic solvents, choline chloride/glycerol; choline chloride/ethylene glycol; choline chloride/urea; and choline chloride/oxalic acid, in a dilute state concentration of the ionic liquid at different temperatures, T = (298.15-318.15) K. Based on the obtained density and speed of sound data, the apparent molar isentropic compressibility and apparent molar volume were computed. The solute-solvent interactions between the ionic liquid and the deep eutectic solvent are stronger for choline chloride/urea systems than for the other deep eutectic solvents investigated, according to the findings. The Pitzer model was also used to correlate the apparent molar volume and molar isentropic compressibility values, and the data showed good agreement.

Sethi *et al.* (2021) reported volumetric and compressibility studies on aqueous mixtures of deep eutectic solvents based on choline chloride and carboxylic acids at different temperatures using experimental, theoretical, and computational approaches. The density and speed of sound of binary systems of deep eutectic solvents (choline chloride/acetic acid and choline chloride/L-(+)-lactic acid, with a mole ratio of 1:2, respectively) with water were measured over the entire composition range at various temperatures, T = (298.15-313.15) K and air pressures. The thermodynamic parameters were derived and used to discuss intermolecular interactions taking place in the systems. The negative excess molar volume data revealed is attributed to strong hydrogen bonds,

charge transfer, and molecular packing in the binary systems over repulsive interaction. The Prigogine-Flory-Patterson (PFP) theory, which satisfactorily explains the volumetric behaviour of binary mixtures, was used to correlate the excess molar volume values. Furthermore, the isentropic compressibility and change in isentropic compressibility values were positive and negative, respectively, and this is the intermolecular interaction agreement over intra-molecular interactions.

While, Abri *et al.* (2019) studied the spectral and thermophysical properties of certain innovative deep eutectic solvents based on *l*-menthol, as well as their mixtures with ethanol. The list of the studied deep eutectic solvents was as follows: (I) *l*-menthol: salicylic acid, (II) *l*-menthol: (1S)-(+)-camphor-10-sulfonic acid, and (III) *l*-menthol: ethylene glycol. Density and speed of sound measurements were made at T (288.15-308.15) K and air pressures for all the binary systems with ethanol. From the obtained data, the excess molar volume, variation in isentropic compressibility, and speed of sound variation were computed at all the experimental temperatures. The obtained values fitted the Redlich-Kister equation well. Thus, excess molar volumes and variation in isentropic compressibilities were observed to decrease as the temperature was increased and both parameters gave negative values. This indicated strong hydrogen bonds, charge transfer, and molecular packing in the binary systems over repulsive interaction.

Shekaari *et al.* (2020b) investigated the density, speed of sound, viscosity, and refractive index of choline chloride/urea (1:2) in aqueous solutions in the dilute region of deep eutectic solvent concentration were determined at different temperatures T = (298.15-323.15) K and atmospheric pressures. The apparent molar volume, excess molar volume, isentropic compressibility, viscosity, and molar refraction were all calculated using these data. The measured excess molar volume values were negative, and they decreased as the concentration of the examined deep eutectic solvent decreased. These results show that hydrogen bonding between solute (DES) and water molecules is so strong that the mixtures' expansibility is larger than that of pure solvents. The isentropic compressibility values of deep eutectic solvent (choline chloride/urea) (1:2) in aqueous mixtures confirm strong solute (DES) and solvent (water) interaction because of high dipole-dipole interactions and strong hydrogen bondings. The attractive nature of interactions among the molecules of deep eutectic solvent and water can be seen in the negative values of isentropic compressibility.

Nowosielski *et al.* (2022) investigated the properties of novel deep eutectic solvents (DESs) prepared from tetrabutylammonium chloride and 3-amino-1-propanol or tetrabutylammonium bromide and 3-amino-1-propanol or 2-(methylamino) ethanol or 2-(butylamino)ethanol in aqueous solutions. The density, speed of sound, viscosity, and refractive index values of aqueous mixtures

of deep eutectic solvents were measured at T = (293.15-313.15) K over a wide variety of compositions. The Redlich-Kister Equation was used to correlate and connect key physicochemical features, such as excess molar volumes, variation in viscosity, excess isentropic compressibility, and variation in refractive index values with temperature-dependent factors. Excess molar volumes and excess compressibilities were negative over the full range of composition and temperature, although deviations in viscosity and refractive index were positive, showing strong intermolecular interactions among different molecules. The Prigogine-Flory-Patterson theory was used to evaluate the non-ideal behaviour of the studied systems, and the results were interpreted in terms of interactions between the mixture components. The calculated negative values of the excess partial molar volumes of deep eutectic solvents and water revealed sufficient solvent-solute interactions that are stronger than the solvent-solvent or solute-solute interactions, which will most likely aid in the efficient utilization of deep eutectic solvents.

Qualitative results of all the cited studies in the literature are summarised in Table 2-5 for excess molar volume data and 2-6 for isentropic compressibility data.

Table 2-5: Qualitative excess molar volume data of the deep eutectic solvents with common solvents from the literature

Authorship	*Systems*	*Excess molar volume*
(Haghbakhsh and Raeissi, 2018c)	[reline (DES) + ethanol]	Negative (-)
(Haghbakhsh and Raeissi, 2018a)	[ethaline (DES) + methanol]	Negative (-)
(Moghimi and Roosta, 2019)	[(choline chloride + glucose) + water]	Negative (-)
(Kuddushi *et al.*, 2019)	[(choline chloride + malonic acid) + water] [(choline chloride + glutaric acid) + water]	Negative (-) Negative (-)
(Patyar *et al.*, 2021)	[ethaline (DES)+ water] [glyceline (DES) + water] [(choline chloride + 1.4-butenediol) + water]	Negative (-) Negative (-) Negative (-)

(Sethi *et al.*, 2021)	[choline chloride + acetic acid) + water]	Negative (-)
	[(choline chloride + L-(+)-lactic acid) + water]	Negative (-)
(Abri *et al.*, 2019)	[(*l*-menthol + salicylic acid) + ethanol]	Negative (-)
	[(*l*-menthol + (1S) - (+)-camphor-10-sulfonic acid) + ethanol]	Negative (-)
	[(*l*-menthol + ethylene glycol) + ethanol]	Negative (-)
(Shekaari *et al.*, 2020b)	[reline (DES) + water]	Negative (-)
(Haghbakhsh and Raeissi, 2018b)	[ethaline (DES) + water]	Negative (-)
	[ethaline (DES) + DMSO]	Negative (-)
	[reline (DES) + water]	Negative (-)
	[reline (DES) + methanol]	Negative (-)
	[reline (DES) + ethanol]	Negative (-)
	[glycine (DES) + water]	Negative (-)
	[glycine (DES) + methanol]	Negative (-)
	[glycine (DES) + ethanol]	Negative (-)
	[glycine (DES) + isopropanol]	Negative (-)
	[maline (DES) + water]	Negative (-)
	[tegaline (DES) + water]	Negative (-)
	[glucoline (DES) + water]	Negative (-)
(Nowosielski *et al.*, 2022)	[(tetrabutylammonium chloride + 3-amino-1-propanol) + water]	Negative (-)
	[(tetrabutylammonium bromide + 3-amino-1-propanol) + water]	Negative (-)

	[tetrabutylammonium bromide + 2-(methylamino)ethanol) + water] [(tetrabutylammonium bromide: 2-(butylamino)ethanol) + water]	Negative (-) Negative (-)

Table 2-6: Qualitative isentropic compressibility data of the deep eutectic solvents with common solvents from the literature

Authorship	*Systems*	*Isentropic compressibility*
(Shekaari *et al.*, 2020c)	[ethaline (DES) + 1-ethyl-3-methylimidazolium ethyl sulfate] [reline (DES) + 1-ethyl-3-methylimidazolium ethyl sulfate]	Positive (+) Positive (+)
(Karpinska *et al.*, 2017)	[ethaline (DES) + ethanol] [glycine (DES) + ethanol	Positive (+) Positive (+)
Sethi *et al.* (2021)	[choline chloride + acetic acid) + water] [(choline chloride + L-(+)-lactic acid) + water]	Positive (+) Positive (+)
(Abri *et al.*, 2019)	[(*l*-menthol + salicylic acid) + ethanol] [(*l*-menthol + (1S)-(+)-camphor-10-sulfonic acid) + ethanol] [(*l*-menthol + ethylene glycol) + ethanol]	Positive (+) Positive (+) Positive (+)

2.7.2 Infinite Dilution Activity Coefficients and Excess Thermodynamic Properties of Deep Eutectic Solvents

Verevkin *et al.* (2015) studied the separation potential of bio-renewable deep eutectic solvents, choline chloride + glycerol, at mole ratios of 1:1 and 1:2. They measured the infinite dilution activity coefficients (IDACs) of 23 organic solutes, including aromatic and aliphatic hydrocarbons, alcohols, ketones, esters, and ethers, in a deep eutectic solvent as a future extracting solvent. The infinite dilution activity coefficient measurements were carried out using gas-liquid chromatography (GLC) coupled to a thermal conductivity detector (TCD) at a temperature range of T = (298-258) K. For the first time, the perturbed-chain statistical associating fluid theory (PC-SAFT) was used to verify the separation performance of deep eutectic solvents. This approach appears to be a useful tool for identifying acceptable precursors and assessing separation performance at temperatures that are relevant to practical applications. Moreover, the separation performance of deep eutectic solvents has been found to be comparable to that of ionic liquids. However deep eutectic solvents are less expensive and less harmful to the environment.

Nkosi *et al.* (2018c) studied tetramethylammonium chloride + glycerol (1:2), deep eutectic solvent as an extraction agent for 24 different organic solutes using gas-liquid chromatography. They determined infinite dilution activity coefficient data of alk-1-anes, alk-1-enes, alk-1-ynes, alkylbenzenes, cycloalkanes, alkanols, ketones, esters, and heterocyclics, at four different temperatures T = (313.15-343.15) K and atmospheric pressures. The obtained infinite dilution activity coefficients were extremely high for every investigated solute except for methanol and pyridine. Higher infinite dilution activity coefficient values are an indication of lower miscibility and weaker interaction between the deep eutectic solvent and selected solutes. The partial molar excess enthalpy values were computed from the experimental infinite dilution activity coefficient data. The obtained partial molar excess enthalpy values were negative for all the investigated functional groups apart from alcohols, aromatics, and ketones. Negative values were an indication of solute-solvent interaction, while positive values indicated solute-solute and/or solvent-solvent interaction. Furthermore, the negative partial molar excess enthalpy values were an indication of endothermic heat mixing between the investigated deep eutectic solvent and the solutes in the separation. Again, from the infinite dilution activity coefficient data, the selectivity and capacity values of 4 most common different separation problems, including methanol/benzene, hexane/benzene, cyclohexane/benzene, n-hexane/hex-1-ene, n-heptane/cyclohexane, acetone/ethanol, and n-heptane/toluene, were computed. Both parameters revealed poor performance, as according to the literature a good selectivity or capacity should be greater than

unity. It was suggested that this could be possibly due to the selected mole ratio, effect of the hydrogen bond donor, or the effect of temperature.

Sandip and Singh (2022) also determined the activity coefficients of 22 different organic solutes in the deep eutectic solvent, tetramethylammonium chloride + 1.6 hexanediol in a mole ratio of 1:1 at infinite dilution. The studied solutes included alkanes, alkynes, cycloalkanes, alcohols, aromatics, ketones, esters, and heterocyclics. At T = (313.15–343.15) K and p = 101.3 kPa, the infinite dilution activity coefficients (IDACs) were determined using gas-liquid chromatography with a thermal conductivity detector. The intermolecular interactions between the packed solvent (DES) and the selected solutes were discussed using the observed IDACs. The partial molar characteristics, such as enthalpy, entropy, Gibbs free energy values, selectivity, and capacity values, were also estimated using the infinite dilution activity coefficients to obtain further insight into the happening interactions. Solutes such as methyl acetate, pyridine, and thiophene were found to have the strongest solvent-solute interactions. Furthermore, based on selectivity and capacity parameters, the examined deep eutectic solvent showed good separation performance for mixtures containing alkanes and thiophene or pyridine. As a result, the researchers found that DES (tetramethylammonium chloride + 1.6-hexanediol in a 1:1 molar ratio) is an effective approach for denitrogenation and desulfurization of transportation fuels.

Furthermore, Nkosi *et al.* (2018a) investigated the infinite dilution activity coefficients of 23 different organic solutes in a deep eutectic solvent of tetrapropylammonium bromide + 1,6-hexanediol (1:2 mole ratio). Alkanes, alkynes, cycloalkanes, alcohols, aromatics, ketones, esters, and heterocyclics were among the functional groups investigated. At temperatures of T = (313.15-343.15) K and atmospheric pressures, they employed gas-liquid chromatography (GLC). The partial molar excess enthalpy values were calculated using the Gibbs-Helmholtz equation over the temperature range given above, using infinite dilution activity coefficients. In addition, the infinite dilution activity coefficients were utilized to calculate selectivity and capacity values, which were then compared to previous literature for a better understanding of molecular interactions. For mixtures containing alkanes and thiophene or pyridine, as well as alcohols and cycloalkanes, aromatics, or ketones, the investigated deep eutectic solvent with a ratio of 1:2 for hydrogen bond acceptor and hydrogen bond donor respectively, was found to be an effective separating agent.

Moreover, Nkosi *et al.* (2018b) employed gas-liquid chromatography to determine the infinite dilution activity coefficients for 19 various organic solutes in deep eutectic solvents of tetramethylammonium chloride + ethylene glycol at four different temperatures ranging from T = (313.15-343.15) K and atmospheric pressures. Alkanes, alkynes, cycloalkanes, alcohols,

aromatics, ketones, esters, and heterocyclics were among the functional groups investigated. From the investigated solute's infinite dilution activity coefficients, the partial molar excess enthalpy values were derived using the Gibbs-Helmholtz equation. Furthermore, the selectivity and capacity values for all the investigated solutes were computed from the measured infinite dilution activity coefficients. According to the findings, the examined deep eutectic solvent could be used as an alternate solvent for several industrial separation problems, including alkanes, thiophene, alkanes-pyridine, ketones-alcohols, aromatics-alcohols, and cycloalkanes-alcohol systems.

Kabane and Redhi (2020) reported on the excess thermodynamic properties and infinite dilution activity factors of 33 distinct organic solutes in a deep eutectic solvent: glycerol + 1-butyl-3-methylimidazolium chloride. Alkanes, alkenes, alkynes, cycloalkanes, cycloalkenes, alcohols, aromatics, ketones, and water were among the groups investigated. Gas-liquid chromatography coupled to a thermal conductivity detector (TCD) operated at different temperatures (313.15-343.15) K and ambient pressures was used. The infinite dilution activity coefficients obtained were extremely high (>1), making them suitable for the extraction of the selected solutes. Furthermore, the partial molar excess properties such as Gibbs free energy, enthalpy, and entropy, as well as separation parameters, selectivity, and capacity values of separation problems (hexane/benzene; cyclohexane/ethanol; cyclohexane/benzene; and acetone/ethanol), were determined from the measured infinite dilution activity coefficients. The separation parameters revealed the deep eutectic solvent's limited performance as a separation solvent, as the capacity is low, but the high selectivity values are useful. Nevertheless, the authors stated that factors, such as the ratio of hydrogen bond acceptor-hydrogen bond donor and extraction temperature, might influence the deep eutectic solvent selection in the extraction process, affecting the yield.

Recently, Mgxadeni *et al.* (2022) studied the infinite dilution activity coefficients influence of hydrogen bond donors on zinc chloride in binary mixture separation. They employed gas-liquid chromatography to determine the infinite dilution activity coefficients of 34 different organic solutes, including alkanes, alkenes, alcohols, ketones, cycloalkanes, cycloalkenes, aromatics, heterocyclics, thiophene, acetonitrile, tetrahydrofuran, and water in two different deep eutectic solvents ([zinc chloride + acetic acid] (1:4) and [zinc chloride + phosphoric acid] (1:2.5)) at various temperatures T = (313.15-353.15) K and ambient pressures. The obtained values of the infinite dilution activity coefficient were extremely high, showing low solubility and weak intermolecular interactions for both studied deep eutectic solvents. The partial molar properties, i.e., Gibbs free energy, enthalpy, and entropy, were determined from the measured infinite dilution activity coefficient data. The obtained partial excess molar enthalpy revealed mixed values, with positive

for some solutes, mostly nonpolar solutes, and mostly negative values for polar solutes. This suggests solvent-solute interactions for polar solutes and solute-solute and/or solvent-solvent interactions for nonpolar solutes. However, positive Gibbs free energy values were observed for most solutes except for alcohols, water, and acetonitrile. Positive Gibbs free energy data is an indication of poor immiscibility between the selected solutes and the investigated deep eutectic solvent. On the other hand, the obtained entropy values were negative except for alcohols, water, and THF. It appears as if the solute molecules arrange themselves in the center of the solvent for deep eutectic solvents. Moreover, the selectivity and capacity values of different separation problems, including cyclohexane/ethanol, benzene/ethanol, n-octane/acetonitrile, n-heptane/butan-1-ol, and ethylbenzene/butan-1-ol, were also computed from the infinite dilution activity coefficients. These provided a high degree of separation potential, especially the [zinc chloride + phosphoric acid] (1:2.5), deep eutectic solvent.

Li *et al.* (2022) inspected the thermodynamic parameters and infinite dilution activity coefficients for 32 different organic solutes in a deep eutectic solvent: choline chloride + 1,5-pentanediol. Alkanes, alkenes, cycloalkanes, cycloalkenes, alcohols, aromatics, ketones, ethers, esters, monocyclic, heterocyclis, alkyl halides, and water, were among the functional groups investigated. Inverse-gas chromatography was used for the prediction of infinite dilution activity coefficient data at different temperatures T = (303.15-343.15) K. The obtained infinite dilution activity coefficient data revealed higher values for all the solutes, indicating low solubility and weak intermolecular interactions for the studied deep eutectic solvent. The partial molar properties, including Gibbs free energy, entropy, and enthalpy, were computed from the obtained infinite dilution activity coefficient data. Computed partial molar excess enthalpies attributed positive values, suggesting solute-solute and/or solvent-solvent interactions presiding over solvent-solute interaction. Positive entropy values on the other side demonstrates that the dissolution of solutes in the deep eutectic solvent is an entropy-increasing process. The Gibbs free energy takes into account the changes in enthalpy and entropy that occur during the dissolving process, as well as the interactions between the solutes and the deep eutectic solvent. The separation potential of separation problems, benzene/methanol; benzene/thiophene; and n-hexane/benzene was evaluated using selectivity and capacity parameters. The findings revealed that the investigated deep eutectic solvent is effective at separating the benzene/methanol system.

Wang *et al.* (2022) studied the infinite dilution activity coefficients as well as the other thermodynamic properties for 31 different organic solutes in a deep eutectic solvent, choline chloride + oxalic acid (1:1 mole ratio). Alkanes, alkenes, alcohols, aromatics, ketones, esters,

monocyclic, and alkyl halides were among the functional groups investigated. Inverse gas chromatography (IGC) operated at T = (303.15-343.15) K was used for the determination of infinite dilution activity coefficient data. The investigated deep eutectic solvent demonstrated good miscibility with alcohols and acetonitrile. The separation parameters, i.e., selectivity and capacity values of the separation problems (cyclohexane/ethanol; acetone/ethanol; benzene/methanol; n-heptane/thiophene; and tetrachloromethane/methanol) for the investigated deep eutectic solvent were computed from the infinite dilution activity coefficient data. The selectivity and capacity measurements obtained indicated that the deep eutectic solvent is an excellent tetrachloromethane/methanol and acetone/ethanol separation agent.

Mbatha *et al.* (2022) investigated the measurements of the infinite dilution activity coefficient for 1-Methyl-4-(1-methylethenyl)-cyclohexene as a green separation solvent. Solutes from a variety of functional groups were investigated, including the following functional groups: alkanes, alkenes, alkynes, cycloalkanes, aromatics, alcohols, ketones, ethers, nitrile, heterocycles, and water. For infinite dilution activity coefficients prediction, gas-liquid chromatography at temperatures T = (303.15–323.15) K was used. The obtained infinite dilution activity coefficient data gave higher values, indicating low miscibility and weak intermolecular interaction. Furthermore, the partial molar properties, i.e., enthalpy, entropy, and Gibbs free energy, as well as the separation potential parameters, i.e., selectivity and capacity values, were computed from the measured infinite dilution activity coefficient data. Like the activity coefficient, all these properties reveal that the investigated solvent is not suitable for the separation of the selected solutes.

CHAPTER THREE

THEORETICAL FOUNDATION

Overview

The equations and concepts utilized to account for the thermophysical, and thermodynamic properties are detailed in this section. This chapter covers parameter descriptions, derivation processes, and any other developments in equations linked to thermophysical and thermodynamic properties. The parameters and constants used in this study were derived from previous scientific research.

3.1 Thermophysical Properties

When looking for suitable solvents for certain purposes or modifying certain characteristic physicochemical properties that would improve material functions in industrial applications, understanding the thermophysical properties of liquid mixtures is critical (Dohrn and Pfohl, 2002; Bahadur and Deenadayalu, 2013; Oke *et al.*, 2020). As a result, these properties can be utilized to evaluate the intermolecular interactions that occur in a liquid mixture.

3.1.1 Excess Molar Volume

Background

The excess molar volume (V_m^E) is an extremely sensitive property for ascertaining mutual interactions amongst the component molecules of a binary system (Lavanya *et al.*, 2013; Bagheri *et al.*, 2021). It is given by eq. (3-1) below:

$$V_m^E = V_{mixture} - \sum x_i V_i \tag{3-1}$$

Both $V_{mixture}$ and V_i denote molar volumes for pure species, and x_i denotes the mole fraction for the species.

As a result, when two chemicals are mixed as shown in eq. (3-2) below, a volume change occurs:

$$V_m^E = V_{mixture} - (x_1 V_1^0 + x_2 V_1^0) \tag{3-2}$$

Subscripts 1 and 2 are used to indicate the liquid components of the binary mixture (Kgagodi, 2017).

- The analysis of component 1-1 and 2-2 molecular interactions has a positive influence on the volume.
- The occurrence of the 1-2 molecular interactions results in a decrease in the volume of the mixture.
- The effect of packing caused differences in the shape and size of the component species, as they will have a beneficial or negative impact on the species involved.
- Formation of new chemical species.

The behaviour of binary mixtures under constant temperature and pressure is a critical property in thermodynamics. As a result, this feature investigates the deviations that occur in an ideal system, as non-ideality systems might order the application and volume of liquid mixtures. Thus, these mixtures excess molar volume can be calculated through equation (3-3) below.

$$V_M^E = \left(\frac{x_1M_1+x_2M_2}{\rho_{mixture}}\right) - \left(\frac{x_1M_1}{\rho_1} + \frac{x_2M_2}{\rho_2}\right) \quad (3\text{-}3)$$

where M is the molar mass of components 1 and 2, ρ is the density of components 1 and 2 as well as the mixture.

3.1.2 Experimental Determination of Excess Molar Volume

The excess molar volume of binary systems can be determined by direct and indirect methods (Redhi, 2003):

- Direct technique (dilatometric): In this technique, the volume change of mixed liquids is assumed.
- Indirect technique (densitometer): The mixture's density and the density of a pure component liquid are both measured.

3.1.2.1 Direct Technique

When non-similar component liquids are mixed, the volume change is measured using this technique. The continuous dilution dilatometer and the batch dilatometer are two methods for direct measurements of V_m^E (Handa and Benson, 1979). The continuous dilution dilatometer has many configurations for each load at different temperatures, whereas the batch dilatometer only has one configuration for each load at each temperature (Redhi, 2003). Nonetheless, as

documented in studies by Wood and Brusie (1943); Washington and Battino (1968); Wirth and LoSurdo (1968), dilatometry techniques have improved and evolved in many ways in recent years.

Continuous dilution dilatometer

Continuous dilution dilatometer is a more common technique than batch dilatometer because it uses less time as well as generates more data for each load (Bottomley and Scott, 1974). The most prominent continuous dilatometer was developed by Bottomley and Scott (1974). This innovation was later improved by Kumaran and McGlashan (1977). The application procedure comprises the introduction of a liquid into a reservoir that contains another liquid so as to perceive the volume change that occurs in a component solution. Hence, the excess molar volume is obtained from the change in volume and the pressure change observed upon the mixing of component liquids.

The continuous dilution dilatometer is shown schematically in Figure 3-1. In the diagram, the burette (e) is used to measure the volume change caused by an introduced liquid, while the bulb (d) is used to measure the volume change caused by the other liquid. Some components of the mercury in the burette in the capillary (c) change positions during mixing, and an added liquid is transmitted from the burette to the bulb across the upper capillary (b). A calibrated capillary (a) filled with mercury shows a change in level (a) after mixing, which is interpreted as a change in volume.

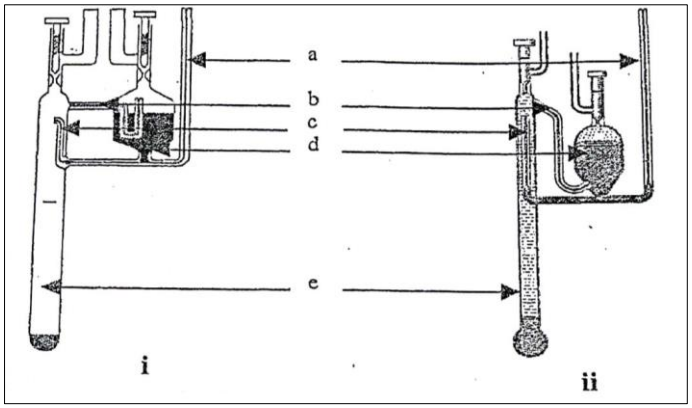

Figure 3-1: Illustration of continuous dilution dilatometer by Bottomley and Scott (1974); Kumaran and McGlashan (1977).

Batch Dilatometer

Figure 3-2 depicts the batch dilatometer device. Mercury is used to help separate the components in a dilatometer in order to identify the exact amount of pure component liquid that is injected into the dilatometer. The height of the mercury in the calibrated capillary column (before and after mixing of liquids) aids in determining the quantity of component liquids. Furthermore, a

dilatometer rotator is used to mix the component liquids, and the volume change is exhibited in a calibrated capillary column. As a result, the V_m^E values are estimated using the volume change and the masses of the constituent liquids. The precision of this technique, according to Prausnitz *et al.* (1998) is approximately 0.003 $cm^3.mol^{-1}$ at a standard temperature ranging between 280 and 350 K. The drawback of this method is that it is difficult to fill the dilatometer accurately because it is generally filled with a small needle, which frequently results in an incorrect reading. The nature of the components causes this inaccuracy, as it is hard to correctly measure the dilatometer because it includes mercury. As a result, the mass measured will be inaccurate. Furthermore, it is commonly recognized that the error associated with calculating the difference between enormous masses is typically quite substantial (Redhi, 2003).

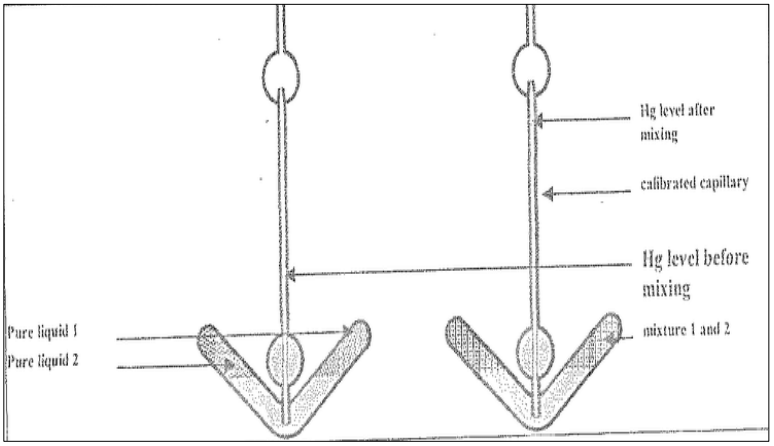

Figure 3-2: A distinctive dilatometer for measurements of volume of mixing (Sibiya, 2009).

3.1.2.2 Indirect Technique

This technique is more accurate than other density measurement techniques for measuring the developed dilatometer (Wood and Brusie, 1943). The pycnometer, the densitometer, and the magnetic float densitometer method are among the methods used to determine the densities of liquids.

Pycnometer

Pycnometers come in a variety of shapes and sizes, as well as distinct handling methods developed by different researchers (Wood and Brusie, 1943; Scatchard *et al.*, 1946; Bauer and Lewin, 1959). The pycnometer is a precision instrument for measuring liquid density. Wood and Brusie (1943) invented a single-arm pycnometer with a high accuracy of one in a hundred thousand, as shown in Figure 3-3. This method employs an 11 cm^3 capacity, a 1mm internal diameter precision capillary,

and 11 lines softly etched around the stems as well as 1 mm away. A hypodermic syringe and cannula are used to load the pycnometer in this manner. In order to determine density, it is critical to determine the composition of mixtures with great precision.

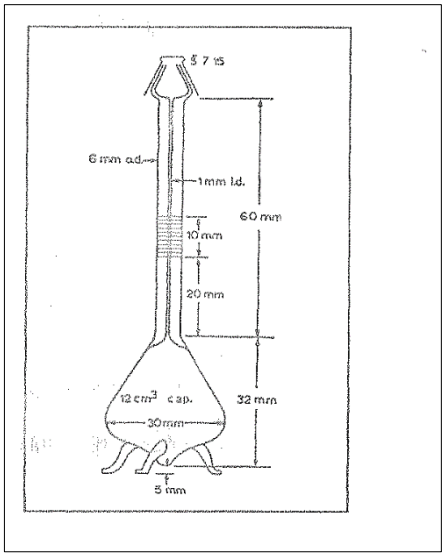

Figure 3-3: A single arm pycnometer by Wood and Brusie (1943)

Mechanical oscillating densitometer

The mechanical oscillating densitometer, also known as a vibrating tube densimeter (Handa and Benson 1979), is connected to digital output displays and is generally employed in the chemical industry and research institutions for the determination of the densities of various pure liquids as well as liquid mixtures. The vibration frequency of the tube carrying a pure liquid or liquid mixture is exposed to constant electric stimulation, which is associated with the density of a liquid. Handa and Benson (1979) reported that the vibration frequency (v) of an undammed tube carrying a liquid connected using a spring with constant elasticity is associated with the composition of the vibrating tube and carried liquid. Eq. 3-4 gives a short description of the above statement.

$$2\pi v = \left[{}^{c}/_{M}\right]^{\frac{1}{2}} \tag{3-4}$$

Where *c* denotes the constant elasticity, M is the composition of the contents in the oscillator and can be calculated using eq. 3-5 below.

$$M = M_o + \rho V \tag{3-5}$$

Thus, M_o is the composition of the unfilled oscillator, ρ is the density of the liquid, and V is the volume of the oscillator.

Hence, substituting for M into (3-4) and solving for density, ρ yields:

$$\rho = -\,{}^{M_o}/_{V} + \left({}^{c}/_{4\pi^2 V}\right)\left({}^{1}/_{v^2}\right) \tag{3-6}$$

Eq. (3-6) could be written as follows:

$$\rho = A + B\left({}^{1}/_{v}\right)^2 \tag{3-7}$$

Since, $C = \left({}^{1}/_{v}\right)$, $A = -\,{}^{M_0}/_{V}$ and $B = \left({}^{c}/_{4\pi^2 V}\right)$

Where constants A and B represent characteristics of the oscillator, and v represents the volume.

Thus, A and B constants can be extracted from the linear calibration. Eq. 3-8 is used to obtain the B constant since the densities are estimated in relation to reference material.

$$\rho - \rho_o = B(\tau - \tau_0^2) \tag{3-8}$$

Where ρ_o represents the density of the reference material (e.g., deionised water) and τ_o is the corresponding period oscillation.

Many of the vibrating tube densimeters can estimate up to 1x 10^{-5} g.cm^{-3}. This suggests a precision of about 0.003 cm^3.mol^{-1} for excess molar volume measurements (Singh, 2017).

Magnetic float densimeter

The magnetic float densimeter is a simple and versatile technique used to estimate the densities of liquids as a function of temperature (Millero Jr, 1967; Blanco and Vargas, 2004). The first magnetic float densimeter was reported by Lamb and Lee (1913). A few decades later, Franks and Smith (1967) modified the original version of the magnetic float densimeter. In this technique, a pyrex cell of 600 cm^3 capacity is attached to a thermostat bath that is constructed of non-magnetic materials. This instrument has a density precision of 3x 10^{-6}g.cm^{-3}. Hence, this results in a point of precision of 0.0008 cm^3.mol^{-1} $V_{m.}^{E}$ The magnetic float densimeter diagram is shown below.

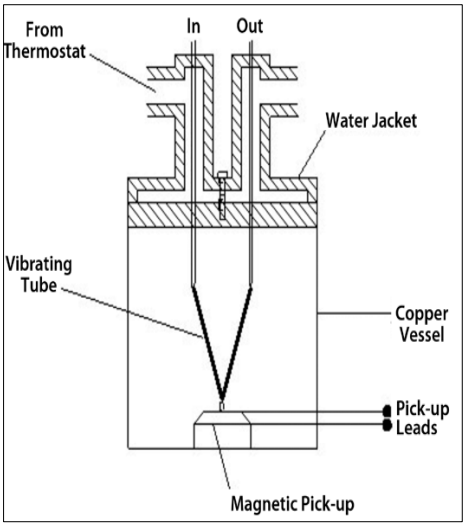

Figure 3-4: Design of Franks and Smith (1967), magnetic float densimeter

In this work, the density and sound velocity of mixtures were measured at different temperatures using an Anton Paar DSA 5000 M instrument.

A sample's density is defined as the mass (m) divided by the volume (v):

$$\rho = {}^{m}/_{v} \tag{3-9}$$

Excess molar volume is calculated using density.

3.1.3. The Newton Laplace Equation

The Newton-Laplace Equation is used to determine the isentropic compressibility (K_s) values of solutions and liquid mixtures. An important thermodynamic quantity has been identified as the isentropic compressibility for a system of defined composition at a fixed temperature and pressure. The readily and precisely measured set of densities, together with the sound velocity (at low frequency), are related by Equation (3-10), the Newton Laplace Equation, in most descriptions of experiments yielding the isentropic properties of solutions and liquid mixtures (Pal *et al.*, 2010; Alvarez *et al.*, 2011; Pal and Kumar, 2011).

$$K_s = (u^2\rho) \tag{3-10}$$

Equation (3-10) is used to calculate the variation in isentropic compressibility (ΔK_s) values of liquid mixture from the ideal value.

$$\Delta K_s = K_s - \sum k_{s,i}^0 \emptyset_i \quad (3\text{-}11)$$

and

$$\emptyset_i = \frac{x_i v_i^0}{\sum x_i v_i^0} \quad (3\text{-}12)$$

where $\emptyset_i$ and x_i denote the volume fraction and mole fraction of (i) in the mixture, expressed in terms of the unmixed components, respectively. $k_{s,i}^0$ and $\emptyset_i$ denote the isentropic compressibility and molar volume for pure component (i), respectively.

In addition, equation (3-13) has been used to compute intermolecular free length (L_f), as shown below.

$$L_f = K_j (K_s)^{\frac{1}{2}} \quad (3\text{-}13)$$

The temperature-dependent Jacobson's constant (K_j) has a value of (93.88 + 0.38 T)10^{-8}.

3.1.4 The Correlation Between Derived Properties

Redlich-Kister Equation

The thermophysical data of the analysed binary systems were derived and fitted to the Redlich-Kister equation (3-14), at fixed temperatures of T = (293.15, 298.15, 303.15, 308.15, and 313.15) K and an atmospheric pressure (Arumugam *et al.*, 2020):

$$Z = x_1 x_2 \sum_{i=1}^{k} A_i (1 - 2x_1)^{i-1} \quad (3\text{-}14)$$

V_m^E and ΔK_s are represented by x. The values of the fitting parameters were determined using the least-square method (A_i). Moreover, the corresponding standard deviations were determined by the following equation (3-15).

$$\sigma = \sum_{i=1}^{n} \left[\frac{W_{exp} - W_{calc}}{(N-K)}\right]^{1/2} \quad (3\text{-}15)$$

W_{exp} and W_{calc} are experimental values, N is the number of experimental points, and K indicates the probability of coefficients in the Redlich-Kister equation.

3.2 Excess Thermodynamic Properties

3.2.1 Activity Coefficients

Background

The activity coefficient (γ_i) is a thermodynamic factor used to quantify the non-ideality of solutes in organic mixtures (Krummen *et al.*, 2002). It details the deviations that take place in an ideal system in a mixture of chemical components. The mathematical equation (3-16) that defines interactions is shown below.

$$\gamma_i = \frac{f_i}{x_i f_i^0} \tag{3-16}$$

The γ_i symbol in equation (3-16) denotes the activity coefficient of the species i, whilst f_i denotes the fugacity of a component i in a mixture, f_i^0denotes the fugacity of the pure component i, and x_i denotes the mole fraction of the component i in a solution.

Now the activity (a_i) is defined by the eq. (3-17) below:

$$a_i = \frac{f_i}{f_i^0} \tag{3-17}$$

and for an ideal solution, $\gamma_i = 1$

Hence, the activity coefficient can be defined as the activity of a material divided by its mole fraction as seen in eq. (3-18):

$$\gamma_i = \frac{a_i}{x_i} \tag{3-18}$$

and can be expressed in monomial form as seen in eq. (3-19) below:

$$a_i = \gamma_i \, x_i \tag{3-19}$$

3.2.2 Infinite Dilution Activity Coefficient (IDAC)

The infinite dilution activity coefficient (γ_i^∞) is a significant thermodynamic property that is used to perform crucial experiments in various fields of study, including chemistry, chemical engineering, physics, and environmental sciences. Scientists (Landau *et al.*, 1991; Seader *et al.*, 1998b) refer to this term as the limiting value of a solute activity coefficient when its concentration goes to zero. Infinite dilution is used to study the properties of a solution. It can be well-defined as a hypothetical state where only solute-solvent interactions occur. In this state, the concentration

of a solution cannot be altered by adding more liquid to the solution (Debenedetti and Kumar, 1986a; Debenedetti and Kumar, 1986b).

Muhlbauer (1997) detailed a few reasons why the infinite dilution region of a solution fascinates chemical separation experts. These include:

- High purity products are obtained for system behavior in the extremely dilute state, which remains instrumental.
- In a highly diluted state, there are more deviations.
- It is very expensive and more challenging to remove the remaining traces of impurities in a separation process.

3.2.3 Gas Liquid Chromatography

Gas liquid chromatography (GLC) is a highly preferred technique by numerous chemical industries (Harrison *et al.*, 1994; Karpińska *et al.*, 2018; Paiva and Hantao, 2020). This technique is most used to investigate high boiling solvents, including deep eutectic solvents, ionic liquids, and other new innovative solvents. It is always assumed that as the solute flows in and out of the column:

- The gas phase consists of an ideal mixture of carrier and solute.
- The stationary phase consists of a real liquid mixture of solvent and solute.

Letcher (1980) described in detail how to determine infinite dilution activity coefficients (IDACs) using gas liquid chromatography (GLC). James and Martin (1952) established this technique for the study of volatile compounds, which is now being utilized to account for IDACs. Porter *et al.* (1956) used the GLC method to invastigate the relationship between retention volume and partitioning coefficients at infinite dilutions of solutes in a solvent.

Conder and Young (1979) offered eq. (3-20) to account for the partition coefficient, K_L of the solutes among two phases.

$$K_L = \frac{C_L}{C_M} \tag{3-20}$$

where C_L and C_M denote concentration of a solute in a liquid and gas phases, respectively. The equations are given below:

$$C_L = \frac{x\, n_3}{V_L} \tag{3-21}$$

and $$C_M = \frac{y\, n_2}{V_G} \tag{3-22}$$

where V_L and V_G donate the volume of the liquid phase and vapour phase respectively, x and y donate mole fractions of solutes in a liquid and gas phases, n_3 represents the number of moles of a solvent in a liquid phase, and n_2 represents the number of moles of a carrier gas in the vapour phase.

Equation (3-23) was founded from eq. (3-20) by means of substitution for C_L and C_M.

$$K_L = \frac{x n_3\, V_G}{y n_2\, V_L} \tag{3-23}$$

Gas phase volume (V_G) was attained from ideal eq. (3-24).

$$V_G = \frac{n_2\, RT}{P} \tag{3-24}$$

Eq. (3-25) was simplified from eq. (3-23) using the modified or revised Raoult's law.

$$K_L = \frac{n_3\, RT}{\gamma_{13}^{\infty}\ P_1^*\, V_L} \tag{3-25}$$

and the revised Raoult's law is given below:

$$yP = x\, P_1^* \gamma_{13}^{\infty} \tag{3-26}$$

where P denotes solute pressure, and the saturated vapour pressure is donated by P_1^*.

For more knowledge of thermodynamic properties, Laub and Pecsok (1978) advised that eq. (3-27) below, can be used to attain the distribution coefficient, K_L at low pressures in the column. This relates the net retention volume, V_N to volume of the stationary phase (V_L) and partition coefficient (K_L).

$$V_N = K_L\, V_L \tag{3-27}$$

After the expression of eq. (3-25), Porter *et al.* (1956) proposed the eq. (3-28) below.

$$\gamma_{13}^{\infty} = \frac{n_3\, RT}{K_L V_L P_1^*} \tag{3-28}$$

This expression can be written in terms of the V_N in following form:

$$\gamma_{13}^{\infty} = \frac{n_3\, RT}{V_N\, P_1^*} \tag{3-29}$$

In an advancement of the method's accuracy and precision (Everett, 1965; Cruickshank *et al.*, 1966a, 1966b) modified eq. (3-29) to establish the derived equation which can be employed to determine the solute-solute and solute-carrier gas imperfections and also account for the pressure drop within the column. The derived eq. (3-30) below was then established (Letcher, 1980).

$$\ln \gamma_{13}^{\infty} = \ln\left(\frac{\mathrm{n_3\ RT}}{\mathrm{V_N\ P_1^*}}\right) - \left(\frac{\mathrm{P_1^*(B_{11} - V_1^*)}}{\mathrm{RT}}\right) + \left(\frac{\mathrm{P_o J_2^3 (2B_{12} - V_1^{\infty})}}{\mathrm{RT}}\right) \tag{3-30}$$

where $\ln\gamma_{13}^{\infty}$ represents the IDAC of a solute in a solvent, n_3 is the number of moles of a solvent, R is the ideal gas constant, T is the temperature of a column, P_i represents inlet pressure as displayed by the instrument, P_o represents column outlet pressure, which is the same as atmospheric pressure, while P_1^* represents the saturated vapour pressure of a solute at a temperature (T), $P_o J_2^3$which signifies the mean column pressure, $J_2^3$is the pressure correction term, V_1^{∞}represents the infinite dilution partial molar volume of a solute, which is equivalent to V_1^*(molar volume of a solute) in this case.

In this work, the saturated vapour pressure (P_1^*) was calculated through the employment of Antione Equations (Poling *et al.*, 2001a). The pressure correction term, J_2^3as revised by Everett (1965), can be determined by eq. (3-31) below:

$$J_2^3 = \left(\frac{\left(\frac{P_i}{P_o}\right)^3 - 1}{\left(\frac{P_i}{P_o}\right)^2 - 1}\right)\left(\frac{2}{3}\right) \tag{3-31}$$

The V_N was obtained from eq. (3-32) below:

$$V_N = (J_2^3)^{-1}(U_o)\ (t_R - t_G) \tag{3-32}$$

where U_o represents the corrected column outlet flow rate, t_R represents the retention time of the solute, and t_G represents the air peak (inert gas).

Eq. (3-33) specifies the corrected column outlet volumetric flow rate from the burette bubble flow meter:

$$U_o = U\left(1 - \left(\frac{P_W}{P_o}\right)\right)\left(\frac{T_f}{T}\right) \tag{3-33}$$

where the volumetric flow rate of the estimated carrier gas by the bubble flow meter at the column outlet is represented by U, P_w represents the vapour pressure of water, and T_f represents the temperature of the flow meter. The vapour pressure of water employed in the calculations was provided by Everett and Powl (1976) and was determined by means of Antione Equations (Poling *et al.*, 2001a).

3.2.4 Determination of Virial Coefficients

McGlashan and Potter (1962) proposed the equation (3-34) to determine the second virial coefficients of the pure solutes (B_{11}):

$$\frac{B}{V_C} = 0.43 - 0.886\left(\frac{T_C}{T}\right) - 0.694\left(\frac{T_C}{T}\right)^2 - 0.0375\left(\frac{T_C}{T}\right)^{4.5}(n-1) \quad (3\text{-}34)$$

The critical properties, T_c and V_c used in the calculations of the second virial coefficients of the solutes were extracted from a study by Poling *et al.* (2001a). Regardless of this fact, McGlashan and Potter (1962) equation is appropriate for the selected nonpolar solutes such as alkanes, alkenes, alkynes, and aromatics (Bruce *et al.*, 2001). A similar equation can be employed for the determination of mixed virial coefficients (B_{12}). Furthermore, Hudson and McCoubrey (1960); Addouni *et al.* (2020) also detailed the method of determining the other mixed properties. Mixing rules are detailed as follows, eq. (3-35) below:

$$T_{c12} = 128\,[\,T_{c11}.T_{c12}]^{1/2}\,.\,[\,I_{c11}.I_{c22}]^{1/2}\,.\left[\frac{[\,V_{c11}.V_{c22}]}{I_{c12}}\right] \quad (3\text{-}35)$$

where I_{c12} can be calculated by eq. (3-36) below:

$$I_{c12} = [\,I_{c11}.I_{c22}]\left[\,(V_{c11})^{1/3} + (V_{c22})^{1/3}\right]^6 \quad (3\text{-}36)$$

and V_{c12} can be calculated as follows, eq. (3-37):

$$V_{c12} = \left[\frac{1}{8}\right]\left[(V_{11})^{1/3} + (V_{c22})^{1/3}\right]^3 \quad (3\text{-}37)$$

and

$$n_{12} = \frac{n_1+n_2}{2} \quad (3\text{-}38)$$

Subscripts 1, 2, and 12 represent the solute, carrier gas, and the component mixtures, respectively. Critical ionization energy, $I_c$was borrowed from the literature (Lide, 2004). The modified *Rackett*

equation was used to calculate the saturated molar volumes, eq. (3-39) below, and is also provided in the literature by Poling *et al.* (2001a).

$$V_1^* = V_c\,[0{,}29056 - 0{,}08775\omega]\left[1 - \frac{T}{T_c}\right]^{2/7} \tag{3-39}$$

The acentric factor, ω of the organic solutes in the equation above was also provided in the literature by Poling *et al.* (2001a). In addition, the V_1^* values were assumed to be equivalent to V_1^∞values of the organic solutes for the purposes of the calculations (Letcher and Whitehead, 1997).

Nevertheless, it is not easy to determine the actual second virial coefficients from experimental data. As a result, Tsonopoulos *et al.* (1989) suggested eq. (3-40) below, to determine the second viral coefficient. Furthermore, this equation was recommended as the most reliable correlation method that could be employed for the determination of the second viral coefficient (Poling *et al.*, 2001a).

$$\frac{B_{virial}P_c}{RT_c} = f^{(0)}(T_r) + \omega f^{(1)}(T_r) + a_t f^{(2)}(T_r) + b_t f^{(3)}(T_r) \tag{3-40}$$

where $f^{(0)}(T_r)$ is given by eq. (3-41) below:

$$f^{(0)}(T_r) = 0.1445 - \frac{0.330}{T_r} - \frac{0.1385}{T_r^2} - \frac{0.0121}{T_r^3} - \frac{0.000607}{T_r^8} \tag{3-41}$$

the $f^{(1)}(T_r)$

$$f^{(1)}(T_r) = 0.0637 - \frac{0.331}{T_r^2} - \frac{0.423}{T_r^3} - \frac{0.008}{T_r^8} \tag{3-42}$$

the $f^{(2)}(T_r)$

$$f^{(2)}(T_r) = \frac{1}{T_r^6} \tag{3-43}$$

and $f^{(3)}(T_r)$

$$f^{(3)}(T_r) = -\frac{1}{T_r^8} \tag{3-44}$$

where f_i is the fugacity of the pure component (i) {kPa}, $\widehat{f_i}$ is the fugacity of the component (i) in a solution (kPa), f^0 is the correlation term of the Tsonopolus, f^1 is the correlation term of the Tsonopolus, f^2 is the correlation term of the Tsonopolus, and f^3 denotes correlation term of Tsonopolus.

Poling *et al.* (2001a) employed these correlations to estimate the experimental second viral coefficients of the untainted components together with the mixtures of polar and nonpolar combinations using the critical properties of the components at a specified temparature. These correlations can apply to certain classes of compounds such as water, ketones, and alcohols which produce hydrogen bonds (Tsonopoulos *et al.*, 1989). In contrast, Smith *et al.* (2001) modified Tsonopolous equation to develop eq. (3-45) below, for non-polar compounds such as aromatics, alkanes, alkenes, and alkynes.

$$\frac{B_{virial}P_c}{RT_c} = f^{(0)}(T_r) + \omega f^{(1)} \tag{3-45}$$

The equation above can be re-arranged to attain eq. (3-46) below:

$$B_{ij} = B^0 + \omega_i B^1 = \left[0{,}083 - \frac{0{,}422}{T_r^{16}}\right] + \omega_i \left[0{,}139 - \frac{0{,}172}{T_r^{4.2}}\right] \tag{3-47}$$

However, Poling *et al.* (2001a) reported that the second viral coefficients modified equation has some restrictions (only true once $T_r > 0{,}6$ and $\omega < 0{,}4$).

The equation developed by Tsonopoulos *et al.* (1989) for polar the compounds to account for the second viral coefficients, including the mixed second viral coefficient (through T_c, P_c, a_t, b_t and ω) is given below:

The critical properties were determined in terms of eq. (3-48, 49, and 50) as:

$$T_{c_{12}} = \sqrt{(1 - k_{12})(T_c)_1(T_c)_2} \tag{3-48}$$

$$P_{c_{12}} = 4\, T_{c_{12}} \left[\frac{\left(\left(\frac{P_c V_c}{T_c}\right)_1 + \left(\frac{P_c V_c}{T_c}\right)_2\right)}{\left(V_c^{1/3}\right)_1 + \left(V_c^{1/3}\right)_2}\right] \tag{3-49}$$

and

$$\omega_{12} = \frac{\omega_1 + \omega_2}{2} \tag{3-50}$$

The k_{12} parameter represents the empirical binary interactions and its value can be attained by means of the procedures provided by Tarakad and Danner (1977).

For polar compounds, a_t and b_t eq. (3-51) and (3-52) given as:

$$a_{t_{12}} = \frac{a_{t_1} + a_{t_2}}{2} \quad (3\text{-}51)$$

and

$$b_{t_{12}} = \frac{b_{t_1} + b_{t_2}}{2} \quad (3\text{-}52)$$

The subscripts 1, 2, and 12 designate the solute, carrier gar, and mixture or binary mixture, respectively.

The determination of infinite dilution activity coefficients can assist in the development of green procedures for the selection of a desirable solvent for a precise separation process. The infinite dilution activity coefficients also enable the determination of other thermodynamic properties, such as enthalpy, entropy, and Gibbs free energy, as well as selectivity and capacity values. These properties are all significant for the inexpensive design of separation equipment. Sandler (1996) reported the practical and theoretical application of infinite dilution activity coefficients in various fields, including chemistry, physics, and chemical engineering.

3.2.5 Infinite Dilution Activity Coefficients: Theoretical and Practical Applications

The applications of IDACs were further detailed by various scientific researchers as follows:

- development and optimization of extraction procedures (Seader *et al.*, 1998b),
- characterization of liquid mixture performance (Seader *et al.*, 1998b),
- prediction of the existence of azeotropes (Seader *et al.*, 1998b),
- determination of Henry's law constants (Halder, 2014),
- determination of limiting partial molar excess properties (Smith, 1950).

The following section gives brief details on the theoretical and practical applications of IDACs.

3.2.5.1 Development and optimization of extraction procedures

The separation of chemical compounds is extremely challenging in a lot of industrial processes (Vishtal and Kraslawski, 2011; Cai *et al.*, 2012; Adewole *et al.*, 2013). This is caused by non-sensitive separation procedures that are currently utilized for extractive distillation in the production of chemical products. The new chemical industry legislation and regulations demand high-purity products with reasonable prices and minimal environmental risks. Thus, the experimental IDAC is a great tool that can be employed in the pre-screening of desirable solvents for separation problems (Sandler, 1996).

Furthermore, the infinite dilution activity coefficient values of the separated solutes can be employed to determine the selectivity, S_{ij}^{∞} and capacities, k_j^{∞} of the desirable solvent for the separation process. These two variables are specifically adopted for extractive distillation and liquid-liquid extraction for the separation problems of azeotropes with closely related boiling points mixtures. Eq. (3-53) and (3-54) are given below:

$$S_{ij}^{\infty} = \frac{\gamma_i^{\infty}}{\gamma_j^{\infty}} \tag{3-53}$$

Thus,

$$k_j^{\infty} = \frac{1}{\gamma_j^{\infty}} \tag{3-54}$$

S_{ij}^{∞} and k_j^{∞} denote the limiting values of selectivity and capacity for a solvent mixture at infinite dilution in a composition containing component i and j, respectively. The γ_i^{∞} and γ_j^{∞} denote the values of the IDACs of the i and j are components in a mixture. Moreover, subscripts, i and j were taken from Seader *et al.* (1998b).

3.2.5.2 Characterization of the performance for liquid mixture

Data on infinite dilution activity coefficients provides critical information about the molecular interactions between solutes and solvents in a mixture at infinite dilution (McMillan Jr and Mayer, 1945; Doyle, 2005). High infinite dilution activity coefficient values will result in weaker solute-solvent molecular interactions, thus lowering the solubility observed in a solution (Cheong, 2003). An ideal solution will result when an IDAC value becomes unity ($\gamma_i^{\infty} = 1$). Hence, the infinite

dilution activity coefficient value of a non-ideal solution at infinite dilution can be either lower or higher than unity.

3.2.5.3 Prediction of the existence of azeotropes

Azeotropes are binary mixtures with boiling points that are closely related (Li *et al.*, 2020; Su *et al.*, 2020; Manyoni and Redhi, 2022). This makes it difficult to predict their existence in a separation process. IDAC's data can be used to predict the circumstances where an azeotrope binary mixture occurs (Seader *et al.*, 1998b). When a mixture displays positive (+) deviation from Raoult's law, an azoetropic mixture holding a minimum temperature and maximum pressure is formed. The relationship between the positive and negative deviations is displayed in eq. (3-55) and (3-56) below.

$$\ln \gamma_j^{\infty} < \ln \left[\frac{P_i^{sat}}{P_j^{sat}}\right] < -\ln \gamma_i^{\infty} \tag{3-55}$$

A negative (-) deviation in Raoult's law means an azeotropic mixture holding a pressure minimum and temperature maximum is formed.

$$\ln \gamma_j^{\infty} > \ln \left[\frac{P_i^{sat}}{P_j^{sat}}\right] > -\ln \gamma_i^{\infty} \tag{3-56}$$

Thus, $\gamma_i^{\infty}$and γ_j^{∞}both denote the activity coefficient at infinite dilution of species (i) and (j), and $P_i^{sat}$and P_j^{sat}denote saturated vapor pressures for species (i) and (j), respectively.

Moreover, the prediction of IDACs can assist in reducing industrial separation costs and helping to develop environmentally friendly separation processes.

3.2.5.4 Determination of Henry's law constants

The infinite dilution activity coefficients are used in the characterization of partitioning coefficients, K for organic compounds. Hence, IDAC's shares some relationship with Henry's law constant, as given in eq. (3-57) below.

$$\gamma_s^{\infty} = \frac{H_i}{P_i^*} \tag{3-57}$$

This equation can be written in monomial form as eq. (3-58) to make Henry's constant the subject.

$$H_i = \gamma_s^{\infty} P_i^* \tag{3-58}$$

The H_i denotes Henry's law constant for the component (i) in a mixture, and P_i^*denotes vapour pressure of the component (i) at a temperature suitable for the IDAC. As shown by eq. (3-58) above, Henry's constant can be calculated from the value of IDAC. Moreover, separation of the gases involves the application of Henry's law constant.

3.2.5.5 Determination of excess partial molar properties

The values of an infinite dilution activity coefficient (IDAC) is required for the determination of excess partial molar properties, i.e., enthalpies, entropies, and Gibbs free energies, which are also useful for separation purpose (Manyoni *et al.*, 2022; Manyoni and Redhi, 2022). The relationship between the excess properties can be expressed in a combination of equations for $G^E$and S^E.

Defined as eq. (3-59), $$H^E = G^E + TS^E \tag{3-59}$$

Knowing that $S^E$is given by eq. (3-60) below.

$$S^E = -\left(\frac{\partial G^E}{\partial T}\right)_{P,x} \tag{3-60}$$

Gibbs free energy is a part of the functions giving directions for the determination of all other properties through simple mathematical procedures (elementary algebra and differentiation) and indirectly, property information. Hence, substituting and differentiating equations. (3-59) and (3-60) result in the Gibbs-Helmholtz Equation (3-61), which expresses the effect of temperature on the activity coefficient.

$$\left[\frac{\partial\left(\frac{G^E}{RT}\right)}{\partial T}\right]_{x,P} = -\left[\frac{H^E}{RT^2}\right] \tag{3-61}$$

Since eq. (3-62)

$$G^E = RT\ln\gamma_i \tag{3-62}$$

Therefore, eq. (3-61) and (3-62) can be substituted to give Gibbs-Denham Equation (3-63) which can be utilized for the relation of the enthalpy and activity coefficient.

$$\left[\frac{\partial \ln\gamma_i}{\partial T}\right]_{P,x} = -\left[\frac{H_i^E}{RT^2}\right] \tag{3-63}$$

Thus,

$$\left[\frac{\partial \ln\gamma_i^{\infty}}{\partial\left(\frac{1}{T}\right)}\right]_{P,x} = -\left[\frac{\Delta H_i^{E,\infty}}{R}\right] \tag{2-64}$$

whereby: $\Delta H_1^{E,\infty}$ denotes the partial molar enthalpy at infinite dilution

: R denotes ideal gas constant value

: T denotes experimental temperature

The partial excess molar enthalpy $\left(\Delta H_i^{E,\infty}\right)$ can be calculated through the straight line derived from eq. (3-64), as eq. (3-65) below:

$$\text{Slope} = -\left[\frac{\Delta H_i^{E,\infty}}{R}\right] \tag{3-65}$$

The eq. (3-66) below was used to fit the experimental infinite dilution activity coefficient data of the selected organic solutes.

$$\ln \gamma_i = A + \left(\frac{B}{T}\right) \tag{3-66}$$

3.2.6 Experimental Technique for determination of Infinite Dilution Activity Coefficient

Several techniques have been designed for the experimental measurements of the infinite dilution activity coefficient, counting the following:

- Inert Gas Stripping Technique (IGS) (Lerol *et al.*, 1977),
- Head Space Chromatography Technique (HSC) (Hussam and Carr, 1985),
- Differential Ebulliometry Method (DEM) (Gautreaux Jr and Coates, 1955),
- Differential Static Cell Technique (DSC) (Pividal *et al.*, 1992)
- Dew Point Method, (DPM) (Suleiman and Eckert, 1994),
- Rayleigh Distillation Method (RDM) (Dohnal and Horáková, 1991)
- Gas Liquid Chromatography (GLC) (Letcher, 1980).

Each of the techniques listed above is intended to certify specific conditions. However, due to a lack of specificity in the data, some of these techniques have been ruled out. This overview provides a brief history of the aforesaid techniques as well as their applications as preferred methods for IDAC prediction.

3.2.6.1 Inert Gas Stripping Technique

The technique was introduced by Fowlis and Scott (1963) for the vapor dilution systems of detector calibration. Lerol *et al.* (1977) advanced this method for fast and accurate determination of the infinite dilution activity coefficients of a volatile solute in a liquid mixture. The inert gas stripping (IGS) technique is alternatively known as the dilutor technique or continuous gas extraction technique (Dobryakov and Vitenberg, 2006).

The experimental procedure of the method is detailed below.

A very diluted solute is stripped from a liquid mixture under constant temperature conditions by the application of a constant inert gas flow. Gas chromatography is used from time to time to analyze the vapor departure from the cell. The peak area of a solute in the vapor phase goes down using units of time in minutes. Furthermore, the infinite dilution activity coefficient of a selected solute through the extracting solvent is compared with the decrease of the resultant peak area as time goes by.

In addition, the inert gas stripping method is suitable for the measurements of both volatile and non-volatile solvents as well as the systems of solvent mixtures. The advantages and limitations are provided in Table 3-1 below:

Table 3-1: Limitations and advantages of inert gas stripping technique

Advantages	Limitations
It has the ability to examine numerous solutes at the same time.	Gas-liquid contact must be good in order to achieve accurate and reliable results.
It works with systems containing highly volatile solvents.	Purification of solutes is required.
GC detector must be calibrated before vapour analysis.	When measuring low volatile solvents, there are numerous challenges.
Apparatus is legitimately direct or straightforward	

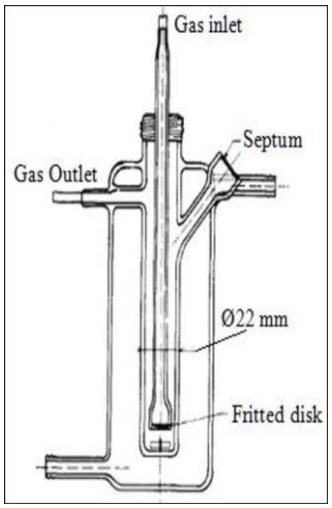

Figure 3-5: Dilutor flask (Lerol *et al.*, 1977)

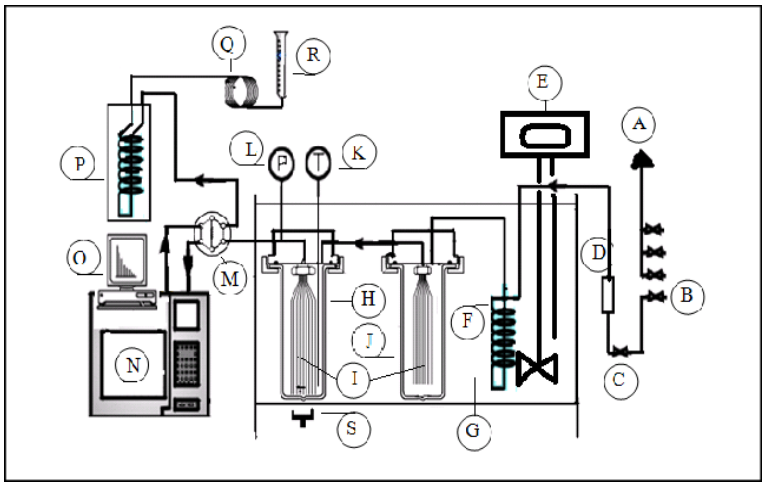

Figure 3-6: IGS schematic diagram

A-Helium, B-Nitrogen line, C-valve, D-Flow meter, E-Immersion temperature control, F-Coiled tube, G-Transparent acrylic bath, H-Dilutor cell, I-Capillaries, J-Pre-saturation cell, K-Platinum resistance thermometer, L-Pressure transducer, M-Sampling valve, N-GC equipment, O-PC monitor, P-Cold trap, Q-Cold tube, R-Soap bubble flowmeter, and S-Magnetic stirrer.

3.2.6.2 Differential ebuliometry method

The differential ebuliometry method (DEM) is well known as the most reliable method for mixtures that contain embroiled water. This method was championed by (Gautreaux Jr and Coates, 1955) to derive equations to obtain the IDACs of binary systems in fixed conditions such as isobaric temperature and isothermal pressure. The derived equations were thermodynamically sound, and the application proved to be good for extrapolation of experimental results.

In addition, Loos and Weir (2005) have highlighted some of the advantages and some of the limitations involved with this method.

Table 3-2: Advantages and limitations of the differential ebuliometry method (DEM)

Advantages	Limitations
It can analyze multiple solutes at once,	Produces inaccurate results for binary mixtures of high boiling temperature variety.
It possesses the ability to measure the systems where solutes and solvents have the same volatility.	Operator must possess much experience in order to get accurate and reliable results.
	Time consuming

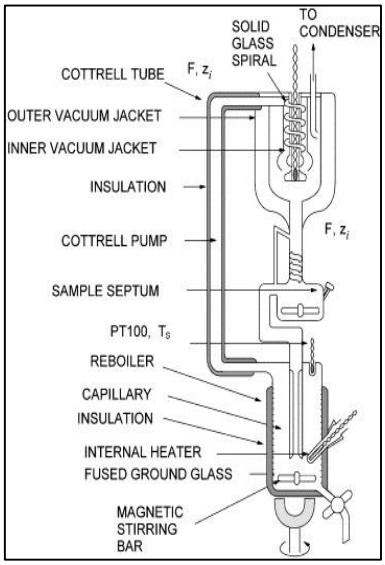

Figure 3-7: DEM schematic diagram

CHAPTER FOUR

EXPERIMENTAL WORK

4.1 Experimental

Instruments, viz., density and sound velocity meter (Anton Paar DSA 5000 M) with an oscillating U-tube and a gas-liquid chromatography (Shimadzu GC-2014) coupled with a thermal conductivity detector (TCD), were used in the present study. The materials used, the experimental setup, and the experimental procedure are detailed in this chapter. For both the density and sound velocity meter as well as the gas-liquid chromatography (GLC) measurements, the experimental procedure was validated by comparing measured values with the previously published data.

4.2 Density and Sound Velocity Measuring Apparatus

4.2.1 Density and Sound Velocity Meter (Anton Paar DSA 5000 M)

The density (ρ) and sound velocity (u) were measured by the use of the DSA 5000 M with an oscillating U-tube. A DSA 5000 M simultaneously measures two autonomous physical properties, i.e., density and sound velocity, using one sample. To combine the oscillating U-tube technology with a precise device for sound velocity quantification, this instrument employs a density cell and a sound velocity cell. The temperature of the two cells is controlled by a built-in Peltier thermostat, and the Peltier thermostat temperature with uncertainty of 0.01 K.

To compute the excess molar volumes (V_m^E), binary mixtures are determined from density measurements by exploitation of the expression below.

$$V_m^E = \frac{x_1M_1+x_2M_2}{\rho} - \frac{x_1M_1}{\rho_1} - \frac{x_2M_2}{\rho_2} \quad (4\text{-}1)$$

Accordingly, $\rho_1$and ρ_2 denote density values, $x_1$and x_2 are mole fractions, and $M_1$and M_2 are molar masses for each component 1 and 2, respectively (Negadi *et al.*, 2017; Dubey and Dhingra, 2021). And density is dependent on temperature.

4.2.2 Oscillating U-tube

An oscillation-type density meter works on the principle of harmonic oscillation, in which the sample to be analysed is packed into a U-tube and exposed to an electromagnetic field. The frequency and period of the tube's vibrations are measured, and the density value of the sample can be determined if it is packed with the sample. Moreover, the fundamental frequency of the U-tube is a function of the system mass (Furtado *et al.*, 2016). This approach provides extremely precise density readings.

4.2.3 Sound Velocity Analyser

The device is equipped with a stainless-steel cell and uses the pulse-echo method, which entails the transmission of a short ultrasound pulse across the middle of the sample. At a frequency of around 3 MHz, the sound velocity is measured. This technique allows for exceedingly exact density measurements. When an impediment is encountered, a portion of the pulse is reflected, and the remaining portion is transmitted (Prak *et al.*, 2017).

As a result, the device records track of the time between the pulse's emission and echo's reception, converting it into a distance (Cunha *et al.*, 2013). Hence, the density is calculated using the quotient of the U-tube and reference oscillator's oscillation time:

$$\rho = KA\ x\ Q^2\ x\ f_1 - KB\ x\ f_2 \tag{4-2}$$

KA, KB denote the apparatus constants, Q denotes the quotient of the U-tube's oscillation time divided by the reference oscillator's oscillation time, whereas f_1, f_2 are correction terms for temperature and non-linearity.

The acquired density value is displayed on the LCD screen. The Anton Paar DSA 5000 M is linked to a computer which has a software that stores all the measured density. A display of Anton Paar DSA 5000 M is given in Figure 4-2.

Figure 4-1: Photograph of Anton Paar DSA 5000 M Densitometer (taken from Anton Paar guideline book)

The sample is placed in the sound velocity measuring cell, which has an ultrasonic transmitter on one side and a sound velocity receiver on the other. The sound velocity is determined by the time and distance travelled by sound waves in the entrance receiver and transmitter. The sound velocity is determined using Equation (4-3).

$$u = \left[\frac{\left(l \, \mathrm{x} \left({}^{1}/_{(1\mathrm{x}10^{-1})\mathrm{x}\,\Delta T} \right) \right)}{\left({}^{P_S}/_{512} \right) - A \, \mathrm{x} \, f_3} \right] \tag{4-3}$$

In this equation, ΔT denotes the temperature deviation, l denotes the path length travelled by sound waves, P_s denotes the oscillation interval of the received sound waves, A is a constant sound velocity, and f_3 denotes temperature correction term. The frequency for the measurements is made at 3 MHz. In addition, both density and sound velocity are temperature dependent.

The Anton Paar DSA 5000 M's advantages include high density measuring precision and accuracy. It has the world's most cutting-edge digital density and sound velocity measurement equipment. The following is a list of the main features of the Anton Paar DSA 5000 M:

- Optical pickups are used to measure the U-oscillation tube's period.
- A thermobalance is a main oscillator that provides long-term stability and allows exact measurements across the instrument's entire temperature range with only one adjustment at T = 293.15 K.
- When samples with high viscosity and high density are utilized, special changes to standards of high viscosity and high-density lead to increased precision.
- The Peltier elements, in combination with two inbuilt Pt 100 platinum thermometers, allow a highly precise thermosetting of the sample.

Gas bubbles in the measuring cells are a common source of measurement mistakes when using a density and sound velocity meter. Anton Paar has added two additional features to reduce the development of gas bubbles:

- U-View

The U-tube can be visually inspected for gas bubbles in the density measuring cell using a real-time camera with zoom capabilities.

- Filling Check

By analysing the oscillation pattern of the density measuring cell, the equipment detects gas bubbles in the cell and sends a warning message.

Given in Table 4-1 are the specifications of Anton Paar DSA 5000 M.

Table 4-1: Specifications of Anton Paar DSA 5000 M

Parameters	Range
Sound velocity range measurements	(1000 to 2000) ms^{-1}
Density range measurements	(0 to 3) $g.cm^{-3}$
Sound velocity repeatability	0.1 m s^{-1}
Density repeatability	1 x 10^{-6} $g.cm^{-3}$
Temperature range measurements	(273.15 to 343.15) K
Pressure range measurements	(0 to 3) MPa
Time per sample range measurements	(1 to 4) minutes
Temperature repeatability	273.15 K
Volume of a sample	approximately 3 mL
Reference oscillator	Yes
Automatic bubble detection	Yes
Atmospheric pressure sensor	Yes
Density measuring cell for visual check	Camera

4.3 Materials Used for the Measurements of Thermophysical Properties

Sigma Aldrich (South Africa) provided the hydrogen bond acceptor, 1-ethyl-1-methylpyrrolidinium bromide, with a purity of > 99 percent (Table 4-2). Glycerol and ethylene glycol, the hydrogen bond donors, were provided by Sigma Aldrich and Merck, respectively, and both had purity values of > 99 percent (Table 4-2). Sigma Aldrich (SA) also provided methanol and ethanol, both of which had purity standards of 99.9% and 99.9%, respectively. To keep the hydrogen bond accepter dry, it was stored in molecular sieves. Additionally, the Karl Fischer Auto Titrator was utilized to determine the water content prior to the start of the experiment.

Table 4-2: Ionic liquid (HBA) and organic solvents (HBDs) are used for the preparation of deep eutectic solvents. The supplier, as well as the purity

Chemical Name	Supplier	Purity
1-ethyl-1-methylpyrrolidinium bromide	Sigma Aldrich	≥ 99%
Glycerol	Sigma Aldrich	≥ 99%
Ethylene glycol	Merck	≥ 99%

Table 4-3: The list of alcohols used in the preparation of binary mixtures, their suppliers, as well as their purity

Chemical Name	Supplier	Purity
Methanol	Sigma Aldrich	≥ 99.9%
Ethanol	Sigma Aldrich	≥ 99%

4.4 Preparation of Deep Eutectic Solvents

Deep eutectic solvents were made by precisely measuring distinct mole ratios of the component materials: hydrogen bond acceptors (HBAs) and hydrogen bond donors (HBDs). An OHAUS analytical balance with a precision of 0.0001g was used to weigh the masses of each component material. During the experiment, extra caution was taken to avoid any possible errors or contamination. Figures 4-2 and 4-3 show the preparation of two deep eutectic solvents for the measurement of thermophysical properties for binary systems.

- [1-ethyl-1-methylpyrrolidinium bromide + glycerol], [(EMPYR) Br + Gly] (1:2 mole ratio)
- [1-ethyl-1-methylpyrrolidinium bromide + ethylene glycol], [(EMPYR) Br + EG] (1:4 mole ratio)

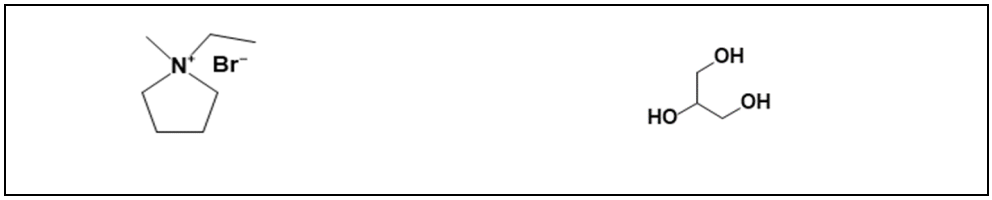

Figure 4-2: [1-ethyl-1-methypyrrolidinium bromide + glycerol], [(EMPYR) Br + Gly]

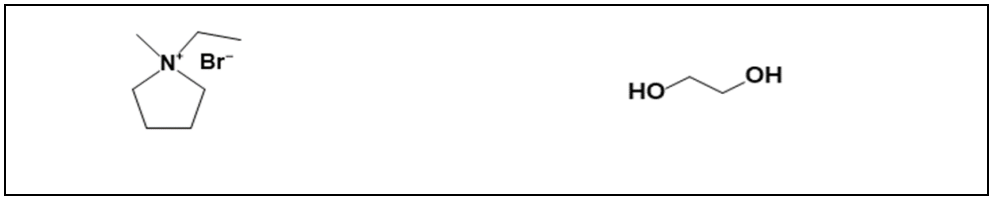

Figure 4-3: [1-ethyl-1-methylpyrrolidinium bromide + ethylene glycol], [(EMPYR) Br + EG]

Table 4-4 shows the experimental densities and sound velocities of the components, which were compared to published data.

Table 4-4: Comparison of component densities and sound velocities; methanol and ethanol, as well as [(EMPYR) Br + Gly] and [(EMPYR) Br + EG] for the current work with literature data.

T/K	ρ (g.cm $^{-3}$)				u (ms^{-1})			
Methanol	Exp	Lit	Ref	σ	Exp	Lit	Ref	σ
293.15	0.793	0.792-0.793	*a,c*	0.006	1126	1119	*d*	7
298.15	0.792	0.787	*c*	0.005	1110	1103	*e*	7
303.15	0.788	0.782-0.783	*a,b,c*	0.005	1094	1088	*d*	8
308.15	0.780	0.777	*c*	0.003	1079	1071	*e*	8
313.15	0.775	0.772-0.774	*a,b,c*	0.002	1065	1055	*d,e*	10
Ethanol	Exp	Lit	Ref	σ	Exp	Lit	Ref	
293.15	0.789	0.790-0.799	*g,h*	0.002	1152	1162	*g*	10
298.15	0.786	0.785-0.786	*f,g,h*	0.001	1135	1145	*g*	10
303.15	0.782	0.781-0.783	*f,g,h*	0.001	1120	1129	*g*	9
308.15	0.777	0.776-0.778	*f,g,h*	0.000	1103	1112	*g*	9
313.15	0.773	0.772-0.774	*f,g,h*	0.000	1087	1096	*g*	9

[(EMPYR) Br + Gly]	Exp	Lit	Ref	σ	Exp	Lit	Ref	σ
293.15	1.264	-	-	-	1917	-	-	-
298.15	1.261	-	-	-	1904	-	-	-
303.15	1.257	-	-	-	1893	-	-	-
308.15	1.254	-	-	-	1881	-	-	-
313.15	1.251	-	-	-	1870	-	-	-
[(EMPYR) Br + EG]	Exp	Lit	Ref	σ	Exp	Lit	Ref	σ
293.15	1.143	-	-	-	1692	-	-	-
298.15	1.139	-	-	-	1681	-	-	-
303.15	1.136	-	-	-	1669	-	-	-
308.15	1.132	-	-	-	1658	-	-	-
313.15	1.129	-	-	-	1646	-	-	-

(Haghbakhsh and Raeissi, 2018a)[a], (Haghbakhsh and Raeissi, 2020)[b], (Gonfa et al., 2015)[c], (Zaoui-Djelloul-Daouadji et al., 2016)[d], (Anwar and Yasmeen, 2016)[e], (Quijada-Maldonado et al., 2013)[f], (Keshapolla et al., 2015)[g], and (Wang et al., 2018b)[h].

It can be concluded to say the literature data presented in this section is in good correspondence with the experimentally determined physical properties, i.e., density and sound velocity.

4.5 Preparation of Binary Systems

The binary systems of the above-mentioned deep eutectic solvents with alcohols, namely methanol and/or ethanol, were prepared using a mole fraction range of x_1= (0-1). An OHAUS analytical balance with a precision of 0.0001g was used to correctly weigh the component masses of the binary systems, just as it was for the preparation of deep eutectic solvents. Furthermore, the binary systems were prepared in airtight vails and shaken to ensure that all of the components were thoroughly mixed. Furthermore, the systems were created immediately prior to the density and sound velocity measurements in the experiment. This was done to prevent the compositions from changing due to solvent evaporation. A list of the investigated binary systems.

- {[1-ethy-1-methylpyrrolidinium bromide + glycerol] (1:2 mole ratio) + methanol/ethanol}, {[(EMPYR) Br + Gly] (1:2 mole ratio) + methanol/ethanol}
- {[1-ethy-1-methylpyrrolidinium bromide + ethylene glycol] (1:4 mole ratio) + methanol/ethanol}, {[(EMPYR) Br + EG] (1:4 mole ratio) + methanol/ethanol}

4.6 Experimental Procedure for Density and Sound Velocity Measurements

A precise amount of each prepared sample system was introduced by an autosampler into an airtight vial. The density and the sound velocity measurements for the systems were investigated using a sound velocity analyser and a digital tube density meter with an accuracy of (0.4-0.5) ms^{-1} for sound velocity and 5×10^{-6} $g.cm^{-3}$ for density. Toluene and acetone were used to clean and dry the cells, respectively. Furthermore, the X sampler 452 was used for cleaning before conducting the experimental analysis. Additionally, the thermostat was used to control and keep the temperature at 0.01K during the density and sound velocity measurements.

The density measurements use the oscillating U-tube to simultaneously measure the sound velocity ranging between (1000-2000) $m.s^{-1}$ and the density ranging between of $0\text{-}3 \times 10^{3}$ $kg.m^{-3}$ at temperatures T = (273.15-343.15) K, pressures (0-0.2) MPa, and the frequency of 3 MHz. The uncertainties for both sound velocity and density were 1 ms^{-1} and 0.002 $g.cm^{-3}$, respectively. From the measured physical properties, i.e., density and sound velocity values, the thermophysical properties, including excess molar volumes (V_m^E), isentropic compressibility (K_s), variation in isentropic compressibility (ΔK_s), and intermolecular free length (L_f) values, were calculated. The calculated properties, i.e., ($V_m^E, k_s,$ and Δk_s) uncertainties, were measured to be 0.005 $cm^3. mol^{-1}$, 2×10^{-7} Pa^{-1}, and 0.7×10^{-7} Pa^{-1}, respectively.

Figure 4-4: Anton Paar DSA 5000 M Densitometer used

4.7 Test System, Thermophysical Properties of [Ethanol + Hexane]

The experimental method was validated by determining the densities, sound velocities, excess molar volumes, and variation in isentropic compressibility for the test system of [ethanol + hexane] at a temperature of 298.15 K and at atmospheric pressure. The results were comparable to the results obtained by (Orge *et al.*, 1997). Table 4-4 as well as Figures 4-3 and 4-4 present the correspondence between the experimental results and the literature data for the densities, sound velocities, excess molar volumes, as well as the variation in isentropic compressibilities. Moreover, the present study adopted the molar fraction from (Orge *et al.*, 1997).

Table 4-5: Experimental and literature results comparison of ρ, u, V_m^E, and ΔK_s for the test system, [Ethanol + Hexane] at 298.15 K.

x_i	ρ/ g.cm^{-3}			$V_m^E.10^9$/ cm^3.mol^{-1}			u/ ms^{-1}			ΔK_s/Pa^{-1}		
	Exp	Lit	σ	Exp	Lit	σ	Exp	Lit	σ	Exp	Lit	σ
0	0.650	0.650	0.000	0	0	0	1082	1077	5	0	0	0
0.057	0.659	0.658	0.001	177	156	21	1078	1071	7	31	28	3
0.150	0.664	0.663	0.001	312	305	7	1068	1069	1	59	56	3
0.273	0.673	0.671	0.002	402	390	12	1067	1068	1	87	83	4
0.439	0.687	0.686	0.001	435	423	12	1071	1070	1	110	106	4
0.598	0.706	0.704	0.002	408	409	1	1078	1077	1	114	112	2
0.724	0.725	0.722	0.003	365	356	9	1086	1087	1	105	102	3
0.828	0.744	0.741	0.003	250	257	7	1104	1101	3	81	79	2
0908	0.760	0.759	0.001	154	143	9	1117	1117	0	52	49	7
0.967	0.777	0.775	0.002	40	43	3	1140	1133	7	21	19	2
1	0.788	0.781	0.007	0	0	0	1151	1141	10	0	0	0

(Orge *et al.*, 1997)

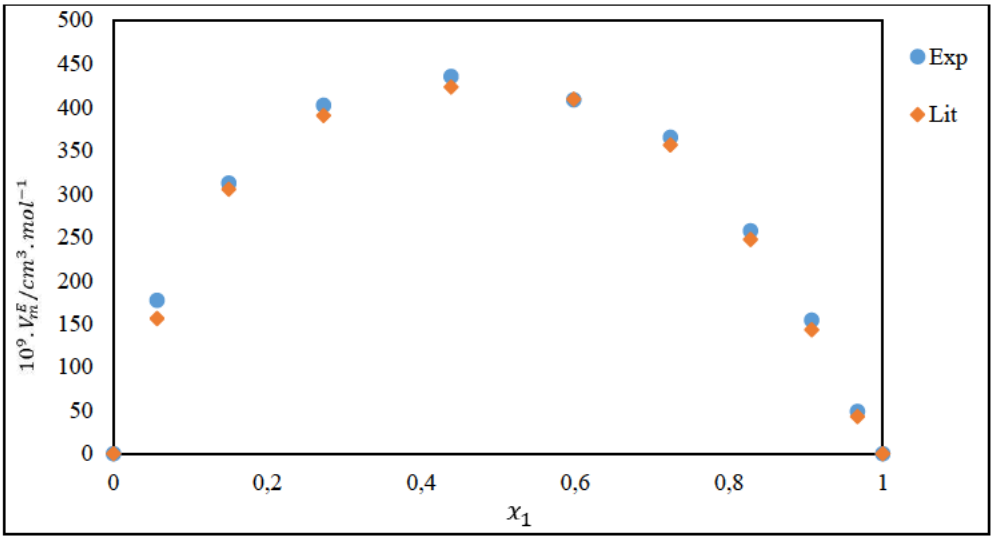

Figure 4-5: Comparison of V_m^E values between the experimental results and literature data of [ethanol (x_1) + hexane (x_2)], test system

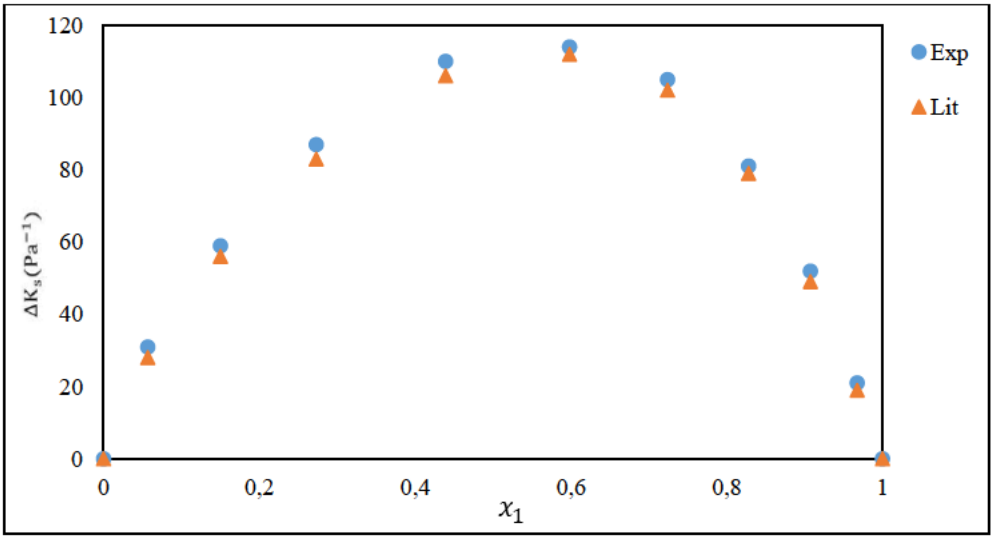

Figure 4-6: Comparison of ΔK_s values between the experimental results and literature data of [ethanol (x_1) + hexane (x_2)], test system

4.8 Approach for Infinite Dilution Activity Coefficient Measurements

4.8.1 Gas Liquid Chromatography (GLC)

Scientific researchers have begun the quest for special methods regarding the determination of infinite dilution activity coefficients (IDACs) (Wilson and Deal, 1962; Seader *et al.*, 1998a). Gas liquid chromatography (GLC) has become the most preferred of all techniques for the determination of IDACs. In this technique, the deep eutectic solvent is used as the stationary phase coated with a solid support material, W HP, 80-100 mesh particle size before being packed into the stainless-steel column. A volatile solute (mobile phase) is injected through a septum into a chromatographic stainless-steel column using a microlitre syringe. A thermal conductivity detector (TCD) uses helium as a carrier gas to drive a solute from one end of the packed column to the other, and the solute is detected at a peak (response) retention time by the thermal conductivity detector (TCD). The infinite dilution activity coefficients (γ_{13}^{∞}) are then computed using the retention times, and these are exploited for intermolecular interpretation of the injected solute.

To produce accurate and repeatable results, it's critical to choose the right method. When the following parameters are taken into account, this GLC technique is accurate and reliable (Guiochon and Guillemin, 1988):

- A solute must be in a liquid phase form.
- It is necessary for a solute to be volatile.
- Solute vapour pressure must be negligible at certain experimental temperatures to avoid evaporation in a column.
- Carrier gas should be insoluble in a solute.

In addition, Table 4-6 lists the benefits and limitations of gas liquid chromatography (Adlercreutz, 1971; Guiochon and Guillemin, 1988).

Table 4-6: List of benefits and limitations of the GLC technique

Benefits	Limitations
A very small amount of a solvent and the solute (μL) is needed for measurements.	Only low-volatility solvents are suited for this method.
Several solutes can be injected at the same time.	The IDAC of a solute cannot be determined straight away (thermodynamic application required)
Solutes should not be of a high purity	Only reaches up to certain experimental temperatures
It considers reactive systems	No adsorption effects

Figure 4-7 is a gas liquid chromatography schematic diagram used in the present study.

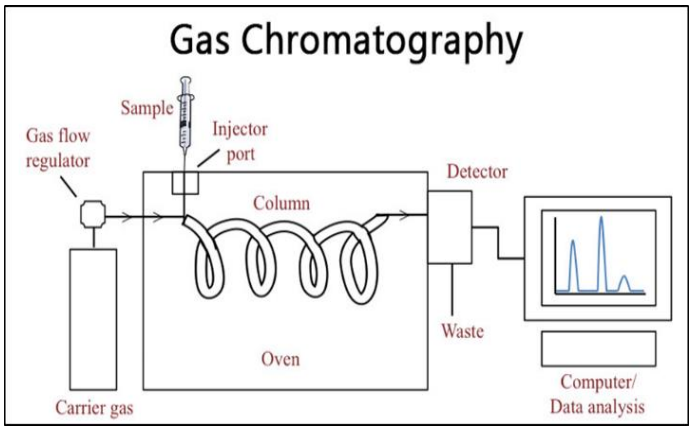

Figure 4-7: Gas liquid chromatography schematic diagram

Thermal Conductivity Detector

Because it is sensitive to the concentrations of chemicals in the mixture rather than the entire mass of a sample, the thermal conductivity detector (TCD) is ideal for miniaturization (Sun *et al.*, 2011).

A filament in the thermal conductivity detector (TCD) is heated electrically to make it hotter than the detector body. While alternate streams of reference gas and column outflow pass over the filament, the temperature is kept constant. The power required to keep the filament temperature constant changes when the sample is injected. While inert gas (helium) is utilized as a carrier gas,

the conductivity of the sample decreases. When the sample elutes from the column, it reaches the detector, where it is detected as a change in conductivity. Temperature and flow affect retention time; conductivity has little effect. Figure 4-8 is a schematic diagram of a thermal conductivity detector (TCD).

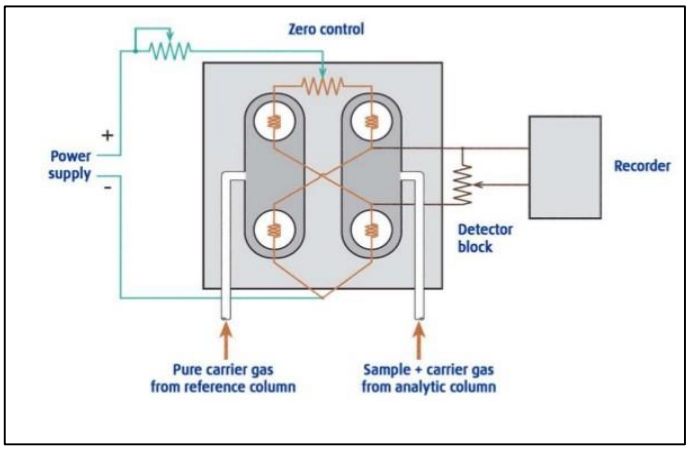

Figure 4-8: Schematic diagram of TCD, also known as Katharometer

Benefits of the Thermal Conductivity Detector (TCD)

TCD has the following list of benefits:

- Accommodates many compounds,
- Satisfactory sensitive for countless compounds,
- Simple construction,
- Excellent linear range,
- Good detection limit,
- Produces a good signal when a carrier gas flow rate, temperature block, and power filament are excellently controlled.

4.8.2 Materials Used for Infinite Dilution Activity Coefficients

All materials used in the experiments (e.g., helium, chromosorb, solvents, and ILs for DES preparation) were obtained from various suppliers and were within the purity margin (95–99) %, as shown in Table 4-6 (organic solutes). As a result, these materials were used without additional purification since it was known that this method could separate impurities from organic solutes.

Helium

Helium, which is an inert gas, was used as a carrier gas for the injection of solutes in a GLC instrument. It was purchased from Afrox SA (Pty) with a minimum purity of < 99.99%.

Chromosorb

Chromosorb (SiO_2) is a coating material. In this case, it was utilized as a solid support material for the stationary phase. It is a product of SUPELCO supplied by Merck (SA) with a W HP, 80-100 mesh particle size.

Table 4-7: List of all the studied organic solutes

Organic solute	*Supplier*	*Purity*
2.2-dimethylbutane	Sigma Aldrich	≥ 99%
Pentane	Sigma Aldrich	≥ 98%
Hexane	Sigma Aldrich	≥ 97%
Heptane	Sigma Aldrich	≥ 99%
Octane	Fluka	≥ 95%
n-Nonan	Merck	≥ 99%
n-Decan	Merck	≥ 99%
1-Pentane	Alfa Aesar	≥ 97%
1-Hexene	Alfa Aesar	≥ 98%
1-Nonene	Sigma Aldrich	≥ 96%
1-Decene	Sigma Aldrich	≥ 96%
1-Pentyne	Alfa Aesar	≥ 99%
1-Hexyne	Alfa Aesar	≥ 98%
1-Heptyne	Alfa Aesar	≥ 99%
o-Xylene	Fluka	≥ 99%
m-Xylene	Fluka	≥ 99%
p-Xylene	Fluka	≥ 99%
Benzene	Riedel-de Haën	≥ 99%
Ethylbenzene	Fluka	≥ 99%
Toluene	Sigma Aldrich	≥ 99.5%
Cyclopentane	Sigma Aldrich	≥ 98%
Cyclohexane	Sigma Aldrich	≥ 99.5%
Methylcyclohexane	Alfa Aesar	≥ 99%

Cyclopentene	Sigma Aldrich	≥ 96%
Methanol	Sigma Aldrich	≥ 99.9%
Ethanol	Sigma Aldrich	≥ 99%
2-Propanol	Sigma Aldrich	≥ 99.5%
Butan-1-ol	Saarchem	≥ 99%
Acetone	Sigma Aldrich	≥ 99.8%
MEK	Allied Signal	≥ 99.9%
Thiophene	Sigma Aldrich	≥ 99%

Table 4-8: List of ionic liquids (HBAs) used for the preparation of deep eutectic solvents, their suppliers, as well as their assay

Chemical Name	*Supplier*	*Assay*
1-ethyl-1-methylpyrrolidinium bromide	Sigma Aldrich	≥ 99%
Trihexyltetradecylphosphonium decanoate	Sigma Aldrich	≥ 95%

Table 4-9: List of organic solvents (HBDs) used in the preparation of deep eutectic solvents, as well as the supplier and purity.

Chemical Name	*Supplier*	*Purity*
Glycerol (Gly)	Sigma Aldrich	≥ 99%
Ethylene glycol (EG)	Merck	≥ 99%
1.5-pentanediol (1.5-PDO)	Sigma Aldrich	≥ 99%
1.6-hexanediol (1.6-HDO)	Sigma Aldrich	≥ 99%

4.8.3 Preparation of Deep Eutectic Solvents

This method employed a procedure similar to the one described earlier in this chapter in the method section of thermophysical properties. A list of all the deep eutectic solvents that have been explored can be seen below. In addition, structural compounds employed for the preparation of the examined deep eutectic solvents for the measurements of infinite dilution activity coefficient can be shown in Figures 4-6 to 4-10.

- 1-ethyl-1-methypyrrolidinium bromide + glycerol, [(EMPYR) Br + Gly]
- 1-ethyl-1-methylpyrrolidinium bromide + ethylene glycol, [(EMPYR) Br + EG]

- 1-ethyl-1-methylpyrrolidinium bromide + 1.5-pentanediol, [(EMPYR) Br + 1.5-PDO]
- 1-ethyl-1-methylpyrrolidinium bromide + 1.6-hexanediol, [(EMPYR) Br + 1.6-HDO]
- Trihexyltetradecylphosphonium decanoate + ethylene glycol, [(THTDP) Dc + EG]

Figure 4-9: 1-ethyl-1-methypyrrolidinium bromide + glycerol, [(EMPYR) Br + Gly]

Figure 4-10: 1-ethyl-1-methylpyrrolidinium bromide + ethylene glycol, [(EMPYR) Br + EG]

Figure 4-11: 1-ethyl-1-methylpyrrolidinium bromide + 1.5-pentanediol, [(EMPYR) Br + 1.5-PDO]

Figure 4-12: 1-ethyl-1-methylpyrrolidinium bromide + 1.6-hexanediol, [(EMPYR) Br + 1.6-HDO]

Figure 4-13: Trihexyltetradecylphosphonium decanoate + ethylene glycol, [(THTDP) Dc + EG]

4.8.4 Preparation of the Stationary Phase

Preparation of Deep Eutectic Solvent Mixture

- A clean round-bottomed flask rinsed with acetone was used to accurately weigh two rationed component materials using a OHAUS Analytical Balance with an accuracy of 0.000g.
- An accurate mass of W HP, 80-100 mesh chromosorb material was added in a round-bottom flask to mix with a prepared deep eutectic solvent.
- The mass loading of all the prepared deep eutectic solvents was in the required range of (25-35) % solvent mass.

Evaporation of Dichloromethane

Dichloromethane is a polar aprotic solvent that has a wide range of applications. This solvent was employed to evenly disperse deep eutectic solvent on the solid support material in this study.

The Hei-VAP Rotatory Evaporator was utilized to ensure that deep eutectic solvent was evenly distributed on the solid support material and that the solvent (dichloromethane) was entirely evaporated from the mixture as follows:

- A round-bottomed flask contained a deep eutectic solvent mixture was sequestrated in a rotatory evaporator.
- The vacuum pump set at 60 kPa was used to remove dichloromethane from the deep eutectic solvent mixture for 4 hours, to ensure the complete removal of the dichloromethane.
- The mixture was then cooled for few hours before the column packing.

4.8.5 Experimental Setup

Experiments were conducted by gas liquid chromatography (Shimadzu GC-2014) coupled with a thermal conductivity detector (TCD). Figures 4-11 to 4-14 display the experimental setup for the instrument.

Figure 4-14: Shimadzu GC-2014 setup

Figure 4-15: Coiled and packed column tube with a DES stationary phase

Figure 4-16: Installed column in GLC

4.8.6 Experimental Procedure

Column preparation

The 1 m length and 4 mm internal diameter stainless steel column (Figure 4-15 and 4-16) was thoroughly washed with hot water and soap, rinsed with distilled water, and then dried with

acetone. The column tube was finely packed in a vacuum pump to maintain the conditions of the stationary phase and installed as shown in Figure 4-14 to Figure 4-16.

Conditioning

After the installation of the stainless-steel column, the column was conditioned for at least for 3 hours, to make sure that the pressure drop remains constant, and moisture is completely removed. Mass changes on the column were then monitored, to ensure no solvent was lost.

Flow Rate Measurements

The flow meter located at the outlet of the TCD was used to ascertain the carrier gas flow rates with the use of soap bubbles. The flow rate ranged from (15-40) ml/min with uncertainties of 0.50%. In addition, the capacity of the flow meter was calibrated at 30 ml.

For all of the measurements, the temperature of the detector and injector was held at T = 523.15 K. At temperatures ranging from (313.15 to 343.15) K, retention times (t_g and t_r) and other parameters for measuring IDACs of various organic solutes were determined. Each solute was injected one at a time, in volumes ranging from (0.1 to 0.5) µL. The solute detection and signal response display, as shown in Figure 4-17 on the computer screen, were also recorded following the injection. In chapter three, some thermodynamic equations were discussed in detail. Furthermore, for the sake of accuracy, two replicates of each solute analysis were performed.

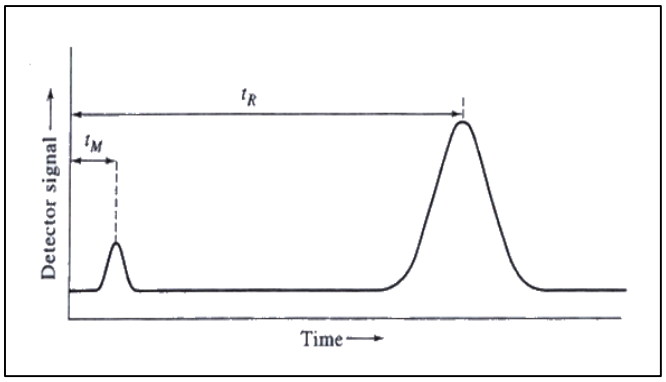

Figure 4-17: Chromatogram response as a function of time

Measurement of inlet and outlet pressure

In the experiment, the column opening was exposed to the atmosphere. Hence, the outlet pressure (P_o) was measured by the digital barometer to the atmospheric pressure with an uncertainty of 5

Pa. The pressure drop was displayed on the screen to determine the inlet pressure contingent on the gas flow set for experimental measurements. Thus, it was calculated as eq. (4-4):

$$P_i = P + \Delta P \tag{4-4}$$

The level of uncertainty was 5 Pa.

4.9 Test System, Infinite Dilution Activity Coefficients in Hexadecane

In the present section, the full details of the findings of the test system (hexadecane) were utilised to validate the experimental procedure before the investigation of the deep eutectic solvents for the new systems was used to confirm the reliability and consistency of the instrumental setup and the experimental method used. Several organic solutes, including 2,2-dimethylbutane, pentane, hexane, heptane, cyclopentane, cyclohexane, benzene, and toluene, were experimentally examined in hexadecane as a stationary phase and helium as a mobile phase at various temperatures varying from (323.15–343.15) K and at atmospheric pressure. Table 4-10 illustrates the results.

Table 4-10: Comparison of literature and experimental results for the infinite dilution activity coefficients in hexadecane as a stationary phase, test system with various organic solutes.

Organic Solutes	Temp (T/K)	Exp (γ_{13}^{∞})	Lit (γ_{13}^{∞})	R.D (%)
2.2-Dimethylbutane	323.15	0.861	0.872 [a]	1.23
	333.15	0.879	0.886 [a]	0.79
	343.15	0.824	0.832 [a]	0.96
Pentane	323.15	0.808	0.814 [a]	0.74
	333.15	0.845	0.833-0.850[ab]	1.90
	343.15	0768	0.776 [a]	1.03
Hexane	323.15	0.875	0.860-0.905[abc]	1.81
	333.15	0.870	0.867-0.911[abc]	1.79
	343.15	0.815	0.824 [a]	1.09
Heptane	323.15	0.878	0.867-0.921[abc]	1.75
	333.15	0.922	0.879-0.923[abc]	1.79

	343.15	0.848	0.855 [a]	0.82
Cyclopentane	323.15	0.709	0.686 [a]	3.35
	333.15	0.713	0.702 [a]	1.57
	343.15	0.668	0.659 [a]	1.37
Cyclohexane	323.15	0.755	0.739-0.787[ab]	2.10
	333.15	0.761	0.757-0.782[ab]	2.08
	343.15	0.712	0.704 [a]	1.14
Benzene	323.15	0.958	0.932-0.977[ab]	1.67
	333.15	0.877	0.620-0.957[abc]	1.80
	343.15	0.971	0.876 [a]	10.8
Toluene	323.15	0.918	0.941 [a]	2.44
	333.15	0.779	0.621-0.948[ac]	1.02
	343.15	0.873	0.870 [a]	0.34

(Schult et al., 2001)[a], (Castells et al., 1990)[b], and (Snyder and Thomas, 1968)[c]

The relative deviation of the experimental and literature data was obtained through the following eq. (4-5):

$$R.D = \frac{\left(\gamma_{13}^{\infty,Exp} - \gamma_{13}^{\infty,Exp}\right)}{\gamma_{13}^{\infty,Lit}} \times 100\% \qquad (4\text{-}5)$$

CHAPTER FIVE

EXPERIMENTAL RESULTS

Overview

This chapter details the physical and thermophysical properties results for four different systems with their mole ratios listed below that were experimentally examined as extracting solvents at various temperatures varying from T = (293.15-313.15) K and atmospheric pressure of 0.1 MPa.

- {[1-ethyl-1-methylpyrrolidinium bromide + ethylene glycol] (1,001: 3,999 mole ratio) + methanol}, {[(EMPYR) Br + EG] (1,001: 3,999 mole ratio) + methanol},
- {[1-ethyl-1-methylpyrrolinium bromide + ethylene glycol] (1,000: 4,000 mole ratio) + ethanol}, {[(EMPYR) Br + EG] (1,000: 4,000 mole ratio) + ethanol]},
- {[1-ethyl-1-methypyrrolidinium bromide + glycerol] (1,000: 2,000 mole ratio) + methanol}, {[(EMPYR) Br + Gly] (1,000: 2,000 mole ratio) + methanol]},
- {[1-ethyl-1-methylpyrrolidinium bromide + glycol] (1,002: 1,998 mole ratio) + ethanol}, {[(EMPYR) Br + Gly] (1,002: 1,998 mole ratio) + ethanol}

During the experiments, the physical properties, i.e., densities and sound velocities, of the prepared systems were estimated simultaneously using an Anton Paar DSA 5000 M, which is a density and sound velocity meter. The measured density and sound velocity values were used to compute the experimental thermophysical properties, such as excess molar volumes (V_m^E), isentropic compressibilities (K_s), the variation in isentropic compressibilities (ΔK_s), and the intermolecular free length (L_f) of each system at different temperatures.

The results for both physical and thermophysical properties are listed in Tables 5-1 to 5-8 and displayed in plots from figures 5-1 to 5-16. Moreover, the Redlich-Kister Equation (5-1) given below, was used for correlating or smoothing functions such as $V_m^E, K_s, \Delta K_s,$ as well as L_f experimental data.

$$\sigma(X) = \sum_{i=1}^{n} \left[{(X_{exp} - X_{calc})} \Big/ {(N - K)} \right]^{\frac{1}{2}} \quad (5\text{-}1)$$

Thus, N represents the number of experimental points and K denotes the coefficient used in the equation.

This chapter further presents the infinite dilution activity coefficients (γ_{13}^{∞}) results of five different systems with their mole ratios:

- 1-ethyl-1-methypyrrolidinium bromide + glycerol, [(EMPYR) Br + Gly] (1,000: 2,000 ratio)
- 1-ethyl-1-methylpyrrolidinium bromide + ethylene glycerol, [(EMPYR) Br + EG] (1,002: 3,998 mole ratio)
- 1-ethyl-1-methylpyrrolidinium bromide + 1.5-pentanediol, [(EMPYR) Br + 1.5-PDO] (1,001: 1,999 mole ratio)
- 1-ethyl-1-methylpyrrolinium bromide + 1.6-hexanediol, [(EMPYR) Br + 1.6-HDO] (1,000: 2,000 mole ratio)
- Trihexyltetradecylphosphonium decanoate + ethylene glycol, [(THTDP) Dc + EG] (1,003: 3,997 mole ratio)

These were experimentally investigated at various temperatures varying from T = 313.15-343.15 K and the atmospheric pressure of 0.1 MPa. During the experimental study, the retention times of various organic solutes were estimated in gas-liquid chromatography (GLC) to obtain the experimental infinite dilution activity coefficients in each system for all five investigated systems at a specific temperature. Furthermore, the plots of experimental infinite dilution activity coefficients as a function of temperature are listed in Tables 5-9, 5-11, 5-13, 5-15, and 5-17, as well as in Figures 5-17 to 5-55.

In addition, the partial molar properties, i.e., enthalpies, entropies, and Gibbs free energies, of all the investigated systems are listed in this section in Tables 5-10, 5-12, 5-14, 5-16, and 5-18 through the utilization of the Gibbs-Helmholtz Equation, which was detailed in the previous chapters.

5.1 Measured Physical Properties and Derived Thermophysical Properties

5.1.1 {[1-ethyl-1-methylpyrrolidiium bromide + ethylene glycol] + methanol}, {[(EMPYR) Br + EG] + methanol}

Table 5-1: Mole fractions (x_1), densities (ρ), sound velocities (u), excess molar volumes (V_m^E), isentropic compressibilities (K_s), variation in isentropic compressibilities (ΔK_s), and intermolecular free length values (L_f), for {[(EMPYR) Br + EG] (x_1) + methanol (x_2)}, binary systems at different temperatures and at p = 0.1 MPa.

x_1	ρ $(g.cm^{-3})$	u (ms^{-1})	V_m^E $(cm^3.mol^{-1})$	$10^7.\Delta K_s$ (Pa^{-1})	$10^7.K_s$ (Pa^{-1})	$10^{-10}.L_f$ (m)
			293.15 K			
0	0.792	1126	0	0	99.63	20.53
0.010	0.795	1129	-0.277	-0.008	98.84	20.49
0.041	0.910	1289	-0.772	-3.031	66.11	16.72
0.081	0.976	1390	-1.222	-4.088	53.03	14.97
0.104	0.999	1429	-1.328	-4.332	49.04	14.40
0.199	1.060	1537	-1.577	-4.583	39.85	12.98
0.302	1.096	1599	-1.660	-4.280	35.66	12.28
0.398	1.115	1633.7	-1.623	-3.809	33.61	11.92
0.499	1.128	1659.4	-1.543	-3.243	32.18	11.66
0.598	1.137	1675.9	-1.336	-2.632	31.31	11.50
0.709	1.144	1689.5	-1.089	-1.924	30.62	11.38
0.800	1.147	1694.9	-0.795	-1.311	30.34	11.33
0.901	1.150	1701.4	-0.297	-0.635	30.03	11.27
1	1.155	1715.5	0	0	29.42	11.16
			298.15 K			
0	0.787	1110	0	0	103.1	20.89

0.010	0.790	1113	-0.304	-0.014	102.3	20.80
0.041	0.906	1275	-0.823	-3.217	67.93	16.95
0.081	0.972	1377	-1.306	-4.289	54.28	15.15
0.104	0.995	1416	-1.397	-4.541	50.14	14.56
0.199	1.058	1525	-1.631	-4.796	40.64	13.11
0.302	1.093	1587	-1.678	-4.475	36.32	12.40
0.398	1.111	1622	-1.690	-3.981	34.21	12.03
0.499	1.125	1648	-1.609	-3.389	32.74	11.77
0.598	1.134	1664	-1.389	-2.751	31.84	11.61
0.709	1.141	1678	-1.164	-2.012	31.13	11.47
0.800	1.144	1683	-0.840	-1.373	30.86	11.42
0.901	1.147	1690	-0.345	-0.668	30.53	11.36
1	1.150	1704	0	0	29.95	11.25
			303.15 K			
0	0.783	1094	0	0	106.8	21.45
0.010	0.785	1099	-0.359	-0.051	105.5	21.32
0.041	0.902	1261	-0.854	-3.384	69.80	17.34
0.081	0.968	1363	-1.391	-4.498	55.60	15.48
0.104	0.991	1402	-1.475	-4.760	51.29	14.86
0.199	1.055	1512	-1.707	-5.017	41.46	13.36
0.302	1.089	1575	-1.772	-4.677	37.01	12.63
0.398	1.108	1610	-1.763	-4.160	34.83	12.25
0.499	1.121	1636	-1.641	-3.540	33.33	11.98
0.598	1.130	1653	-1.450	-2.873	32.40	11.81
0.709	1.137	1666	-1.220	-2.101	31.67	11.68
0.800	1.140	1672	-0.890	-1.434	31.38	11.62

0.901	1.143	1678	-0.388	-0.698	31.05	11.57
1	1.146	1692	0	0	30.46	11.46
			308.15 K			
0	0.778	1079	0	0	110.4	22.01
0.010	0.780	1085	-0.388	-0.074	108.9	21.85
0.041	0.897	1246	-0.888	-3.537	71.76	17.74
0.081	0.964	1350	-1.427	-4.699	56.95	15.80
0.104	0.987	1389	-1.512	-4.970	52.48	15.17
0.199	1.051	1500	-1.782	-5.233	42.30	13.62
0.302	1.085	1563	-1.830	-4.875	37.71	12.86
0.398	1.104	1598	-1.809	-4.334	35.47	12.47
0.499	1.118	1624	-1.691	-3.687	33.92	12.19
0.598	1.127	1641	-1.503	-2.992	32.97	12.02
0.709	1.134	1655	-1.262	-2.188	32.22	11.88
0.800	1.137	1660	-0.937	-1.493	31.93	11.83
0.901	1.140	1667	-0.417	-0.727	31.59	11.77
1	1.143	1681	0	0	30.97	11.66
			313.15 K			
0	0.773	1065	0	0	114.0	22.56
0.010	0.776	1070	-0.417	-0.065	112.5	22.41
0.041	0.893	1232	-0.897	-3.683	73.77	18.15
0.081	0.960	1337	-1.440	-4.899	58.34	16.14
0.104	0.983	1376	-1.517	-5.183	53.70	15.49
0.199	1.047	1487	-1.792	-5.460	43.18	13.89
0.302	1.082	1551	-1.880	-5.096	38.44	13.10
0.398	1.100	1581	-1.775	-4.542	36.13	12.70

0.499	1.114	1612	-1.748	-3.878	34.54	12.42
0.598	1.123	1629	-1.526	-3.166	33.56	12.24
0.709	1.130	1643	-1.289	-2.341	32.79	12.10
0.800	1.133	1643	-1.013	-1.628	32.49	12.04
0.901	1.136	1648	-0.437	-0.842	32.13	11.97
1	1.141	1655	0	0	32.47	12.04

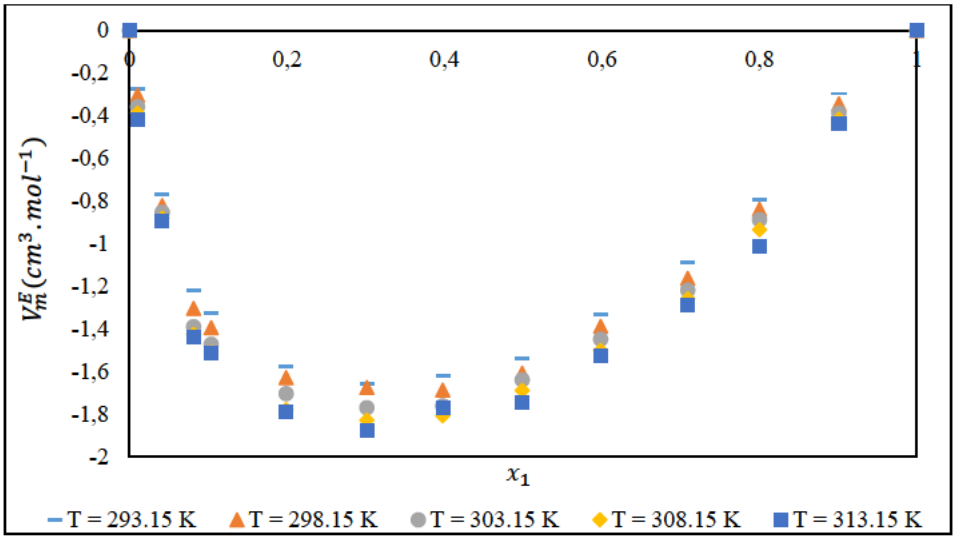

Figure 5-1: Excess molar volumes (V_m^E) for {[(EMPYR) Br + EG] (x_1) + methanol (x_2)}, binary systems as a function of mole fraction of x_1= (0-1) at T = (293.15; 298.15; 303.15; 308.15; and 313.15) K

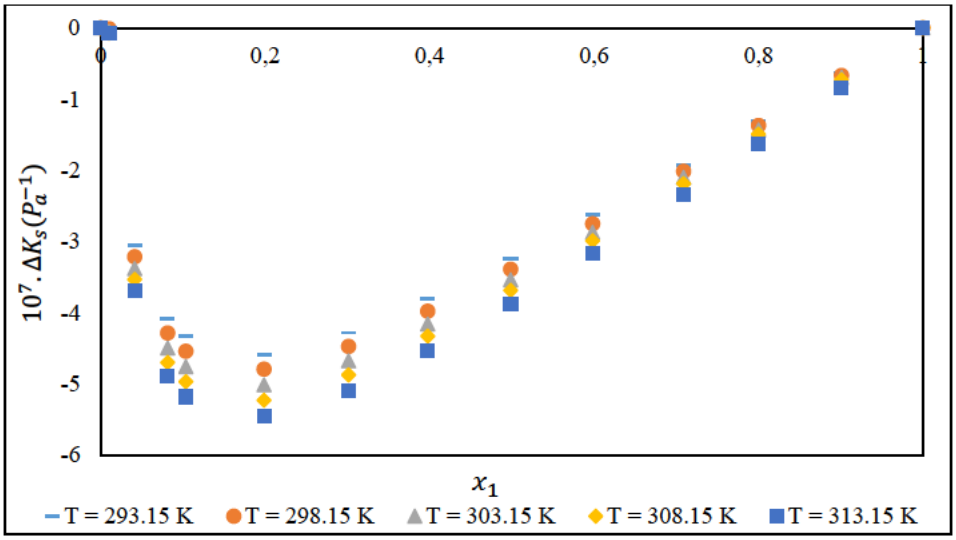

Figure 5-2: Variation in isentropic compressibilities (ΔK_s) for {[(EMPYR) Br + EG] (x_1) + methanol (x_2)}, binary systems as a function of mole fraction x_1 = (0-1) at T = (293.15; 298.15; 303.15; 308.15; and 313.15) K

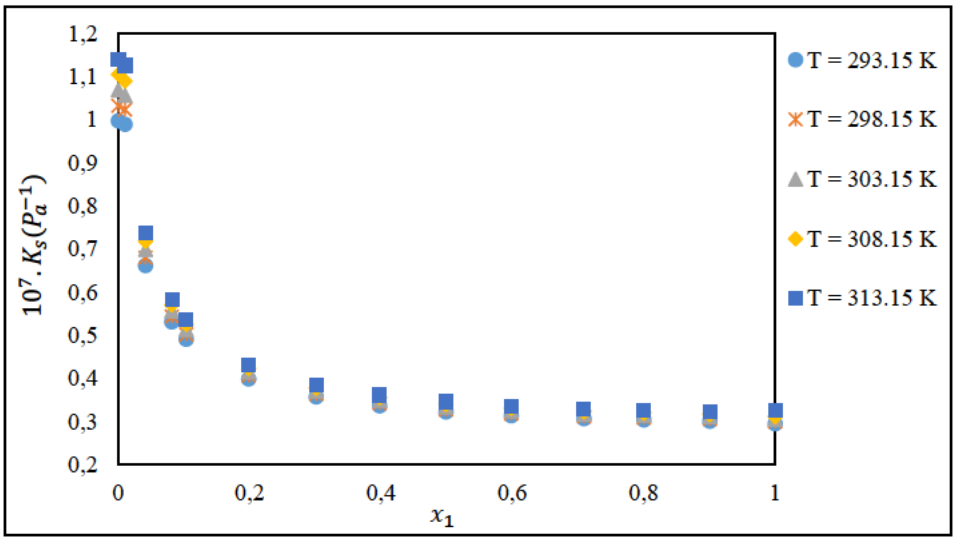

Figure 5-3: Isentropic compressibilities (K_s) for {[(EMPYR) Br + EG] (x_1) + methanol (x_2)}, binary systems as a function of mole fraction of x_1 = (0-1) at T = (293.15; 298.15; 303.15; 308.15; and 313.15) K

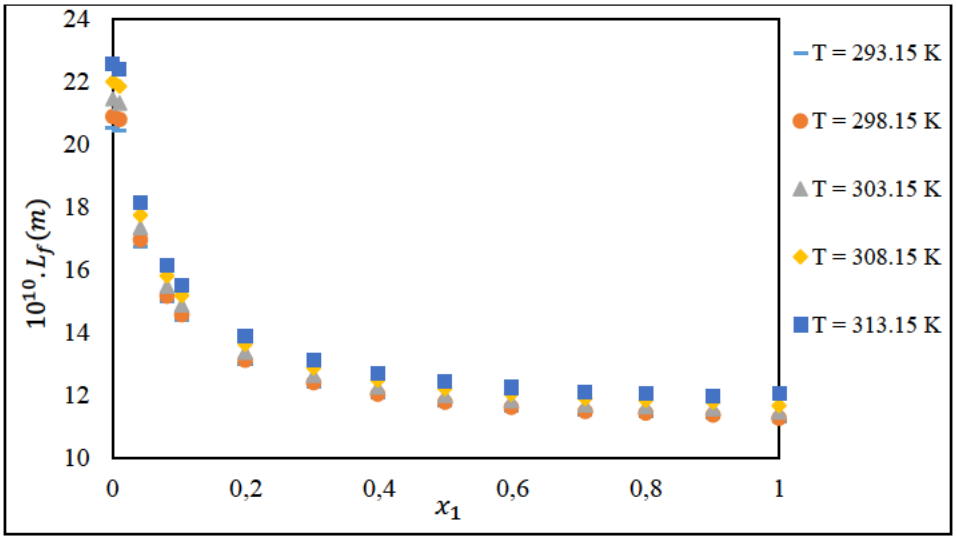

Figure 5-4: Intermolecular free length values (L_f) for {[(EMPYR) Br + EG] (x_1) + methanol (x_2)}, binary systems as a function of mole fraction of x_1 = (0-1) at T = (293.15; 298.15; 303.15; 308.15; and 313.15) K

5.1.2 {[1-ethyl-1-methylpyrrolidiium bromide + ethylene glycol] + ethanol}, {[(EMPYR) Br + EG] + ethanol}

Table 5-2: Mole fractions (x_1), densities (ρ), sound velocities (u), **e**xcess molar volumes (V_m^E), isentropic compressibilities (K_s), deviation in isentropic compressibilities (ΔK_s), and intermolecular free length values (L_f), for {[(EMPYR) Br + EG] (x_1) + ethanol (x_2)}, binary systems at different temperatures and at p = 0.1 MPa.

x_1	ρ $(g.cm^{-3})$	u (ms^{-1})	V_m^E $(cm^3.mol^{-1})$	$10^7.\Delta K_s$ (Pa^{-1})	$10^7.K_s$ (Pa^{-1})	$10^{-10}.L_f$ (m)
			293.15 K			
0	0.791	1165	0	0	93.24	19.68
0.010	0.821	1204	-0.576	-0.858	84.03	18.68
0.041	0.885	1280	-1.323	-2.173	68.97	16.92
0.080	0.939	1351	-2.448	-2.981	58.39	15.57
0.102	0.965	1389	-2.815	-3.317	53.67	14.93
0.200	1.035	1498	-3.398	-3.764	43.05	13.37
0.300	1.069	1556	-3.585	-3.577	38.65	12.67
0.400	1.099	1607	-3.570	-3.291	35.25	12.10
0.501	1.115	1636	-3.255	-2.832	33.52	11.80
0.600	1.118	1640	-2.840	-2.236	33.25	11.75
0.700	1.131	1663	-2.356	-1.738	31.97	11.52
0.801	1.135	1673	-1.593	-1.155	31.47	11.43
0.901	1.136	1684	-0.894	-0.572	31.02	11.35
1	1.143	1692	0	0	30.56	11.27
			298.15 K			
0	0.787	1148	0	0	96.46	20.20
0.010	0.817	1188	-0.587	-0.902	86.78	19.16

0.041	0.880	1265	-1.360	-2.285	70.96	17.33
0.080	0.935	1337	-2.610	-3.132	59.88	15.91
0.102	0.962	1376	-2.930	-3.481	54.97	15.25
0.200	1.031	1486	-3.456	-3.941	43.95	13.64
0.300	1.066	1543	-3.641	-3.741	39.41	12.91
0.400	1.095	1595	-3.627	-3.440	35.90	12.32
0.501	1.111	1624	-3.361	-2.958	34.12	12.01
0.600	1.114	1628	-2.887	-2.336	33.84	11.97
0.700	1.127	1652	-2.411	-1.814	32.53	11.73
0.801	1.131	1662	-1.679	-1.206	32.02	11.63
0.901	1.133	1673	-0.982	-0.597	31.55	11.55
1	1.139	1681	0	0	31.07	11.46
			303.15 K			
0	0.782	1131	0	0	99.90	20.74
0.010	0.812	1171	-0.598	-0.951	89.70	19.66
0.041	0.876	1250	-1.390	-2.406	73.07	17.74
0.080	0.931	1322	-2.751	-3.295	61.45	16.27
0.102	0.958	1362	-3.028	-3.658	56.33	15.58
0.200	1.027	1472	-3.599	-4.132	44.90	13.91
0.300	1.062	1530	-3.727	-3.918	40.21	13.16
0.400	1.091	1583	-3.686	-3.599	36.58	12.55
0.501	1.107	1611	-3.460	-3.090	34.78	12.24
0.600	1.111	1616	-2.971	-2.443	34.46	12.18
0.700	1.123	1640	-2.446	-1.897	33.11	11.94
0.801	1.123	1650	-1.742	-1.260	32.58	11.84
0.901	1.129	1661	-1.023	-0.624	32.10	11.75

1	1.136	1669	0	0	31.60	11.66
			308.15 K			
0	0.778	1114	0	0	103.5	21.31
0.010	0.808	1155	-0.609	-1.004	92.75	20.17
0.041	0.872	1234	-1.420	-2.526	75.35	18.18
0.080	0.927	1308	-2.792	-3.468	63.09	16.63
0.102	0.954	1347	-3.176	-3.846	57.75	15.92
0.200	1.023	1459	-3.653	-4.332	45.89	14.19
0.300	1.058	1518	-3.781	-4.105	41.03	13.41
0.400	1.088	1570	-3.746	-3.768	37.28	12.79
0.501	1.104	1599	-3.517	-3.230	35.45	12.47
0.600	1.107	1604	-3.107	-2.557	35.10	12.41
0.700	1.120	1628	-2.462	-1.984	33.70	12.16
0.801	1.124	1638	-1.825	-1.318	33.16	12.06
0.901	1.126	1649	-1.125	-0.652	32.66	11.97
1	1.132	1658	0	0	32.14	11.87
			313.15 K			
0	0.774	1098	0	0	107.3	21.89
0.010	0.804	1139	-0.622	-1.059	95.93	20.70
0.041	0.868	1217	-1.452	-2.646	77.80	18.64
0.080	0.923	1293	-2.835	-3.649	64.79	17.01
0.102	0.950	1333	-3.379	-4.044	59.22	16.26
0.200	1.020	1444	-3.715	-4.531	47.03	14.49
0.300	1.055	1505	-3.836	-4.300	41.88	13.67
0.400	1.084	1558	-3.809	-3.945	38.00	13.03
0.501	1.100	1585	-3.675	-3.372	36.20	12.71

0.600	1.105	1592	-3.278	-2.676	35.76	12.64
0.700	1.116	1616	-2.509	-2.076	34.31	12.38
0.801	1.121	1626	-1.883	-1.379	33.76	12.28
0.901	1.122	1637	-1.222	-0.682	33.24	12.18
1	1.129	1646	0	0	32.71	12.09

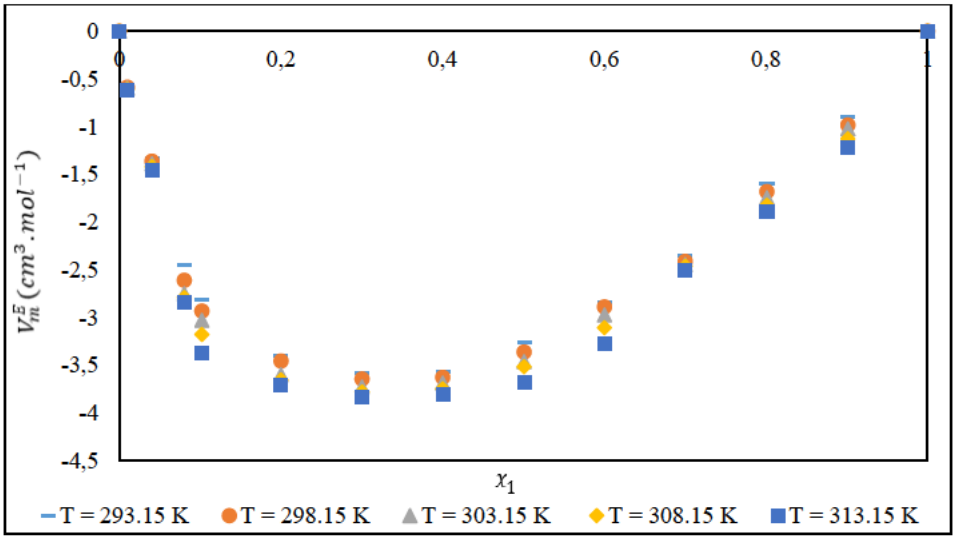

Figure 5-5: Excess molar volumes (V_m^E) for {[(EMPYR) Br + EG] (x_1) + ethanol (x_2)}, binary systems as a function of mole fraction of x_1= (0-1) at T = (293.15; 298.15; 303.15; 308.15; and 313.15) K

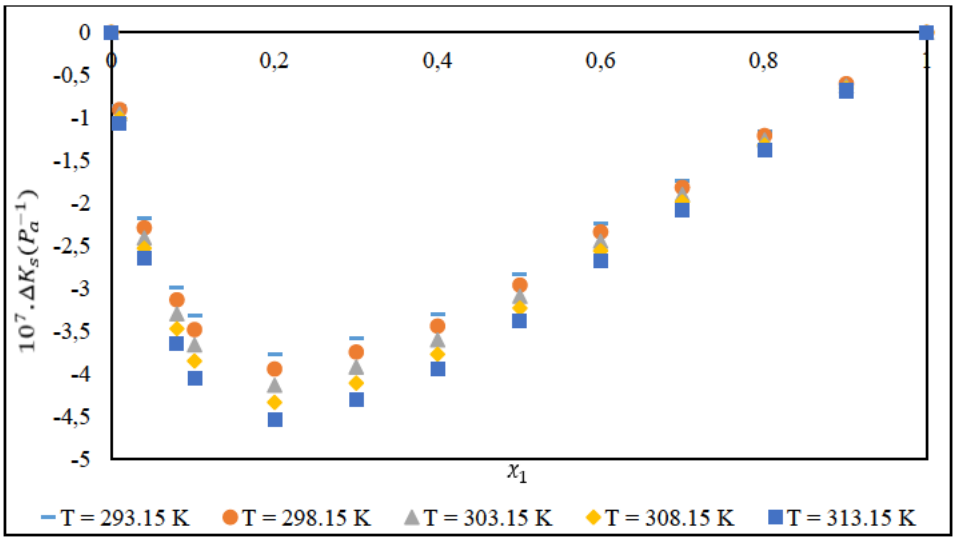

Figure 5-6: Variation in isentropic compressibilities (ΔK_s) for {[(EMPYR) Br + EG] (x_1) + ethanol (x_2)}, binary systems as a function of mole fraction of x_1= (0-1) at T = (293.15; 298.15; 303.15; 308.15; and 313.15) K

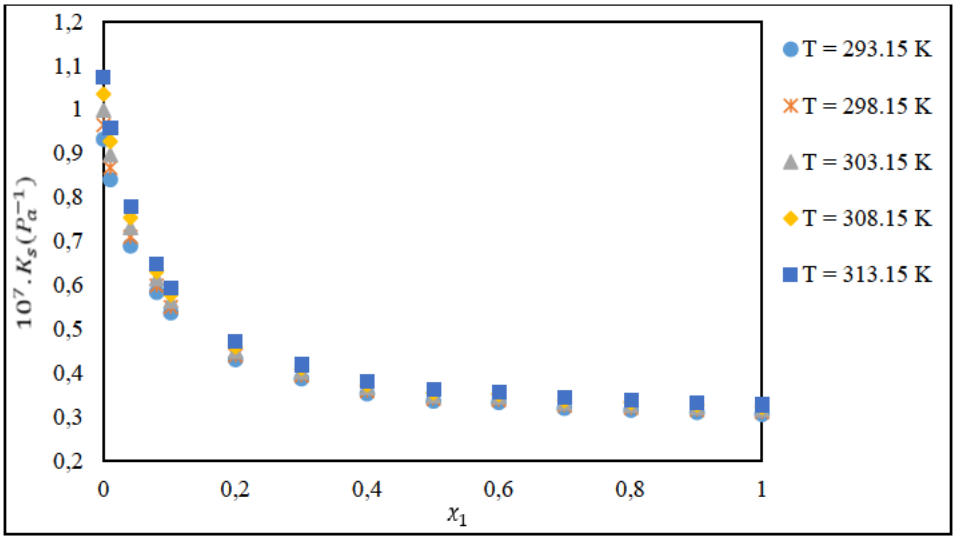

Figure 5-7: Isentropic compressibilities (K_s) for {[(EMPYR) Br + EG] (x_1) + ethanol (x_2)}, binary systems as a function of mole fraction of x_1 = (0-1) at T = (293.15; 298.15; 303.15; 308.15; and 313.15) K

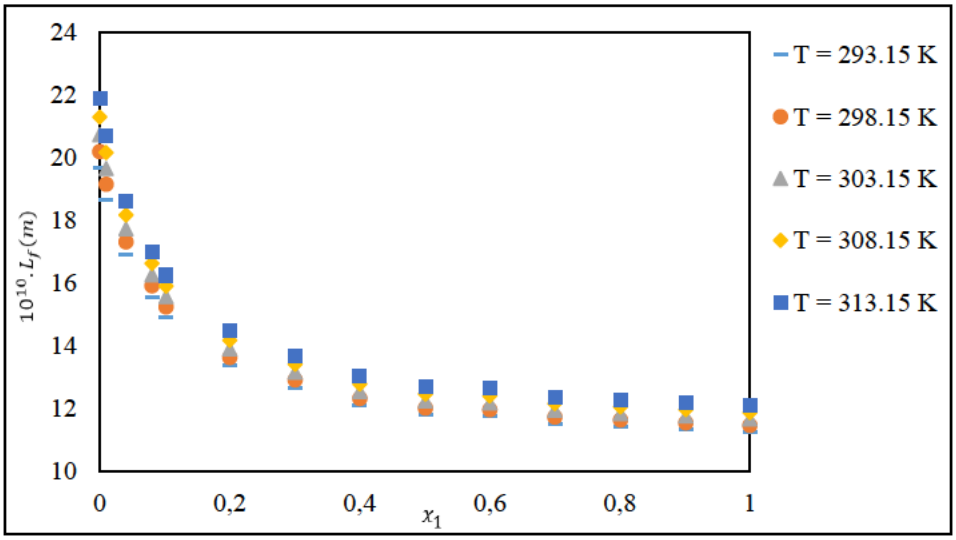

Figure 5-8: Intermolecular free length values (L_f) for {[(EMPYR) Br + EG] (x_1) + ethanol (x_2)}, binary systems as a function of mole fraction of x_1 = (0-1) at T = (293.15; 298.15; 303.15; 308.15; and 313.15) K

5.1.3 {[1-ethyl-1-methylpyrrolidiium bromide + glycerol] + methanol}, {[(EMPYR) Br + Gly] + methanol}

Table 5-3: Mole fractions (x_1), densities (ρ), sound velocities (u), excess molar volumes (V_m^E), isentropic compressibilities (K_s), variation in isentropic compressibilities (ΔK_s), and intermolecular free length values (L_f), for {[(EMPYR) Br + Gly] (x_1) + methanol (x_2)} binary systems at different temperatures and at p = 0.1 MPa.

x_1	ρ $(g.cm^{-3})$	u (ms^{-1})	V_m^E $(cm^3.mol^{-1})$	$10^7.\Delta K_s$ (Pa^{-1})	$10^7.K_s$ (Pa^{-1})	$10^{-10}.L_f$ (m)
			293.15 K			
0	0.792	1122	0	0	100.3	20.41
0.011	0.831	1169	-0.244	-1.141	88.07	19.12
0.041	0.919	1283	-0.812	-3.097	66.13	16.57
0.081	0.994	1392	-1.091	-4.197	51.95	14.69
0.105	1.031	1453	-1.224	-4.607	45.95	13.82
0.205	1.118	1607	-1.324	-4.949	34.64	11.99
0.306	1.165	1701	-1.256	-4.6562	29.67	11.10
0.405	1.196	1765	-1.205	-4.156	26.84	10.56
0.507	1.216	1808	-1.050	-3.525	25.14	10.21
0.605	1.231	1840	-0.834	-2.863	24.01	9.987
0.707	1.243	1867	-0.605	-2.157	23.09	9.794
0.807	1.247	1876	-0.384	-1.397	22.79	9.729
0.904	1.254	1891	-0.175	-0.680	22.32	9.628
1	1.264	1917	0	0	21.54	9.460
			298.15 K			
0	0.788	1106	0	0	103.9	20.96
0.011	0.827	1157	-0.253	-1.269	90.36	19.55

0.041	0.915	1268	-0.840	-3.261	67.95	16.95
0.081	0.990	1378	-1.129	-4.406	53.18	15.00
0.105	1.026	1440	-1.248	-4.831	46.95	14.09
0.205	1.114	1595	-1.351	-5.178	35.27	12.21
0.306	1.162	1690	-1.300	-4.866	30.16	11.29
0.405	1.193	1754	-1.211	-4.340	27.26	10.74
0.507	1.213	1797	-1.087	-3.680	25.53	10.39
0.605	1.228	1828	-0.874	-2.989	24.37	10.15
0.707	1.240	1855	-0.644	-2.250	23.44	9.958
0.807	1.244	1864	-0.414	-1.458	23.13	9.892
0.904	1.250	1879	-0.217	-0.711	22.65	9.789
1	1.261	1904	0	0	21.87	9.619
			303.15 K			
0	0.783	1089	0	0	107.7	21.54
0.011	0.822	1137	-0.263	-1.274	94.03	20.13
0.041	0.911	1254	-0.870	-3.433	69.86	17.35
0.081	0.986	1365	-1.165	-4.627	54.47	15.32
0.105	1.024	1427	-1.311	-5.067	48.00	14.38
0.205	1.110	1583	-1.410	-5.418	35.93	12.44
0.306	1.158	1678	-1.337	-5.087	30.67	11.49
0.405	1.189	1743	-1.247	-4.534	27.69	10.92
0.507	1.209	1786	-1.112	-3.843	25.92	10.56
0.605	1.224	1817	-0.925	-3.120	24.74	10.32
0.707	1.237	1845	-0.686	-2.349	23.79	10.12
0.807	1.241	1853	-0.455	-1.523	23.47	10.05
0.904	1.247	1867	-0.239	-0.743	22.99	9.952

1	1.257	1893	0	0	22.20	9.779
			308.15 K			
0	0.778	1073	0	0	111.6	22.12
0.011	0.818	1122	-0.273	-1.346	97.21	20.65
0.041	0.906	1239	-0.900	-3.614	71.85	17.75
0.081	0.982	1351	-1.164	-4.859	55.80	15.64
0.105	1.020	1414	-1.344	-5.314	49.10	14.67
0.205	1.106	1571	-1.416	-5.669	36.62	12.67
0.306	1.155	1666	-1.373	-5.318	31.20	11.69
0.405	1.186	1731	-1.288	-4.738	28.14	11.11
0.507	1.206	1775	-1.131	-4.014	26.33	10.75
0.605	1.221	1806	-0.927	-3.258	25.12	10.49
0.707	1.234	1832	-0.719	-2.452	24.15	10.29
0.807	1.237	1842	-0.484	-1.590	23.83	10.22
0.904	1.244	1856	-0.274	-0.777	23.33	10.11
1	1.254	1881	0	0	22.53	9.940
			313.15 K			
0	0.773	1057	0	0	115.7	22.73
0.011	0.813	1106	-0.284	-1.424	100.5	21.18
0.041	0.902	1224	-0.930	-3.803	73.92	18.17
0.081	0.978	1336	-1.175	-5.089	57.31	16.00
0.105	1.012	1398	-1.369	-5.541	50.54	15.02
0.205	1.101	1558	-1.443	-5.924	37.41	12.92
0.306	1.151	1653	-1.385	-5.555	31.79	11.91
0.405	1.183	1720	-1.332	-4.950	28.60	11.30
0.507	1.203	1763	-1.146	-4.192	26.74	10.93

0.605	1.218	1794	-0.952	-3.403	25.50	10.67
0.707	1.230	1821	-0.771	-2.560	24.51	10.46
0.807	1.234	1830	-0.545	-1.661	24.18	10.39
0.904	1.241	1845	-0.313	-0.811	23.68	10.28
1	1.251	1870	0	0	22.86	10.10

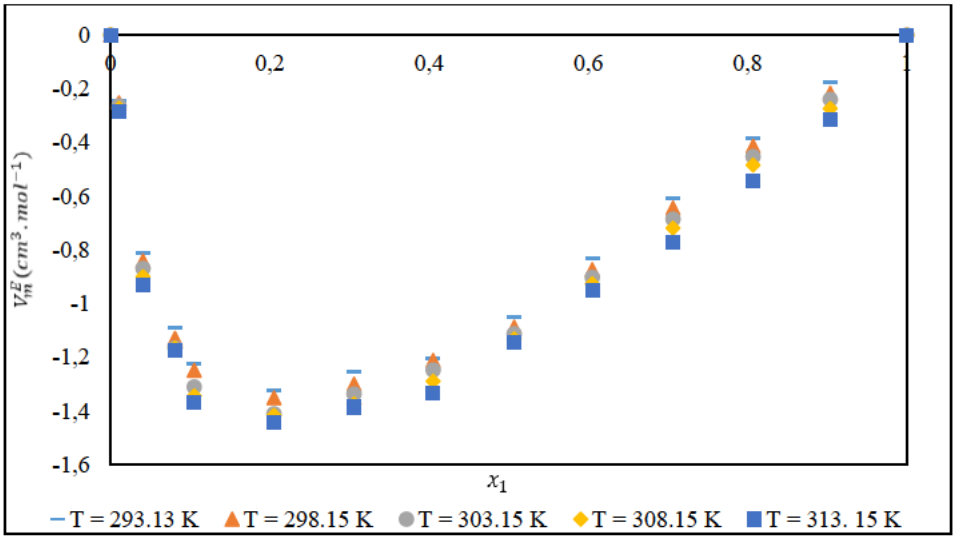

Figure 5-9: Excess molar volumes (V_m^E) for {[(EMPYR) Br + Gly] (x_1) + methanol (x_2)}, binary systems as a function of mole fraction of x_1 = (0-1) at T = (293.15; 298.15; 303.15; 308.15; and 313.15) K

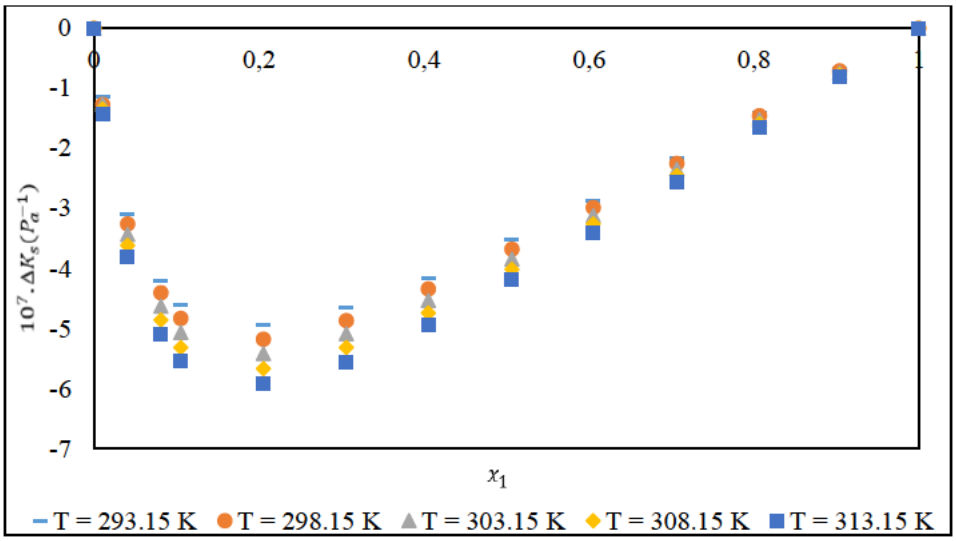

Figure 5-10: Variation in isentropic compressibilities (ΔK_s) for {[(EMPYR) Br + Gly] (x_1) + methanol (x_2)}, binary systems as a function of mole fraction of x_1 = (0-1) at T = (293.15; 298.15; 303.15; 308.15; and 313.15) K

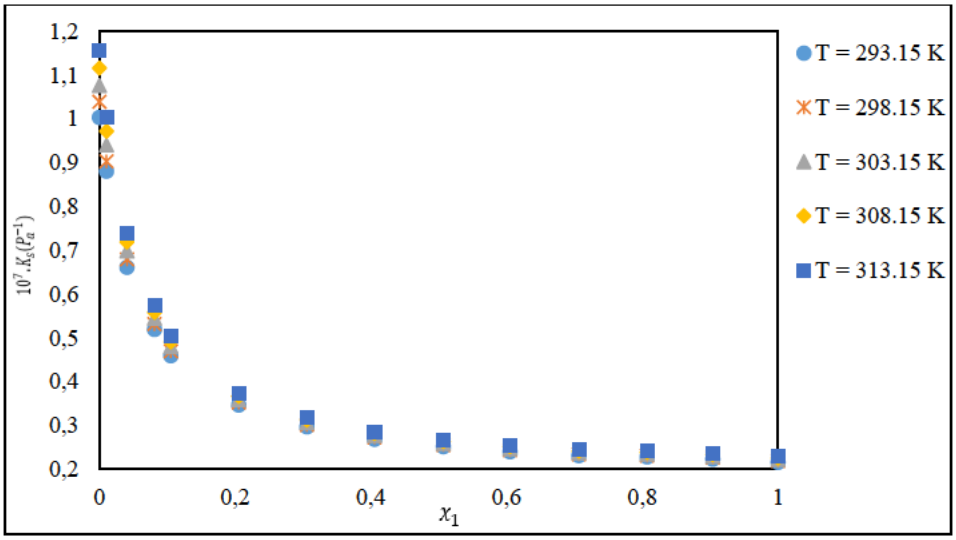

Figure 5-11: Isentropic compressibilities (K_s) for {[(EMPYR) Br + Gly] (x_1) + methanol (x_2)}, binary systems as a function of mole fraction of x_1 = (0-1) at T = (293.15; 298.15; 303.15; 308.15; and 313.15) K

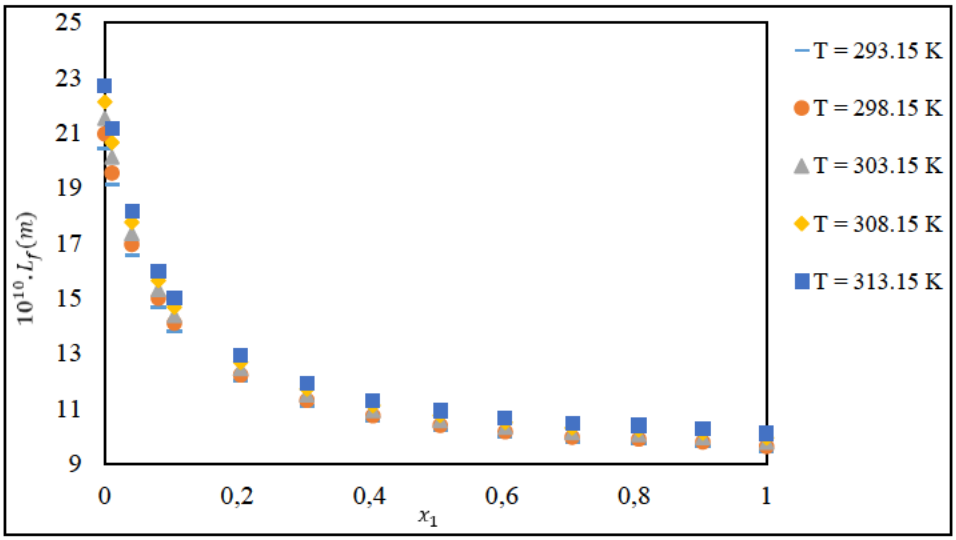

Figure 5-12: Intermolecular free length values (L_f) for {[(EMPYR) Br + Gly] (x_1) + methanol (x_2)}, binary systems as a function of mole fraction of x_1= (0-1) at T = (293.15; 298.15; 303.15; 308.15; and 313.15) K

5.1.4 {[1-ethyl-1-methylpyrrolidiium bromide + glycerol] + ethanol}, {[(EMPYR) Br + Gly] + ethanol}

Table 5-4: Mole fractions (x_1), densities (ρ), sound velocities (u), excess molar volumes (V_m^E), isentropic compressibilities (K_s), variation in isentropic compressibilities (ΔK_s), and intermolecular free length values (L_f), for {[(EMPYR) Br + Gly] (x_1)+ ethanol (x_2)}, binary systems at different temperatures and at p = 0.1 MPa.

x_1	ρ $(g.cm^{-3})$	u (ms^{-1})	V_m^E $(cm^3.mol^{-1})$	$10^7.\Delta K_s$ (Pa^{-1})	$10^7.K_s$ (Pa^{-1})	$10^{-10}.L_f$ (m)
			293.15 K			
0	0.772	1120	0	0	103.3	20.71
0.011	0.811	1167	-1.065	-1.183	90.56	19.40
0.040	0.899	1281	-3.409	-3.219	67.83	16.78
0.080	0.974	1390	-4.569	-4.356	53.18	14.86
0.104	1.011	1451	-5.350	-4.781	46.99	13.97
0.200	1.098	1605	-6.050	-5.165	35.36	12.12
0.300	1.145	1699	-5.734	-4.859	30.26	11.21
0.400	1.176	1763	-5.289	-4.338	27.36	10.66
0.503	1.196	1806	-4.470	-3.679	25.62	10.32
0.601	1.211	1838	-3.645	-2.995	24.46	10.08
0.701	1.223	1865	-2.970	-2.271	23.52	9.884
0.801	1.227	1874	-1.630	-1.493	23.21	9.819
0.900	1.233	1889	-0.135	-0.734	22,73	9.717
1	1.244	1915	0	0	21.94	9.546
			298.15 K			
0	0767	1104	0	0	107.0	21.28

0.011	0.806	1155	-1.088	-1.316	92.91	19.83
0.040	0.895	1267	-3.477	-3.390	69.70	17.17
0.080	0.970	1376	-4.659	-4.574	54.44	15.18
0.104	1.007	1438	-5.450	-5.015	48.02	14.25
0.200	1.094	1593	-6.158	-5.404	36.01	12.34
0.300	1.142	1688	-5.836	-5.078	30.76	11.41
0.400	1.173	1752	-5.384	-4.531	27.79	10.84
0.503	1.193	1795	-4.550	-3.841	26.01	10.49
0.601	1.207	1826	-3.721	-3.126	24.83	10.25
0.701	1.220	1853	-3.036	-2.370	23.88	10.05
0.801	1.224	1862	-1.694	-1.558	23.56	9.984
0.900	1.230	1877	-0.127	-0.767	23.07	9.880
1	1.240	1902	0	0	22.27	9.707
			303.15 K			
0	0.763	1087	0	0	110.9	21.86
0.011	0.802	1135	-1.111	-1.322	96.72	20.41
0.040	0.890	1252	-3.550	-3.569	71.67	17.57
0.080	0.966	1363	-4.750	-4.804	55.76	15.50
0.104	1.004	1425	-5.550	-5.260	49.10	14.54
0.200	1.090	1581	-6.260	-5.656	36.69	12.57
0.300	1.138	1676	-5.931	-5.309	31.28	11.61
0.400	1.169	1741	-5.475	-4.734	28.23	11.02
0.503	1.190	1784	-4.619	-4.011	26.42	10.67
0.601	1.204	1815	-3.785	-3.264	25.21	10.42
0.701	1.217	1842	-3.087	-2.473	24.24	10.21
0.801	1.221	1851	-1.715	-1.628	23.91	10.15

0.900	1.227	1865	-0.015	-0.801	23.42	10.04
1	1.237	1891	0	0	22.61	9.869
			308.15 K			
0	0.757	1071	0	0	115.1	22.47
0.0109	0.796	1120	-1.139	-1.399	100.1	20.96
0.040	0.885	1237	-3.627	-3.764	73.80	17.99
0.080	0.961	1349	-4.859	-5.053	57.20	15.84
0.104	0.998	1412	-5.656	-5.526	50.28	14.85
0.200	1.085	1569	-6.344	-5.927	37.43	12.81
0.300	1.134	1664	-6.044	-5.560	31.85	11.82
0.400	1.165	1729	-5.585	-4.955	28.71	11.22
0.503	1.185	1773	-4.696	-4.196	26.86	10.85
0.601	1.200	1804	-3.857	-3.415	25.62	10.60
0.701	1.212	1830	-3.143	-2.586	24.62	10.39
0.801	1.216	1840	-1.748	-1.703	24.29	10.32
0.900	1.223	1854	-0.206	-0.839	23.78	10.21
1	1.233	1879	0	0	22.96	10.04
			313.15 K			
0	0.752	1055	0	0	119.4	23.09
0.011	0.792	1104	-1.164	-1.481	103.6	21.50
0.040	0.881	1223	-3.700	-3.962	75.94	18.41
0.080	0.957	1334	-4.955	-5.294	58.75	16.20
0.104	0.991	1396	-5.476	-5.764	51.76	15.20
0.200	1.080	1556	-6.323	-6.195	38.24	13.07
0.300	1.130	1651	-6.115	-5.808	32.46	12.04
0.400	1.162	1718	-5.685	-5.178	29.18	11.41

0.503	1.182	1761	-4.756	-4.383	27.28	11.03
0.601	1.200	1792	-3.920	-3.566	26.01	10.78
0.701	1.209	1819	-3.191	-2.700	24.99	10.56
0.801	1.213	1828	-1.800	-1.778	24.67	10.49
0.900	1.220	1843	-0.235	-0.877	24.14	10.38
1	1.230	1868	0	0	23.30	10.20

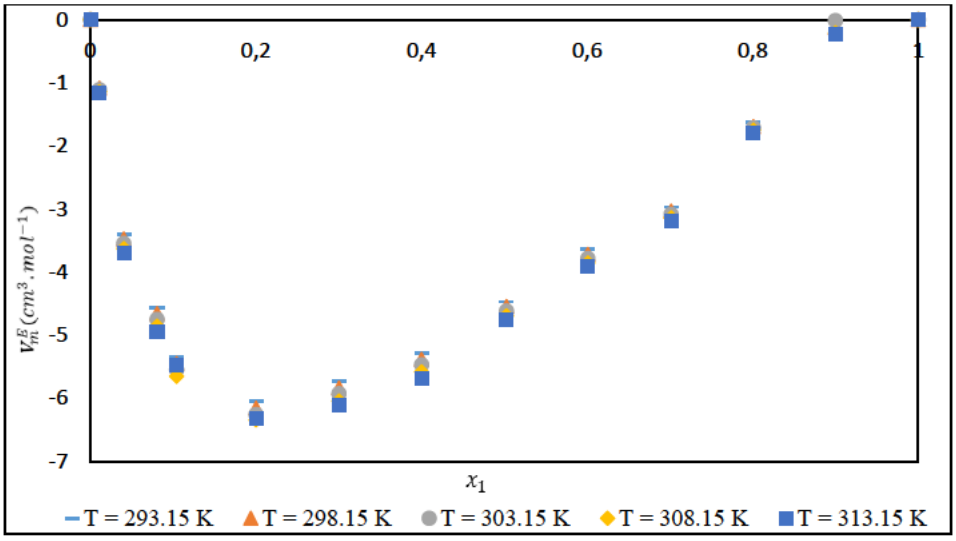

Figure 5-13: Excess molar volumes (V_m^E) for {[(EMPYR) Br + Gly] (x_1) + ethanol (x_2)}, binary systems as a function of mole fraction of x_1 = (0-1) at T = (293.15; 298.15; 303.15; 308.15; and 313.15) K

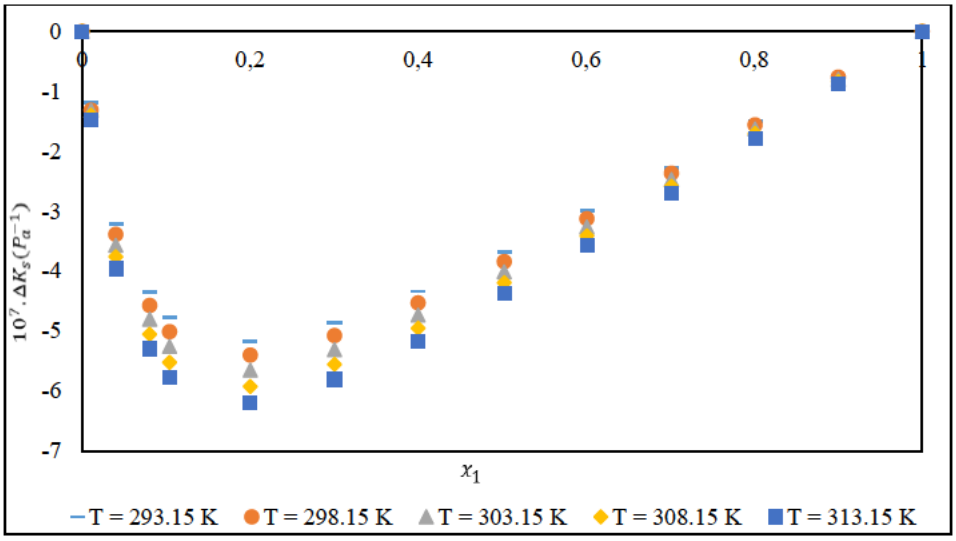

Figure 5-14: Variation in isentropic compressibilities (ΔK_s) for {[(EMPYR) Br + Gly] (x_1) + ethanol (x_2)}, binary systems as a function of mole fraction of x_1 = (0-1) at T = (293.15; 298.15; 303.15; 308.15; and 313.15) K

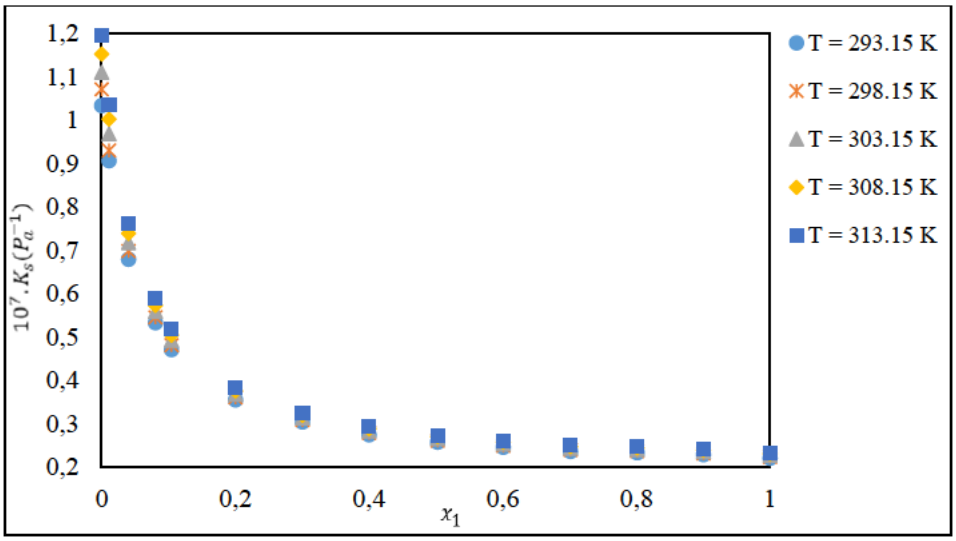

Figure 5-15: Isentropic compressibilities (K_s) for {[[EMPYR]Br + Gly] (x_1) + ethanol (x_2)}, binary systems as a function of mole fraction of x_1 = (0-1) at T = (293.15; 298.15; 303.15; 308.15; and 313.15) K

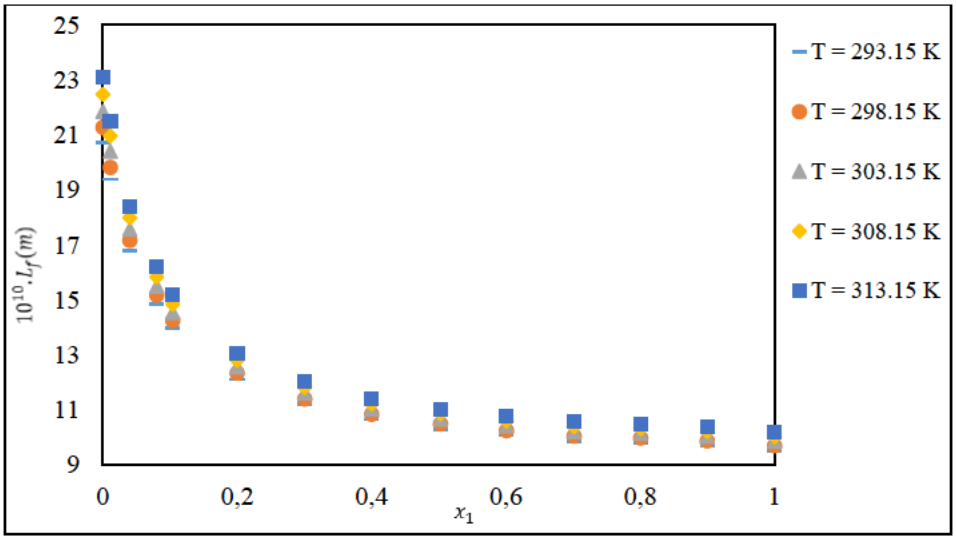

Figure 5-16: Intermolecular free length values (L_f) for {[(EMPYR) Br + Gly] (x_1) + ethanol (x_2)}, binary systems as a function of mole fraction of x_1= (0-1) at T = (293.15; 298.15; 303.15; 308.15; and 313.15) K

Table 5-5 to 5-8 lists the standard deviations and constants coefficients for all investigated binary systems.

Table 5-5: Standard deviations (σ) and constant coefficients (A_i) for {[(EMPYR) Br + EG] (x_1) + methanol (x_2)}, binary systems at different temperatures and at atmospheric pressure

Properties	T/K	A_0	A_1	A_2	A_3	σ
V_m^E/cm^3.mol^{-1}	293.15	-6.542	-3.138	-2.982	-2.939	0.018
	298.15	-6.645	-3.183	-3.038	-3.001	0.021
	303.13	-6.752	-3.214	-3.085	-3.061	0.021
	308.15	-6.864	-3.262	-3.149	-3.129	0.022
	313.15	-6.976	-3.300	-3.199	-3.179	0.023
$10^7.\Delta K_s$/Pa^{-1}	T/K	A_0	A_1	A_2	A_3	σ
	293.15	-15.61	-7.286	-6.688	-6.782	0.056
	298.15	-16.44	-7.606	-6.944	-7.267	0.057
	303.13	-17.35	-7.944	-6.228	-7.566	0.061

	308.15	-18.29	-8.178	-7.736	-8.576	0.078
	313.15	-19.33	-8.716	-7.745	-8.274	0.080
$10^{-10}.L_f$/m	T/K	A_0	A_1	A_2	A_3	σ
	293.15	6.253	-4.364	25.28	17.84	0.413
	298.15	6.374	-4.567	25.67	18.62	0.422
	303.13	6.526	-4.782	25.88	18.48	0.512
	308.15	6.596	-4.894	26.19	18.88	0.541
	313.15	6.716	-5.079	26.46	19.24	0.538

Table 5-6: Standard deviations (σ) and constant coefficients (A_i) for {[(EMPYR) Br + EG] (x_1) + ethanol (x_2)}, binary systems at different temperatures and at atmospheric pressure

Properties	T/K	A_0	A_1	A_2	A_3	σ
V_m^E/cm^3.mol^{-1}	293.15	-8.078	-4.066	-2.682	-2.626	0.025
	298.15	-8.466	-4.138	-2.744	-2.788	0.025
	303.13	-8.676	-4.182	-2.816	-2.979	0.026
	308.15	-8.788	-4.246	-2.897	-3.145	0.028
	313.15	-8.892	-4.312	-2.958	-3.268	0.030
$10^7.\Delta K_s$/Pa^{-1}	T/K	A_0	A_1	A_2	A_3	σ
	293.15	-21.38	-6.371	-5.188	-6.703	0.071
	298.15	-22.09	-6.842	-5.562	-7.248	0.072
	303.13	-23.14	-7.453	-5.904	-7.708	0.072
	308.15	-24.32	-7.861	-6.324	-8.025	0.074
	313.15	-26.02	-8.222	-6.868	-8.486	0.074
$10^{-10}.L_f$/m	T/K	A_0	A_1	A_2	A_3	σ
	293.15	7.246	-4.644	26.38	18.84	0.398
	298.15	7.581	-4.617	26.74	19.62	0.444

	303.13	7.688	-4.872	26.96	19.48	0.456
	308.15	7.789	-4.984	26.97	20.88	0.462
	313.15	7.982	-5.209	27.36	20.24	0.462

Table 5-7: Standard deviations (σ) and constant coefficients (A_i) for {[(EMPYR) Br + Gly] (x_1) + methanol (x_2)}, binary systems at different temperatures and at atmospheric pressure

Properties	T/K	A_0	A_1	A_2	A_3	σ
V_m^E/cm^3.mol^{-1}	293.15	-6.542	-3.138	-2.982	-2.939	0.018
	298.15	-6.645	-3.182	-3.038	-3.001	0.021
	303.13	-6.752	-3.214	-3.085	-3.061	0.021
	308.15	-6.864	-3.262	-3.149	-3.129	0.022
	313.15	-6.976	-3.300	-3.299	-3.179	0.023
ΔK_s/Pa^{-1}	T/K	A_0	A_1	A_2	A_3	σ
	293.15	-15.61	-7.286	-6.688	-6.782	0.056
	298.15	-16.44	-7.606	-6.944	-7.267	0.057
	303.13	-17.35	-7.944	-7.228	-7.566	0.061
	308.15	-18.29	-8.178	-7.736	-8.578	0.078
	313.15	-19.33	-8.716	-7.745	-8.274	0.080
10^{-10}.L_f/m	T/K	A_0	A_1	A_2	A_3	σ
	293.15	7.253	-4.364	25.28	17.84	0.422
	298.15	7.374	-4.567	25.67	18.62	0.422
	303.13	7.526	-4.782	25.88	18.48	0.438
	308.15	7.596	-5.494	25.91	18.68	0.436
	313.15	7.716	-5.079	26.46	19.31	0.458

Table 5-8: Standard deviations (σ) and constant coefficients (A_i) for {[(EMPYR) Br + Gly] (x_1) + ethanol (x_2)}, binary systems at different temperatures and at atmospheric pressure

Properties	T/K	A_0	A_1	A_2	A_3	σ
V_m^E/cm^3.mol^{-1}	293.15	-8.078	-4.066	-2.682	-2.626	0.025
	298.15	-8.466	-4.138	-2.744	-2.788	0.025
	303.13	-8.676	-4.182	-2.816	-2.979	0.026
	308.15	-8.788	-4.246	-2.897	-3.145	0.028
	313.15	-8.892	-4.312	-2.958	-3.268	0.030
ΔK_s/Pa^{-1}	T/K	A_0	A_1	A_2	A_3	σ
	293.15	-21.38	-6.372	-5.188	-6.703	0.071
	298.15	-22.09	-7.843	-5.562	-7.248	0.072
	303.13	-23.14	-7.452	-5.904	-7.708	0.072
	308.15	-24.32	-8.861	-6.324	-8.025	0.074
	313.15	-26.02	-8.225	-6.868	-8.486	0.074
10^{-10}.L_f/m	T/K	A_0	A_1	A_2	A_3	σ
	293.15	7.553	-4.664	26.48	18.52	0.434
	298.15	7.674	-4.867	26.67	18.68	0.442
	303.13	8.226	-5.882	26.88	19.39	0.442
	308.15	8.496	-5.394	27.19	19.68	0.440
	313.15	8.716	-5.679	27.46	20.02	0.448

5.2 Experimental Infinite Dilution Activity Coefficient Data

5.2.1 1-ethyl-1-methylpyrrolidinium bromide + glycerol, [(EMPYR) Br + Gly]

Table 5-9: Averages of infinite dilution activity coefficients for the chosen organic solutes in the [(EMPYR) Br + Gly], DES at a mole ratio of 1,000: 2,000 and at four different temperatures: With the standard state of the solute's hypothetical liquid at zero pressure.

Organic Solutes	Average of infinite dilution activity coefficients (γ^{∞}_{13}) at T/K			
	T = 313.15K	T = 323.15K	T = 333.15K	T = 343.15K
2,2-dimethylbutane	113.1	81.84	66.62	52.39
Pentane	62.49	44.01	38.93	30.76
Hexane	169.8	123.5	112.3	89.27
Heptane	364.7	257.8	223.8	199.7
Octane	500.6	462.0	437.1	414.7
n-Nonane	865.2	529.3	479.9	408.8
n-Decane	1392	931.0	806.9	659.3
1-Pentene	45.72	37.31	30.59	25.29
1-Hexene	123.1	96.20	87.01	69.44
1-Heptene	280.7	232.9	215.0	176.5
1-Nonene	577.3	514.8	464.0	389.5
1-Decene	835.7	685.1	582.7	505.5
Cyclopentane	57.55	47.67	38.31	28.17
Cyclohexene	116.0	89.31	62.61	35.54
Cyclohexane	159.4	119.7	92.47	66.18
Methylcyclohexane	441.2	349.1	289.4	217.6
1-Pentyne	41.80	36.07	30.84	26.08
1-Hexyne	103.4	92.10	73.82	67.18
1-Heptyne	162.5	152.7	145.4	128.6
o-Xylene	106.1	104.0	101.5	98.30
m-Xylene	162.8	160.1	158.0	156.9
p-Xylene	142.3	140.3	138.9	136.2
Toluene	71.58	68.06	66.16	62.63
Benzene	34.12	32.44	30.81	28.79
Ethylbenzene	130.5	127.6	124.8	120.0
Methanol	1.221	1.201	1.188	1.167

Ethanol	3.116	3.033	2.829	2.727
2-Propanol	7.278	7.091	6.920	6.704
Butan-1-ol	8.600	8.281	8.099	7.974
Acetone	5.992	5.941	5.902	5.653
MEK	11.30	11.08	10.71	10.60
Thiophene	17.47	17.30	17.19	17.07

Standard uncertainties (u): u (γ^{∞}_{13}) = 5%; u (T) = 0.01 K; u (p) = 1kPa; and u (x) = 0.05

Table 5-10: Partial molar excess properties such as enthalpies ($\Delta H_1^{E,\infty}$), Gibbs free energies ($\Delta G_1^{E,\infty}$), and entropies ($T_{ref}\,\Delta S_1^{E,\infty}$) for the organic solutes in the [(EMPYR) Br + Gly], DES at the reference temperature $T_{ref} = 313.15$ K.

Organic solutes	$\Delta H_1^{E,\infty}$/kJ.mol^{-1}	$\Delta G_1^{E,\infty}$/kJ.mol^{-1}	$T_{ref}\,\Delta S_1^{E,\infty}$/kJ.mol^{-1}
2,2-dimethylbutane	-24.21	12.34	-36.54
Pentane	-12.42	9.874	-22.30
Hexane	-21.01	15.17	-36.18
Heptane	-19.05	13.33	-32.37
Octane	-20.88	15.55	-36.43
n-Nonane	-12.91	16.75	-29.66
n-Decane	-16.89	18.33	-35.22
1-Pentene	-14.05	9.719	-23.77
1-Hexene	-17.05	12.53	-29.58
1-Heptene	-13.82	14.68	-28.50
1-Nonene	-11.72	16.56	-28.27
1-Decene	-14.97	17.52	-32.49
Cyclopentane	21.28	8.692	12.58
Cyclohexene	31.31	9.640	21.67
Cyclohexane	26.18	10.92	15.26
Methylcyclohexane	21.05	14.01	7.036
1-Pentyne	-17.63	8.411	-26.04
1-Hexyne	-12.85	10.95	-23.81
1-Heptyne	-6.741	12.67	-19.66

o-Xylene	2.271	11.95	-9.675
m-Xylene	1.097	13.16	-12.07
p-Xylene	1.315	12.79	-11.48
Toluene	3.978	10.77	-6.795
Benzene	5.056	8.749	-3.693
Ethylbenzene	2.512	12.46	-9.952
Methanol	1.347	0.412	1.359
Ethanol	3.971	2.612	0.945
2-Propanol	2.445	4.954	-2.509
Butan-1-ol	2.251	5.406	-3.154
Acetone	1.734	1.734	-2.776
MEK	1.905	1.905	-4.242
Thiophene	0.397	0.397	-7.001

Standard uncertainties (u): u ($\Delta G_1^{E,\infty}$) = 5%; u ($\Delta H_1^{E,\infty}$) = 5%; u ($\Delta S_1^{E,\infty}$) = 5%; u (T) = 0.01 K; u (p) = 0.1kPa; and u (x) = 0.05

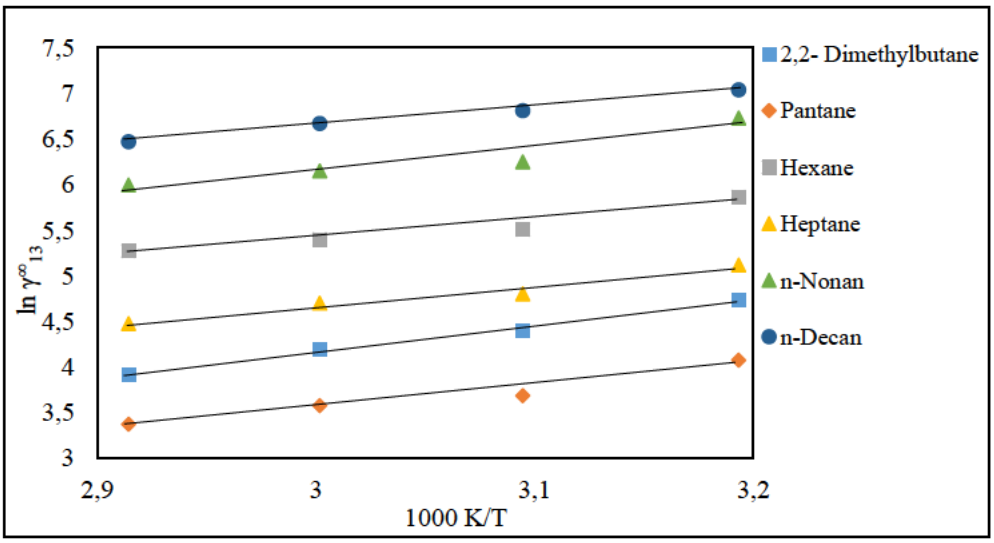

Figure 5-17: Plot of ln γ_{13}^{∞} versus 1000 K/T for the selected alkanes in [(EMPYR) Br + Gly] at T = (313.15-343.15) K

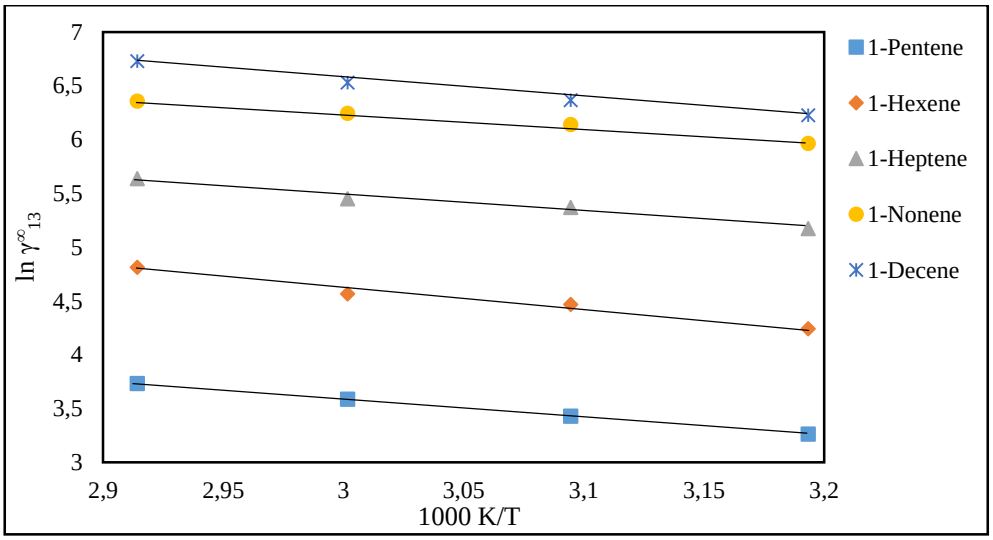

Figure 5-18: Plot of ln γ^{∞}_{13} versus 1000 K/T for the selected alkenes in [(EMPYR) Br + Gly] at T = (313.15-343.15) K

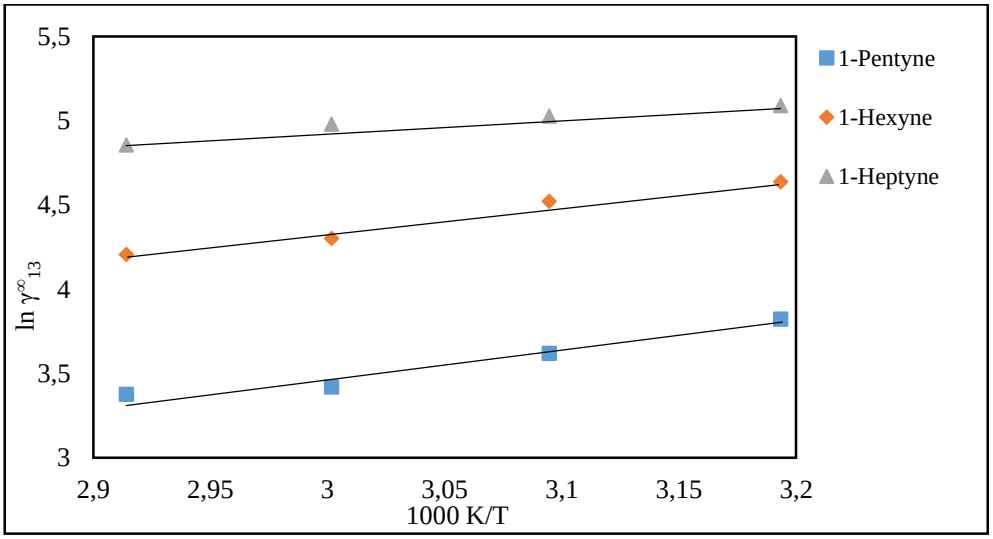

Figure 5-19: Plot of ln γ^{∞}_{13} versus 1000 K/T for the selected alkynes in [(EMPYR) Br + Gly] at T = (313.15-343.15) K

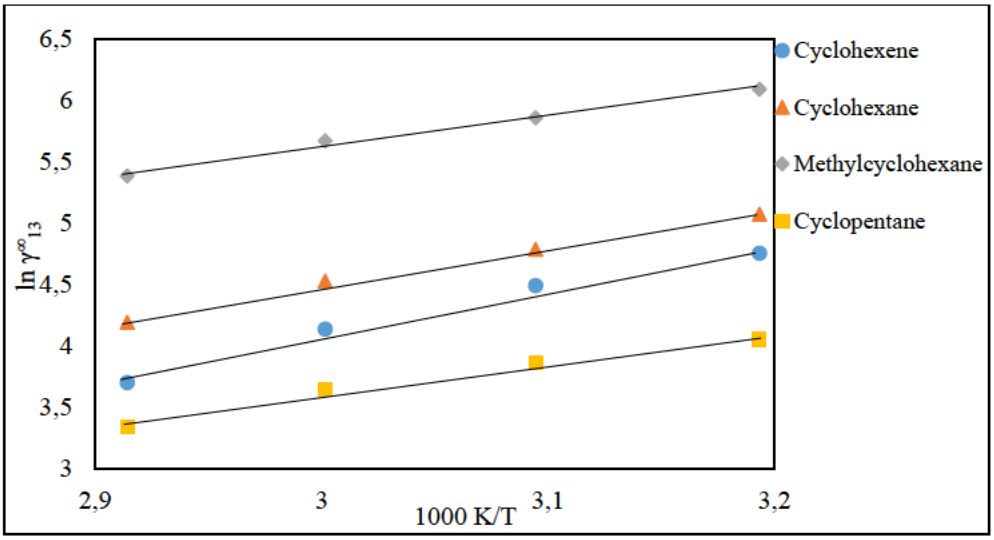

Figure 5-20: Plot of ln γ_{13}^{∞} [redacted]us 1000 K/T for the selected cycloalkanes in [(EMPYR) Br + Gly] at T = (313.15-343.15) K

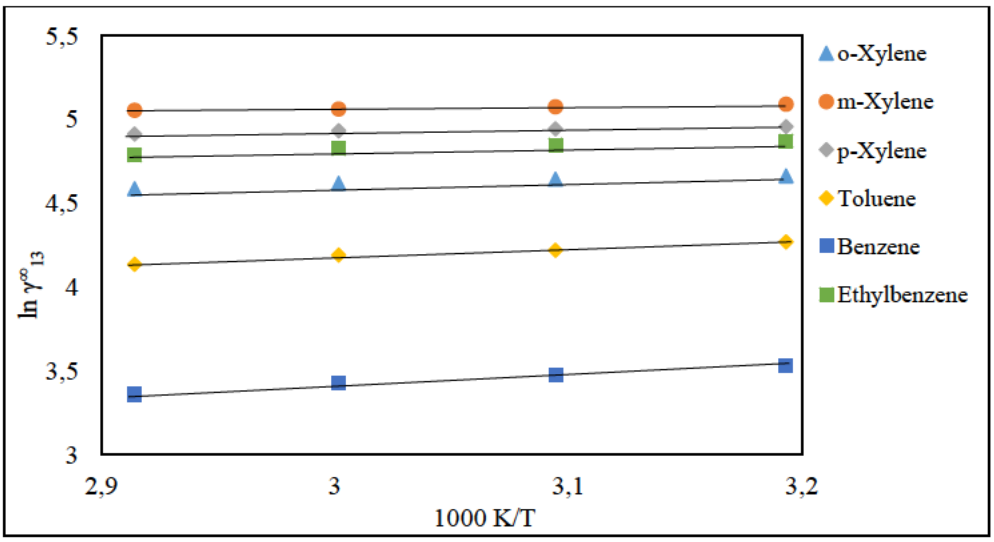

Figure 5-21: Plot of ln γ_{13}^{∞} versus 1000 K/T for the selected alkyl benzenes in [(EMPYR) Br + Gly] at T = (313.15-343.15) K

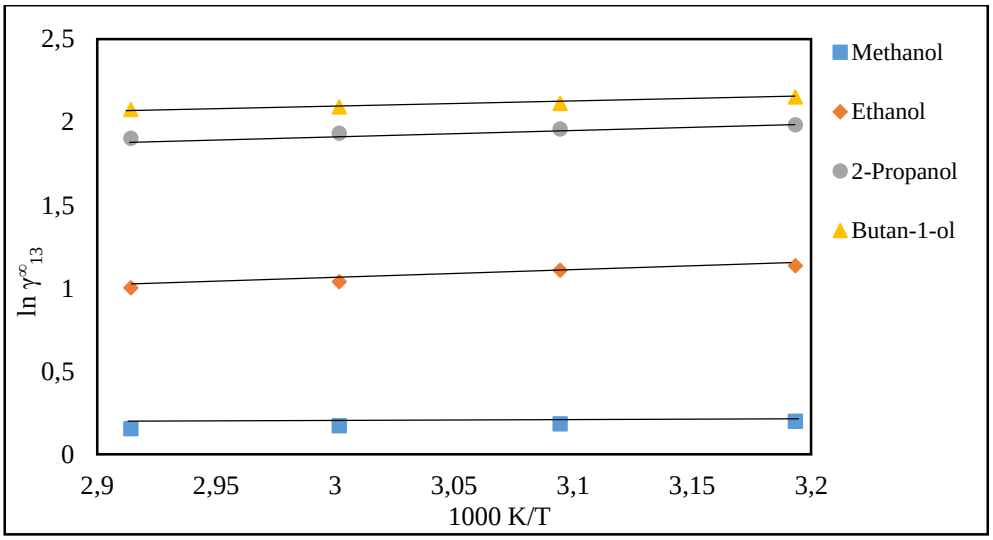

Figure 5-22: Plot of ln γ^{∞}_{13} versus 10[redacted]K/T for the selected alcohols in [(EMPYR)Br + Gly] at T = (313.15-343.15) K

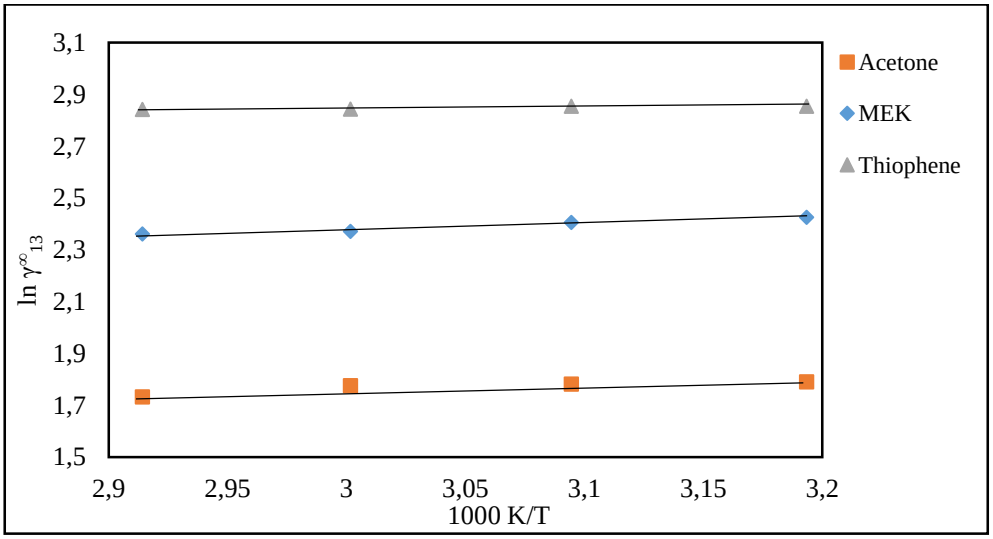

Figure 5-23: Plot of ln γ^{∞}_{13} versus 1000 K/T for the selected ketones and thiophene in [(EMPYR) Br + Gly] at T = (313.15-343.15) K

5.2.2 1-ethyl-1-methylpyrrolidinium bromide + ethylene glycol, [(EMPYR)Br + EG]

Table 5-11: Averages of infinite dilution activity coefficients for the chosen organic solutes in the [(EMPYR) Br + EG], DES at a mole ratio of 1,002: 3,998 and at four different temperatures: With the standard state of the solute's hypothetical liquid at zero pressure.

	Averages of infinite dilution activity coefficients (γ^{∞}_{13}) at T/K			
Organic solutes	T= 313.15 K	T= 323.15 K	T= 333.15 K	T= 343.15 K
1-Pentyne	1.010	1.064	1.111	1.171
1-Hexyne	1.086	1.151	1.215	1.274
1-Heptyne	1.130	1.199	1.260	1.319
1-Pentene	1.327	1.392	1.474	1.537
1-Hexene	1.400	1.473	1.573	1.671
1-Nonene	1.699	1.793	1.888	1.988
1-Decene	1.818	1.921	2.009	2.118
2,2-Dimethylbutane	1.361	1.430	1.479	1.539
Pentane	1.412	1.476	1.526	1.581
Hexane	1.669	1.763	1.846	1.928
Heptane	1.787	1.893	2.038	2.118
Octane	1.898	2.007	2.128	2.249
n-Nonane	2.010	2.193	2.243	2.368
n-Decane	2.095	2.199	2.323	2.439
Cyclopentane	1.232	1.274	1.309	1.342
Cyclohexane	1.319	1.358	1.397	1.414
Methylcyclohexane	1.475	1.522	1.587	1.623
Cyclooctane	1.506	1.571	1.628	1.710
Cyclopentene	0.725	0.786	0.845	0.913
Cyclohexene	1.000	1.099	1.159	1.242
o-Xylene	1.003	1.058	1.099	1.140
m-Xylene	1.192	1.249	1.304	1.389
p-Xylene	1.149	1.203	1.258	1.307
Benzene	0.920	0.971	1.006	1.045

Toluene	0.969	1.019	1.059	1.101
Ethylbenzene	1.099	1.145	1.198	1.249
Methanol	0.781	0.833	0.886	0.930
Ethanol	0.805	0.884	0.968	1.039
2-Propanol	0.882	0.968	1.057	1.135
Butan-1-ol	0.937	1.030	1.109	1.207
Acetone	1.032	1.068	1.111	1.147
MEK	1.110	1.153	1.207	1.262

Standard uncertainties (u): u (γ^{∞}_{13}) = 5%; u (T) = 0.01 K; u (p) = 1kPa and u (x) = 0.05

Table 5-12: Partial molar properties such as enthalpies ($\Delta H_1^{E,\infty}$), Gibbs free energies ($\Delta G_1^{E,\infty}$), and entropies ($T_{ref}\,\Delta S_1^{E,\infty}$) for the organic solutes in the [(EMPYR) Br + EG], DES at the reference temperature, $T_{ref} = 313.15$ K.

Organic solutes	$\Delta H_1^{E,\infty}$/kJ.mol^{-1}	$\Delta G_1^{E,\infty}$/kJ.mol^{-1}	$T_{ref}\Delta S_1^{E,\infty}$/kJ.mol^{-1}
1-Pentyne	-4.405	51.81	-56.21
1-Hexyne	-4.893	49.34	-54.23
1-Heptyne	-4.611	47.26	-51.87
1-Pentene	-4.375	0.559	-3.816
1-Hexene	-5.270	-0.514	-4.756
1-Nonene	-4.678	-0.626	-5.305
1-Decene	-4.547	-1.597	-2.952
2,2-Dimethylbutane	-3.673	0.692	-4.365
Pentane	-3.367	0.782	-4.149
Hexane	-4.292	1.429	-5.720
Heptane	-5.055	0.440	-5.496
Octane	-5.053	0.675	-5.729
n-Nonan	-4.882	0.266	-5.147
n-Decan	-4.528	0.461	-4.989
Cyclopentane	-2.544	1.771	-4.315
Cyclohexane	-2.483	2.506	-4.989

Methylcyclohexane	-2.848	2.714	-5.562
Cyclooctane	-3.777	0.371	-4.149
Cyclopentene	-6.867	1.465	-8.331
Cyclohexene	-6.454	0.215	-6.669
o-Xylene	-3.810	1.387	-5.197
m-Xylene	-4.549	0.556	-5.105
p-Xylene	-3.828	1.086	-4.914
Benzene	-3.791	1.355	-5.147
Toluene	-3.795	1.418	-5.213
Ethylbenzene	-3.795	1.202	-4.997
Methanol	-5.211	-11.41	6.194
Ethanol	-7.596	-3.539	-4.058
2-Propanol	-7.532	7.892	-15.42
Butan-1-ol	-7.559	4.914	-12.47
Acetone	-3.146	0.553	-3.700
MEK	-3.832	1.032	-4.864

Standard uncertainties (u): u ($\Delta G_1^{E,\infty}$) = 5%; u ($\Delta H_1^{E,\infty}$) = 5%; u ($\Delta S_1^{E,\infty}$) = 5%; u (T) = 0.01 K; u (p) = 0.1kPa; and u (x) = 0.05

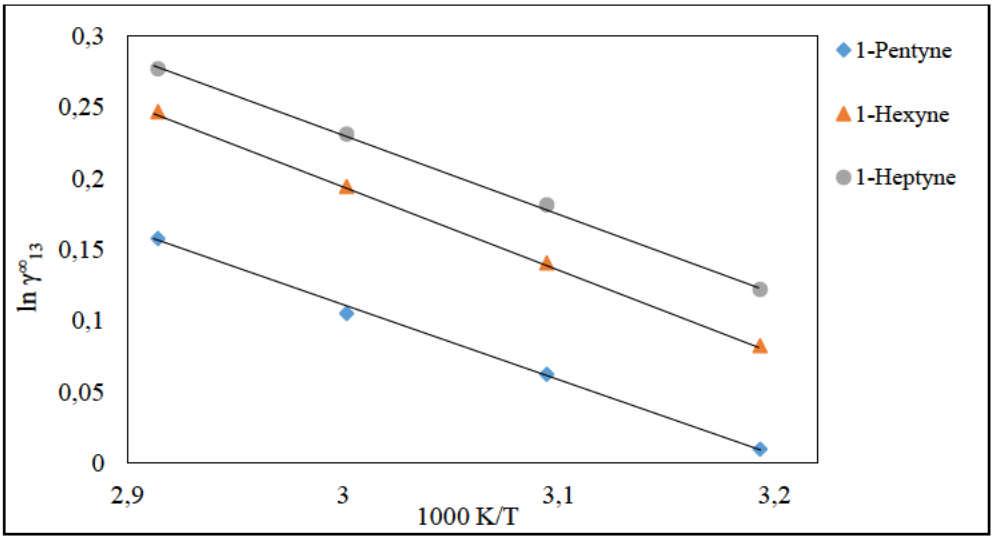

Figure 5-24: Plot of ln γ_{13}^{∞} versus 1000 K/T for the selected alkynes in [(EMPYR) Br + EG] at T = (313.15-343.15) K

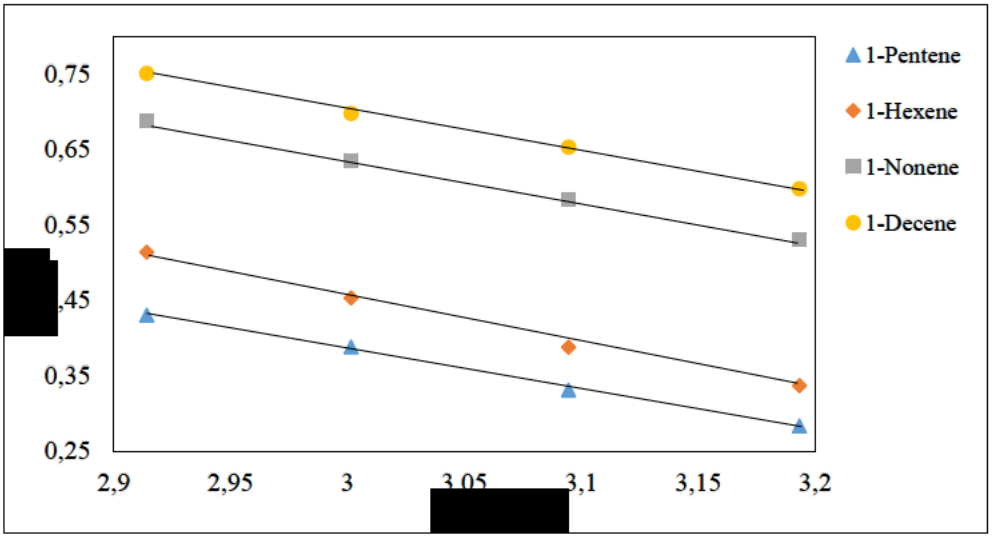

Figure 5-25: Plot of ln γ_{13}^{∞} versus 1000 K/T for the selected alkenes in [(EMPYR) Br + EG] at T = (313.15-343.15) K

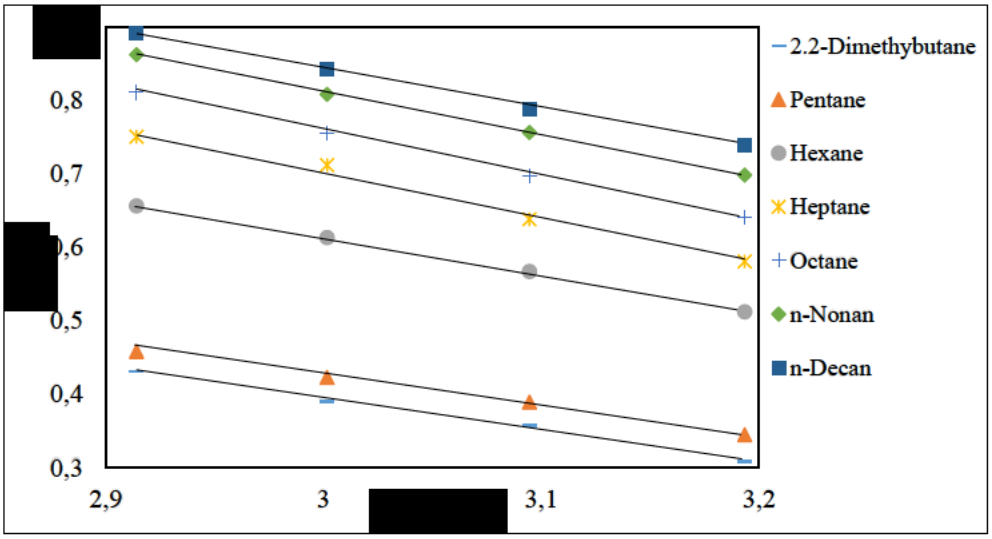

Figure 5-26: Plot of ln γ_{13}^{∞} versus 1000 K/T for the selected alkanes in [(EMPYR) Br + EG] at T = (313.15-343.15) K

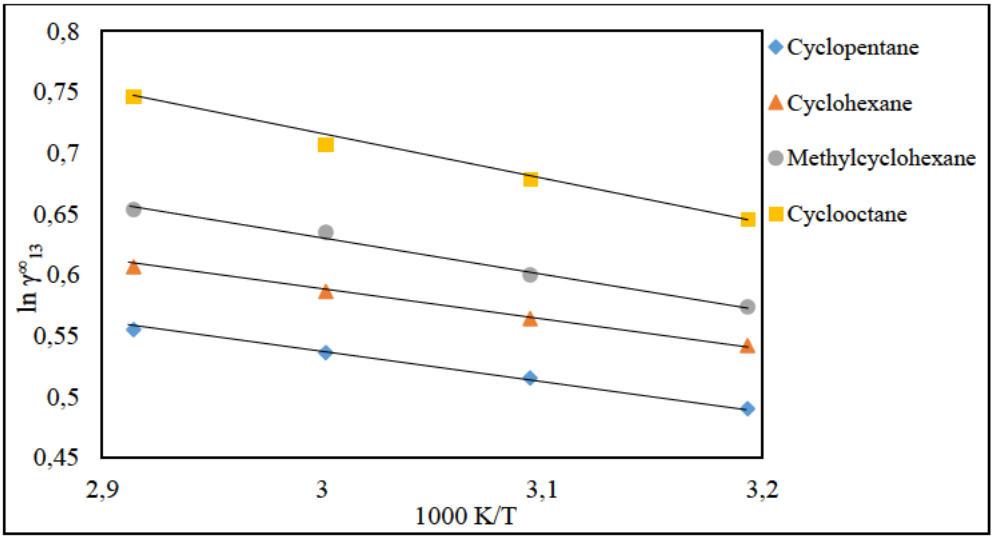

Figure 5-27: Plot of ln γ_{13}^{∞} versus 1000 K/T for the selected cycloalkanes in [(EMPYR) Br + EG] at T = (313.15-343.15) K

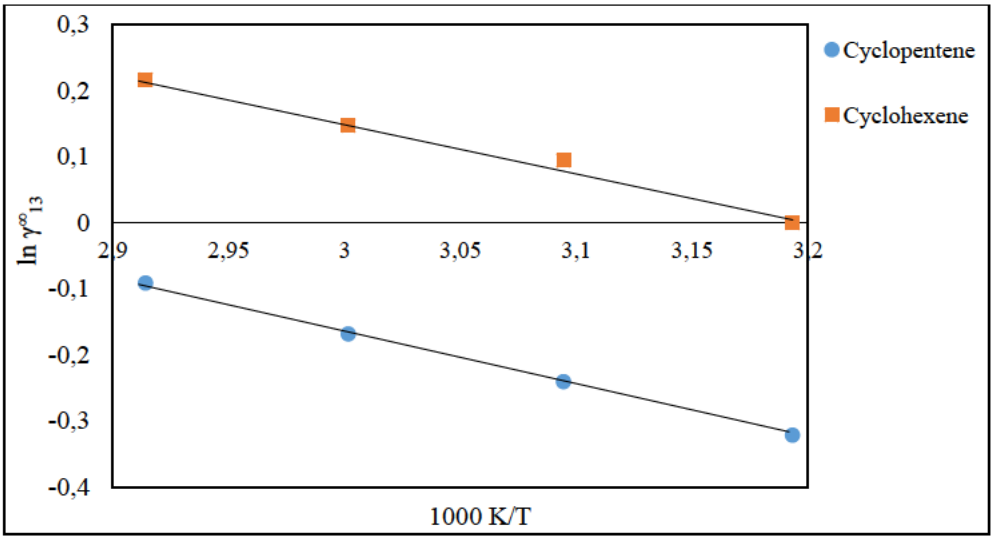

Figure 5-28: Plot of ln γ^{∞}_{13} versus 1000 K/T for the selected cycloalkenes in [(EMPYR) Br + EG] at T = (313.15-343.15) K

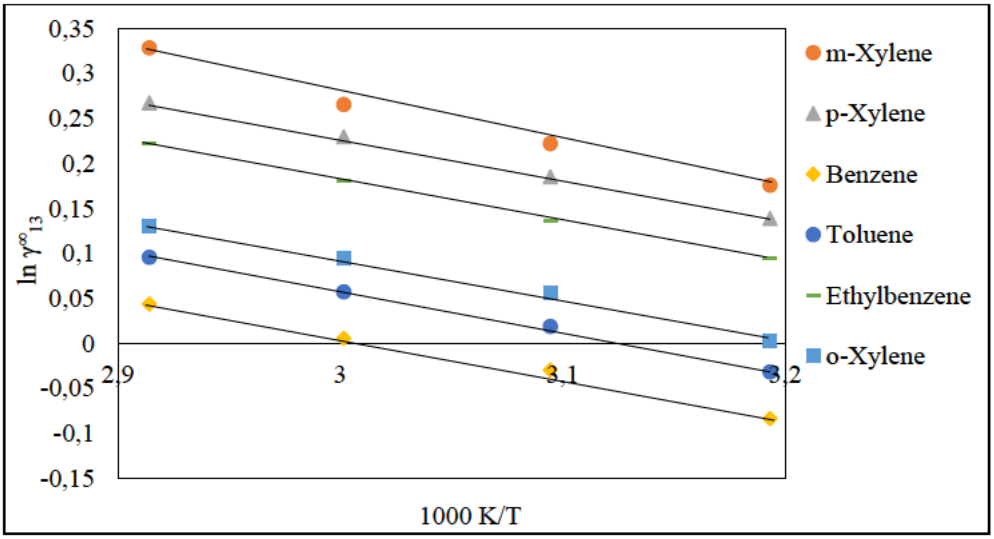

Figure 5-29: Plot of ln γ^{∞}_{13} versus 1000 K/T for the selected aromatics in [(EMPYR) Br + EG] at T = (313.15-343.15) K

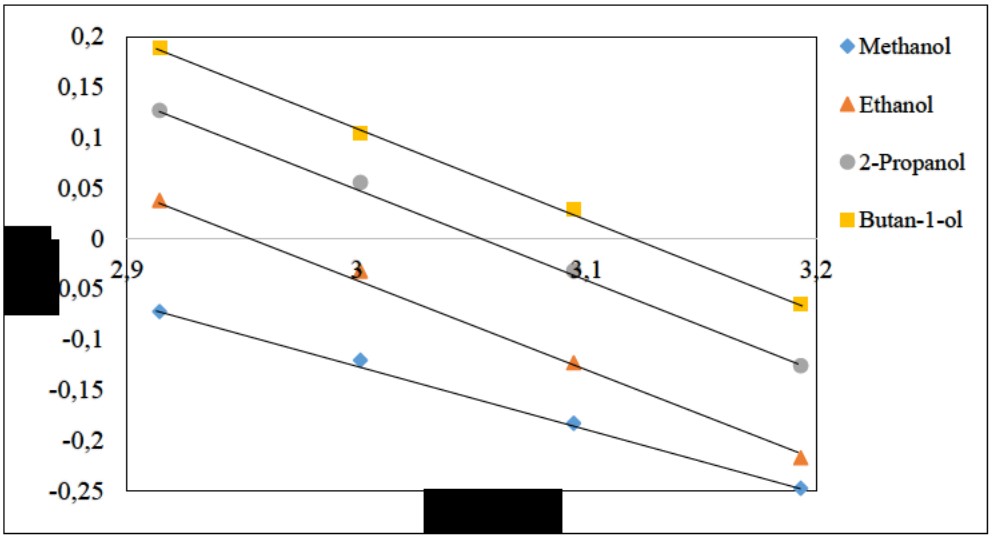

Figure 5-30: Plot of ln γ_{13}^{∞} versus 1000 K/T for the selected alcohols in [(EMPYR) Br + EG] at T = (313.15-343.15) K

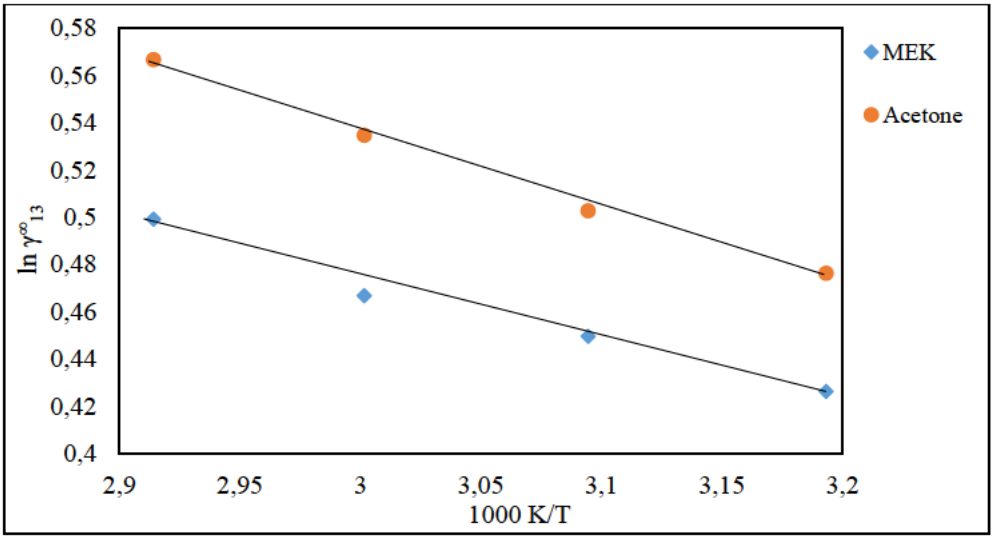

Figure 5-31: Plot of ln γ_{13}^{∞} versus 1000 K/T for the selected ketones in [(EMPYR) Br + EG] at T = (313.15-343.15) K

5.2.3 1-ethyl-1-methylpyrrolidinium bromide + 1.5-pentanediol, [(EMPYR) Br + 1.5-PDO]

Table 5-13: Averages of infinite dilution activity coefficients for the chosen organic solutes in the [(EMPYR) Br + 1.5-PDO], DES at a mole ratio of 1,001: 1,998 and at four different temperatures: With the standard state of the solute's hypothetical liquid at zero pressure.

	Averages of infinite dilution activity coefficients (γ^{∞}_{13}) at T/K			
Organic solutes	T = 313.15 K	T = 323.15 K	T = 333.15 K	T = 343.15 K
2,2-Dimethylbutane	2.902	2.922	2.942	2.967
Pentane	2.826	2.851	2.887	2.984
Hexane	2.889	2.994	3.095	3.184
Heptane	2.999	3.180	3.300	3.510
Octane	3.241	3.497	3.718	3.916
n-Nonan	3.736	3.985	4.292	4.519
n-Decan	3.952	4.267	4.607	4.912
1-Pentane	2.021	2.181	2.309	2.436
1-Hexene	2.295	2.457	2.559	2.685
1-Nonene	2.510	2.649	2.746	2.832
1-Decane	3.125	3.383	3.480	3.601
1-Pentyne	1.600	1.808	1.839	1.844
1-Hexyne	1.990	2.136	2.166	2.203
1-Heptyne	2.487	2.645	2.673	2.702
Cyclopentane	2.502	2.555	2.613	2.644
Cyclohexane	2.545	2.601	2.642	2.685
Methylcyclohexane	2.660	2.731	2.773	2.836
Cyclooctane	2.619	2.665	2.720	2.771
Cyclopentene	1.449	1.515	1.590	1.657
Cyclohexene	1.614	1.672	1.705	1.744
o-Xylene	1.331	1.480	1.600	1.715
m-Xylene	1.449	1.598	1.709	1.819
p-Xylene	1.538	1.636	1.738	1.853
Benzene	1.188	1.298	1.401	1.499

Toluene	1.208	1.310	1.424	1.537
Ethylbenzene	1.394	1.527	1.652	1.791
Methanol	0.175	0.251	0.341	0.459
Ethanol	0.222	0.303	0.409	0.542
2-Propanol	0.321	0.387	0.471	0.629
Butan-1-ol	0.347	0.482	0.576	0.704
Acetone	1.163	1.257	1.351	1.432
MEK	1.328	1.446	1.539	1.626
Water	0.174	0.250	0.340	0.454

Standard uncertainties (u): u (γ^{∞}_{13}) = 5%; u (T) = 0.01 K; u (p) = 1kPa; and u (x) = 0.05

Table 5-14: Partial molar properties such as enthalpies ($\Delta H_1^{E,\infty}$), Gibbs free energies ($\Delta G_1^{E,\infty}$), and entropies ($T_{ref}\,\Delta S_1^{E,\infty}$) for the organic solutes in the [(EMPYR) Br + 1.5-PDO], DES at the reference temperature $T_{ref} = 313.15$ K

Organic solutes	$\Delta H_1^{E,\infty}$/kJ.mol^{-1}	$\Delta G_1^{E,\infty}$/kJ.mol^{-1}	$T_{ref}\Delta S_1^{E,\infty}$/kJ.mol^{-1}
1-Pentyne	-4.234	5.809	-10.04
1-Hexyne	-3.030	6.174	-9.204
1-Heptyne	-2.467	5.914	-8.381
1-Pentene	-5.561	2.828	-8.389
1-Hexene	-4.683	3.732	-8.414
1-Nonene	-3.594	5.037	-8.631
1-Decene	-4.231	5.821	-10.05
2,2-Dimethylbutane	-0.717	8.263	-8.980
Pentane	-1.621	6.951	-8.572
Hexane	-2.902	5.695	-8.597
Heptane	-4.685	4.029	-8.714
Octane	-5.639	3.440	-9.079
n-Nonan	-5.669	3.301	-8.971
n-Decan	-6.476	2.321	-8.797
Cyclopentane	-1.645	6.453	-8.098

Cyclohexane	-1.595	6.637	-8.231
Methylcyclohexane	-1.909	6.745	-8.655
Cyclooctane	-1.679	6.760	-8.439
Cyclopentene	-3.992	10.24	-14.23
Cyclohexene	-2.313	8.047	-10.36
o-Xylene	-7.551	-2.662	-4.889
m-Xylene	-5.763	-0.708	-5.055
p-Xylene	-5.549	-0.468	-5.080
Benzene	-6.933	-1.928	-5.005
Toluene	-7.165	-2.135	-5.030
Ethylbenzene	-7.472	-2.334	-5.138
Methanol	-28.78	-35.13	6.352
Ethanol	-26.62	-31.51	4.897
2-Propanol	-19.73	-23.42	3.692
Butan-1-ol	-19.17	-24.05	3.226
Acetone	-5.569	-0.971	-4.598
MEK	-6.033	-2.607	-3.426
Water	-28.66	-24.88	-3.778

Standard uncertainties (u): u ($\Delta G_1^{E,\infty}$) = 5%; u ($\Delta H_1^{E,\infty}$) = 5%; u ($\Delta S_1^{E,\infty}$) = 5%; u (T) = 0.01 K; u (p) = 1kPa; and u (x) = 0.05

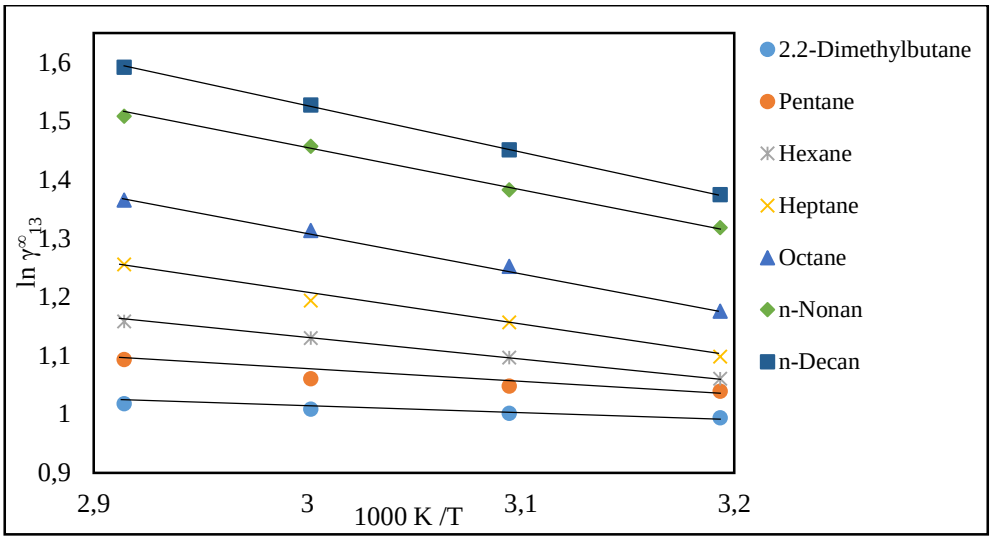

Figure 5-32: Plot of ln γ_{13}^{∞} versus 1000 K/T for the selected alkanes in [(EMPYR) Br + 1.5-PDO] at T = (313.15-343.15) K

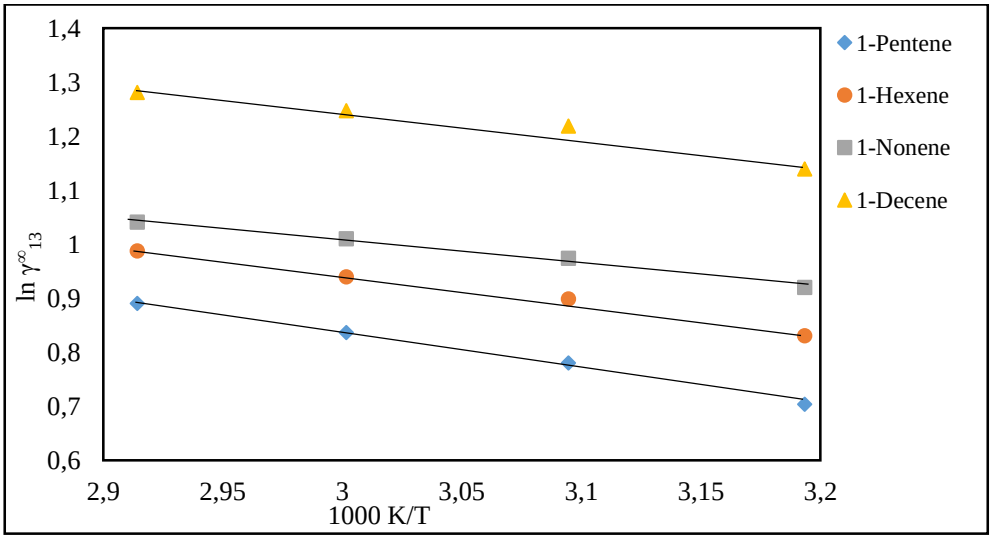

Figure 5-33: Plot of ln γ_{13}^{∞} versus 1000 K/T for the selected alkenes in [(EMPYR) Br + 1.5-PDO] at T = (313.15-343.15) K

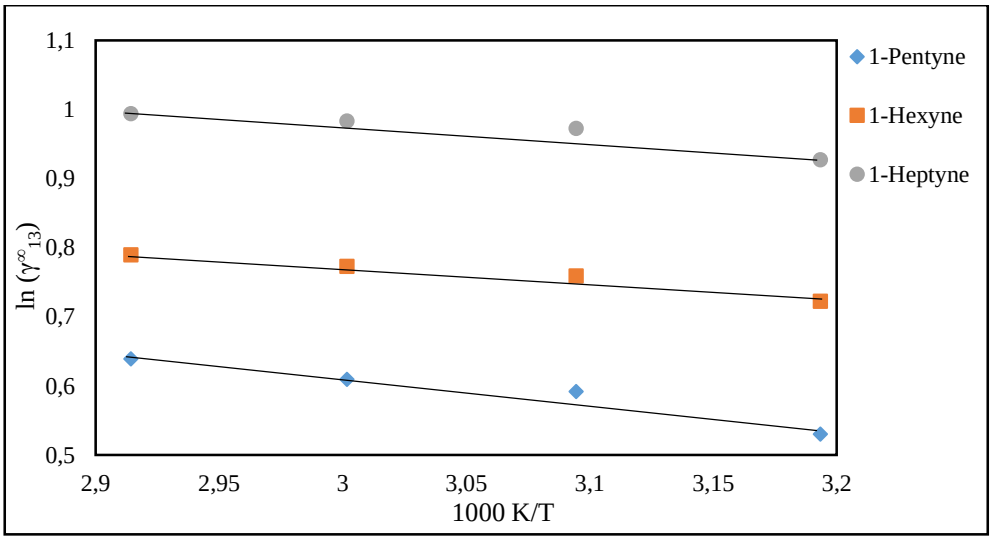

Figure 5-34: Plot of ln γ^{∞}_{13} versus 1000 K/T for the selected alkynes in [(EMPYR) Br + 1.5-PDO] at T = (313.15-343.15) K

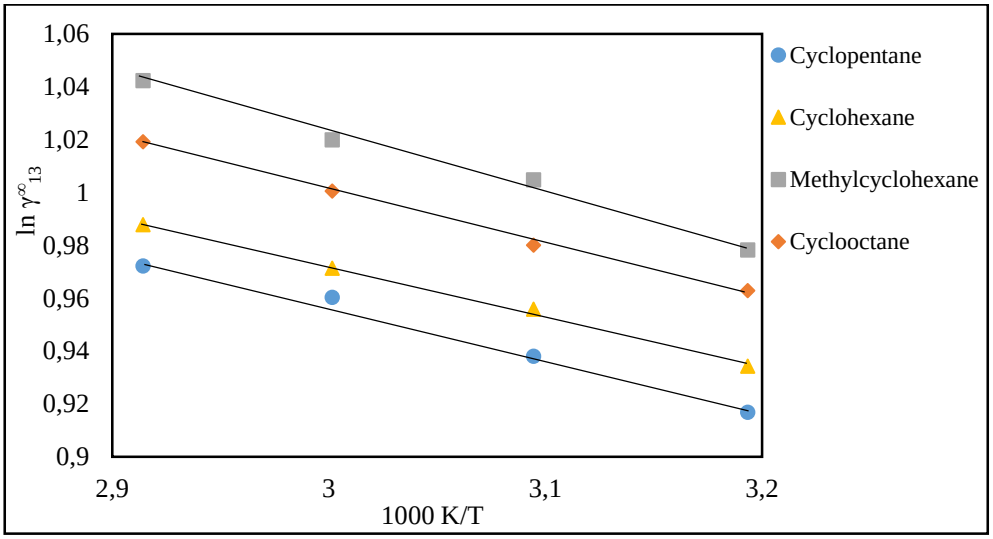

Figure 5-35: Plot of ln γ^{∞}_{13} versus 1000 K/T for the selected cycloalkanes in [(EMPYR) Br + 1.5-PDO] at T = (313.15-343.15) K

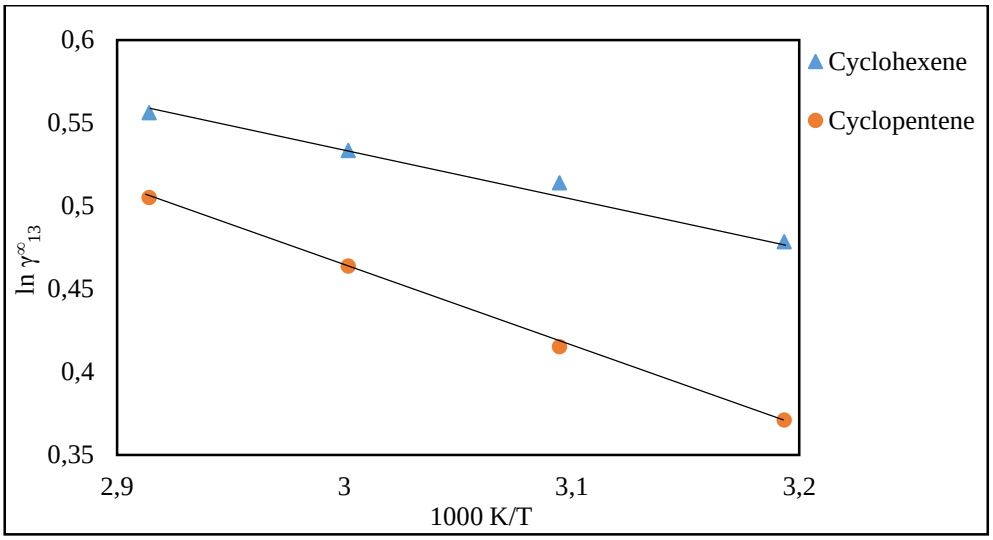

Figure 5-36: Plot of ln γ_{13}^{∞} versus 1000 K/T for the selected cycloalkenes in [(EMPYR) Br + 1.5-PDO] at T = (313.15-343.15) K

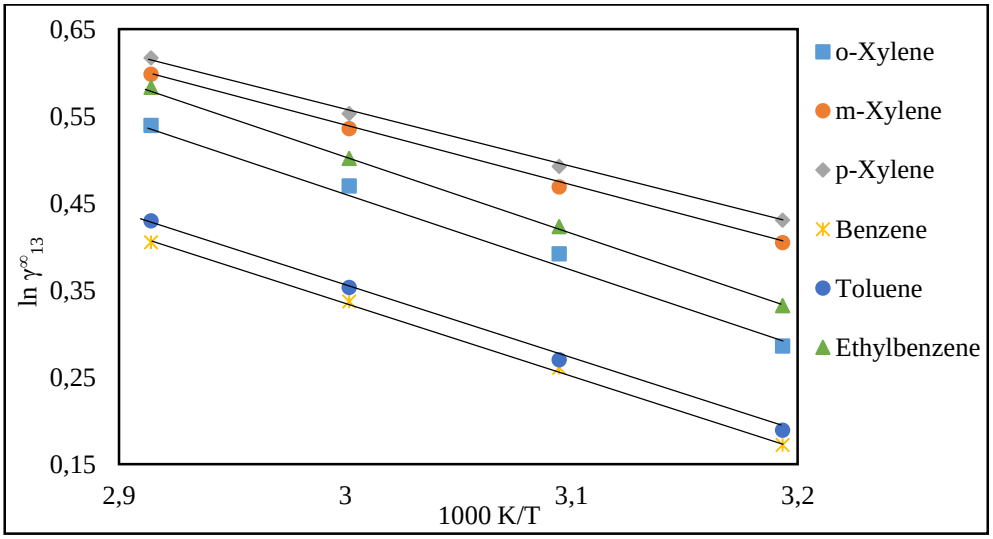

Figure 5-37: Plot of ln γ_{13}^{∞} versus 1000 K/T for the selected alkyl benzenes in [(EMPYR) Br + 1.5-PDO] at T = (313.15-343.15) K

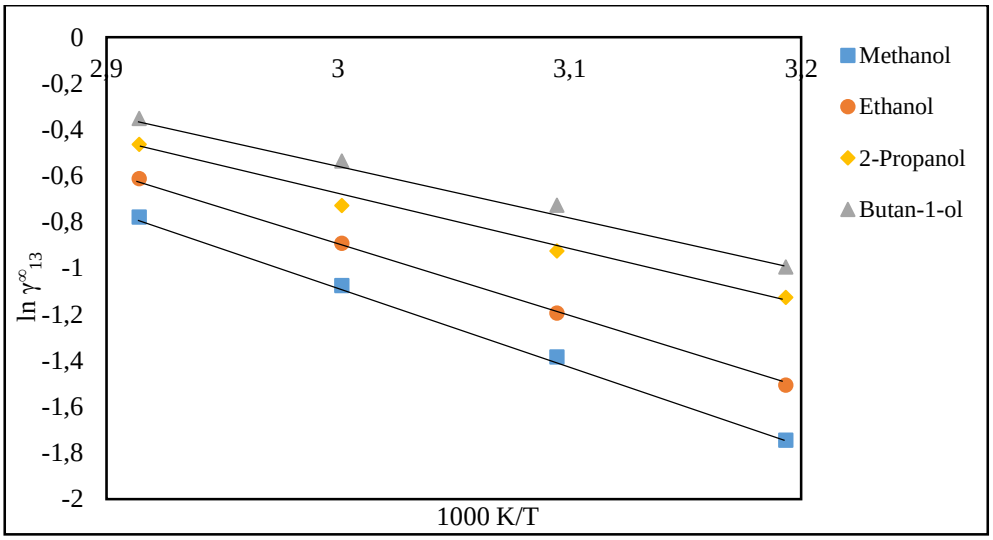

Figure 5-38: Plot of ln γ_{13}^{∞} versus 1000 K/T for the selected alcohols in [(EMPYR) Br + 1.5-PDO] at T = (313.15-343.15) K

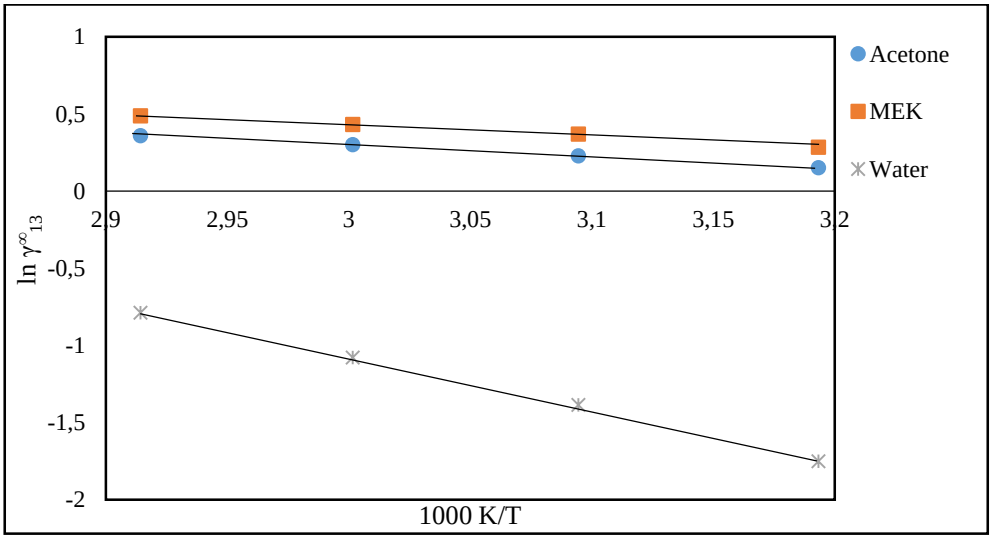

Figure 5-39: Plot of ln γ_{13}^{∞} versus 1000 K/T for the selected ketones and water in [(EMPYR) Br + 1.5-PDO] at T = (313.15-343.15) K

5.2.4 1-ethyl-1-methylpyrrolidinium bromide + 1.6-hexanediol, [(EMPYR) Br + 1.6-HDO]

Table 5-15: Averages of infinite dilution activity coefficients for the chosen organic solutes in the [(EMPYR) Br + 1.6-HDO], DES at a mole ratio of 1,000: 2,000 and at four different temperatures: With the standard state of the solute's hypothetical liquid at zero pressure.

	Average of infinite dilution activity coefficients (γ^{∞}_{13}) at T/K			
Organic Solutes	T = 313.15 K	T = 323.15 K	T = 333.15 K	T = 343.15 K
1-Pentene	2.505	2.608	2.729	2.814
1-Hexene	2.601	2.721	2.841	2.942
1-Nonene	3.087	3.262	3.390	3.517
1-Decene	3.570	3.635	3.858	3.994
1-Pentyne	1.787	1.791	1.800	1.813
1-Hexyne	2.100	2.105	2.122	2.134
1-Heptyne	2.636	2.674	2.733	2.774
2,2-Dimethylbutane	2.702	2.780	2.829	2.916
Pentane	2.892	2.949	3.005	3.059
Hexane	3.086	3.153	3.243	3.312
Heptane	3.226	3.283	3.366	3.420
Octane	3.348	3.451	3.569	3.689
n-Nonane	3.488	3.643	3.725	3.949
n-Decane	3.629	3.795	3.990	4.209
Cyclopentane	1.690	1.771	1.853	1.962
Cyclohexane	2.403	2.500	2.650	2.725
Methylcyclohexane	2.754	2.880	2.999	3.092
Cyclooctane	2.057	2.103	2.212	2.266
Cyclopentene	1.367	1.417	1.480	1.529
Cyclohexene	2.344	2.386	2.440	2.494
Benzene	1.630	1.746	1.851	1.947
Toluene	2.033	2.108	2.218	2.283
o-Xylene	3.037	3.097	3.175	3.203
m-Xylene	2.786	2.890	2.966	3.027

p-Xylene	2.575	2.695	2.793	2.875
Ethylbenzene	1.838	1.964	2.080	2.188
Methanol	0.979	1.063	1.131	1.202
Ethanol	1.081	1.189	1.297	1.401
2-Propanol	1.177	1.308	1.432	1.558
Butan-1-ol	1.340	1.460	1.594	1.726
Acetone	0.645	0.744	0.957	1.151
MEK	1.025	1.217	1.369	1.635
Water	0.511	0.630	0.780	0.891

Standard uncertainties (u): u (γ^{∞}_{13}) = 5%; u (T) = 0.01 K; u (p) = 1kPa; and u (x) = 0.05

Table 5-16: Partial molar properties such as enthalpies ($\Delta H_1^{E,\infty}$), Gibbs free energies ($\Delta G_1^{E,\infty}$), and entropies ($T_{ref}\,\Delta S_1^{E,\infty}$) for the organic solutes in the [(EMPYR) Br + 1.6-HDO], DES at the reference temperature $T_{ref} = 313.15$ K

Organic solutes	$\Delta H_1^{E,\infty}$/kJ.mol^{-1}	$\Delta G_1^{E,\infty}$/kJ.mol^{-1}	$T_{ref}\Delta S_1^{E,\infty}$/kJ.mol^{-1}
1-Pentyne	-0.435	12.29	-12.72
1-Hexyne	-0.475	11.52	-11.73
1-Heptyne	-1.571	9.554	-11.13
1-Pentene	-3.464	5.865	-9.329
1-Hexene	-3.665	6.162	-9.827
1-Nonene	-3.884	6.160	-10.04
1-Decene	-3.344	8.280	-11.62
2.2-Dimethylbutane	-2.263	7.878	-10.14
Pentane	-1.671	7.789	-9.459
Hexane	-2.108	7.936	-10.04
Heptane	-1.691	8.594	-10.29
Octane	-2.889	7.272	-10.16
n-Nonan	-3.697	6.448	-10.15
n-Decan	-4.417	4.921	-9.337
Cyclopentane	-4.441	2.211	-6.652

Cyclohexane	-3.749	5.048	-8.796
Methylcyclohexane	-3.446	5.492	-8.938
Cyclooctane	-2.882	3.842	-6.725
Cyclopentene	-3.325	4.410	-7.736
Cyclohexene	-1.887	5.685	-7.572
o-Xylene	-1.589	8.322	-9.911
m-Xylene	-2.477	7.134	-9.612
p-Xylene	-3.290	6.206	-9.496
Benzene	-5.291	0.430	-5.720
Toluene	-3.467	3.501	-6.968
Ethylbenzene	-5.194	1.449	-6.643
Methanol	-6.108	-4.878	-1.231
Ethanol	-7.719	-3.628	-4.091
2-Propanol	-8.360	-3.721	-4.639
Butan-1-ol	-7.543	-2.488	-5.055
Acetone	-17.27	-16.53	-0.748
MEK	-13.91	-10.86	-3.047
Water	-16.55	-9.143	-7.408

Standard uncertainties (u): u ($\Delta G_1^{E,\infty}$) = 5%; u ($\Delta H_1^{E,\infty}$) = 5%; u ($\Delta S_1^{E,\infty}$) = 5%; u (T) = 0.01 K; u (p) = 0.1kPa; and u (x) = 0.05

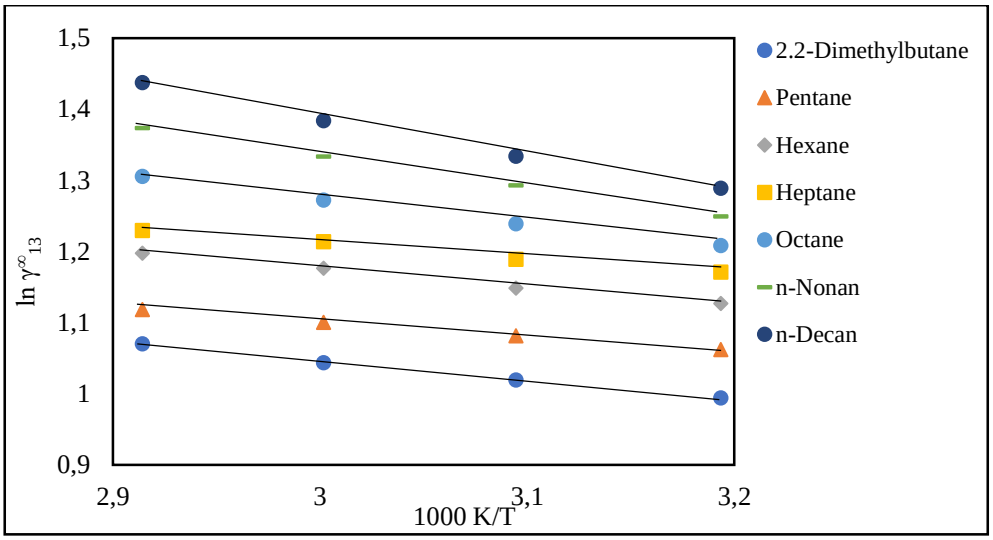

Figure 5-40: Plot of ln γ_{13}^{∞} versus 1000 K/T for the selected alkanes in [(EMPYR) Br + 1.6-HDO] at T = (313.15-343.15) K

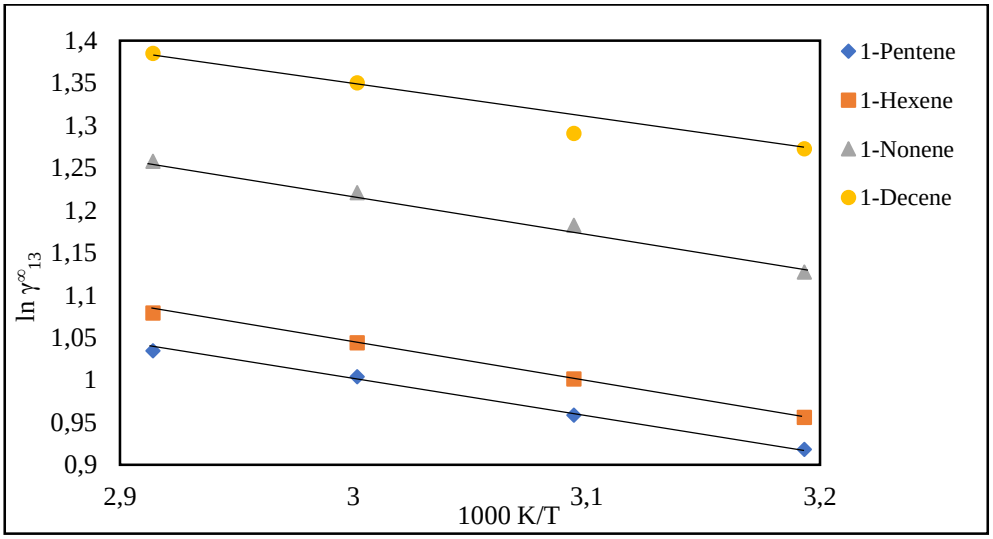

Figure 5-41: Plot of ln γ_{13}^{∞} versus 1000 K/T for the selected alkenes in [(EMPYR) Br + 1.6-HDO] at T = (313.15-343.15) K

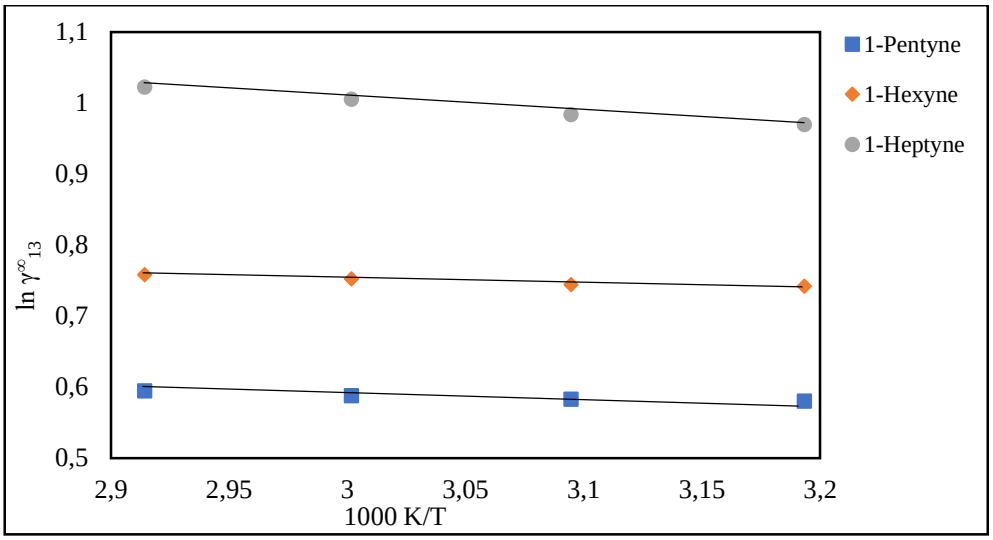

Figure 5-42: Plot of ln γ_{13}^{∞} versus 1000 K/T for the selected alkynes in [(EMPYR) Br + 1.6-HDO] at T = (313.15-343.15) K

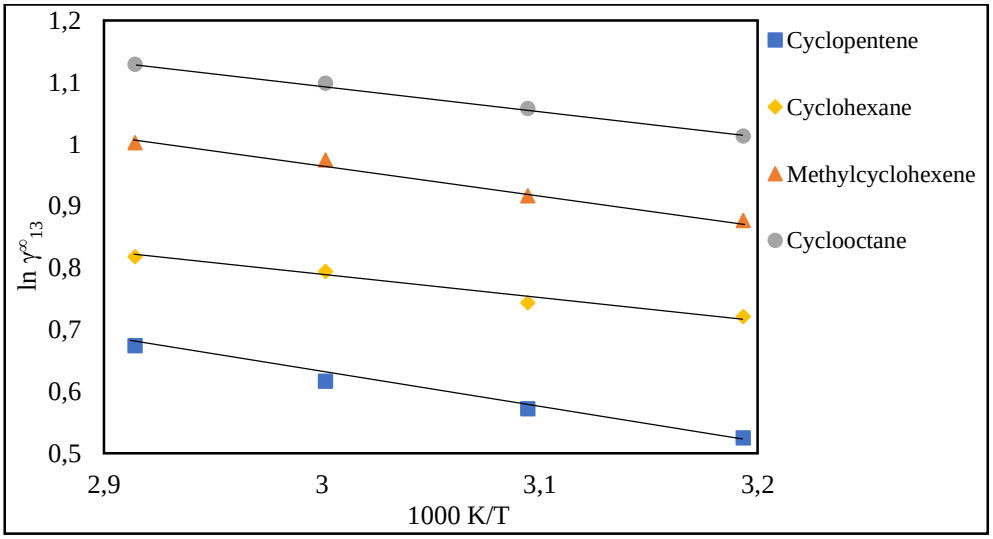

Figure 5-43: Plot of ln γ_{13}^{∞} versus 1000 K/T for the selected cycloalkanes in [(EMPYR) Br + 1.6-HDO] at T = (313.15-343.15) K

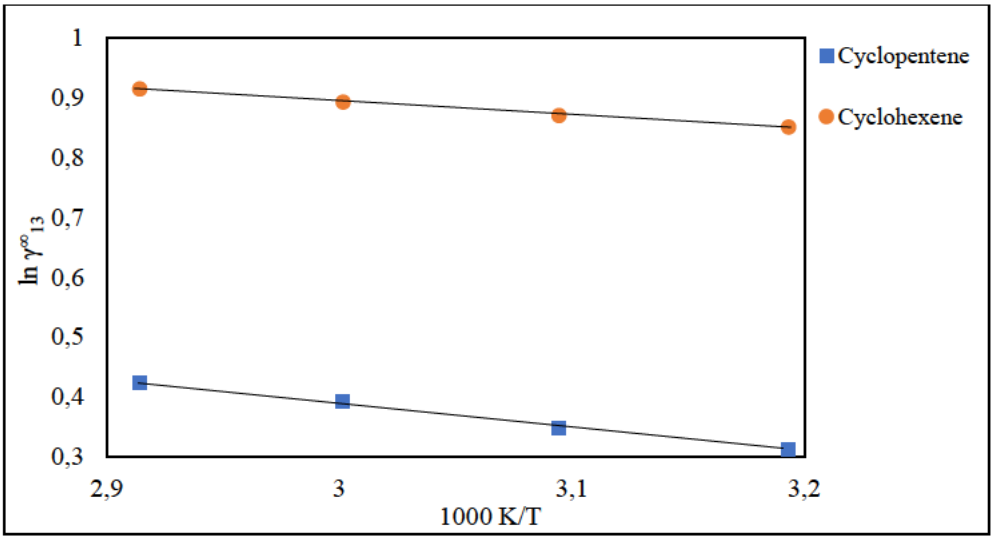

Figure 5-44: Plot of ln γ_{13}^{∞} versus 1000 K/T for the selected cycloalkenes in [(EMPYR) Br + 1.6-HDO] at T = (313.15-343.15) K

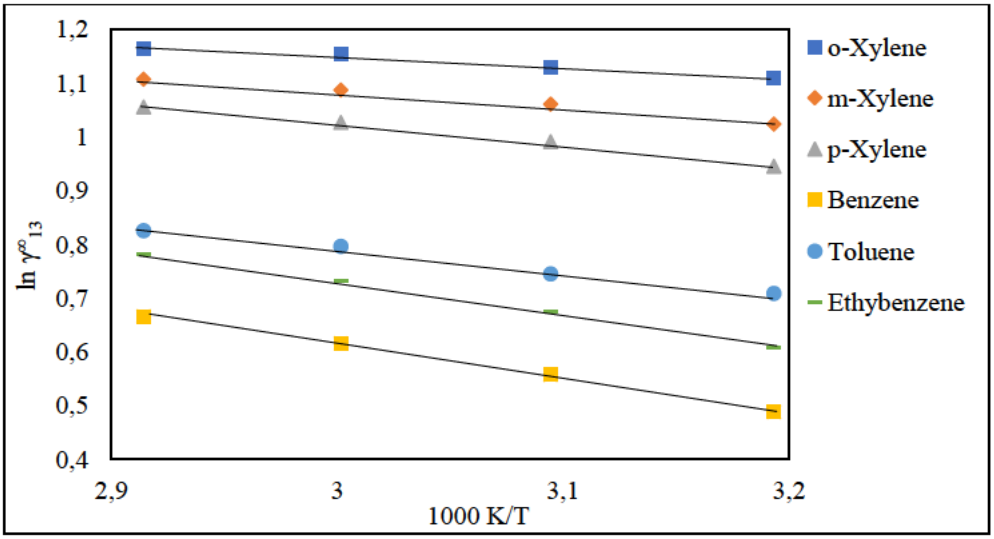

Figure 5-45: Plot of ln γ_{13}^{∞} versus 1000 K/T for the selected alkyl benzenes in [(EMPYR) Br + 1.6-HDO] at T = (313.15-343.15) K

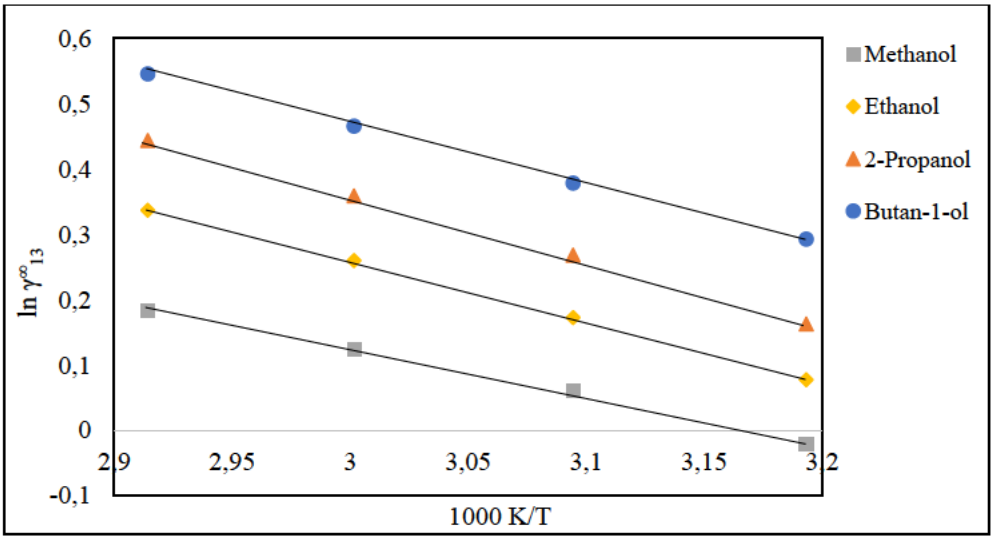

Figure 5-46: Plot of ln γ_{13}^{∞} versus 1000 K/T for the selected alcohols in [(EMPYR) Br + 1.6-HDO] at T = (313.15-343.15) K

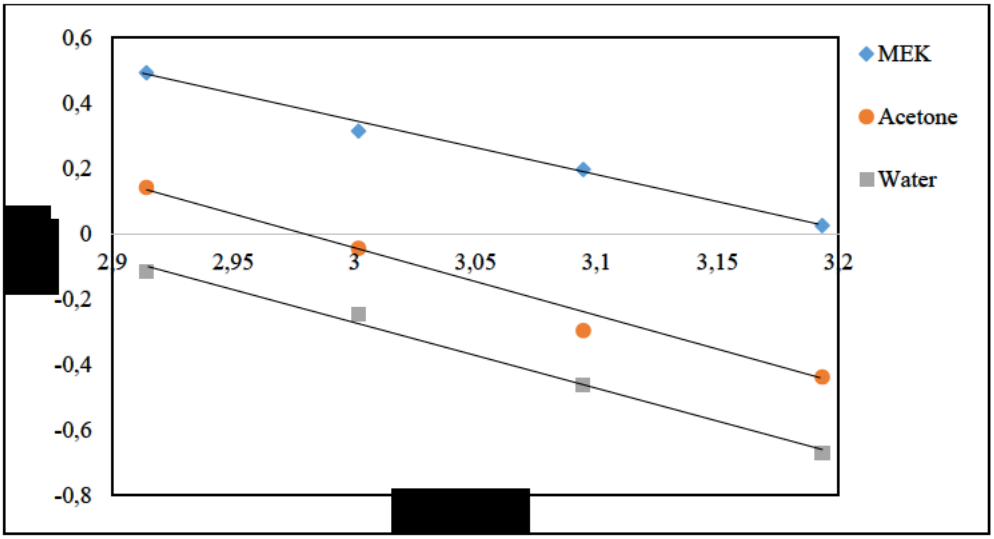

Figure 5-47: Plot of ln γ_{13}^{∞} versus 1000 K/T for the selected water and ketones in [(EMPYR) Br + 1.6-HDO] at T = (313.15-343.15) K

5.2.5 Trihexyltetradecylphosphonium decanoate + ethylene glycol, [(THTDP) Dc + EG]

Table 5-17: Averages of infinite dilution activity coefficients for the chosen organic solutes in the [(THTDP) Dc + EG], DES at a mole ratio of 1,003: 3,997 and at four different temperatures: With the standard state of the solute's hypothetical liquid at zero pressure.

	Average of infinite dilution activity coefficients (γ^{∞}_{13}) at T/K			
Organic solutes	T= 313.15 K	T= 323.15 K	T= 333.15 K	T= 343.15 K
2,2-Dimethylbutane	1.972	2.371	2.659	3.045
Pentane	3.787	4.406	4.906	5.376
Hexane	6.386	7.049	7.991	9.149
Heptane	9.155	11.31	13.45	15.58
Octane	12.06	14.77	17.46	20.15
n-Nonane	18.50	22.41	26.30	30.18
n-Decane	28.22	32.25	35.11	38.38
1-Pentene	2.682	3.496	4.503	5.098
1-Hexene	5.154	6.466	7.790	9.093
1-Nonene	8.900	11.20	13.41	17.05
1-Decene	15.08	18.85	22.71	28.58
1-Pentyne	4.774	4.998	5.258	5.451
1-Hexyne	8.628	8.829	8.930	9.383
1-Heptyne	10.30	10.66	10.89	11.19
Cyclopentane	3.679	4.235	4.771	5.305
Cyclohexane	5.990	6.702	7.302	8.212
Methylcyclohexane	6.888	7.831	8.671	9.575
Cyclopentene	1.772	1.824	1.898	1.953
Cyclohexene	3.563	3.600	3.618	3.660
o-Xylene	1.936	2.210	2.570	2.851
m-Xylene	3.500	4.721	6.078	7.365
p-Xylene	2.599	3.488	4.419	5.525
Benzene	1.458	1.695	2.100	2.450
Toluene	1.755	2.042	2.351	2.626

Ethylbenzene	2.200	2.498	2.886	2.223
Methanol	0.150	0.251	0.400	0.603
Ethanol	0.170	0.310	0.530	0.921
2-Propanol	0.230	0.403	0.655	1.099
Butan-1-ol	0.366	0.649	1.242	1.881
Acetone	1.671	2.097	3.140	3.842
MEK	5.024	5.557	5.928	6.336
Water	0.139	0.230	0.381	0.580

Standard uncertainties (u): u (γ^{∞}_{13}) = 5%; u (T) = 0.01 K; u (p) = 0.1kPa and u (x) = 0.05

Table 5-18: Partial molar properties, enthalpies ($\Delta H_1^{E,\infty}$), Gibbs free energies ($\Delta G_1^{E,\infty}$), and entropies ($T_{ref}\Delta S_1^{E,\infty}$) for the various organic solutes in [(THTDP) Dc + EG], DES at the reference temperature, $T_{ref} = 313.15$ K.

Organic solutes	$\Delta H_1^{E,\infty}$/kJ.mol^{-1}	$\Delta G_1^{E,\infty}$/kJ.mol^{-1}	$T_{ref}\Delta S_1^{E,\infty}$/kJ.mol^{-1}
1-Pentyne	-2.484	10.50	-12.99
1-Hexyne	-2.500	8.866	-11.37
1-Heptyne	-3.950	5.936	-9.886
1-Pentene	-19.13	9.950	-29.08
1-Hexene	-16.93	5.726	-22.65
1-Nonene	-19.36	2.986	-22.35
1-Decene	-17.56	-6.990	-10.57
2,2-Dimethylbutane	-12.94	14.08	-27.02
Pentane	-10.43	17.13	-27.56
Hexane	-10.71	15.06	-25.77
Heptane	-15.83	2.880	-18.71
Octane	-15.29	-0.783	-14.51
n-Nonan	-14.57	-4.141	-10.43
n-Decan	-9.158	-13.19	-22.35
Cyclopentane	-2.484	12.14	-12.99

Cyclohexane	-2.500	5.644	-11.37
Methylcyclohexane	-3.950	-2.313	-9.886
Cyclopentene	-2.892	10.26	-13.15
Cyclohexene	-0.795	9.881	-10.68
o-Xylene	-28.91	-19.65	-9.262
m-Xylene	-12.61	-3.759	-8.848
p-Xylene	-12.62	-3.759	-8.857
Benzene	-22.16	-4.307	-17.85
Toluene	-43.11	-27.95	-15.16
Ethylbenzene	-11.38	-1.033	-10.35
Methanol	-41.46	-40.58	-0.878
Ethanol	-46.93	-43.74	-3.194
2-Propanol	-46.61	-46.53	-0.074
Butan-1-ol	-48.75	-41.99	-6.756
Acetone	-50.42	-31.50	-18.92
MEK	-0.055	-14.56	-14.62
Water	-42.54	-37.72	-4.822

Standard uncertainties (u): u ($\Delta G_1^{E,\infty}$) = 5%; u ($\Delta H_1^{E,\infty}$) = 5%; u ($\Delta S_1^{E,\infty}$) = 5%; u (T) = 0.01 K; u (p) = 0.1kPa; and u (x) = 0.05

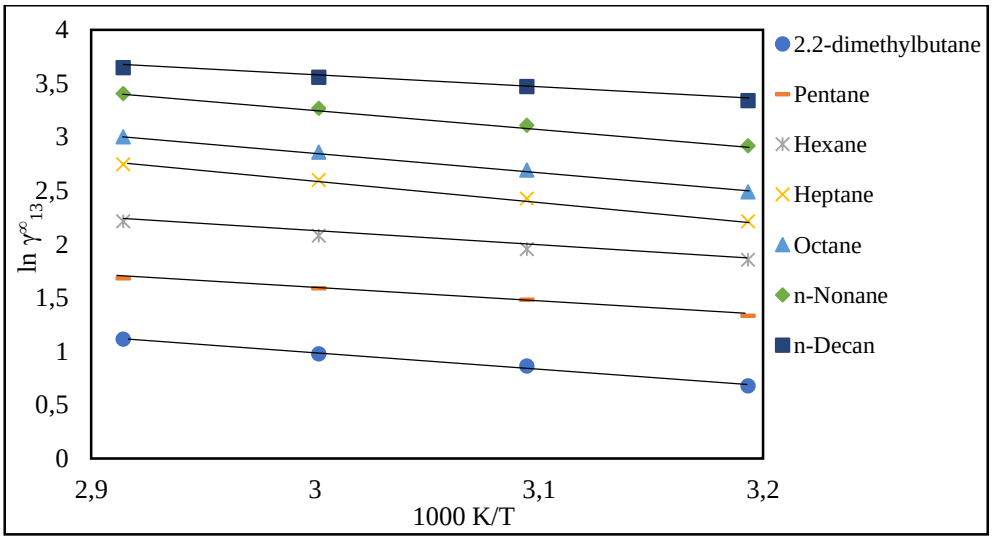

Figure 5-48: Plot of ln γ_{13}^{∞} versus 1000 K/T for the selected alkanes in [(THTDP) Dc + EG] at T = (313.15-343.15) K

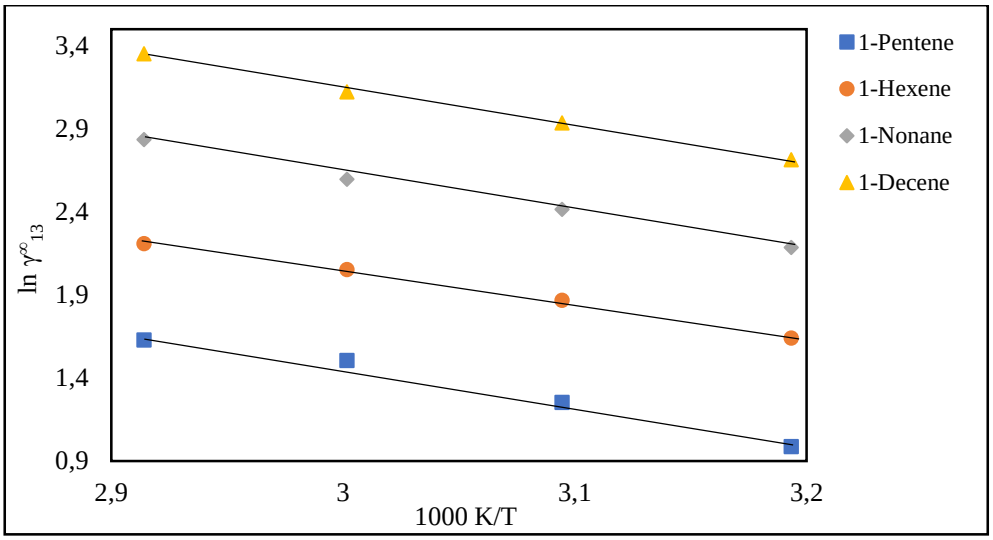

Figure 5-49: Plot of $\ln \gamma_{13}^{\infty}$ versus 1000 K/T for the selected alkenes in [(THTDP) Dc + EG] at T = (313.15-343.15) K

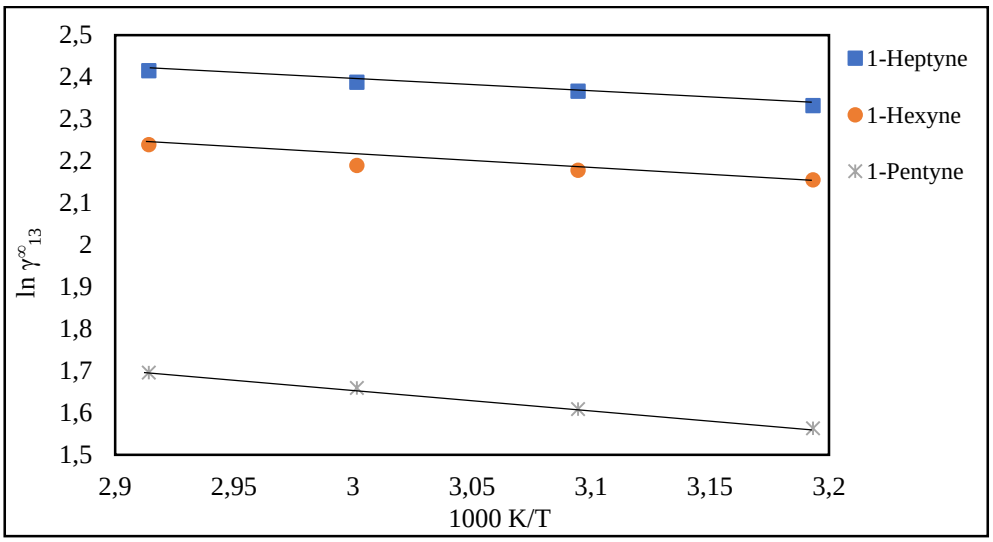

Figure 5-50: Plot of $\ln \gamma_{13}^{\infty}$ versus 1000 K/T for the selected alkynes in [(THTDP) Dc + EG] at T = (313.15-343.15) K

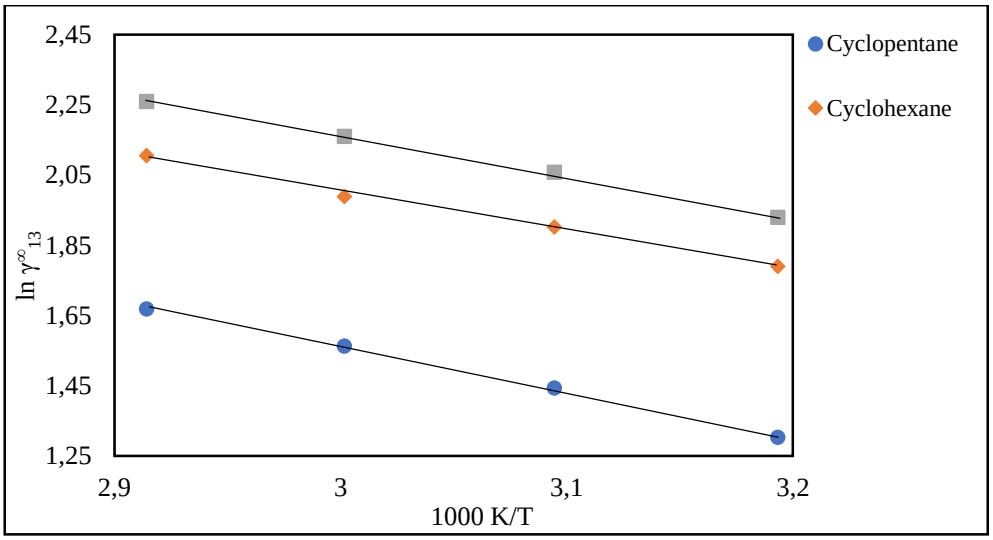

Figure 5-51: Plot of ln γ^{∞}_{13} versus 1000 K/T for the selected cycloalkanes in [(THTDP) Dc + EG] at T = (313.15-343.15) K

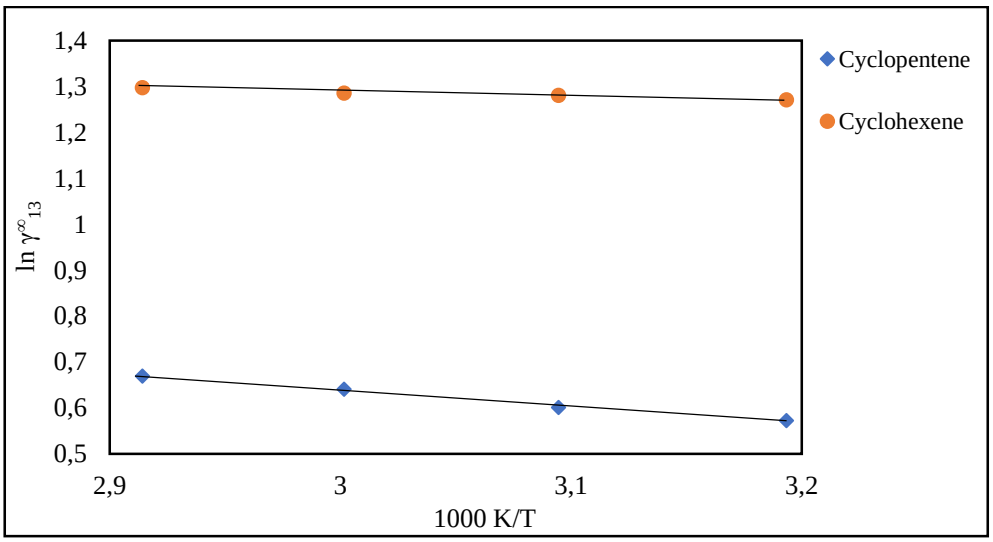

Figure 5-52: Plot of ln γ^{∞}_{13} versus 1000 K/T for the selected cycloalkenes in [(THTDP) Dc + EG] at T = (313.15-343.15) K

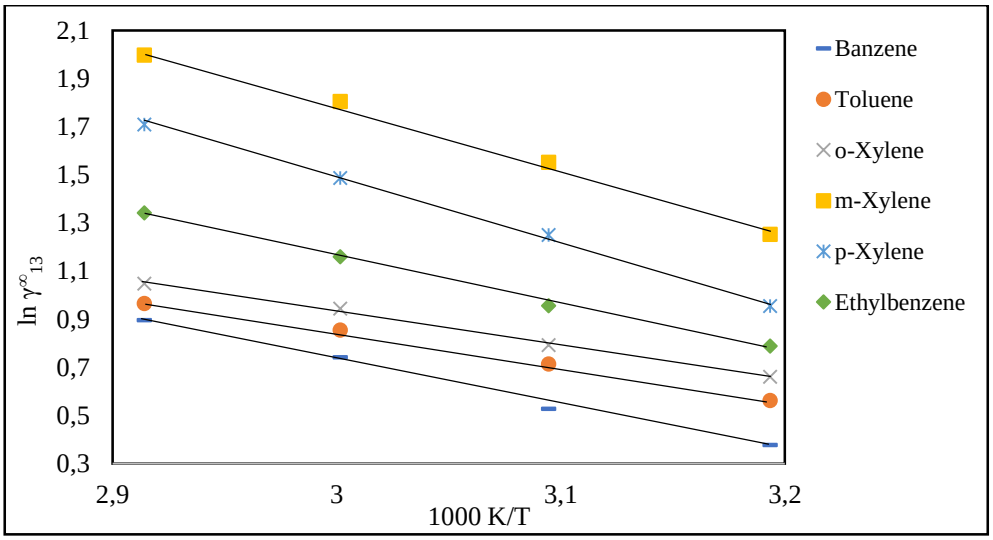

Figure 5-53: Plot of ln γ_{13}^{∞} versus 1000 K/T for the selected alkyl benzenes in [(THTDP) Dc + EG] at T = (313.15-343.15) K

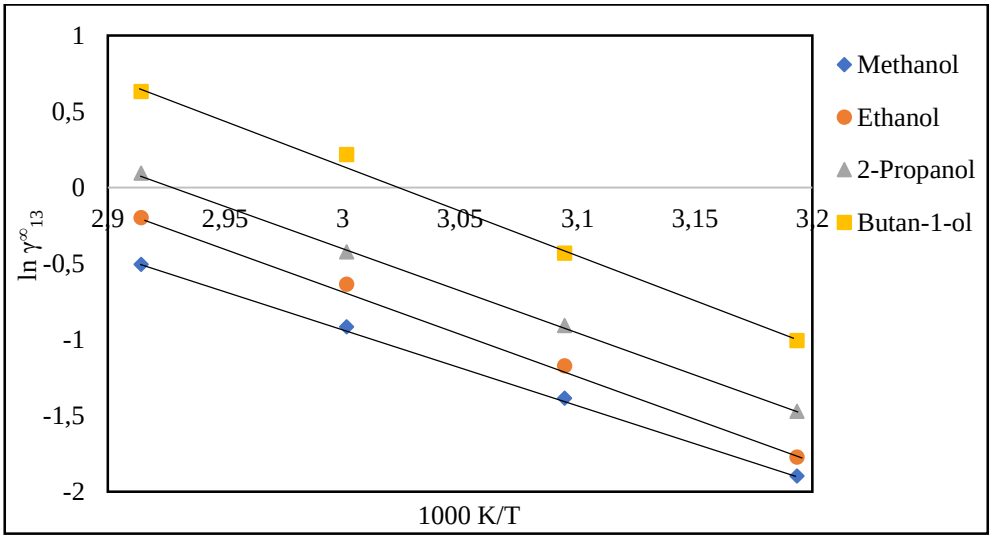

Figure 5-54: Plot of ln γ_{13}^{∞} versus 1000 K/T for the selected alcohols in [(THTDP) Dc + EG] at T = (313.15-343.15) K

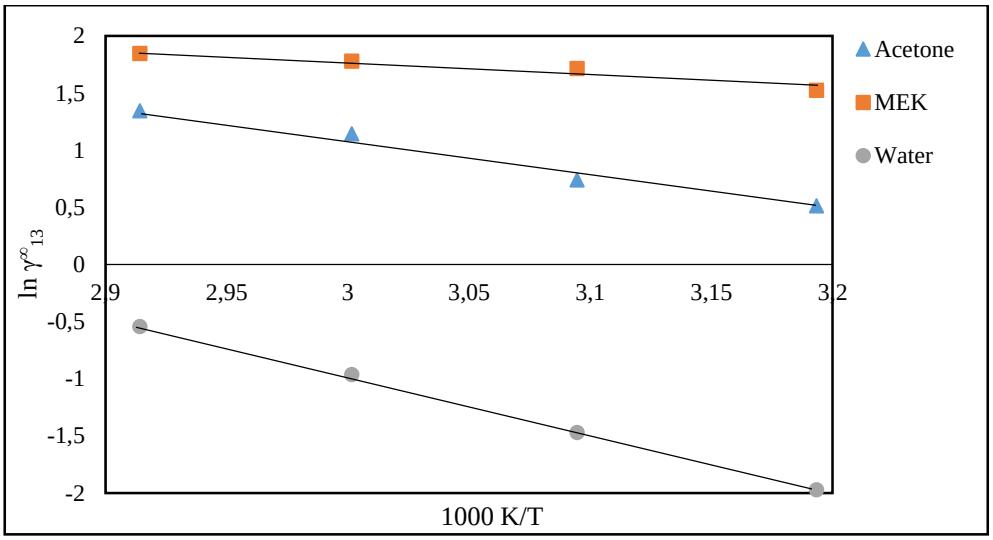

Figure 5-55: Plot of $\ln \gamma_{13}^{\infty}$ versus 1000 K/T for the selected water and ketones in [(THTDP) Dc + EG] at T = (313.15-343.15) K

CHAPTER SIX

DISCUSSION

Overview

The present chapter discusses the results achieved in the present study, as detailed in the results section. The studied deep eutectic solvents (DESs) possess a large range of properties, such as low toxicity and good thermal stability. The importance of deep eutectic solvents as extracting solvents was investigated by means of converting commonly utilised industrial solvents as well as ionic liquids (ILs) to extract solvents with closely related boiling temperatures. The obtained thermophysical data included density (ρ), sound velocity (u), excess molar volume (V_m^E), isentropic compressibility (K_s), variation in isentropic compressibility (ΔK_s), and intermolecular free length (L_f). The studied systems are listed below:

- {[1-ethyl-1-methylpyrrolidinium bromide + ethylene glycol] + methanol}, {[(EMPYR) Br + EG] + methanol}
- {[1-ethyl-1-methylpyrrolidinium bromide + ethylene glycol] + ethanol}, {[(EMPYR) Br + EG] + ethanol}
- {[1-ethyl-1-methylpyrrolidinium bromide + glycerol] + methanol}, {[(EMPYR) Br + Gly] + methanol}
- {[1-ethyl-1-methylpyrrolidinium bromide + glycerol] + ethanol}, {[(EMPYR) Br + Gly] + ethanol}

Moreover, the obtained thermodynamic data included the infinite dilution activity coefficients (γ_{13}^{∞}), partial molar properties (i.e., $\Delta G_1^{E,\infty}, \Delta H_1^{E,\infty}$, and $\Delta S_1^{E,\infty}$), as well as selectivity values (S_{ij}^{∞}) and capacities (k_j^{∞}) for the common industrial separation problems, i.e., toluene/benzene, acetone/ethanol, and cyclohexane/benzene, were chosen to compare the extraction potential of the investigated deep eutectic solvents. In addition, the studied systems were as follows:

- 1-ethyl-1-methylpyrrolidinium bromide + glycerol, [(EMPYR) Br + Gly]
- 1-ethyl-1-methylpyrrolidinium bromide + ethylene glycol, [(EMPYR) Br + EG]

- 1-ethyl-1-methylpyrrolidinium bromide + diethylene glycol, [(EMPYR) Br + 1.5-PDO]
- 1-ethyl-1-methylpyrrolidinium bromide + triethylene glycol, [(EMPYR) Br + 1.6-HDO]
- Trihexyltetradecylphosphonium decanoate + ethylene glycol, [(THTDP) Dc + EG]

6.1 Experimental Physical Properties

6.1.1 Density

As mentioned in previous chapters, density is one of the most important properties in the study of organic solvents. This property should also be one of the most studied physical properties for the new class of organic solvents called deep eutectic solvents (DESs). The physical data in relation to pyrrolidinium and phosphonium based-DESs densities is still very limited in particular.

The density measurements are usually examined at numerous temperatures so as to observe the performance of the solvents, mostly by the Anton Paar DMA 5000 M digital vibrating tube densitometer. Furthermore, densities are used to characterize materials, which informs scientists about the fluidity of the materials, also provides information about the sound velocities of materials. As it is well-known, the higher the density of the medium, the lower the sound velocity. Moreover, density and sound velocity are used to compute the thermophysical properties such as excess molar volume (V_m^E), isentropic compressibility (K_s), variation in isentropic compressibility (ΔK_s), and the intermolecular free length (L_f).

6.1.1.1 Temperature effect on density

The experimental densities of the investigated binary systems were increased with an increase in the set temperature. Figures 6-1 to 6-4 show this trend for all of the investigated binary systems, including [(EMPYR) Br + Gly] + methanol, [(EMPYR) Br + Gly] + ethanol, [(EMPYR) Br + EG] + methanol, and [(EMPYR) Br + EG] + ethanol, at temperatures ranging from T = 293.15-313.15 K. Figures 6-1 to 6-4 also showed almost similar prominence of the temperature effects of densities and sound velocities for all the investigated systems. To achieve strong solvent-solute interaction in all of the investigated systems, small amounts of hydrogen bond donors (HBDs) and hydrogen bond acceptors (HBAs) were used, (25-32) % by mass.

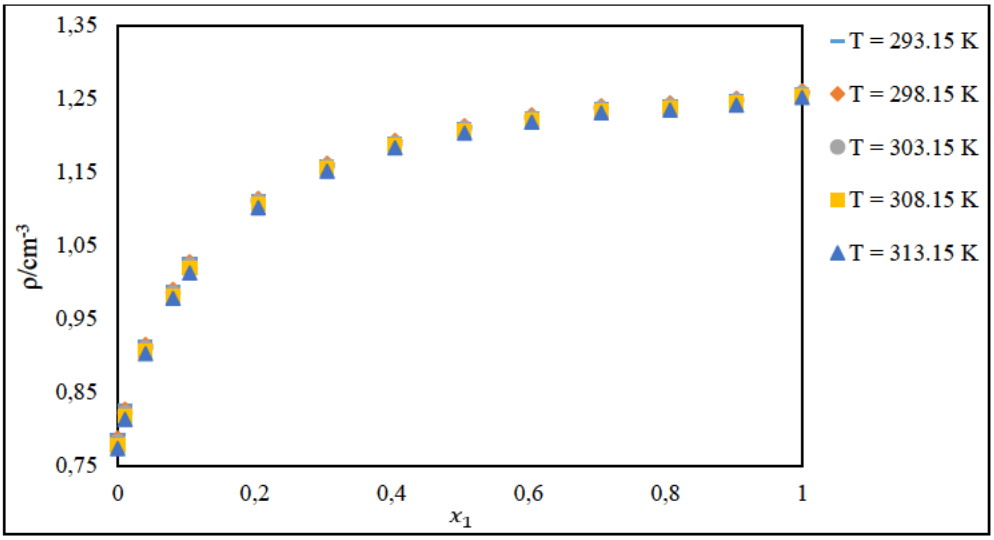

Figure 6-1: Plot of experimental densities (ρ) for binary systems of {[(EMPYR) Br + Gly] (x_1) + methanol (x_2)} against the mole fraction of x_1= (0-1) at T = (293.15-313.15) K

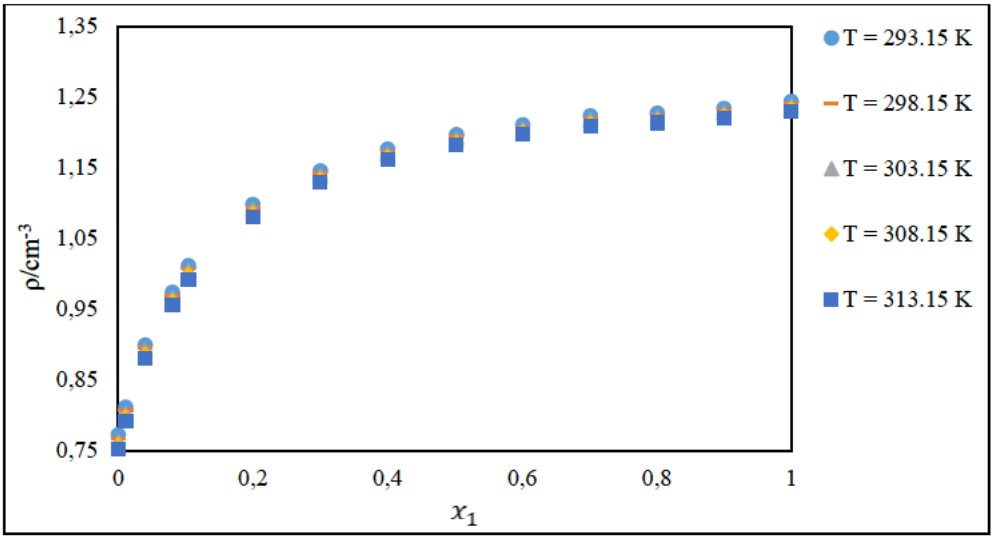

Figure 6-2: Plot of experimental densities (ρ) for binary systems of {[(EMPYR) Br + Gly] (x_1) + ethanol (x_1)} against the mole fraction of x_1= (0-1) at T = (293.15-313.15) K

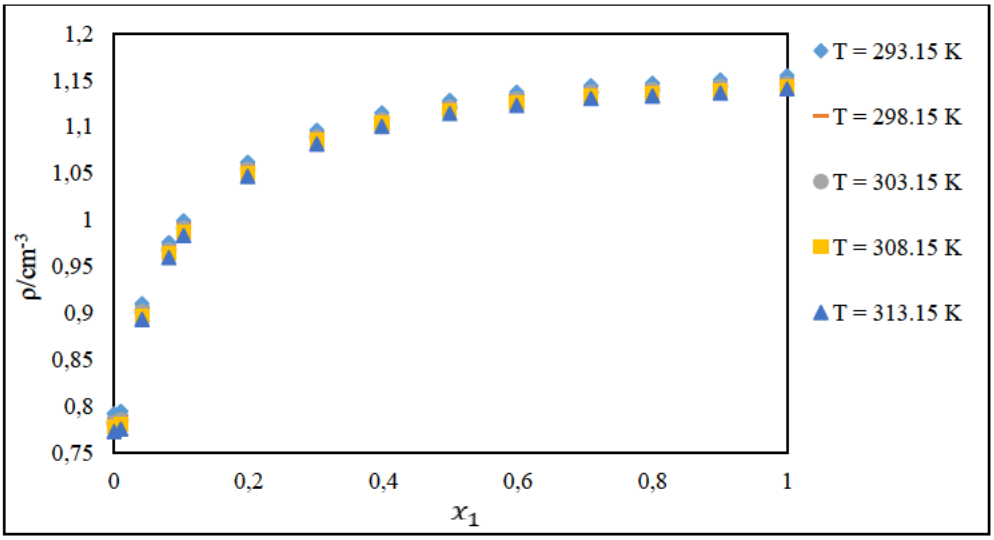

Figure 6-3: Plot of experimental densities (ρ) for binary systems of {[(EMPYR) Br + EG] (x_1) + methanol (x_2)} against the mole fraction of x_1= (0-1) at T = (293.15-313.15) K

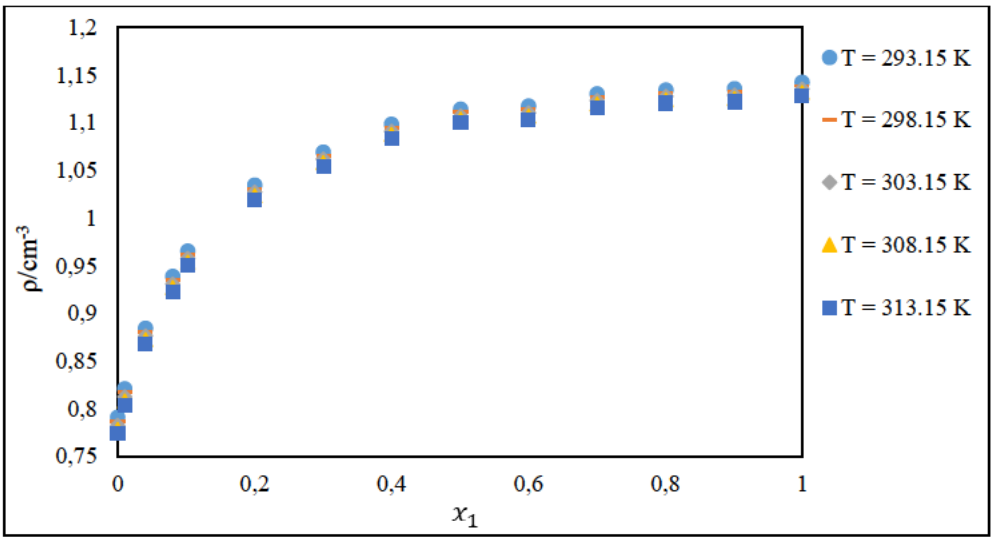

Figure 6-4: Plot of experimental densities (ρ) for binary systems of {[(EMPYR) Br + EG] (x_1) + ethanol (x_1)} against the mole fraction of x_1= (0-1) at T = (293.15-313.15) K

6.1.1.2 Composition effects on the density

The density values of the investigated systems, i.e., {[(EMPYR) Br + Gly] + methanol or ethanol} and {[(EMPYR) Br + EG] + methanol or ethanol}, were increased with an increase in the composition, suggested by the above figures. Both [(EMPYR) Br + Gly] and [(EMPYR) Br + EG] systems, can contribute significantly when interacting with alcohols as methanol and ethanol through various types of intermolecular interactions, including (I) weak hydrogen bonds, (II) π-π interactions, and (III) n-π interactions, where symbol n denotes O and N atoms, attached on the alcohol compound or deep eutectic solvent component structures. The oxygen atom on methanol or ethanol creates hydrogen bondings with the hydrogen atoms from [(EMPYR) Br + Gly] or [(EMPYR) Br + EG] complex structures or with hydrogen situated on the CH_3 group from either a hydrogen bond donor or hydrogen bond accepter on the complex structure. The composition effect gave strong interactions with alcohol molecules since the complex structure was willing to share a hydrogen atom. Hence, it contributes to the increase solubility of the solvent.

6.1.2 Sound Velocity

Sound velocity is one of the tools to analyse intermolecular interactions such as association, dissociation, complex formation, calculation of isothermal compressibility, isobaric thermal expansion coefficient, thermal pressure coefficient, ratio of isobaric and isochoric heat capacities, and the Joule-Thomson coefficient (Widegren and Magee, 2007; Laesecke *et al.*, 2012; Gowrisankar *et al.*, 2013). In the present study, sound velocity was measured simultaneously with density at various temperatures and atmospheric pressure. The obtained data was used to compute the experimental thermophysical properties, yielding more information. As is known, the higher the density of the medium, the lower the sound velocity. For both [(EMPYR) Br + EG] and [(EMPYR) Br + Gly] systems, a slight increase in the sound velocity as the solute chain length increased was observed. Furthermore, in terms of sound velocity, a 1:4 mole ratio of [(EMPYR) Br + EG] and a 1:2 mole ratio of [(EMPYR) Br + Gly produced relatively similar results.

6.1.2.1 Composition and temperature effect on sound velocity

The sound velocities of the investigated binary systems increased with an increase in experimental temperature. Figures 6-5 to 6-8 show this trend for all binary systems, {[[EMPYR]Br + Gly] + methanol}, {[[EMPYR]Br + Gly] + ethanol}, {[[EMPYR]Br + EG] + methanol}, and {[[EMPYR]Br + EG] + ethanol} over the mole fraction range, 0-1 at temperatures ranging from

T = (293.15-313.15) K and at 0.1MPa. Thus, there is an effect of temperature on sound velocities and densities for all investigated systems, as indicated in Figures 6-5 to 6-8. Furthermore, relatively small amounts of hydrogen bond donors and acceptor were used to prepare respective deep eutectic solvents, which resulted in some significant good interactions with all of the investigated alcohols.

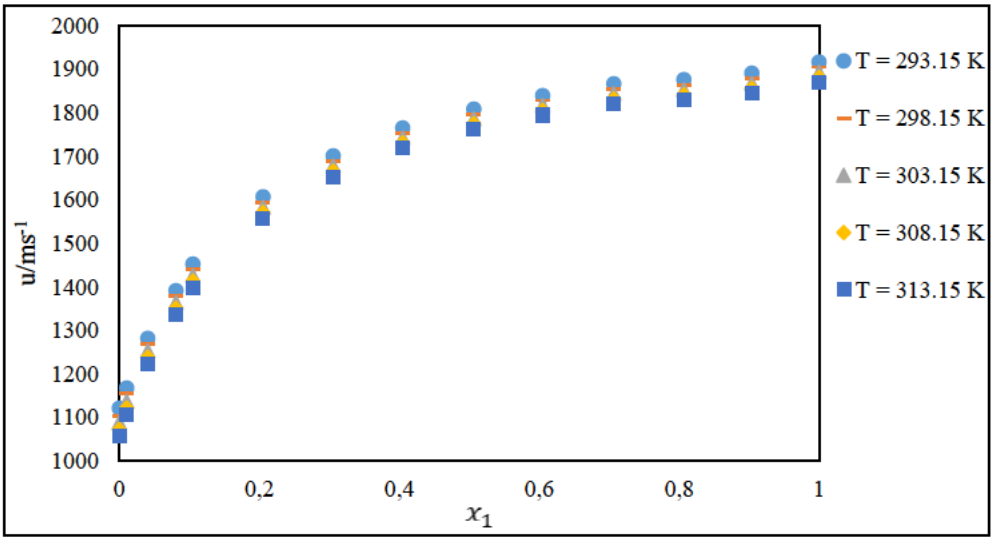

Figure 6-5: Plot of experimental sound velocities (u) for binary systems of {[(EMPYR) Br + Gly] (x_1) + methanol (x_2)} against the mole fraction of x_1= (0-1) at T = (293.15-313.15) K

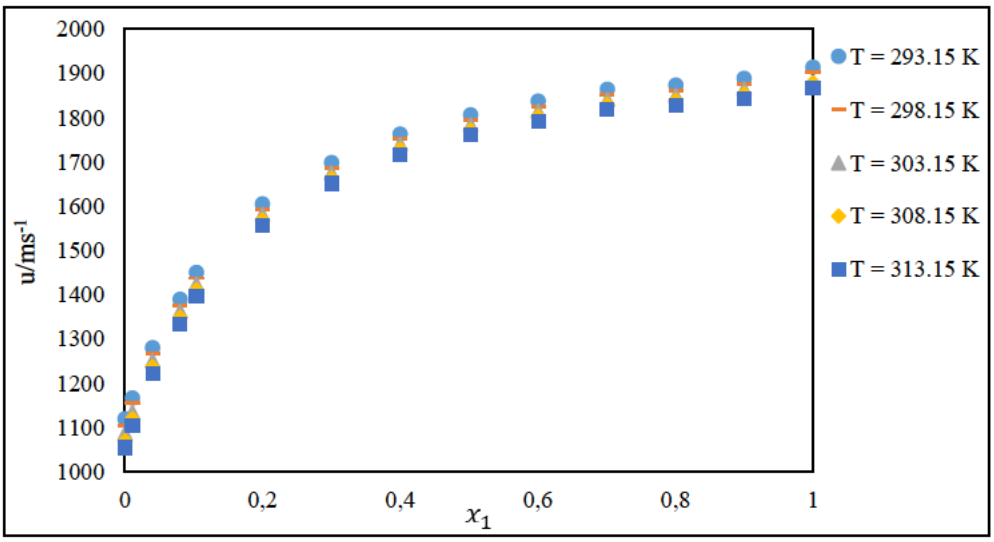

Figure 6-6: Plot of experimental sound velocities (u) for binary systems of {[(EMPYR) Br + Gly] (x_1) + ethanol (x_2)} against the mole fraction of x_1= (0-1) at T = (293.15-313.15) K

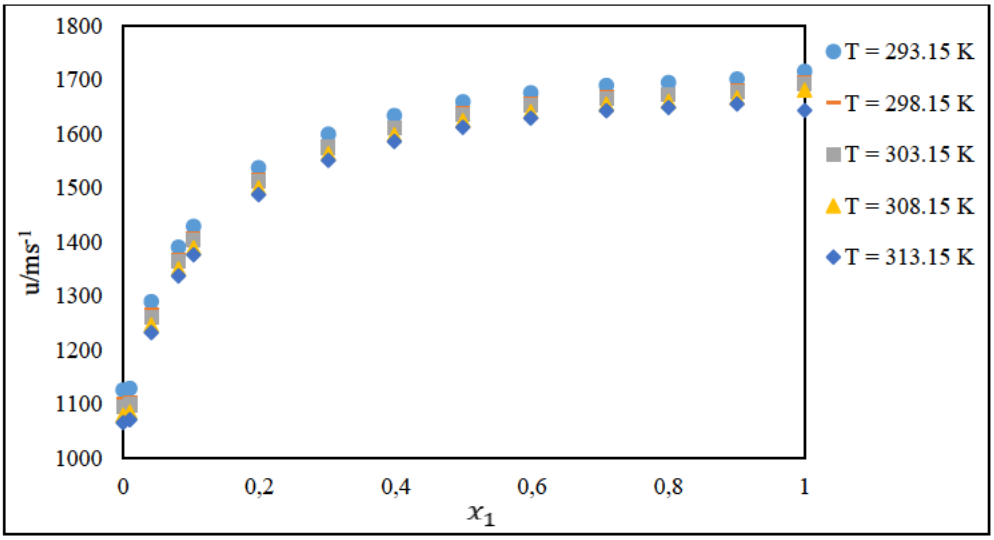

Figure 6-7: Plot of experimental sound velocities (u) for binary systems of {[[EMPYR]Br + EG] + methanol} against the molar fraction at T = (293.15-313.15) K

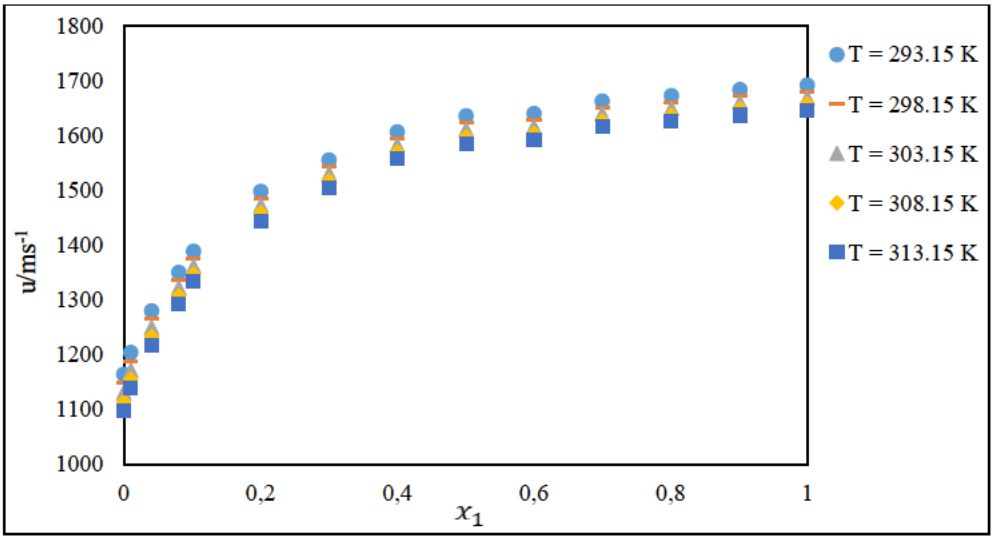

Figure 6-8: Plot of experimental sound velocities (u) for binary systems of {[(EMPYR) Br + EG] (x_1) + ethanol (x_2)} against the mole fraction of x_1= (0-1) at T = (293.15-313.15) K

6.2 Experimental Thermophysical Properties

6.2.1 Excess Molar Volume

(I) Intermolecular interactions, such as hydrogen bonds, dipole-dipole interactions, charger transfer forces, and other complex forming interactions, are important factors influencing excess molar volume behaviour in binary systems.

(II) The shape, size, and packing ability of component molecules, as well as geometric factors in solution (Iloukhani and Almasi, 2009; Laesecke *et al.*, 2012).

Moreover, the investigated excess molar volumes for all the investigated systems were obtained by using eq. (6-1).

$$V_m^E = \sum_{i=1}^{2} x_i M_i (\rho^{-1} - \rho_i^{-1}) \quad (6\text{-}1)$$

According to Redhi (2003), the positive excess molar volumes designate strong interactions amongst similar molecules, whereas negative excess molar volumes designate strong interactions among various molecules or in the association of additional species involved. Hence, this organises the molecules together in a liquid mixture. The V_m^E reported in the present study were all negative, which reveals those strong interactions of various molecules in a liquid mixture.

6.2.1.1 Temperature effects on excess molar volume

The values of V_m^E for all the investigated binary systems, {[(EMPYR) Br + Gly] + methanol}, {[(EMPYR) Br + Gly] + ethanol}, {[(EMPYR) Br + EG] + methanol}, and {[(EMPYR) Br + EG] + ethanol}, were negative across all the investigated experimental temperatures. The negative values for all the obtained V_m^E values increased as the temperature increased. This sequence was also observed in the previously studied binary systems made of deep eutectic solvents (Leron *et al.*, 2012). A close examination of the values in Tables 5-1 to 5-4 reveals that [(EMPYR) Br + Gly] and [(EMPYR) Br + EG], deep eutectic solvents, have strongly interacted with methanol and/or ethanol molecules, resulting in a decrease in volume. This effect is potentially caused by the occurrence of hydrogen bondings and dipole-dipole interactions that have occurred (McAtee and Heitz, 2016). Furthermore, the negative values also imply that more attractive interactions took place as the studied deep eutectic solvents and alcohol molecules were interacting. Furthermore, the additional distinct molecular interactions could have resulted in charge transfer, hydrogen bonding, and packing effects of component molecules.

6.2.1.2 Composition effects on the excess molar volume

As shown in Figures 5-1, 5-5, 5-9, and 5-13, the V_m^E values for all the investigated binary systems, {[(EMPYR) Br + Gly] + methanol}, {[(EMPYR) Br + Gly] + ethanol}, {[(EMPYR) Br + EG] + methanol}, and {[(EMPYR) Br + EG] + ethanol} were negative across the entire examined experimental mole fraction range. The minimum V_m^E was reached at 0.2 mole fraction for {[(EMPYR) Br + EG] + methanol/ethanol} binary systems and 0.3 mole fraction for {[(EMPYR) Br + Gly] + methanol/ethanol} binary systems, respectively. Additionally, the values of V_m^E for methanol systems were less negative than the values for ethanol systems. The rest of the findings provide information about the close packing of the ions to the surrounding solvent molecules and/or potentially other more attractive forces among the deep eutectic solvent complex and the solvent molecules in the liquid mixture. This also suggests that [(EMPYR) Br + Gly] or [(EMPYR) Br + EG] interacted well with methanol or ethanol molecules in a liquid mixture via various interactions such as hydrogen bonding, dipolar interactions, dipole-dipole interactions, and dispersive forces.

6.2.2 Isentropic Compressibility, Variation in Isentropic Compressibility, and Intermolecular Free Length

The term isentropic informs that as sound waves pass through a fluid, the pressure and temperature fluctuate in each infinitesimal volume, whilst the entropy of the entire mixture stays constant (Rao *et al.*, 2017). The same authors mentioned that in order for the conditions to become true, the sound velocity should be measured through the application of a low frequency generator. Hence, DSA 5000M transducer gave a frequency of about 3 MHz though, at high frequency (> 100 MHz) there is a velocity dispersion and adsorption of sound waves because of the pairing with the molecular processes within the fluid (Fortin *et al.*, 2013; Rao *et al.*, 2017). Therefore, the variation of isentropic compressibility as a function of the composition ratio of the system mixture will provide some evidence about the existence of the intermolecular interactions in liquid solutions (Fort and Moore, 1965).

6.2.2.1 Isentropic compressibility

In this work, the data for isentropic compressibility (K_s) with respect to the binary mixtures, {[(EMPYR) Br + Gly] + methanol/ethanol} and {[(EMPYR) Br + EG] methanol/ethanol} in a

variety of temperatures are given in Tables 5-1 to 5-4. The data from the Tables are also plotted as isentropic compressibility versus molar fraction, (K_s vs x_i) as shown in Figures 5-3, 5-7, 5-11 to 5-15. The study utilized the Newton-Laplace Equation from Rice and Hirschfelder (1954) to determine the $K_s$of the studied systems. The terms or symbols used in Newton-Laplace Equation were detailed in Chapter Four.

$$K_S = \frac{1}{\rho\mu^2} \tag{6-2}$$

From Figures 5-3, 5-7, 5-11, and 5-15, it can be clearly seen that as experimental K_s decreased, the mole fraction increase. Stronger interactions occurred between [(EMPYR) Br + Gly] or [(EMPYR) Br + EG] components and alcohols (i.e., methanol and ethanol) molecules forming a compressible bulk solvent than in the ideal system. Furthermore, all the experimental $K_s$values were positive for the whole composition ratio and the whole temperature range. According to volumetric studies, this is a most likely effect, and it denotes a decrease in compressibility of the mixtures. As a result, the data was in good agreement with strong solvent-solute interactions (Chaudhary and Nain, 2020; Pathania *et al.*, 2020).

6.2.2.2 Variation in isentropic compressibility

The experimental variation in isentropic compressibilities (ΔK_s) for the studied systems, [(EMPYR) Br + EG] + methanol or ethanol and [(EMPYR) Br + Gly] + methanol or ethanol, were computed using eq. (6-3) at various temperatures and atmospheric pressures of 0.1 MPa, as well as in a composition range of (0-1).

$$\Delta K_S = K_S - \sum_{i=1}^{N} x_i K_{S_i} \tag{6-3}$$

The experimental ΔK_svalues are extrapolated in Figures 5-2, 5-6, 5-10, and 5-8. All ΔK_svalues were negative across the whole composition range and the whole temperature range. The hydrogen bondings, dipole-dipole interactions, charge transfer forces, dispersive forces as well as the other various reactive forces of [(EMPYR) Br + Gly] or [(EMPYR) Br + EG] and methanol or ethanol molecules for the binary systems resulted in a decrease in the compressibility of the systems. It was established that the obtained data was in good agreement with strong solvent-solute interactions (Arumugam *et al.*, 2020; Chaudhary and Nain, 2020).

6.2.2.3 Intermolecular free length

In order to fully understand the intermolecular interactions of various organic mixtures, Jacobson proposed an empirical equation to compute the intermolecular free length (L_f). As given by eq. (6-4) below,

$$L_f = K_j\sqrt{K_s} \tag{6-4}$$

Where K_j denotes Jacobson's constant, it is the value of (93.88 + 0.375T) 10^{-8} since it's a temperature-dependent constant.

The experimental values for all four different investigated binary systems, namely [(EMPYR) Br + Gly] + methanol or ethanol and [(EMPYR) Br + EG] + methanol or ethanol, were computed using the same equation for the entire series of composition and temperature range in this study. The experimental results are detailed in Tables 5-1 to 5-4 as well as displayed in Figures 5-4, 5-8, 5-12, and 5-16. As shown in Figures 5-4, 5-8, 5-12, and 5-16, the L_f values for the investigated binary systems were all positive and increased with an increase in temperature but decreased with an increase in molar composition of the deep eutectic solvent. This is most likely attributed to a variety of intermolecular interactions which include physical interactions such as hydrogen bonding, weak dipole-dipole interaction or dispersive forces that may have led to positive L_f values. While the chemical interactions such as the strong dipole-dipole interactions during the complex formation as well as the charge transfer between the component molecules could only lead to negative L_f values, thus, all of the studied systems showed lower compressibility values.

6.2.3 Redlich-Kister Equation

The corresponding data for all four investigated systems were correlated to obtain a mathematical description of the derived properties with composition for use in precisely determining compositions in the compositional analysis of mixtures derived from VLE experiments. The Redlich-Kister Equation (6-5) was used for correlation of binary systems. The obtained correlation constants (A_i) are given in Chapter Five, Tables 5-5 to 5-8.

$$X = x_1x_2\ \sum_{i=1}^{k} A_i\ (1-2x_1)^{i-1} \tag{6-5}$$

In the above equation, *x* denotes the deviation in V_m^E or ΔK_s. The least square method was used to determine the parameter values of A_i. Furthermore, the standard deviation (σ) for the correlation was calculated by eq. (6-7):

$$\sigma(X) = \sum_{i=1}^{N} \left[\left(X_{exp} - X_{calc} \right) \Big/ (N - K) \right]^{\frac{1}{2}} \tag{6-6}$$

In eq. (6-6) above, K denotes the coefficients used in eq. (6-5), N denotes the number of experimental points. Moreover, the standard deviation and correlation constants provided a strong correlation for all the computed or derived properties as the low values were produced.

6.3 Thermodynamic Data at Infinite Dilution

In the present section, the importance of deep eutectic solvents (DESs) in separation processes as separating agents was confirmed by comparing the conventionally organic solvents and ionic liquids (ILs) from the literature for the separation of various azeotropic systems with closely interrelated boiling points. Therefore, various industrial separation problems were selected to estimate the potential use of the studied deep eutectic solvents in terms of selectivity as well as capacity values.

Computing Constant Properties

The constant properties, i.e., critical temperature, critical volume, critical pressure, and acentric factor, of all the chemical solutes utilised in this study were taken from the following textbooks: (I) The Properties of Gas and Liquids (Poling *et al.*, 2001b) and CRC Handbook of Chemistry and Physics 97th Edition (Haynes *et al.*, 2016). These constant properties were used to compute the infinite dilution activity coefficients (IDACs) since they designate the nature of these chemical components. As the computation of the IDACs (γ_{13}^{∞})of solutes is highly dependent on the constant properties of the pure components to determine the second viral coefficient values, i.e., B_{11} and B_{12}. In addition, the molar volumes utilized in this work were computed using the modified *Rackett Equation* (1970) as detailed in Chapter Three.

6.3.1 Measurements of Infinite Dilution Activity Coefficient

6.3.1.1 Test system

To test the system, the infinite dilution activity coefficients of seven selected organic solutes, including 2,2-dimethylbutane; pentane; hexane; heptane; cyclopentane; cyclohexane; as well as benzene in hexadecane at three different temperatures and an atmospheric pressure of 0.1 MPa, were determined and compared to the literature data. The experimental data is presented in Table 4-6 in Chapter Four. The test system results were in good correspondence with the literature data.

6.3.1.2 Analysis of infinite dilution activity coefficients of pyrrolidinium and phosphonium-based DESs

The experimental infinite dilution activity coefficients of different organic solutes in the deep eutectic solvent systems are recorded in Tables 5-9 to 5-11, 5-13 to 5-15, 5-17 to 5-19, 5-21 to 5-23, and 5-25 to 5-27 for all the listed systems below.

- 1-ethyl-1-methylpyrrolidinium bromide + glycerol, [(EMPYR) Br + Gly]
- 1-ethyl-1-methylpyrrolidinium bromide + ethylene glycol, [(EMPYR) Br + EG]
- 1-ethyl-1-methylpyrrolidinium bromide + 1.5-pentanediol, [(EMPYR) Br + 1.5-PDO]
- 1-ethyl-1-methylpyrrolidinium bromide + 1.6-hexanediol, [(EMPYR) Br + 1.6-HDO]
- Trihexyltetradeclyphosphonium decanoate + ethylene glycol, [(THTDP) Dc + EG]

There were two experimental infinite dilution activity coefficients obtained for each investigated system in different column loadings: {e.g., 27.76% and 28.22% in $^{m}/_{m}$ for the [(EMPYR) Br + EG] system} at all four temperatures, T = (298.15-343.15) K and an atmospheric pressure of 0.1 MPa. The infinite dilution activity coefficients were independent of the carrier gas flow and revealed that there was no significant adsorption. Furthermore, this shows that the column load had enough solvent (deep eutectic solvent). As known, lower infinite dilution activity coefficients are an indication of an increased interaction between solvent and solute, whereas higher infinite dilution activity coefficients are an indication of a decrease in the measured retention time and a decrease in the interaction between the solvent and solutes. Normally, a magnitude 1 is an ideal activity coefficient. For better intermolecular interpretations, the natural logarithms (ln γ_{13}^{∞}) are plotted as a function of inverse absolute temperature (1000 K/T), for every investigated system and per functional group. Details are presented for each studied system.

For all the studied solutes, the [(EMPYR) Br + Gly] system gave higher infinite dilution activity coefficients, e.g., pentane (γ_{13}^{∞}= 62.49), 1-pentene (γ_{13}^{∞}= 45.72), 1-pentyne (γ_{13}^{∞}= 41.80), cyclopentane (γ_{13}^{∞}= 67.55), benzene (γ_{13}^{∞}= 34.12), butan-1-ol (γ_{13}^{∞}= 8.600), and methyl ethyl ketone (γ_{13}^{∞}= 11.30), all at 313.15 K. Also, this system solutes' infinite dilution activity coefficients decreased with the temperature increase. For example, toluene had infinite dilution activity coefficients of (γ_{13}^{∞}= 71.51, 68.06, 66.16, and 62.63) at 313.15 K, 323.15 K, 333.15 K, and 343.15 K, respectively. This trend has been observed in previously published pyrrolidinium-based ILs for

alkanes and alkenes (Domanska *et al.*, 2009; Acree Jr *et al.*, 2012; Kabane *et al.*, 2019a; Mutelet *et al.*, 2019; Krolikowski *et al.*, 2020). It is due to weak forces between the investigated solvent system and the selected solutes, in this case, [(EMPYR) Br + Gly]. This trend definitely proves that a mole ratio of [(EMPYR) Br] (1) and Gly (2) won't be an ideal solvent for future extraction purposes.

The system of [EMPYR) Br + EG] gave rational and adequate infinite dilution activity coefficients, e.g., pentane (γ_{13}^{∞}= 1.412), 1-pentene (γ_{13}^{∞}= 1.327), 1-pentyne (γ_{13}^{∞}= 1.010), cyclopentane (γ_{13}^{∞}= 1.232), benzene (γ_{13}^{∞}= 0.920), toluene (γ_{13}^{∞}= 0.969), methanol (γ_{13}^{∞}= 0.781), and acetone (γ_{13}^{∞}= 1.032) all at 313.15 K. In this system, the infinite dilution activity coefficients of the investigated solutes increased with the temperature increase. For instance, ethanol had infinite dilution activity coefficients of (γ_{13}^{∞}= 0.805, 0.884, 0.968, 1.039) at 313.15 K, 323.15 K, 333.15 K, and 343.15 K, respectively. This arising trend was observed from previous studies (Mutelet *et al.*, 2019; Kabane and Redhi, 2020), including pyrrolidinium based studies (Marcinkowski *et al.*, 2020; Manyoni *et al.*, 2022) and ethylene glycol solvent studies (Zhang *et al.*, 2003; Krolikowski *et al.*, 2022). Furthermore, this effect was prompted by strong hydrogen bonds, dipole-dipole interactions, dispersive forces, charge transfer forces, as well as many other attractive forces in the solution between the above system and the selected solutes (Khachatrian *et al.*, 2020; Singh *et al.*, 2020). Furthermore, this demonstrates that a 1:4 mole ratio of [(EMPYR) Br] (1) and EG (4) is a potential ideal extracting solvent.

On the other hand, [(EMPYR) Br + 1.5-PDO] gave slightly higher infinite dilution activity coefficients for the investigated nonpolar solutes (e.g., alkanes and alkenes), but were more practical for alkyl benzenes and were more accommodative for polar solutes, including water. Examples: 1-pentene (γ_{13}^{∞}= 2.021), benzene (γ_{13}^{∞}= 1.188), ethanol (γ_{13}^{∞}= 0.222), and water (γ_{13}^{∞}= 0.741), all at 313.15 K. Again, for this system, the infinite dilution activity coefficients increased with an increase in experimental temperature. Meanwhile, in infinite dilution activity coefficients, the [(EMPYR) Br + 1.6-HDO] system behaved similarly to the [(EMPYR) Br + 1.5-PDO] system., the infinite dilution activity coefficients of polar solutes differed slightly. Because the [(EMPYR) Br + 1.6-HDO] system was slightly higher than the [(EMPYR) Br + 1.5-PDO] system. However, both systems gave appropriated infinite dilution activity coefficients for polar solutes. Once more, this effect is evoked through hydrogen bondings, dipole forces, charge transfer, dispersive forces, as well as many other attractive forces (Singh *et al.*, 2020). As a result, both systems with a similar mole ratio of 1:2 would be appropriate extraction solvent systems for polar solvents.

Similarly, the phosphonium-based DES, [(THTDP) Dc + EG] gave appropriate infinite dilution activity coefficients for alcohols and water, but higher for the rest of the investigated compounds. Examples: pentane (γ_{13}^{∞}= 3.787), cyclopentane (γ_{13}^{∞}= 3.679), toluene (γ_{13}^{∞}= 1.755), ethanol (γ_{13}^{∞}= 0.170), and water (γ_{13}^{∞}= 0.139), all at 313.15 K. Again, this system would be appropriate for extraction of solutes such as alcohols and water. For the last time, with this system, the infinite dilution activity coefficients increased with an increase in experimental temperature. All of the above outcomes are the result of large and strong hydrogen bondings, dipole-dipole forces, and charge transfer caused by both the hydrogen bond accepter [(THTDP) Dc] and the hydrogen bond donor [EG].

The separation potential in terms of infinite dilution activity coefficients per functional group was determined in the following order for all of the examined systems:

- Alkanes > alkenes > cycloalkanes > cycloalkenes > alkynes > alkyl benzenes > ketones > alcohols > thiophene, for [(EMPYR) Br + Gly] system.
- Alkanes > alkenes > cycloalkanes > cycloalkenes > alkynes > alkyl benzenes > ketones > alcohols, for [(EMPYR) Br + 1.5-PDO] system.
- Alkanes > alkenes > cycloalkanes > cycloalkenes > alkynes > alkyl benzenes > ketones > alcohols > water, for [(EMPYR) Br + 1.6-HDO] system.
- Alkanes > alkenes > cycloalkanes > cycloalkenes > alkynes > alkyl benzenes > ketones > alcohols, for [(EMPYR) Br + EG] system.
- Alkanes > alkenes > cycloalkanes > cycloalkenes > alkynes > alkyl benzenes > ketones > alcohols > water, for [(THTDP) Dc + EG] system.

It was clear from the results that nonpolar solutes, including water, always had greater infinite dilution activity coefficients than polar solutes. Hydrogen bonds appear to be stronger than other forces, such as the Van der Waals forces for alkanes, alkenes, and alkynes. In comparison to the examined polar solutes, this also shows that nonpolar solutes moved quickly in the stationary phase packed with pyrrolidinium and/or phosphonium-based DES.

Again, for nonpolar solutes, it was observed that both alkanes and alkenes interactions were always higher than for cycloalkanes and cycloalkenes. This is so because of the stronger attractive forces between the cyclic structure and the pyrrolidinium ring or phosphonium chain of a hydrogen bond

acceptor in a deep eutectic solvent complex structure. The alkanes infinite dilution activity coefficients were always higher than the alkene of the similar chain length or mother structure, and this was because of the double bond effect, which was difficult to break compared to single bonds in the interaction with the polar deep eutectic solvent complex. Furthermore, this hypothesis was like that of cycloalkanes and cycloalkenes. Alkanes, alkenes, alkynes, cycloalkanes and cycloalkenes always had higher infinite dilution activity coefficients when compared to alkyl benzenes, and this could be due to the strong interactions caused by the charge delocalization that occurred between the hydrogen bond accepter, hydrogen bond donor, and the polar deep eutectic solvent complex structure as well as benzene structures. As it is known, π-bonds can carry only two electrons but in a benzene ring there are six delocalised electrons. Possibly, these have strongly interacted with the deep eutectic solvent components, i.e., hydrogen bond acceptor and hydrogen bond donor, and resulted to the formation of n-π forces. Yet again, n-π forces are known to be stronger than Vaal der Waals forces.

For polar solutes, the alcohols, including methanol, ethanol, 2-propanol, and butan-1-ol, as well as ketones, including acetone and methyl ethyl ketone, were always lower in infinite dilution activity coefficients compared to nonpolar solutes for all the investigated systems. This suggests stronger interactions for polar compounds with the deep eutectic solvent components, and this is due to hydrogen bonds, which are known to be strong forces compared to intermolecular forces, except for ionic bonds. Moreover, the alcohol infinite dilution activity coefficients were always lower compared to the ketones, and this is because of the polarity contributed by the carbonyl group (C=O), which may have slightly increased the infinite dilution activity coefficients of ketones. In addition, water was the only solute lower than selected polar solutes. This was due to the presence of hydrogen bonds in water molecules, which allowed molecules to bind more firmly with the deep eutectic solvent in the stationary phase.

6.3.1.3 Impact of hydrogen bond donor on the infinite dilution activity coefficients

A hydrogen bond donor (HBD) is a critical participant component in a deep eutectic solvent, as it's the one that determines the separation potential of deep eutectic solvents (Maugeri *et al.,* 2012; Tiecco *et al.,* 2019; Ma *et al.,* 2021). In this study, four different HBDs, counting glycerol, ethylene glycol, 1.5-pentanediol, and 1.6-hexanediol, were used for the preparation of deep eutectic solvents to separate various organic solutes that are highly volatile and have closely related boiling points. The structural compounds of these hydrogen bond donors are given below:

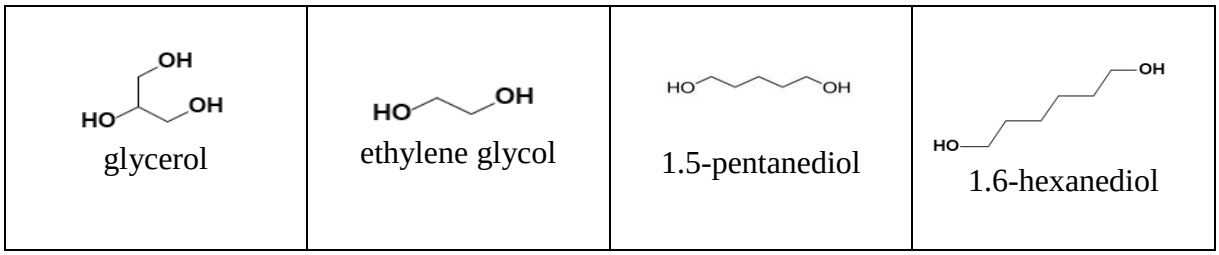

Figure 6-9: Structural compounds of the investigated hydrogen bond donors

In Figures 5-17 to 5-55, it is evident that the selected hydrogen bond donors have impacted the infinite dilution activity coefficient data. The separation potential order was found as follows:

- Glycerol (Gly): alkanes > alkenes > cycloalkanes > cycloalkenes > alkynes > alkyl benzenes > ketones > alcohols > thiophene,
- Ethylene glycol (EG): alkanes > alkenes > cycloalkanes > cycloalkenes > alkynes > alkyl benzenes > ketones > alcohols,
- 1.5-pentanediol (1.5-PDO): alkanes > alkenes > cycloalkanes > cycloalkanes > alkynes > alkyl benzenes > ketones > alcohols > water, and
- 1.6-hexanediol (1.5-HDO): alkanes > alkenes > cycloalkanes > cycloalkenes > alkynes > alkyl benzenes > ketones > alcohols > water.

The polarity of molecules is used to provide a comprehensive explanation, through the number of hydroxyl groups and their locations and the chain length of the compound. It was found that the hydroxyl group had a greater impact compared to alkyl chain length. For each of the above orders, it could be observed that the long alkyl chain HBDs were associated with low polarity, prompted by the existence of a hydroxyl group in a molecular structure.

From Figure 6-9, glycerol consists of three hydroxyl groups, one located in the middle of the molecular structure, while the other two HBD hydroxyl groups are located at the ends of the molecular structure. Both 1.5-pentanediol and 1.6-hexanediol consist of two hydroxyl groups located at the end of each compound, with five carbons and six carbons, respectively.

As a result, glycerol produced higher experimental infinite dilution activity coefficients than all the other investigated hydrogen bond donors. This was due to the hydroxyl group located in the middle of the molecular structure. In the meantime, the other hydrogen bond donors, which consist of two hydroxyl groups located at the ends of their molecular structures, gave low experimental infinite dilution activity coefficients. Hence, the oxygen-oxygen lone pair repulsion in the

molecular structures of the other hydrogen bond donors could possibly have reduced the hydrogen bonding exhibition and vice versa for glycerol.

Furthermore, the CH_3 number contributed to an increase in the infinite dilution activity coefficients. For example, at T = 313.15 K, the average infinite dilution activity coefficient for 2,2-dimethylbutane was [(EMPYR) Br + EG] = 1.361, [(EMPYR) Br + 1.5-PDO] = 2.902, and [(EMPYR) Br + 1.6-HDO] = 3.002. This means that the longer the alkyl chain length of the HBD, the higher the magnitude of the experimental infinite dilution activity coefficients, as seen in the figures.

In addition, the ionic liquid anion (Br^- or decanoate) interrupted the complex structure as the hydrogen bond donor exhibited hydroxyl group that interacted with the anion instead of interacting with each other.

6.3.2 Partial Molar Properties

The partial molar properties, i.e., Gibbs free energies ($\Delta G_1^{E,\infty}$), enthalpies ($\Delta H_1^{E,\infty}$), and entropies ($\Delta S_1^{E,\infty}$), were determined from the experimental infinite dilution activity coefficients at the temperature, T = 313.15 K. The obtained values are presented in Chapter Five, Tables 5-12, 5-16, 5-20, 5-24, and 5-28. Additionally, the Gibbs-Helmholtz Equation (6-7) given below was used to compute enthalpy values.

$$\Delta(\ln\gamma_{13}^{\infty})\Big/_{\Delta(1/T)} = \Delta H_1^{E,\infty}\Big/_{R} \qquad (6\text{-}7)$$

The experimental data was interpreted in terms of the intermolecular interactions between the studied solvents, viz., pyrrolidinium and phosphonium based DESs, as well as various organic solutes. From Tables 5-12, 5-16, 5-20, 5-24, and 5-8, the partial molar excess enthalpy ($\Delta H_i^{E\prime\infty}$)values obtained by the Gibbs-Helmholtz Equation were negative for straight alkyl chain nonpolar solutes and positive for cyclic solutes as well as polar solutes in the [(EMPYR) Br + Gly]. For example: pentane ($\Delta H_1^{E,\infty}$= -12.42 kJ/mol), cyclopentane ($\Delta H_1^{E,\infty}$= 21.28 kJ/mol), and ethanol ($\Delta H_1^{E,\infty}$= 3.971 kJ/mol). The systems [(EMPYR) Br + EG], [(EMPYR) Br + 1.5-PDO], [(EMPYR) Br + 1.6-HDO], and [(THTDP) Dc + EG], on the other hand, all had negative enthalpies. This suggests strong interactions for all the above systems apart from the system [(EMPYR) Br + Gly], and this is not good for cyclic and polar solutes. Moreover, negative

enthalpies imply solute-solvent interactions for the investigated systems, whereas positive enthalpies indicate a larger dissociation impact in a dilute mixture of a deep eutectic solvent and a solute. Furthermore, a large number of hydroxyl groups for polar solute interactions with hydrogen bond donors led to a large dissociation impact to overcome the association impact in a low concentration of deep eutectic solvent and solute mixture. Hence, this indicates the breaking of hydrogen bondings during the dissolution process in a deep eutectic solvent complex. In addition, negative enthalpies indicate exothermic mixing, whereas positive enthalpies indicate endothermic mixing.

The other partial molar properties, such as entropy and Gibbs free energy, were computed from equation (6-8).

$$\Delta G_1^{E,\infty} = \mathrm{RT} \ln \gamma_{13}^{\infty} = \Delta H_1^{E,\infty} - T\Delta S_1^{E,\infty} \tag{6-8}$$

Equation (6-8) can be also expressed as.

$$\ln \gamma_{13}^{\infty} = \frac{\Delta H_1^{E,\infty}}{RT} - \frac{T\Delta S_1^{E,\infty}}{R} \tag{6-9}$$

For these properties, the date is also displayed in Tables 5-12, 5-16, 5-20, 5-24, and 5-8. At T = 313.15 K, the [(EMPYR) Br + Gly] system produced positive (+) Gibbs free energy values for all of the investigated solutes. For example, pentane was $\Delta G_1^{E,\infty}$= 9.874 kJ/mol and ethanol was $\Delta G_1^{E,\infty}$= 2.612 kJ/mol. The system [(EMPYR) Br + 1.5-PDO] gave positive (+) Gibbs free energy values for all the studied solutes at T = 313.15 K, except for aromatics and polar solutes. For example, pentane ($\Delta G_1^{E,\infty}$ = 6.951 kJ/mol), cyclohexane ($\Delta G_1^{E,\infty}$ = 6.637 kJ/mol), benzene ($\Delta G_1^{E,\infty}$ = -1.928 kJ/mol), and ethanol ($\Delta G_1^{E,\infty}$ = -31.51 kJ/mol). At T = 313.15 K, the system gave positive (+) Gibbs free energy values for all the studied solutes, except for the polar solutes. For example, pentane ($\Delta G_1^{E,\infty}$ =7.789 kJ/mol), cyclohexane ($\Delta G_1^{E,\infty}$ = 5.048 kJ/mol), benzene ($\Delta G_1^{E,\infty}$ = 0.430 kJ/mol), and ethanol ($\Delta G_1^{E,\infty}$ =-3.628 kJ/mol). On the other hand, the [(EMPYR) Br + EG] system gave highly positive Gibbs free energy values for alkynes (e.g., 1-petnyne gave $\Delta G_1^{E,\infty}$ = 51.81 kJ/mol), low and negative (-) Gibbs free energy values for alkenes (e.g., 1-hexene gave $\Delta G_1^{E,\infty}$ = -0.514 kJ/mol), negative (-) Gibbs free energy values for short chain alcohols (e.g., ethanol gave $\Delta G_1^{E,\infty}$ = -3.539 kJ/mol), and the rest of the solutes were positive (+) (e.g., benzene gave $\Delta G_1^{E,\infty}$ = 1.355 kJ/mol and hexane gave $\Delta G_1^{E,\infty}$ = 0.782 kJ/mol). [(THTDP) Dc + EG] on the other hand gave positive (-) Gibbs free energy values for alkanes, alkenes, and alkynes, as well as

their cyclic compounds. However, these gave negative values for long chains such as n-decane ($\Delta G_1^{E,\infty}$ = -13.19 kJ/mol), 1-decene ($\Delta G_1^{E,\infty}$ = -6.990 kJ/mol), as well as methylcyclohexane ($\Delta G_1^{E,\infty}$ = -2.313 kJ/mol). The high positive (+) values are a weak interaction sign for Gibbs free energy values, whereas the less positive values are due to hydrogen bonds, dipole-dipole forces, charge transfer, and other attractive forces, with the studied deep eutectic solvents. Negative (-) Gibbs free energy values are typically associated with good IDAC ($\gamma_{13}^{\infty} > 1$) and solvent-solute interactions (Domanska *et al.*, 2020; Kabane and Redhi, 2020; Zhang *et al.*, 2020a).

Negative entropy values were obtained for the systems [(EMPYR) Br + 1.6-HDO], [(THTDP) Dc + EG], [(EMPYR) Br + 1.5-PDO], and [(EMPYR) Br + EG]. However, [(EMPYR) Br + 1.5-PDO] yielded positive entropy values for alcohols (e.g., methanol $\Delta S_1^{E,\infty}$= 6.352 kJ/mol), and [(EMPYR) Br + EG] yielded a positive value for methanol (($\Delta S_1^{E,\infty}$= 6.194 kJ/mol). The positive (+) entropy values for alcohols were triggered by the breaking of bonds during the dissolution process (Blahut and Dohnal, 2013; Domanska *et al.*, 2020). While the negative entropy for the rest of the solutes and all the investigated systems could indicate that the solute molecules were arranging themselves in the components of the deep eutectic solvents (Nkosi *et al.*, 2018c).

6.3.3. Selectivity and Capacity Potential

Selectivity(S_{ij}^{∞}) and capacity(k_j^{∞}) are two parameters used to denote the separation performance of a specific adsorbent from a mixture of two or more components. This study used selectivity and capacity values to determine the separation performance of various deep eutectic solvent systems, such as [(EMPYR) Br + Gly], [(EMPYR) Br + EG], [(EMPYR) Br + 1.5-PDO], [(EMPYR) Br + 1.6-HDO], and [(THTDP) Dc + EG], in the separation of various organic solutes for closely related boiling components. Equations (6-10) and (6-11) were used to calculate the two parameters from infinite dilution activity coefficients.

$$S_{ij}^{\infty} = \frac{\gamma_i^{\infty}}{\gamma_j^{\infty}} \tag{6-10}$$

$$k_j = \frac{1}{\gamma_j^{\infty}} \tag{6-11}$$

In the above equations, i and j denote the solutes of interest.

The obtained data for the studied separation problems is given in Tables 6-1 to 6-4. Furthermore, the obtained data were compared to previously published ionic liquids as well as commonly used conventional organic solvents, as shown in Tables 6-1 to 6-4 and Figures 6-9 to 6-12.

6.3.3.1 Selectivity and capacity values for benzene/toluene, separation problem

Table 6-1 and Figure 6-9 provide the selectivity and capacity values as well as the comparison of benzene/toluene, binary mixture to the previously studied ionic liquids and conventional organic solvents at temperatures of T = (313.15-343.15) K.

Table 6-1: Comparison of the selectivity and capacity values of the benzene/toluene separation problems for all the investigated systems at various temperatures T = (313.15-343.15) K, using deep eutectic solvents, ionic liquids, and conventional organic solvents

	Selectivity, S_{ij}^{∞}				Capacity, K_j^{∞}			
	Benzene/toluene				Toluene			
Deep eutectic solvent	313.15	323.15	333.15	343.15	313.15	323.15	333.15	343.15
[(EMPYR) Br + Gly][a]	0.460	0.466	0.477	0477	0.016	0.015	0.015	0.014
[(EMPYR) Br + EG][a]	0.966	0.966	0.964	0.963	0.730	0.705	0.685	0.666
[(EMPYR) Br + 1.5-PDO][a]	0.983	0.991	0.984	0.995	0.828	0.763	0.702	0.651
[(EMPYR) Br + 1.6-HDO][a]	0.802	0.828	0.835	0.853	0.492	0.474	0.451	0.438
[(THTDP) Dc + EG][a]	0.830	0.830	0.893	0.853	0.570	0.490	0.425	0.381
Ionic liquids								
[BMPYR] $[B(CN)_4]$[b]	0.737	0.731	0.733	0.734	0.885	0.870	0.855	0.840

[HMPYR] [Tf_2N][c]	-	0.760	0.762	0.750	-	1.000	0.990	0.962
[$P_{6,6,6,14}$] [DCA][d]	0.761	0.793	0.824	0.841	2.387	2.183	2.045	1.912
[OMIM] [NO_3][e]	0.681	0.683	0.685	0.688	0.709	0.704	0.699	0.694
Conventional organic solvent								
[Hexadecane][f]	-	0.990	0.984	1.007	-	1.063	1.055	1.149
[TEG][g]	-	0.650	0.644	0.654	-	0.141	0.147	0.154
[Gly][h]	0.504	0.560	0.593	0.632	0.009	0.011	0.013	0.017

This work[a]; (Blahut and Dohnal, 2013)[b]; (Acree Jr et al., 2012)[c]; (Kabane and Redhi, 2019)[d]; (Duan et al., 2012)[e]; (Schult et al., 2001)[f]; (Sun et al., 2003)[g]; (Ge et al., 2010)[h].

The results presented in Table 6-1 for the separation problem of benzene/toluene are plotted in Figure 6-9 as selectivity values for five investigated deep eutectic solvents, four literature ionic liquids, as well as three conventional organic solvents from the literature data, all at numerous temperatures, T = (313.15-343.15) K.

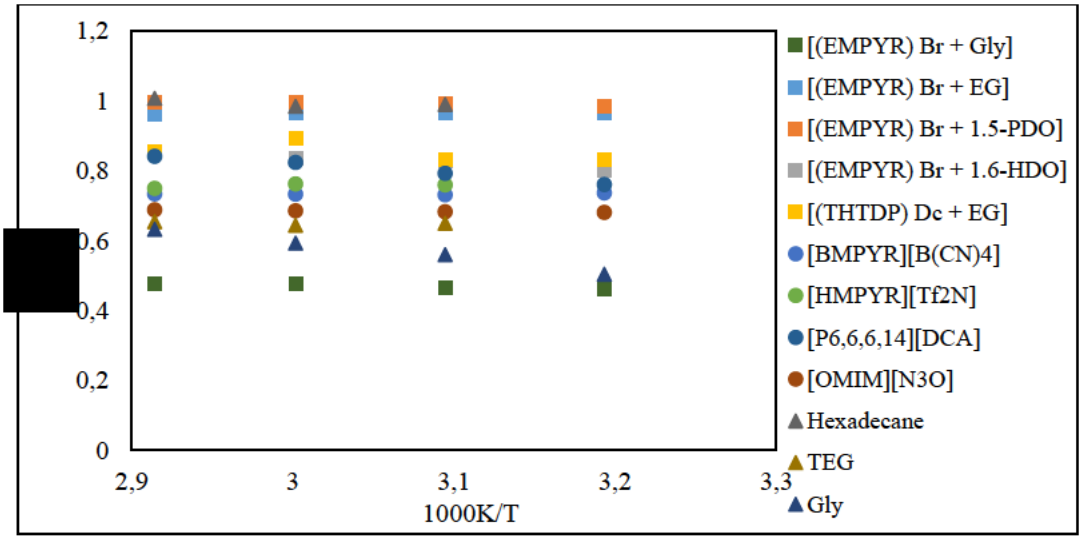

Figure 6-10: Plot of the selectivity values for the selected solvents, including deep eutectic solvents, ionic liquids, and conventional organic solvents versus 1000 K/T for the separation problem, benzene/toluene

Table 6-1 and Figure 6-9 indicate that all the studied deep eutectic solvents for the separation problem of benzene/toluene in terms of the selectivity values were independent of the experimental temperature. Figure 6-9 also shows that the selectivity values for the [(EMPYR) Br + Gly] system was far lower than all the other deep eutectic solvent systems such as [(EMPYR) Br + EG], [(EMPYR) Br + 1.5-PDO], [(EMPYR) Br + 1.6-HDO], and [(THTDP) Dc + EG]. Furthermore, all the four abovementioned DESs systems gave more acceptable selectivity values compared to all the previously investigated ionic liquid systems and all conventional organic solvents except for the glycerol system. Due to their selectivity values, [(EMPYR) Br + EG], [(EMPYR) Br + 1.5-PDO], [(EMPYR) Br + 1.6-HDO], and [(THTDP) Dc + EG] systems would be advantageous for the separation of the chosen separation problem, benzene/toluene. Again, since [(EMPYR) Br + Gly] gave extremely low selectivity values for this separation problem, this suggests poor performance compared to all the solvent systems investigated.

The capacity at infinite dilution values was also evaluated for the selection of a desirable solvent for the separation problem, benzene/toluene (toluene). The systems [(EMPYR) Br + EG], [(EMPYR) Br + 1.5-PDO], [(EMPYR) Br + 1.6-HDO], and [(THTDP) Dc + EG] were discovered to provide acceptable values, implying good performance for all four deep eutectic solvent systems studied above. However, the [(EMPYR) Br + Gly] system produced extremely low and unacceptable capacity values, implying poor performance. As a result, the separation of benzene/toluene using the first four deep eutectic solvent systems via liquid-liquid extraction (LLE) is useful to the separation industry. Furthermore, [(EMPYR) Br + 1.5-PDO] and [(EMPYR) Br + 1.6-HDO] systems would help reduce operation costs because a low volume solvent (1:2 of 30% solvent) would be required in a process and would then be retrieved after use (Petsev *et al.*, 1974; Mohd, 2012).

6.3.3.2 Selectivity and capacity values for cyclohexane/benzene, separation problem

Table (6-2) and Figure (6-10) provide the selectivity and capacity values as well as the comparison of cyclohexane/benzene, binary mixture to the previously studied ionic liquids and conventional organic solvents at temperatures, T = (313.15-343.15) K.

Table 6-2: Comparison of the selectivity and capacity values of cyclohexane/benzene, separation problem for all the investigated systems at various temperatures T = (313.15-343.15) K, using deep eutectic solvents, ionic liquids, and conventional organic solvents

Deep eutectic solvents	Selectivity, S_{ij}^{∞}				Capacity, K_j^{∞}			
	Cyclohexane/benzene				Benzene			
	313.15	323.15	333.15	343.15	313.15	323.15	333.15	343.15
[(EMPYR) Br + Gly][a]	3.685	4.297	4.923	5.844	0.035	0.033	0.031	0.029
[(EMPYR) Br + EG][a]	1.302	1.282	1.278	1.255	0.758	0.729	0.771	0.692
[(EMPYR) Br + 1.5-PDO][a]	0.461	0.487	0.518	0.546	0.842	0.770	0.714	0.667
[(EMPYR) Br + 1.6-HDO][a]	1.474	1.432	1.432	1.400	0.613	0.573	0.540	0.514
[(THTDP) Dc + EG][a]	4.794	4.834	4.905	4.984	0.686	0.590	0.476	0.408
Ionic liquids								
[BMPYR][B(CN)$_4$][b]	10.22	9.822	9.126	8.513	1.200	1.189	1.166	1.144
[HMPYR][Tf$_2$N][c]	-	6.789	5.792	5.987	-	1.316	1.299	1.282
[P$_{6,6,6,14}$][DCA][d]	2.298	2.149	2.065	2.048	3.135	2.755	2.481	2.273
[OMIM][NO$_3$][e]	6.531	6.072	5.694	5.323	1.042	1.031	1.020	1.010
Conventional organic solvents								
[Hexadecane][f]	-	0.793	0.811	0.804	-	1.073	1.072	1.142

[Gly][g]	3.649	3.542	3.681	3.826	0.018	0.020	0.022	0.026
[2-PYR][h]	7.786	7.323	6.797	-	0.354	0.352	0.350	-

This work[a]; (Blahut and Dohnal, 2013)[b]; (Acree Jr et al., 2012)[c]; (Kabane and Redhi, 2019)[d]; (Duan et al., 2012)[e]; (Schult et al., 2001)[f]; (Ge et al., 2010)[g]; (Gruber et al., 1998)[h].

The results presented in Table 6-2 for the cyclohexane/benzene are plotted in Figure 6-10 as selectivity values for five investigated deep eutectic solvents, four literature ionic liquids, as well as three conventional organic solvents from the literature data, all at numerous temperatures, T = (313.15-343.15) K.

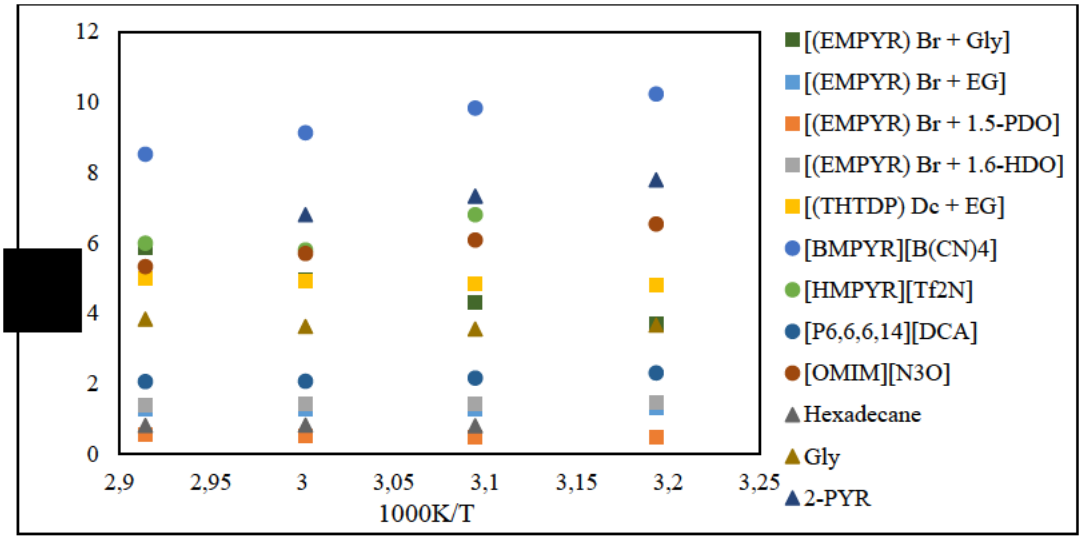

Figure 6-11: Plot of the selectivity values for all the selected solvents, including deep eutectic solvents, ionic liquids, and conventional organic solvents versus 1000 K/T for the separation problem, cyclohexane/benzene

Table 6-2 and Figure 6-10 shows that the system, [(EMPYR) Br + 1.5-PDO] in the separation problem, cyclohexane/benzene had lower and unacceptable selectivity values (<1), whereas both [(EMPYR) Br + EG] and [(EMPYR) Br + 1.6-HDO] gave reasonable selectivity values, i.e., S_{ij}^{∞} = 1.302 and S_{ij}^{∞}= 1.474, respectively, at T = 313.15 K, but lower compared to the literature values of ionic liquids and conventional solvents except for hexadecane (S_{ij}^{∞} = 0.793 at T = 323.15 K). However, both [(EMPYR) Br + Gly] and [(THTPD) Dc + EG] were higher but acceptable and more comparable to ionic liquids and conventional organic solvents from the literature. For [(EMPYR) Br + 1.5-PDO], this indicates poor separation for the chosen separation problem,

cyclohexane/benzene. All the other investigated deep eutectic solvents could be utilized for the separation of mixtures of cyclohexane from benzene.

Nevertheless, all these solvents, [(EMPYR) Br + 1.5-PDO], [(THTPD) Dc + EG], [(EMPYR) Br + 1.6-HDO], and [(THTPD) Dc + EG] gave low but reasonable capacity values, meanwhile [(EMPYR) Br + Gly] gave the lowest and non-acceptable capacity values. As a result, the separation of cyclohexane from benzene using some deep eutectic solvents, such as [(EMPYR) Br + EG], [(EMPYR) Br + 1.6-HDO], [(THTPD) Dc + EG]) via liquid-liquid extraction is possible.

6.3.3.3 Selectivity and capacity values for acetone/ethanol, separation problem

Table 6-3 and Figure 6-11 provide the selectivity and capacity values as well as the comparison of acetone/ethanol, binary mixture to the previously studied ionic liquids and conventional organic solvents at temperatures, T = 313.15-343.15 K.

Table 6-3: Comparison of the selectivity and capacity values of acetone/ethanol separation problems for all the investigated systems at various temperatures, T = (313.15-343.15) K, using deep eutectic solvents, ionic liquids, and conventional organic solvents

Deep eutectic solvents	Selectivity, S_{ij}^{∞}				Capacity, K_j^{∞}			
	Acetone/ethanol				Ethanol			
	313.15	323.15	333.15	343.15	313.15	323.15	333.15	343.15
[(EMPYR) Br + Gly][a]	2.073	2.086	1.959	1.923	0.367	0.354	0.330	0.321
[(EMPYR) Br + EG][a]	1.903	1.751	1.648	1.585	1.242	1.131	1.033	0.962
[(EMPYR) Br + 1.5-PDO][a]	5.914	4.667	3.680	2.930	4.505	3.300	2.445	1.845
[(EMPYR) Br + 1.6-HDO][a]	0.948	1.004	0.984	1.047	0.925	0.825	0.719	0.640
[[THTDP) Dc + EG][a]	9.829	6.765	5.925	4.172	5.882	3.226	1.887	1.086

Ionic liquids								
[BMPYR][B(CN)$_4$][b]	0.337	0.354	0.394	0.432	0.885	0.870	0.855	0.917
[(OH)$_2$C$_3$MPYR][Cl][c]	3.282	3.146	2.927	2.761	4.854	3.559	2.625	1.931
[P$_{14,6,6,6}$][(C$_8$H$_{17}$)$_2$PO$_2$][d]	-	18.00	15.60	13.83	-	20.00	16.67	14.29
[P$_{6,6,6,14}$][DCA][e]	1.032	1.011	1.000	1.010	2.950	2.786	2.611	2.494
Conventional organic solvents								
[2-PYR][f]	2.161	2.153	2.145	-	0.954	0.971	0.977	-
[Sulfolane][g]	-	-	0.627	-	-	-	0.428	-

This work[a]; (Blahut and Dohnal, 2013)[b]; (Kabane et al., 2019a)[c]; (Kabane et al., 2019b)[d]; (Kabane and Redhi, 2019)[e]; (Gruber et al., 1998)[f]; (Letcher and Moollan, 1995)[g].

The results presented in Table 6-3 for the acetone/ethanol separation problem are plotted in Figure 6-11, as selectivity values for five investigated deep eutectic solvents, four literature ionic liquids, as well as two conventional organic solvents from the literature data, all at numerous temperatures, T = (313.15-343.15) K.

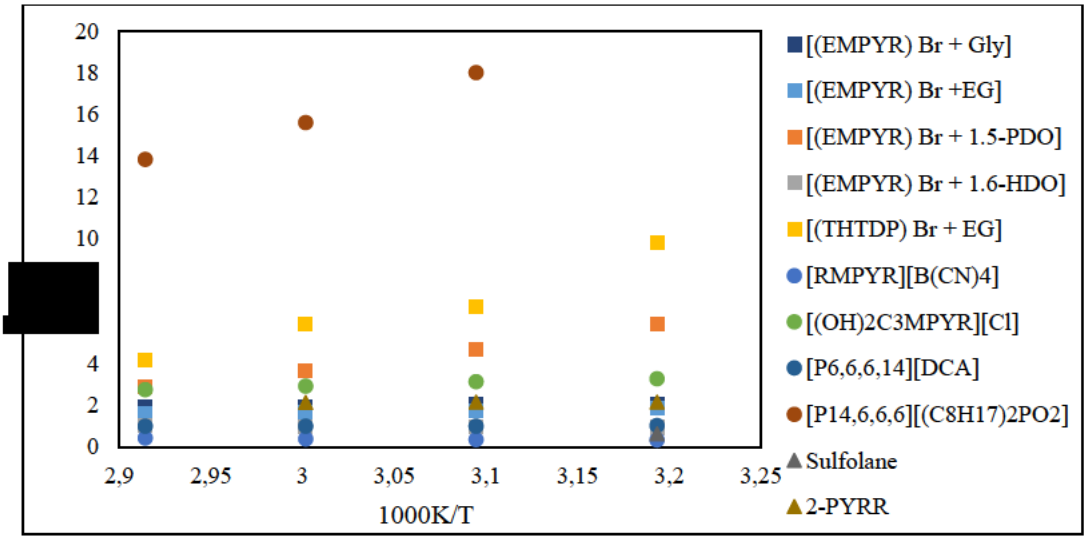

Figure 6-12: Plot of the selectivity values for all the selected solvents, including deep eutectic solvents, ionic liquids, and conventional organic solvents versus 1000 K/T for the separation problem, acetone/ethanol

Table 6-3 and Figure 6-11 signifies that the systems, [(EMPYR) Br + 1.5-PDO] and [(THTDP) Dc + EG] in a separation problem for acetone/ethanol mixture, gave higher values, while the other systems, such as [(EMPYR) Br + EG], [(EMPYR) Br + 1.6-HDO], and [(EMPYR) Br + Gly] also gave high values but relatively acceptable selectivity values which were also comparable to the ionic liquids as well as conventional organic solvents from the literature except $[P_{14,6,6,6}][(C_8H_{17})_2PO_2]$, as this was the highest compared to all evaluated systems in terms of separation problem, acetone/ethanol. Nevertheless, all the above investigated systems suggested that they could all be used in the separation industry for the separation of acetone from ethanol. Moreover, except for [(EMPYR) Br + 1.6-HDO], the obtained values for all investigated systems were acceptable. In addition, all investigated systems could help minimize the costs associated with the operation, as less solvent (approx. 30% solvent) would be required in a process and could then be retrieved after use (Petsev *et al.*, 1974; Mohd, 2012).

6.3.3.4 Selectivity and capacity values for hexane/1-hexene, separation problem

Table 6-4 and Figure 6-12 compare hexane/1-hexene binary mixture selectivity and capacity to previously studied ionic liquids and conventional organic solvents at T = 313.15–343.15 K.

Table 6-4: Comparison of the selectivity and capacity values of hexane/1-hexene separation problem for all the investigated systems at various temperatures, T = (313.15-343.15) K, using deep eutectic solvents, ionic liquids, and conventional organic solvents

	Selectivity, S_{ij}^{∞}				Capacity, K_j^{∞}			
	Hexane/1-hexene				1-hexene			
Deep eutectic solvent	313.15	323.15	333.15	343.15	313.15	323.15	333.15	343.15
[(EMPYR) Br + Gly][a]	1.286	1.291	1.284	1.379	0.367	0.354	0.330	0.321
[(EMPYR) Br + EG][a]	0.839	0.870	0.901	0.945	0.599	0.591	0.573	0.563
[(EMPYR) Br + 1.5-PDO][a]	1.258	1.219	1.209	1.186	0.436	0.407	0.391	0.372
[(EMPYR) Br + 1.6-HDO][a]	1.186	1.159	1.141	1.126	0.384	0.368	0.352	0.340
[(THTDP) Dc + EG][a]	0.698	0.682	0.645	0.610	0.135	0.105	0.083	0.067
Ionic liquids								
[HMPYR][BTI][b]	1.695	1.585	1.476	-	0.216	0.220	0.225	-
[OMPYR][BTI][b]	1.535	1.522	1.524	-	0.304	0.311	0.317	-
[HMPYR][Tf_2N][c]	-	1.697	1.594	1.601	-	0.219	0.216	0.225
[$P_{6,6,6,14}$][DCA][d]	1.272	1.263	1.249	1.249	1.093	1.021	0.946	0.898
Conventional organic solvents								
[Hexadecane][e]	-	1.006	0.987	1.009	-	1.170	1.139	1.225
[2-PYR][h]	2.004	1.927	1.867	-	0.052	0.054	0.056	-

This work[a]; (Nebig et al., 2009)[b]; (Acree Jr et al., 2012)[c]; (Kabane and Redhi, 2019)[d]; (Schult et al., 2001)[e]; (Gruber et al., 1998)[h].

The results tabled in Table 6-4 for hexane/1-hexene, separation problem are also plotted in Figure 6-12, as selectivity values for five investigated deep eutectic solvents, four literature ionic liquids, as well as two conventional organic solvents from the literature data, all at numerous temperatures varying from T = (313.15-343.15) K.

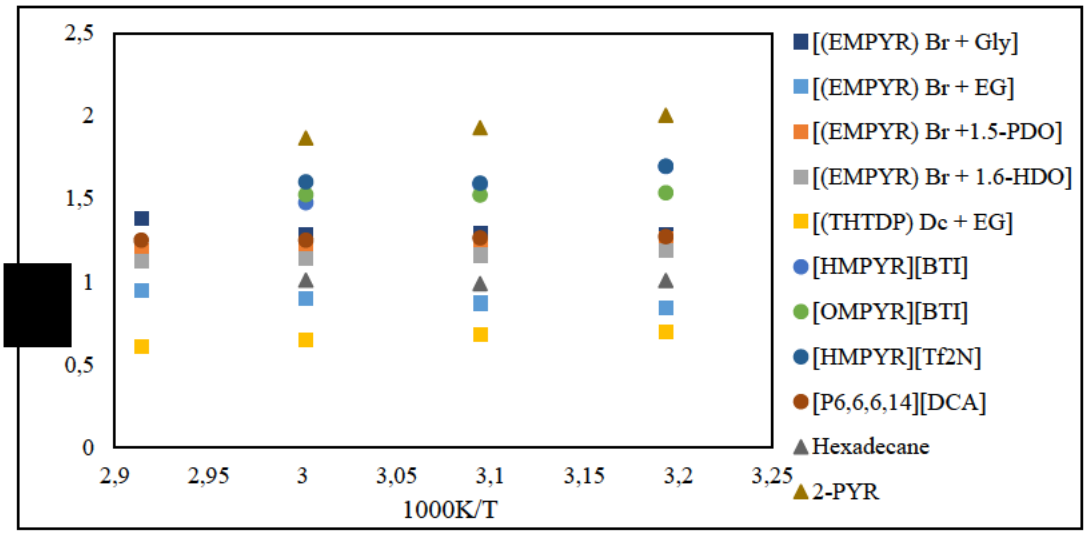

Figure 6-13: Plot of the selectivity values for all the selected solvents, including deep eutectic solvents, ionic liquids, and conventional organic solvents versus 1000 K/T for the separation problem, hexane/1-hexene

Table 6-4 and Figure 6-12 indicates that the investigated deep eutectic solvents, such as [(EMPYR) Br + 1.5-PDO], [(EMPYR) Br + 1.6-HDO], and [(EMPYR) Br + Gly] for the separation of hexane from 1-hexene gave acceptable selectivity values which are also comparable to the previously studied ionic liquids, including $[P_{6,6,6,14}][DCA]$, while the other deep eutectic solvents, such as [(THTDP) Br + EG] and [(EMPYR) Br + EG] gave lower selectivity values render them not suitable for hexane/1-hexene at the temperatures investigated. Likewise, of all the deep eutectic solvents investigated in terms of the separation problem, hexane/1-hexene had lower capacity values. This could lead to these DESs not being selected for future separation purposes.

6.3.4 Impact of Hydrogen Bond Donor on the Selectivity and Capacity

The effect of the hydrogen bond donor in terms of the selectivity and capacity potential for various industrial separation problems has yielded the following order:

- ***Benzene/toluene***

  Selectivity: 1.5-pentanediol > ethylene glycol > 1.6-hexanediol > glycerol

  Capacity: 1.5-pantanediol > ethylene glycol > 1.6-hexanediol > glycerol

- ***Cyclohexane/benzene***

  Selectivity: Glycerol > 1.6-hexanediol > ethylene glycol > 1.5-pentanediol

  Capacity: 1.5-pentanediol > ethylene glycol > 1.6-hexanediol > glycerol

- ***Acetone/ethanol***

  Selectivity: Glycerol > 1.5-pentanediol > ethylene glycol > 1.6-hexanediol

  Capacity: 1.5-pentanediol > ethylene glycol > 1.6-hexanediol > glycerol

- ***Hexane/1-hexene***

  Selectivity: Glycerol > 1.5-pentanediol > 1.6-hexanediol > ethylene glycol

  Capacity: Ethylene glycol > 1.5-pentanediol > 1.6-hexanediol > glycerol

In the above selectivity order, glycerol had higher selectivity values for cyclohexane/benzene and hexane/1-hexene, and this was also supported by its infinite dilution activity coefficients. For the 1.5-pentanediol and 1.6-hexanediol HBDs, 1.5-pentanediol produced better selectivity values for the aromatic separation problem (benzene/toluene) followed by ethylene glycol, 1.6-hexanediol, and glycerol, respectively, whereas for the polar mixture separation problem (acetone/ethanol), glycerol was higher followed by 1.5-pentanediol, ethylene glycol, and 1.6-hexanediol, respectively. This could possibly be due to hydrogen bond donor alkyl chain length, as well as the number of hydroxyl groups. Moreover, the hydroxyl group was more effective compared to the chain length.

In terms of the capacity order, glycerol produced lower capacity values for all the investigated solutes, while diethylene glycol had higher capacity values for all the investigated HBDs and for

all studied separation problems, apart from hexane/1-hexene. In this separation problem, ethylene glycol performed better compared to 1.5-pentanediol, and this was due to the non-polarity of these solutes. Again, this behaviour may possibly be attributed to hydrogen bond donor alkyl chain length, as well as the number of hydroxyl groups. Similarly, as explained earlier for selectivity values and infinite dilution activity coefficients.

In order to understand the molecular nature and interactions of deep eutectic solvent (DES) and their mixtures with other substances, as well as to predict their phase equilibria and thermodynamic properties, a number of theoretical approaches have thus been developed over the past years. Depending on how accurate these approaches are and how they are grounded in theory, these approaches have had varying degrees of success. Additionally, there are no rules for choosing a suitable modelling strategy for prediction of the aforementioned properties of DESs remains an issue to be resolved. This contribution is focused on presenting a study and a concise classification of the different theoretical procedures implemented to the description of the thermodynamic behaviour of DESs and their mixtures in various industrial applications.

CHAPTER SEVEN

CONCLUSIONS AND RECOMMENDATIONS

The primary objectives of the present research project were to investigate the effects of temperature, hydrogen bond donors (HBDs), a hydrogen bond accepter (HBA), and the complex structures of various deep eutectic solvents (DESs), as well as their separation performance with various volatile organic solvents. Thermophysical properties were calculated from experimental physical properties such as density and sound velocity in order to determine the capability or effectiveness of the deep eutectic solvents as promising separation agents.

The physical properties, i.e., density and sound velocity, of alcohols, including methanol and ethanol, were studied at numerous temperatures, T = (293.15-313.15) K, with the employment of the Anton Paar DMA 5000 M digital vibrating tube densitometer analyser to the two deep eutectic solvents:

- {[1-ethyl-1-methylpyrrolidinium bromide + ethylene glycol] + methanol/ethanol}, {[(EMPYR) Br + Gly] + methanol/ethanol}
- {[1-ethyl-1-methylpyrrolidinium bromine + glycol] + methanol/ethanol}, {[(EMPYR) Br + EG] + methanol/ethanol}

The intermolecular interactions in binary mixtures of methanol and/or ethanol in [(EMPYR) Br + Gly] and/or [(EMPYR) Br + EG] systems were studied using thermophysical parameters such as excess molar volume (V_m^E), isentropic compressibility (K_s), variation isentropic compressibility (ΔK_s), and intermolecular free length (L_f), computed from density and sound velocity. The V_m^Evalues computed on the mixture were correlated or smoothed using the Redlich-Kister Equation. The obtained V_m^Edata had negative (-) values, favouring the high dominance of solute-solvent/ion-solvent interactions over self-ionizations such ion-ion/solute-solute/solvent-solvent interactions for all of the analysed systems. All of the examined systems had positive (+) and negative (-), K_s and ΔK_svalues, respectively. It's possible that the resulting effect is due to the near proximity of the striking molecules. Importantly, strong interactions between [(EMPYR) Br + EG] components and methanol/ethanol molecules resulted in the binary mixtures being less compressible. As a result, all the K_s and ΔK_svalues obtained were acceptable and in good agreement with the theoretical values.

Furthermore, in this study, the infinite dilution activity coefficients (γ_{13}^{∞}) for various organic solutes at different temperatures, T = (313.15-343.15) K, were determined with the use of gas liquid chromatography (GLC) for all five investigated and listed deep eutectic solvent systems:

- 1-ethyl-1-methylpyrrolidinium bromide + glycol, [(EMPYR) Br + Gly]
- 1-ethyl-1-methylpyrrolidinium bromide + ethylene glycol, [(EMPYR) Br + EG]
- 1-ethyl-1-methylpyrrolidinium bromide + 1.5-pentanediol, [(EMPYR) Br + 1.5-PDO]
- 1-ethyl-1-methylpyrrolidinium bromide + 1.6-hexanediol, [(EMPYR) Br + 1.6-HDO]
- Trihexyltetredecylphosphonium decanoate + ethylene glycol, [(THTDP) Dc + EG]

This research work found that GLC was the appropriate method to study innovative deep eutectic solvents because of its high preference in the chemical industry and its simple operational procedures when computing γ_{13}^{∞}values for various organic solutes. During the measurements, the GLC instrument detector, thermal conductivity detector (TCD) was calibrated and conditioned before any experimental analysis. The reproducibility and reliability of the experimental results produced by the GLC instrument were confirmed by the determination of γ_{13}^{∞}values for various organic solutes in hexadecane (test system). The obtained results for various organic solutes in the test system, hexadecane, gave good correlation with previous literature findings. This includes ionic liquids and conventional organic solvents.

According to the obtained DESs results, all the investigated systems had sufficient volatility. Thus, the GLC method is deemed suitable since it requires small amounts of deep eutectic solvents (25-35) % and the separation was achieved, resulting in easy calculation of the γ_{13}^{∞} data. Additionally, the obtained γ_{13}^{∞} proves that the studied deep eutectic solvents with the investigated organic solutes are future possible.

The selectivity (S_{ij}^{∞}) and capacity (k_j^{∞})values as well as the partial molar excess properties, i.e., Gibbs free energy ($\Delta G_1^{E,\infty}$), enthalpy ($\Delta H_1^{E,\infty}$), and entropy ($\Delta S_1^{E,\infty}$), were calculated from the infinite dilution activity coefficients also to determine the effectiveness/usefulness of the deep eutectic solvents as the future promising separation agents.

The values of selectivity and capacity provided in-depth knowledge of the applied use of the deep eutectic solvents. The present study also provided more knowledge on the feasibility of the deep

eutectic solvents' application to solvent extraction and extractive distillation. As a result, the γ_{13}^{∞} experimental data was utilised in the inspection of currently studied deep eutectic solvents to perform or enhance the separation of mixtures of closely interrelated boiling mixtures. In addition, the following interpretations were made:

- ***Benzene/toluene:*** In this separation problem, both selectivity and capacity values were acceptable for all the investigated systems except for the [(EMPYR) Br + Gly] system, as this was very low for both selectivity and capacity values. The capacity values of the [(EMPYR) Br + 1.6-HDO] and [(THTDP) Dc + EG] systems were both low but reasonable. Furthermore, all investigated deep eutectic solvents were comparable to the previously investigated ionic liquids as well as hexadecane but not to other conventional organic solvents, such as 1.6-hexanediol (1.6-HDO) and glycerol (Gly).

- ***Cyclohexane/benzene:*** For this separation problem, both [(EMPYR) Br + Gly] and [(THTDP) Dc + EG] systems gave higher selectivity values but lower capacity values, which might have been caused by this deep eutectic solvents' viscosity, as they were highly viscous. All the other investigated deep eutectic solvents gave acceptable selectivity values except for [(EMPYR) Br + 1.5-PDO], which gave lower values. On the other hand, all the obtained capacity values were low but reasonable. Hence, all the investigated deep eutectic solvents were potentially useful for this separation problem except for [(EMPYR) Br + 1.5-PDO]. Additionally, both ionic liquids and conventional organic solvents, except hexadecane, showed better performance for selectivity and capacity values compared to the investigated deep eutectic solvents.

- ***Acetone/ethanol:*** For this separation problem, all the investigated deep eutectic solvents were potentially useful, as revealed by both selectivity values and capacity values, except for [(EMPYR) Br + Gly]. Moreover, all the investigated deep eutectic solvents proved to be significantly acceptable for this separation problem and were comparable with the most ionic liquids as well as conventional organic solvents, such as 2-pyrrolidone.

- ***Hexane/1-hexene:*** All the investigated deep eutectic solvents were acceptable in terms of the selectivity values, except for the [(THTDP) Dc + EG], as this was a little low compared to the other deep eutectic solvents. All the deep eutectic solvents generally had lower capacity values.

According to the data attained, this proved to be significant in dealing with the issue caused by volatile organic solvents in the environment. Based on the performance index and high selectivity produced by the presently investigated solvents for industrial separation processes, some deep eutectic solvents were found to be plausible alternatives to replace some ionic liquids and conventional organic solvents.

Nevertheless, other various properties, such as viscosity, refractive index, conductivity, thermal stability, and surface tension, should be studied to elaborate on the present study. Furthermore, additional separation problems should be investigated in the future for these deep eutectic solvents. In addition, multicomponent deep eutectic solvents (> 2) could also provide enhanced separation potential and need to be investigated.

References

[1] Abbott, A. P., Al-Barzinjy, A. A., Abbott, P. D., Frisch, G., Harris, R. C., Hartley, J. and Ryder, K. S. 2014. Speciation, physical and electrolytic properties of eutectic mixtures based on CrCl3.H2O and urea. *Physical Chemistry Chemical Physics*, 16 (19): 9047-9055.

[2] Abbott, A. P., Boothby, D., Capper, G., Davies, D. L. and Rasheed, R. K. 2004. Deep eutectic solvents formed between choline chloride and carboxylic acids: versatile alternatives to ionic liquids. *Journal of the American Chemical Society*, 126 (29): 9142-9147.

[3] Abbott, A. P., Capper, G., Davies, D. L., Rasheed, R. K. and Tambyrajah, V. 2003. Novel solvent properties of choline chloride/urea mixtures. *Chemical communications*, (1): 70-71.

[4] Abdussalam-Mohammed, W., Qasem Ali, A. and O Errayes, A. 2020. Green chemistry: principles, applications, and disadvantages. *Chemical Methodologies*, 4 (4): 408-423.

[5] Abranches, D. O. and Coutinho, J. A. 2022. Type V Deep Eutectic Solvents: Design and Applications. *Current Opinion in Green and Sustainable Chemistry*, 35: 100612.

[6] Abri, A., Babajani, N., Zonouz, A. M. and Shekaari, H. 2019. Spectral and thermophysical properties of some novel deep eutectic solvent based on l-menthol and their mixtures with ethanol. *Journal of Molecular Liquids*, 285: 477-487.

[7] Acree Jr, W. E., Baker, G. A., Revelli, A.-L., Moise, J.-C. and Mutelet, F. 2012. Activity coefficients at infinite dilution for organic compounds dissolved in 1-alkyl-1-methylpyrrolidinium bis (trifluoromethylsulfonyl) imide ionic liquids having six-, eight-, and ten-carbon alkyl chains. *Journal of Chemical & Engineering Data*, 57 (12): 3510-3518.

[8] Addouni, M., Benyounes, H., Jin, S. and Shen, W. 2020. Extraction process design for the separation of aromatic and aliphatic hydrocarbons using organic solvent, ionic liquid or their mixture: a comparative study. *Brazilian Journal of Chemical Engineering*, 37: 307-322.

[9] Adewole, J., Ahmad, A., Ismail, S. and Leo, C. 2013. Current challenges in membrane separation of CO2 from natural gas: A review. *International Journal of Greenhouse Gas Control*, 17: 46-65.

[10] Adlercreutz, H. 1971. Evaluation of gas-liquid chromatographic techniques for the estimation of oestrogens. *Clinica Chimica Acta*, 34 (2): 231-240.

[11] Albuquerque, B. R., Heleno, S. A., Oliveira, M. B. P., Barros, L. and Ferreira, I. C. 2021. Phenolic compounds: current industrial applications, limitations and future challenges. *Food and Function*, 12 (1): 14-29.

[12] Alimoradi, V., Mogaddam, M. R. A., Farajzadeh, M. A., Nemati, M. and Lotfipour, F. 2022. Surfactant-assisted salting-out homogenous liquid-liquid extraction based on deep eutectic solvents using central composite design; Application in the extraction of natamycin from fruit juices before its determination by HPLC-UV. *Microchemical Journal*: 107504.

[13] Alizadehdakhel, A. and Golzary, A. 2020. An environmental friendly process for extraction of active constituents from herbal plants. *Environmental Energy and Economic Research*, 4 (1): 69-81.

[14] Alkhatib, I. I., Bahamon, D., Llovell, F., Abu-Zahra, M. R. and Vega, L. F. 2020. Perspectives and guidelines on thermodynamic modelling of deep eutectic solvents. *Journal of Molecular Liquids*, 298: 112183.

[15] Alvarez, V. H., Mattedi, S., Martin-Pastor, M., Aznar, M. and Iglesias, M. 2011. Thermophysical properties of binary mixtures of {ionic liquid 2-hydroxy ethylammonium acetate+(water, methanol, or ethanol)}. *The Journal of Chemical Thermodynamics*, 43 (7): 997-1010.

[16] Anwar, N. and Yasmeen, S. 2016. Volumetric, compressibility and viscosity studies of binary mixtures of [EMIM][NTf2] with ethylacetate/methanol at (298.15–323.15) K. *Journal of Molecular Liquids*, 224: 189-200.

[17] Armenta, S., Garrigues, S., Esteve-Turrillas, F. A. and de la Guardia, M. 2019. Green extraction techniques in green analytical chemistry. *Trends in Analytical Chemistry*, 116: 248-253.

[18] Arumugam, V., Moodley, K. G., Ogundele, O. P., Redhi, G. G., Moodley, A. and Gao, Y. 2020. Physicochemical and thermodynamic properties of pyrrolidinium-based ionic liquids and their binary mixtures with carboxylic acids. *Journal of Molecular Liquids*, 310: 113183.

[19] Bagheri, H., Karimi, N., Dan, S., Notej, B. and Ghader, S. 2021. Ionic liquid excess molar volume prediction: A conceptual comparison. *Journal of Molecular Liquids*, 336: 116581.

[20] Bahadur, I. and Deenadayalu, N. 2013. Apparent molar volume and apparent molar isentropic compressibility for the binary systems {methyltrioctylammoniumbis (trifluoromethylsulfonyl) imide+ ethyl acetate or ethanol} at different temperatures under atmospheric pressure. *Thermochimica Acta*, 566: 77-83.

[21] Bauer, N. and Lewin, S. 1959. Measurement of Density of Liquids. *Part I of Physical Methods of Organic Chemistry, 3rd Ed., A Weissberger, Ed., Interscience, New York*: 132-190.

[22] Blahut, A. and Dohnal, V. 2013. Interactions of volatile organic compounds with the ionic liquids 1-butyl-1-methylpyrrolidinium tetracyanoborate and 1-butyl-1-methylpyrrolidinium bis (oxalato) borate. *The Journal of Chemical Thermodynamics*, 57: 344-354.

[23] Blanco, L. H. and Vargas, E. F. 2004. An improved magnetic float densimeter. *Instrumentation Science & Technology*, 32 (1): 13-20.

[24] Bottomley, G. and Scott, R. 1974. A grease-free continuous dilution dilatometer; excess volumes for benzene+ carbon tetrachloride. *The Journal of Chemical Thermodynamics*, 6 (10): 973-981.

[25] Brouwer, T. and Schuur, B. 2020. Bio-based solvents as entrainers for extractive distillation in aromatic/aliphatic and olefin/paraffin separation. *Green Chemistry*, 22 (16): 5369-5375.

[26] Bruce, E. P., John, M. P. and John, P. C. 2001. *Properties of gases and liquids*: McGraw-Hill Companies.

[27] Bryant, S. J., Christofferson, A. J., Greaves, T. L., McConville, C. F., Bryant, G. and Elbourne, A. 2022. Bulk and interfacial nanostructure and properties in deep eutectic solvents: Current perspectives and future directions. *Journal of Colloid and Interface Science*, 608: 2430-2454.

[28] Cai, J., Xing, Y. and Zhao, X. 2012. Quantum sieving: feasibility and challenges for the separation of hydrogen isotopes in nanoporous materials. *RSC advances*, 2 (23): 8579-8586.

[29] Calvo-Flores, F. G., Monteagudo-Arrebola, M. J., Dobado, J. A. and Isac-García, J. 2018. Green and bio-based solvents. *Topics in Current Chemistry*, 376 (3): 1-40.

[30] Castells, R. C., Arancibia, E. L., Nardillo, A. M. and Castells, C. 1990. Thermodynamics of hydrocarbon solutions using glc n-Hexane, n-heptane, benzene, and toluene as solutes each at infinite dilution in n-hexadecane, in n-octadecane, and in n-eicosane. *The Journal of Chemical Thermodynamics*, 22 (10): 969-977.

[31] Chabib, C. M., Ali, J. K., Abi Jaoude, M., Alhseinat, E., Adeyemi, I. A. and Al Nashef, I. M. 2022. Application of deep eutectic solvents in water treatment processes: A review. *Journal of Water Process Engineering*, 47: 102663.

[32] Charles, E. 1934. *The twilight of parenthood*. WW Norton, Incorporated.

[33] Chaudhary, N. and Nain, A. K. 2020. Densities, speeds of sound, viscosities, refractive indices, excess and partial molar properties of binary mixtures of 1-butyl-3-methylimidazolium tetrafluoroborate with formamide at temperatures from 293.15 to 318.15 K. *Journal of Molecular Liquids*, 305: 112816.

[34] Cheng, M.-H., Sekhon, J. J., Rosentrater, K. A., Wang, T., Jung, S. and Johnson, L. A. 2018. Environmental impact assessment of soybean oil production: Extruding-expelling process, hexane extraction and aqueous extraction. *Food and Bioproducts Processing*, 108: 58-68.

[35] Cheong, W. J. 2003. A critical examination of the limiting activity coefficients of normal alkanes in common organic liquids. *Bulletin of the Korean Chemical Society*, 24 (11): 1708-1710.

[36] Cheremisinoff, N. P. 2003. *Industrial solvents handbook, revised and expanded*. 2nd ed. Boca Raton: CRC press.

[37] Choi, Y. H. and Verpoorte, R. 2019. Green solvents for the extraction of bioactive compounds from natural products using ionic liquids and deep eutectic solvents. *Current Opinion in Food Science*, 26: 87-93.

[38] Conder, J. and Young, C. 1979. Physicochemical Measurements by Gas Chromatography. *Willey, NY*.

[39] Coto, B., Suárez, I., Tenorio, M. J. and Huerga, I. 2022. Extraction of aromatic and polyaromatic compounds with NMP: experimental and model description. *Fluid Phase Equilibria*, 554: 113293.

[40] Cruickshank, A., Windsor, M. and Young, C. 1966a. The use of gas-liquid chromatography to determine activity coefficients and second virial coefficients of mixtures I. Theory and verification of method of data analysis. *Proceedings of the Royal Society of London. Series A. Mathematical and Physical Sciences*, 295 (1442): 259-270.

[41] Cruickshank, A., Windsor, M. and Young, C. 1966b. The use of gas-liquid chromatography to determine activity coefficients and second virial coefficients of mixtures II. Experimental studies on hydrocarbon solutes. *Proceedings of the Royal Society of London. Series A. Mathematical and Physical Sciences*, 295 (1442): 271-287.

[42] Cseri, L., Razali, M., Pogany, P. and Szekely, G. 2018. Organic solvents in sustainable synthesis and engineering. In: *Green Chemistry*. Elsevier, 513-553.

[43] Cunha, D. L., Coutinho, J. A., Daridon, J. L., Reis, R. A. and Paredes, M. L. 2013. An atomic contribution model for the prediction of speed of sound. *Fluid Phase Equilibria*, 358: 108-113.

[44] Cunha, S. C. and Fernandes, J. O. 2018. Extraction techniques with deep eutectic solvents. *Trends in Analytical Chemistry*, 105: 225-239.

[45] Curzons, A., Constable, D. and Cunningham, V. 1999. Solvent selection guide: a guide to the integration of environmental, health and safety criteria into the selection of solvents. *Clean Products and Processes*, 1 (2): 82-90.

[46] Cvetanovic, A. 2019. Extractions without organic solvents: advantages and disadvantages. *Chemistry Africa*, 2 (3): 343-349.

[47] Debenedetti, P. and Kumar, S. 1986a. Infinite dilution fugacity coefficients and the general behavior of dilute binary systems. *AIChE journal*, 32 (8): 1253-1262.

[48] Debenedetti, P. G. and Kumar, S. K. 1986b. Thermodynamics and statistical mechanics of dilute binary mixtures.

[49] Dobryakov, Y. G. and Vitenberg, A. 2006. Determination of distribution coefficients of volatile sulfur-containing compounds among aqueous solutions and gas phase by continuous gas extraction. *Russian Journal of Applied Chemistry*, 79 (8): 1244-1250.

[50] Dohnal, V. and Horáková, I. 1991. A new variant of the Rayleigh distillation method for the determination of limiting activity coefficients. *Fluid phase equilibria*, 68: 173-185.

[51] Dohrn, R. and Pfohl, O. 2002. Thermophysical properties-Industrial directions. *Fluid Phase Equilibria*, 194-197: 15-29.

[52] Domanska, U., Redhi, G. G. and Marciniak, A. 2009. Activity coefficients at infinite dilution measurements for organic solutes and water in the ionic liquid 1-butyl-1-methylpyrrolidinium trifluoromethanesulfonate using GLC. *Fluid phase equilibria*, 278 (1-2): 97-102.

[53] Domanska, U., Wlazło, M. and Karpinska, M. 2020. [DCA]-based ionic liquids for the extraction of sulfur and nitrogen compounds from fuels: Activity coefficients at infinite dilution. *Fluid Phase Equilibria*, 507: 112424.

[54] Doyle, A. C. 2005. Emmerich Wilhelm. *Measurement of the Thermodynamic Properties of Multiple Phases*: 137.

[55] Duan, J.-D., Wang, L.-S., Jiang, K. and Wang, X.-X. 2012. Activity coefficients at infinite dilution of organic solutes in 1-octyl-3-methylimidazolium nitrate using gas–liquid chromatography. *Fluid phase equilibria*, 328: 1-8.

[56] Dubey, G. P. and Dhingra, L. 2021. Excess thermodynamic properties and FT-IR studies of binary mixtures of 2-butoxy ethanol+ amines at different temperatures. *The Journal of Chemical Thermodynamics*, 157: 106388.

[57] El Achkar, T., Greige-Gerges, H. and Fourmentin, S. 2021. Basics and properties of deep eutectic solvents: a review. *Environmental Chemistry Letters*, 19 (4): 3397-3408.

[58] Everett, D. 1965. Effect of gas imperfection on GLC measurements: a refined method for determining activity coefficients and second virial coefficients. *Transactions of the Faraday Society*, 61: 1637-1645.

[59] Everett, D. H. and Powl, J. C. 1976. Adsorption in slit-like and cylindrical micropores in the henry's law region. A model for the microporosity of carbons. *Journal of the Chemical Society, Faraday Transactions 1: Physical Chemistry in Condensed Phases*, 72: 619-636.

[60] Fan, W., Yan, H., Huang, H., Ma, Y., Gao, J., Xu, D. and Wang, Y. 2020. Measurement and Thermodynamic Modeling of Ternary Liquid–Liquid Equilibrium for Extraction of 2, 6-Xylenol from Aromatic Hydrocarbon Mixtures with Different Solvents. *Journal of Chemical & Engineering Data*, 66 (1): 330-337.

[61] Fort, R. and Moore, W. 1965. Adiabatic compressibilities of binary liquid mixtures. *Transactions of the Faraday Society*, 61: 2102-2111.

[62] Fortin, T. J., Laesecke, A., Freund, M. and Outcalt, S. 2013. Advanced calibration, adjustment, and operation of a density and sound speed analyzer. *The Journal of Chemical Thermodynamics*, 57: 276-285.

[63] Fowlis, I. and Scott, R. P. W. 1963. A vapour dilution system for detector calibration. *Journal of Chromatography A*, 11: 1-10.

[64] Franks, F. and Smith, H. 1967. Apparent molal volumes and expansibilities of electrolytes in dilute aqueous solution. *Transactions of the Faraday Society*, 63: 2586-2598.

[65] Furtado, A., Moura, S., Pereira, J., Moutinho, J., Oliveira, F. and Godinho, I. 2016. The importance of the use of adequate reference materials in density measurements performed in hemodialysis treatments. *Measurement*, 79: 349-353.

[66] Garcia-Vaquero, M., Rajauria, G. and Tiwari, B. 2020. Conventional extraction techniques: Solvent extraction. In: *Sustainable Seaweed Technologies*. Elsevier, 171-189.

[67] Gautreaux Jr, M. and Coates, J. 1955. Activity coefficients at infinite dilution. *AIChE Journal*, 1 (4): 496-500.

[68] Ge, M.-L., Ma, J.-L. and Wu, C.-G. 2010. Activity Coefficients at Infinite Dilution of Alkanes, Alkenes, and Alkyl Benzenes in Glycerol Using Gas− Liquid Chromatography. *Journal of Chemical & Engineering Data*, 55 (4): 1714-1717.

[69] Ghaedi, H., Ayoub, M., Sufian, S., Hailegiorgis, S. M., Murshid, G. and Khan, S. N. 2018. Thermal stability analysis, experimental conductivity and pH of phosphonium-based deep eutectic solvents and their prediction by a new empirical equation. *The Journal of Chemical Thermodynamics*, 116: 50-60.

[70] Gonfa, G., Bustam, M. A., Muhammad, N. and Ullah, S. 2015. Density and excess molar volume of binary mixture of thiocyanate-based ionic liquids and methanol at temperatures 293.15–323.15 K. *Journal of Molecular Liquids*, 211: 734-741.

[71] Gowrisankar, M., Venkateswarlu, P., Sivakumar, K. and Sivarambabu, S. 2013. Ultrasonic studies on molecular interactions in binary mixtures of N-methyl aniline with methyl isobutylketone,+ 3-pentanone, and+ cycloalkanones at 303.15 K. *Journal of solution chemistry*, 42 (5): 916-935.

[72] Gruber, D., Topphoff, M. and Gmehling, J. 1998. Measurement of Activity Coefficients at Infinite Dilution Using Gas− Liquid Chromatography. 9. Results for Various Solutes with the Stationary Phases 2-Pyrrolidone and N-Methylformamide. *Journal of Chemical & Engineering Data*, 43 (6): 935-940.

[73] Grundtvig, I. P. R., Heintz, S., Krühne, U., Gernaey, K. V., Adlercreutz, P., Hayler, J. D., Wells, A. S. and Woodley, J. M. 2018. Screening of organic solvents for bioprocesses using aqueous-organic two-phase systems. *Biotechnology advances*, 36 (7): 1801-1814.

[74] Guiochon, G. and Guillemin, C. L. 1988. *Quantitative gas chromatography for laboratory analyses and on-line process control*. Amsterdam, The Netherlands: Elsevier.

[75] Gullón, P., Gullón, B., Romaní, A., Rocchetti, G. and Lorenzo, J. M. 2020. Smart advanced solvents for bioactive compounds recovery from agri-food by-products: A review. *Trends in Food Science & Technology*, 101: 182-197.

[76] Haghbakhsh, R. and Raeissi, S. 2018a. Densities and volumetric properties of (choline chloride+ urea) deep eutectic solvent and methanol mixtures in the temperature range of 293.15–323.15 K. *The Journal of Chemical Thermodynamics*, 124: 10-20.

[77] Haghbakhsh, R. and Raeissi, S. 2018b. Excess volumes of mixtures consisting of deep eutectic solvents by the Prigogine-Flory-Patterson theory. *Journal of Molecular Liquids*, 272: 731-737.

[78] Haghbakhsh, R. and Raeissi, S. 2018c. Investigation of solutions of ethyl alcohol and the deep eutectic solvent of Reline for their volumetric properties. *Fluid Phase Equilibria*, 472: 39-47.

[79] Haghbakhsh, R. and Raeissi, S. 2020. Experimental investigation on the volumetric properties of mixtures of the deep eutectic solvent of Ethaline and methanol in the temperature range of 283.15 to 323.15 K. *The Journal of Chemical Thermodynamics*, 147: 106124.

[80] Haghbakhsh, R., Raeissi, S. and Duarte, A. R. C. 2021. Group contribution and atomic contribution models for the prediction of various physical properties of deep eutectic solvents. *Scientific reports*, 11 (1): 1-19.

[81] Halder, G. 2014. *Introduction to chemical engineering thermodynamics*. 2nd Ed ed. PHI Learning Pvt. Ltd.

[82] Hammad, S. F., Abdallah, I. A., Bedair, A. and Mansour, F. R. 2022. Homogeneous liquid–liquid extraction as an alternative sample preparation technique for biomedical analysis. *Journal of Separation Science*, 45 (1): 185-209.

[83] Handa, Y. P. and Benson, G. C. 1979. Volume changes on mixing two liquids: A review of the experimental techniques and the literature data. *Fluid Phase Equilibria*, 3 (2-3): 185-249.

[84] Hansen, B. B., Spittle, S., Chen, B., Poe, D., Zhang, Y., Klein, J. M., Horton, A., Adhikari, L., Zelovich, T. and Doherty, B. W. 2020. Deep eutectic solvents: A review of fundamentals and applications. *Chemical reviews*, 121 (3): 1232-1285.

[85] Harrison, I., Leader, R., Higgo, J. and Tjell, J. C. 1994. Determination of organic pollutants in small samples of groundwaters by liquid-liquid extraction and capillary gas chromatography. *Journal of chromatography A*, 688 (1-2): 181-188.

[86] Hassanshahi, N., Hu, G. and Li, J. 2020. Application of ionic liquids for chemical demulsification: A review. *Molecules*, 25 (21): 4915.

[87] Haynes, W. M., Lide, D. R. and Bruno, T. J. 2016. *CRC handbook of chemistry and physics*. 97 ed. CRC press.

[88] Hayyan, A., Mjalli, F. S., AlNashef, I. M., Al-Wahaibi, T., Al-Wahaibi, Y. M. and Hashim, M. A. 2012. Fruit sugar-based deep eutectic solvents and their physical properties. *Thermochimica Acta*, 541: 70-75.

[89] Hudson, G. and McCoubrey, J. 1960. Intermolecular forces between unlike molecules. A more complete form of the combining rules. *Transactions of the Faraday Society*, 56: 761-766.

[90] Hussam, A. and Carr, P. W. 1985. Rapid and precise method for the measurement of vapor/liquid equilibria by headspace gas chromatography. *Analytical Chemistry*, 57 (4): 793-801.

[91] Ijardar, S. P., Singh, V. and Gardas, R. L. 2022. Revisiting the Physicochemical Properties and Applications of Deep Eutectic Solvents. *Molecules*, 27 (4): 1368.

[92] Iloukhani, H. and Almasi, M. 2009. Densities, viscosities, excess molar volumes, and refractive indices of acetonitrile and 2-alkanols binary mixtures at different temperatures: experimental results and application of the Prigogine-Flory-Patterson theory. *Thermochimica acta*, 495 (1-2): 139-148.

[93] Jakobsen, H. A., Lindborg, H. and Dorao, C. A. 2005. Modeling of bubble column reactors: progress and limitations. *Industrial and engineering chemistry research*, 44 (14): 5107-5151.

[94] Jalili, V., Barkhordari, A. and Ghiasvand, A. 2020. New extraction media in microextraction techniques. A review of reviews. *Microchemical Journal*, 153: 104386.

[95] James, A. and Martin, A. 1952. Gas-liquid partition chromatography. A technique for the analysis of volatile materials. *Analyst*, 77 (921): 915-932.

[96] Jangir, A. K., Mandviwala, H., Patel, P., Sharma, S. and Kuperkar, K. 2020. Acumen into the effect of alcohols on choline chloride: L-lactic acid-based natural deep eutectic solvent (NADES): A spectral investigation unified with theoretical and thermophysical characterization. *Journal of Molecular Liquids*, 317: 113923.

[97] Jhong, H.-R., Wong, D. S.-H., Wan, C.-C., Wang, Y.-Y. and Wei, T.-C. 2009. A novel deep eutectic solvent-based ionic liquid used as electrolyte for dye-sensitized solar cells. *Electrochemistry Communications*, 11 (1): 209-211.

[98] Jiao, T., Ren, C., Lin, S., Zhang, L., Xu, X., Zhang, Y., Zhang, W. and Liang, P. 2022. The extraction mechanism research for the separation of indole through the formation of deep eutectic solvents with quaternary ammonium salts. *Journal of Molecular Liquids*, 347: 118325.

[99] Joshi, D. R. and Adhikari, N. 2019. An overview on common organic solvents and their toxicity. *Journal of Pharmaceutical Research International*: 1-18.

[100] Kabane, B., Arumugam, V., Chokkareddy, R. and Redhi, G. G. 2019a. Assessment of Pyrrolidinium-Based Ionic Liquid for the Separation of Binary Mixtures Based on Activity Coefficients at Infinite Dilution. *Journal of Chemical & Engineering Data*, 64 (12): 5105-5112.

[101] Kabane, B., Chokkareddy, R. and Redhi, G. G. 2019b. Separation of (water/butan-1-ol) binary systems based on activity coefficients at infinite dilution with phosphonium ionic liquid. *The Journal of Chemical Thermodynamics*, 137: 7-12.

[102] Kabane, B. and Redhi, G. G. 2019. Application of trihexyltetradecylphosphonium dicyanamide ionic liquid for various types of separations problems: Activity coefficients at infinite dilution measurements utilizing GLC method. *Fluid Phase Equilibria*, 493: 181-187.

[103] Kabane, B. and Redhi, G. G. 2020. Thermodynamic properties and activity coefficients at infinite dilution for different solutes in deep eutectic solvent: 1-butyl-3-methylimidazolium chloride+ glycerol. *Journal of Molecular Liquids*, 311: 113216.

[104] Karpinska, M., Wlazlo, M. and Domanska, U. 2017. Separation of binary mixtures based on gamma infinity data using [EMIM][TCM] ionic liquid and modilling of thermodynamic functions *Journal of Molecular Liquids* 225: 382-390.

[105] Karpińska, M., Wlazło, M. and Domańska, U. 2018. The ethylbenzene/styrene preferential separation with ionic liquids in liquid–liquid extraction. *Journal of Solution Chemistry*, 47 (10): 1578-1596.

[106] Keshapolla, D., Singh, V., Gupta, A. and Gardas, R. L. 2015. Apparent molar properties of benzyldimethylammonium based protic ionic liquids in water and ethanol at different temperatures. *Fluid Phase Equilibria*, 385: 92-104.

[107] Kgagodi, O. W. 2017. Molecular dynamics study of 2, 2′-difurylmethane with n-propanol and n-butanol binary liquid mixtures.

[108] Khachatrian, A. A., Rakipov, I. T., Solomonov, B. N. and Verevkin, S. P. 2020. Intermolecular interaction of organic solutes with protic [MIM][NO3] and aprotic [EMIM][NO3] ionic liquids. *Journal of Molecular Liquids*, 299: 112243.

[109] Khatibi, S. A., Hamidi, S. and Siahi-Shadbad, M. R. 2022. Application of liquid-liquid extraction for the determination of antibiotics in the foodstuff: recent trends and developments. *Critical reviews in analytical chemistry*, 52 (2): 327-342.

[110] Kohli, K., Katuwal, S., Biswas, A. and Sharma, B. K. 2020. Effective delignification of lignocellulosic biomass by microwave assisted deep eutectic solvents. *Bioresource technology*, 303: 122897.

[111] Koshekov, S. 2020. Evaluating Deep Eutectic Solvent as a Novel Enhanced Oil Recovery Method. Master of Science in Petroleum Engineering Politecnico di Torino.

[112] Kravchyk, K. V., Seno, C. and Kovalenko, M. V. 2020. Limitations of chloroaluminate ionic liquid anolytes for aluminum-graphite dual-ion batteries. *ACS Energy Letters*, 5 (2): 545-549.

[113] Krolikowski, M., Kasprzyk-Niedzicka, M., Krolikowska, M. and Gasiorowska, B. 2022. Physicochemical characterization and activity coefficients at infinite dilution of molecular compound in poly (ethylene glycol) dimethyl ether and the eutectic mixture composed of poly (ethylene glycol) with cyclic carbonate. *The Journal of Chemical Thermodynamics*, 169: 106747.

[114] Krolikowski, M., Krolikowska, M., Wieckowski, M. and Piłowski, A. 2020. The influence of the ionic liquids functionalization on interaction in binary systems with organic solutes and water–Thermodynamic data of activity coefficients at infinite dilution. *The Journal of Chemical Thermodynamics*, 147: 106117.

[115] Krummen, M., Wasserscheid, P. and Gmehling, J. 2002. Measurement of activity coefficients at infinite dilution in ionic liquids using the dilutor technique. *Journal of Chemical & Engineering Data*, 47 (6): 1411-1417.

[116] Kuddushi, M., Nangala, G. S., Rajput, S., Ijardar, S. P. and Malek, N. I. 2019. Understanding the peculiar effect of water on the physicochemical properties of choline chloride based deep eutectic solvents theoretically and experimentally. *Journal of Molecular Liquids*, 278: 607-615.

[117] Kumaran, M. and McGlashan, M. 1977. An improved dilution dilatometer for measurements of excess volumes. *The Journal of Chemical Thermodynamics*, 9 (3): 259-267.

[118] Laesecke, A., Fortin, T. J. and Splett, J. D. 2012. Density, speed of sound, and viscosity measurements of reference materials for biofuels. *Energy & fuels*, 26 (3): 1844-1861.

[119] Lamb, A. B. and Lee, R. E. 1913. The densities of certain dilute aqueous solutions by a new and precise method. *Journal of the American Chemical Society*, 35 (11): 1666-1693.

[120] Landau, I., Belfer, A. J. and Locke, D. C. 1991. Measurement of limiting activity coefficients using non-steady-state gas chromatography. *Industrial & engineering chemistry research*, 30 (8): 1900-1906.

[121] Laub, R. J. and Pecsok, R. L. 1978. *Physicochemical applications of gas chromatography*. U.S.A: John Wiley and Sons.

[122] Lavanya, T., Saravanakumar, K., Baskaran, R. and Kubendran, T. 2013. Density, Viscosity, Sound Speed, and Thermoacoustical Parameters of Benzaldehyde with Chlorobenzene or Nitrobenzene at 303.15 K, 308.15 K, and 313.15 K. *International Journal of Thermophysics*, 34 (7): 1280-1287.

[123] Lee, A. K., Lewis, D. M. and Ashman, P. J. 2012. Disruption of microalgal cells for the extraction of lipids for biofuels: Processes and specific energy requirements. *Biomass and bioenergy*, 46: 89-101.

[124] Lee, J., Kim, H., Kang, S., Baik, N., Hwang, I. and Chung, D. S. 2020. Applications of deep eutectic solvents to quantitative analyses of pharmaceuticals and pesticides in various matrices: a brief review. *Archives of pharmacal research*: 1-20.

[125] Lerol, J.-C., Masson, J.-C., Renon, H., Fabries, J.-F. and Sannier, H. 1977. Accurate measurement of activity coefficient at infinite dilution by inert gas stripping and gas chromatography. *Industrial & Engineering Chemistry Process Design and Development*, 16 (1): 139-144.

[126] Leron, R. B., Soriano, A. N. and Li, M.-H. 2012. Densities and refractive indices of the deep eutectic solvents (choline chloride+ ethylene glycol or glycerol) and their aqueous mixtures at the temperature ranging from 298.15 to 333.15 K. *Journal of the Taiwan Institute of Chemical Engineers*, 43 (4): 551-557.

[127] Letcher, T. and Moollan, W. 1995. The determination of activity coefficients of hydrocarbons at infinite dilution using a glc technique with the polar solvent tetrahydrothiophene-1, 1-dioxide, c-(CH2) 4SO2,(sulfolane) at the temperature 303.15 K. *The Journal of Chemical Thermodynamics*, 27 (8): 867-872.

[128] Letcher, T. and Whitehead, P. 1997. The determination of activity coefficients of alkanes, alkenes, cycloalkanes, and alkynes at infinite dilution with the polar solvents dimethyl sulphoxide (DMSO), orN, N-dimethylformamide (DMF), orN-methyl-2-pyrrolidinone (NMP) using a glc technique at the temperatures 283.15 K and 298.15 K. *The Journal of Chemical Thermodynamics*, 29 (11): 1261-1268.

[129] Letcher, T. M. 1980. Activity coefficients at infinite dilution from gas–liquid chromatography. In: Proceedings of *Faraday Symposia of the Chemical Society*. Royal Society of Chemistry, 103-112.

[130] Li, D., Gao, Z., Vasudevan, N. K., Li, H., Gao, X., Li, X. and Xi, L. 2020. Molecular mechanism for azeotrope formation in ethanol/benzene binary mixtures through gibbs ensemble monte carlo simulation. *The Journal of Physical Chemistry B*, 124 (16): 3371-3386.

[131] Li, Y., Wang, W., Wang, Q., Yalikun, N. and Tang, J. 2022. Thermodynamic parameters and infinite dilution activity coefficients for organic solutes in deep eutectic solvent: Choline Chloride+ 1, 5-Pentanediol. *The Journal of Chemical Thermodynamics*: 106784.

[132] Lide, D. R. 2004. *CRC handbook of chemistry and physics*. 85 Ed ed. Boca Raton: CRC press.

[133] Loos, T. W. d. and Weir, R. D. 2005. 1 Introduction. In: Weir, R. D. and De Loos, T. W. eds. *Experimental Thermodynamics*. Elsevier, 1-3. Available: https://www.sciencedirect.com/science/article/pii/S1874564405800037 (Accessed 2022/04/30).

[134] Ma, Y., Zhang, J., Huang, K. and Jiang, L. 2021. Highly efficient and selective separation of ammonia by deep eutectic solvents through cooperative acid-base and strong hydrogen-bond interaction. *Journal of Molecular Liquids*, 337: 116463.

[135] Makos, P., Słupek, E. and Gebicki, J. 2020. Hydrophobic deep eutectic solvents in microextraction techniques-A review. *Microchemical journal*, 152: 104384.

[136] Manyoni, L., Kabane, B. and Redhi, G. G. 2022. Deep eutectic solvent as a possible entrainer for industrial separation problems: Pre-screening tool for solvent selection. *Fluid Phase Equilibria*, 553: 113266.

[137] Manyoni, L. and Redhi, G. G. 2022. Measurements of infinite dilution activity coefficient for aromatic and aliphatic hydrocarbons in Deep Eutectic Solvent, 1-ethyl-1-methylpyrrolidinium bromide+ ethylene glycol at different temperatures and a stated molar ratio. *Chemical Thermodynamics and Thermal Analysis*: 100057.

[138] Marciniak, A. and Wlozlo, M. 2018. Activity coefficients at infinite dilution and physicochemical properties for organic solutes and water in the ionic liquid trihexyl-tetradecyl-phosphonium tricyanomethanide. *The Journal of Chemical Thermodynamics*, 120: 72-78.

[139] Marcinkowski, Ł., Eichenlaub, J., Ghasemi, E., Polkowska, Ż. and Kloskowski, A. 2020. Measurements of activity coefficients at infinite dilution for organic solutes in the ionic liquids N-ethyl-and N-octyl-N-methylmorpholinium bis (trifluoromethanesulfonyl) imide. A useful tool for solvent selection. *Molecules*, 25 (3): 634.

[140] Martins, P. L. G., Braga, A. R. and de Rosso, V. V. 2017. Can ionic liquid solvents be applied in the food industry? *Trends in Food Science and Technology*, 66: 117-124.

[141] Maugeri, Z., Leitner, W. and de María, P. D. 2012. Practical separation of alcohol–ester mixtures using Deep-Eutectic-Solvents. *Tetrahedron Letters*, 53 (51): 6968-6971.

[142] Mbatha, B. P., Ngema, P. T., Nkosi, N. and Ramsuroop, S. 2022. Infinite Dilution Activity Coefficient Measurements for 1-Methyl-4-(1-methylethenyl)-cyclohexene as a Green Solvent for Separation. *Journal of Chemical & Engineering Data*, 67 (4): 966-974.

[143] McAtee, Z. P. and Heitz, M. P. 2016. Density, viscosity and excess properties in the trihexyltetradecylphosphonium chloride ionic liquid/methanol cosolvent system. *The Journal of Chemical Thermodynamics*, 93: 34-44.

[144] McGlashan, M. and Potter, D. 1962. An apparatus for the measurement of the second virial coefficients of vapours; the second virial coefficients of some n-alkanes and of some mixtures of n-alkanes. *Proceedings of the Royal Society of London. Series A. Mathematical and Physical Sciences*, 267 (1331): 478-500.

[145] McMillan Jr, W. G. and Mayer, J. E. 1945. The statistical thermodynamics of multicomponent systems. *The Journal of Chemical Physics*, 13 (7): 276-305.

[146] Mgxadeni, N., Mmelesi, O., Kabane, B. and Bahadur, I. 2022. Influence of hydrogen bond donor on zinc chloride in separation of binary mixtures: Activity coefficients at infinite dilution. *Journal of Molecular Liquids*: 118596.

[147] Millero Jr, F. J. 1967. High precision magnetic float densimeter. *Review of Scientific Instruments*, 38 (10): 1441-1444.

[148] Moghimi, M. and Roosta, A. 2019. Physical properties of aqueous mixtures of (choline chloride+ glucose) deep eutectic solvents. *The Journal of Chemical Thermodynamics*, 129: 159-165.

[149] Mohd, M. A. 2012. *Advanced gas chromatography: progress in agricultural, biomedical and industrial applications*. BoD–Books on Demand.

[150] Muhlbauer, A. 1997. *Phase Equilibria: Measurement & Computation*. CRC press.

[151] Mukhamatdinov, I. I., Salih, I. S., Khelkhal, M. A. and Vakhin, A. V. 2020. Application of Aromatic and Industrial Solvents for Enhancing Heavy Oil Recovery from the Ashalcha Field. *Energy & Fuels*, 35 (1): 374-385.

[152] Murador, D. C., de Souza Mesquita, L. M., Vannuchi, N., Braga, A. R. C. and de Rosso, V. V. 2019. Bioavailability and biological effects of bioactive compounds extracted with natural deep eutectic solvents and ionic liquids: Advantages over conventional organic solvents. *Current opinion in food science*, 26: 25-34.

[153] Mutelet, F., Baker, G. A., Ravula, S., Qian, E., Wang, L. and Acree Jr, W. E. 2019. Infinite dilution activity coefficients and gas-to-liquid partition coefficients of organic solutes dissolved in 1-sec-butyl-3-methylimidazolium bis (trifluoromethylsulfonyl) imide and in 1-tert-butyl-3-methylimidazolium bis (trifluoromethylsulfonyl) imide. *Physics and Chemistry of Liquids*, 57 (4): 453-472.

[154] Nebig, S., Liebert, V. and Gmehling, J. 2009. Measurement and prediction of activity coefficients at infinite dilution ($\gamma\infty$), vapor–liquid equilibria (VLE) and excess enthalpies (HE) of binary systems with 1, 1-dialkyl-pyrrolidinium bis (trifluoromethylsulfonyl) imide using mod. UNIFAC (Dortmund). *Fluid phase equilibria*, 277 (1): 61-67.

[155] Negadi, L., Feddal-Benabed, B., Bahadur, I., Saab, J., Zaoui-Djelloul-Daouadji, M., Ramjugernath, D. and Negadi, A. 2017. Effect of temperature on density, sound velocity, and their derived properties for the binary systems glycerol with water or alcohols. *The Journal of Chemical Thermodynamics*, 109: 124-136.

[156] Nkosi, N., Tumba, K. and Ramsuroop, S. 2018a. Activity coefficients at infinite dilution of various solutes in tetrapropylammonium bromide+ 1, 6-hexanediol deep eutectic solvent. *Journal of Chemical & Engineering Data*, 63 (12): 4502-4512.

[157] Nkosi, N., Tumba, K. and Ramsuroop, S. 2018b. Measurements of activity coefficient at infinite dilution for organic solutes in tetramethylammonium chloride+ ethylene glycol deep eutectic solvent using gas-liquid chromatography. *Fluid Phase Equilibria*, 462: 31-37.

[158] Nkosi, N., Tumba, K. and Ramsuroop, S. 2018c. Tetramethylammonium chloride þ glycerol deep eutectic solvent as separation agent for organic liquid mixtures: Assessment from experimental limiting activity coefficients. *Fluid Phase Equilibria*, 473: 98-105.

[159] Nowosielski, B., Jamrógiewicz, M., Łuczak, J. and Warmińska, D. 2022. Novel Binary Mixtures of Alkanolamine Based Deep Eutectic Solvents with Water: Thermodynamic Calculation and Correlation of Crucial Physicochemical Properties. *Molecules*, 27 (3): 788.

[160] Obeten, M., Ugi, B. and Alobi, N. 2017. A review on electrochemical properties of choline chloride based eutectic solvent in mineral processing. *Journal of Applied Sciences and Environmental Management*, 21 (5): 991-998.

[161] Obst, M. and König, B. 2018. Organic synthesis without conventional solvents. *European Journal of Organic Chemistry*, 2018 (31): 4213-4232.

[162] Oke, E. A., Sharma, R., Malek, N. I. and Ijardar, S. P. 2020. Investigation on thermophysical properties of binary systems of [C4mim][NTf2] with cyclic ethers: Application of PFP and ERAS theories. *Journal of Molecular Liquids*, 320: 114411.

[163] Orge, B., Iglesias, M., Rodriguez, A., Canosa, J. and Tojo, J. 1997. Mixing properties of (methanol, ethanol, or 1-propanol) with (n-pentane, n-hexane, n-heptane and n-octane) at 298.15 K. *Fluid Phase Equilibria*, 133 (1-2): 213-227.

[164] Pacheco-Fernández, I. and Pino, V. 2019. Green solvents in analytical chemistry. *Current Opinion in Green and Sustainable Chemistry*, 18: 42-50.

[165] Paiva, A. C. and Hantao, L. W. 2020. Exploring a public database to evaluate consumer preference and aroma profile of lager beers by comprehensive two-dimensional gas chromatography and partial least squares regression discriminant analysis. *Journal of Chromatography A*, 1630: 461529.

[166] Pal, A., Gaba, R., Singh, T. and Kumar, A. 2010. Excess thermodynamic properties of binary mixtures of ionic liquid (1-butyl-3-methylimidazolium hexafluorophosphate) with alkoxyalkanols at several temperatures. *Journal of Molecular Liquids*, 154 (1): 41-46.

[167] Pal, A. and Kumar, B. 2011. Volumetric, acoustic and spectroscopic studies for binary mixtures of ionic liquid (1-butyl-3-methylimidazolium hexafluorophosphate) with alkoxyalkanols at T=(288.15 to 318.15) K. *Journal of Molecular Liquids*, 163 (3): 128-134.

[168] Pathania, V., Sharma, S., Vermani, S. K., Vermani, B. and Grover, N. 2020. Ultrasonic velocity and isentropic compressibility studies of monoalkylammonium salts in binary mixtures of acetonitrile and N, N-dimethylacetamide at variable temperature and atmospheric pressure. *Journal of Solution Chemistry*, 49 (6): 798-813.

[169] Patyar, P., Ali, A. and Malek, N. I. 2021. Experimental and theoretical excess molar properties of aqueous choline chloride based deep eutectic solvents. *Journal of Molecular Liquids*, 324: 114340.

[170] Paucar, N. E., Kiggins, P., Blad, B., De Jesus, K., Afrin, F., Pashikanti, S. and Sharma, K. 2021. Ionic liquids for the removal of sulfur and nitrogen compounds in fuels: a review. *Environmental Chemistry Letters*: 1-24.

[171] Pena-Pereira, F., Kloskowski, A. and Namiesnik, J. 2015. Perspectives on the replacement of harmful organic solvents in analytical methodologies: a framework toward the implementation of a generation of eco-friendly alternatives. *Green Chemistry*, 17 (7): 3687-3705.

[172] Perna, F. M., Vitale, P. and Capriati, V. 2020. Deep eutectic solvents and their applications as green solvents. *Current Opinion in Green and Sustainable Chemistry*, 21: 27-33.

[173] Petsev, N., Nikolov, R. and Kostova, A. 1974. Determination of the amount of stationary phase in packings for gas-liquid chromatography. *Journal of Chromatography A*, 93 (2): 369-374.

[174] Pividal, K. A., Sterner, C., Sandler, S. I. and Orbey, H. 1992. Vapor-liquid equilibrium from infinite dilution activity coefficients: measurement and prediction of oxygenated fuel additives with alkanes. *Fluid phase equilibria*, 72: 227-250.

[175] Płotka-Wasylka, J., De la Guardia, M., Andruch, V. and Vilková, M. 2020. Deep eutectic solvents vs ionic liquids: Similarities and differences. *Microchemical Journal*: 105539.

[176] Poling, B. E., Prausnitz, J. M. and O'connell, J. P. 2001a. *The properties of gases and liquids*. Mcgraw-hill New York.

[177] Poling, B. E., Prausnitz, J. M. and O'Connell, J. P. 2001b. *Properties of gases and liquids*. 5th Ed ed. New York: McGraw-Hill Education, New York.

[178] Porter, P., Deal, C. and Stross, F. 1956. The determination of partition coefficients from gas-liquid partition chromatography. *Journal of the American Chemical Society*, 78 (13): 2999-3006.

[179] Prak, D. J., Lee, B. G., Cowart, J. S. and Trulove, P. C. 2017. Density, viscosity, speed of sound, bulk modulus, surface tension, and flash point of binary mixtures of butylbenzene+ linear alkanes (n-decane, n-dodecane, n-tetradecane, n-hexadecane, or n-heptadecane) at 0.1 MPa. *Journal of Chemical & Engineering Data*, 62 (1): 169-187.

[180] Prausnitz, J. M., Lichtenthaler, R. N. and De Azevedo, E. G. 1998. *Molecular thermodynamics of fluid-phase equilibria*. Pearson Education.

[181] Quijada-Maldonado, E., Meindersma, G. W. and de Haan, A. 2013. Viscosity and density data for the ternary system water (1)–ethanol (2)–ethylene glycol (3) between 298.15 K and 328.15 K. *The Journal of Chemical Thermodynamics*, 57: 500-505.

[182] Ramon, D. J. and Guillena, G. 2020. Deep Eutectic Solvents: Synthesis, Properties, and Applications. *Green Chemistry*, 22 (12): 3668-3692.

[183] Rao, V. S., Krishna, T. V., Mohan, T. M. and Rao, P. M. 2017. Physicochemical properties of green solvent 1-ethyl-3-methylimidazolium tetrafluoroborate with aniline from T=(293.15 to 323.15) K at atmospheric pressure. *The Journal of Chemical Thermodynamics*, 104: 150-161.

[184] Redhi, G. G. 2003. Thermodynamics of liquid mixtures containing carboxylic acids. Doctoral dissertation, University of Natal, Durban.

[185] Reeves, C. J., Kasar, A. K. and Menezes, P. L. 2021. Tribological performance of environmental friendly ionic liquids for high-temperature applications. *Journal of Cleaner Production*, 279: 123666.

[186] Ren, F., Wang, J., Xie, F., Zan, K., Wang, S. and Wang, S. 2020. Applications of ionic liquids in starch chemistry: A review. *Green Chemistry*, 22 (7): 2162-2183.

[187] Rice, W. E. and Hirschfelder, J. O. 1954. Second virial coefficients of gases obeying a modified Buckingham (exp-six) potential. *The Journal of Chemical Physics*, 22 (2): 187-192.

[188] Rodriguez, N. R., Gerlach, T., Scheepers, D., Kroon, M. C. and Smirnova, I. 2017. Experimental determination of the LLE data of systems consisting of {hexane+ benzene+ deep eutectic solvent} and prediction using the Conductor-like Screening Model for Real Solvents. *The Journal of Chemical Thermodynamics*, 104: 128-137.

[189] Ruggeri, S., Poletti, F., Zanardi, C., Pigani, L., Zanfrognini, B., Corsi, E., Dossi, N., Salomäki, M., Kivelä, H. and Lukkari, J. 2019. Chemical and electrochemical properties of a hydrophobic deep eutectic solvent. *Electrochimica Acta*, 295: 124-129.

[190] Sandip and Singh. 2022. Chapter 3 - Production of ionic liquids using renewable sources. *Ionic Liquid-Based Technologies for Environmental Sustainability*: 29-43.

[191] Sandler, S. 1996. Infinite dilution activity coefficients in chemical, environmental and biochemical engineering. *Fluid Phase Equilibria*, 116 (1-2): 343-353.

[192] Santana-Mayor, Á., Rodríguez-Ramos, R., Herrera-Herrera, A. V., Socas-Rodríguez, B. and Rodríguez-Delgado, M. Á. 2020. Deep eutectic solvents. The new generation of green solvents in analytical chemistry. *Trends in Analytical Chemistry*: 116108.

[193] Scatchard, G., Wood, S. E. and Mochel, J. M. 1946. Vapor-Liquid Equilibrium. VI. Benzene-Methanol Mixtures1. *Journal of the American Chemical Society*, 68 (10): 1957-1960.

[194] Schult, C. J., Neely, B. J., Robinson Jr, R., Gasem, K. and Todd, B. A. 2001. Infinite-dilution activity coefficients for several solutes in hexadecane and in n-methyl-2-pyrrolidone (NMP): experimental measurements and UNIFAC predictions. *Fluid phase equilibria*, 179 (1-2): 117-129.

[195] Seader, J. D., Henley, E. J. and Roper, D. K. 1998a. *Separation process principles*. USA: wiley New York.

[196] Sethi, O., Singh, M., Kang, T. S. and Sood, A. K. 2021. Volumetric and compressibility studies on aqueous mixtures of deep eutectic solvents based on choline chloride and carboxylic acids at different temperatures: Experimental, theoretical and computational approach. *Journal of Molecular Liquids*, 340: 117212.

[197] Shang, X.-c., Zhang, Y.-q., Zheng, Y.-f. and Li, Y. 2022. Temperature-responsive deep eutectic solvents as eco-friendly and recyclable media for microwave extraction of flavonoid compounds from waste onion (Allium cepa L.) skins. *Biomass Conversion and Biorefinery*: 1-10.

[198] Shekaari, H., Zafarani-Moattar, M. T. and Mohammadi, B. 2020a. Liquid-liquid equilibria and thermophysical properties of ternary mixtures {(benzene/thiophene)+ hexane+ deep eutectic solvents}. *Fluid Phase Equilibria*, 509: 112455.

[199] Shekaari, H., Zafarani-Moattar, M. T. and Mohammadi, B. 2020b. Thermophysical properties of choline chloride/urea deep eutectic solvent in aqueous solution at infinite dilution at T= 293.15–323.15 K. *Journal of Thermal Analysis and Calorimetry*, 139 (6): 3603-3612.

[200] Shekaari, H., Zafarani-Moattar, M. T., Mokhtarpour, M. and Faraji, S. 2020c. Compatibility of sustainable solvents ionic liquid, 1-ethyl-3-methylimidazolium ethyl sulfate in some choline chloride based deep eutectic solvents: thermodynamics study. *The Journal of Chemical Thermodynamics*, 141: 105961.

[201] Shekaari, H., Zafarani-Moattar, M. T., Mokhtarpour, M. and Faraji, S. 2021. Deep eutectic solvents for antiepileptic drug phenytoin solubilization: thermodynamic study. *Scientific Reports*, 11 (1): 1-14.

[202] Shen, Y., Su, Z., Zhao, Q., Shan, R., Zhu, Z., Cui, P. and Wang, Y. 2022. Molecular simulation and optimization of extractive distillation for separation of dimethyl carbonate and methanol. *Process Safety and Environmental Protection*, 158: 181-188.

[203] Shishov, A., Bulatov, A., Locatelli, M., Carradori, S. and Andruch, V. 2017. Application of deep eutectic solvents in analytical chemistry. A review. *Microchemical Journal*, 135: 33-38.

[204] Shishov, A., Pochivalov, A., Nugbienyo, L., Andruch, V. and Bulatov, A. 2020. Deep eutectic solvents are not only effective extractants. *Trends in Analytical Chemistry*, 129: 115956.

[205] Sibiya, P. 2009. Excess molar volumes, partial molar volumes and isentropic compressibilities of binary systems (ionic liquid + alkanol). Masters Degree in Technology, Durban University Of Technology.

[206] Singh, S. 2017. Thermo-physical properties and activity coefficients at infinite dilution for ionic liquid systems at several temperatures. Doctar of Technology Durban University of Technology

[207] Singh, S., Dash, U. N. and Talukdar, M. 2020. Solubility enhancement and study of molecular interactions of poorly soluble ibuprofen in presence of urea, a hydrotropic agent. *Materials Today: Proceedings*, 30: 246-253.

[208] Singh, S. K. and Savoy, A. W. 2020. Ionic liquids synthesis and applications: An overview. *Journal of Molecular Liquids*, 297: 112038.

[209] Skoronski, E., Fernandes, M., Malaret, F. J. and Hallett, J. P. 2020. Use of phosphonium ionic liquids for highly efficient extraction of phenolic compounds from water. *Separation and Purification Technology*, 248: 117069.

[210] Smink, D., Kersten, S. R. and Schuur, B. 2020. Recovery of lignin from deep eutectic solvents by liquid-liquid extraction. *Separation and purification technology*, 235: 116127.

[211] Smith, E. L., Abbott, A. P. and Ryder, K. S. 2014. Deep eutectic solvents (DESs) and their applications. *Chemical reviews*, 114 (21): 11060-11082.

[212] Smith, J., Van Ness, H. and Abbott, M. 2001. Vapor-liquid equilibrium: introduction. *Introduction to Chemical Engineering Thermodynamics*: 328-367.

[213] Smith, J. M. 1950. *Introduction to chemical engineering thermodynamics*: ACS Publications.

[214] Snyder, P. S. and Thomas, J. F. 1968. Solute activity coefficients at infinite dilution via gas-liquid chromatography. *Journal of Chemical & Engineering Data*, 13 (4): 527-529.

[215] Soleimani, O. 2020. Properties and Applications of Ionic Liquids. *Journal of Chemical Reviews*, 2 (3): 169-181.

[216] Sosa, F. H., da Costa, M. C., Silvestre, A. J. and da Costa Lopes, A. M. 2022. Deep Eutectic Solvents for Sustainable Separation Processes. *Sustainable Separation Engineering: Materials, Techniques and Process Development*: 605-652.

[217] Su, Y., Yang, A., Jin, S., Shen, W., Cui, P. and Ren, J. 2020. Investigation on ternary system tetrahydrofuran/ethanol/water with three azeotropes separation via the combination of reactive and extractive distillation. *Journal of Cleaner Production*, 273: 123145.

[218] Suleiman, D. and Eckert, C. A. 1994. Limiting activity coefficients of diols in water by a dew point technique. *Journal of Chemical and Engineering Data*, 39 (4): 692-696.

[219] Sun, J., Cui, D., Chen, X., Zhang, L., Cai, H. and Li, H. 2011. Design, modeling, microfabrication and characterization of novel micro thermal conductivity detector. *Sensors and Actuators B: Chemical*, 160 (1): 936-941.

[220] Sun, P.-P., Gao, G.-H. and Gao, H. 2003. Infinite dilution activity coefficients of hydrocarbons in triethylene glycol and tetraethylene glycol. *Journal of Chemical & Engineering Data*, 48 (5): 1109-1112.

[221] Szalaty, T. J., Klapiszewski, Ł. and Jesionowski, T. 2020. Recent developments in modification of lignin using ionic liquids for the fabrication of advanced materials–A review. *Journal of Molecular Liquids*, 301: 112417.

[222] Tarakad, R. R. and Danner, R. P. 1977. An improved corresponding states method for polar fluids: correlation of second virial coefficients. *AIChE Journal*, 23 (5): 685-695.

[223] Thompson, M. W., Matsumoto, R., Sacci, R. L., Sanders, N. C. and Cummings, P. T. 2019. Scalable screening of soft matter: A case study of mixtures of ionic liquids and organic solvents. *The Journal of Physical Chemistry B*, 123 (6): 1340-1347.

[224] Tiecco, M., Cappellini, F., Nicoletti, F., Del Giacco, T., Germani, R. and Di Profio, P. 2019. Role of the hydrogen bond donor component for a proper development of novel hydrophobic deep eutectic solvents. *Journal of Molecular Liquids*, 281: 423-430.

[225] Tobiszewski, M. and Namiesnik, J. 2017. Greener organic solvents in analytical chemistry. *Current Opinion in Green and Sustainable Chemistry*, 5: 1-4.

[226] Torres-Valenzuela, L. S., Ballesteros-Gómez, A. and Rubio, S. 2020. Green solvents for the extraction of high added-value compounds from agri-food waste. *Food Engineering Reviews*, 12 (1): 83-100.

[227] Tsonopoulos, C., Dymond, J. H. and Szafranski, A. 1989. Second virial coefficients of normal alkanes, linear 1-alkanols and their binaries. *Pure and applied chemistry*, 61 (8): 1387-1394.

[228] Turosung, S. and Ghosh, B. 2017. Application of ionic liquids in the upstream oil industry-a review. *Int. J. Petrochem. Res*, 1: 50-60.

[229] Uddin, M. N., Basak, D., Hopefl, R. and Minofar, B. 2020. Potential application of ionic liquids in pharmaceutical dosage forms for small molecule drug and vaccine delivery system. *Journal of Pharmacy and Pharmaceutical Sciences*, 23: 158-176.

[230] Vanda, H., Dai, Y., Wilson, E. G., Verpoorte, R. and Choi, Y. H. 2018. Green solvents from ionic liquids and deep eutectic solvents to natural deep eutectic solvents. *Comptes Rendus Chimie*, 21 (6): 628-638.

[231] Vekariya, R. L. 2017. A review of ionic liquids: Applications towards catalytic organic transformations. *Journal of Molecular Liquids*, 227: 44-60.

[232] Verevkin, S. P., Sazonova, A. Y., Frolkova, A. K., Zaitsau, D. H., Prikhodko, I. V. and Held, C. 2015. Separation performance of BioRenewable deep eutectic solvents. *Industrial & Engineering Chemistry Research*, 54 (13): 3498-3504.

[233] Verma, C., Alrefaee, S. H., Quraishi, M., Ebenso, E. E. and Hussain, C. M. 2020. Recent developments in sustainable corrosion inhibitors using ionic liquids: A review. *Journal of Molecular Liquids*: 114484.

[234] Verma, C., Haque, J., Quraishi, M. and Ebenso, E. E. 2019. Aqueous phase environmental friendly organic corrosion inhibitors derived from one step multicomponent reactions: a review. *Journal of Molecular Liquids*, 275: 18-40.

[235] Vishtal, A. G. and Kraslawski, A. 2011. Challenges in industrial applications of technical lignins. *BioResources*, 6 (3): 3547-3568.

[236] Walden, P. 1914. Molecular weights and electrical conductivity of several fused salts. *Bull. Acad. Imper. Sci.(St. Petersburg)*, 1800 (8): 405-422.

[237] Wang, C., Wang, Q., Yalikun, N., Fu, J. and Wang, B. 2022. Infinite Dilution Activity Coefficients and Thermodynamic Properties of Various Organic Solutes in a Choline Chloride+ Oxalic Acid Deep Eutectic Solvent. *Journal of Chemical & Engineering Data*,

[238] Wang, H., Hu, L., Liu, X., Yin, S., Lu, R., Zhang, S., Zhou, W. and Gao, H. 2017. Deep eutectic solvent-based ultrasound-assisted dispersive liquid-liquid microextraction coupled with high-performance liquid chromatography for the determination of ultraviolet filters in water samples. *Journal of Chromatography A*, 1516: 1-8.

[239] Wang, H., Xue, L., Su, W., Li, X., Li, Y. and Li, C. 2018a. Design and control of acetonitrile/N-propanolseparation system via extractive distillation using N-methyl pyrrolidone as entrainer. *Korean Journal of Chemical Engineering*: 1520-5754.

[240] Wang, X., Wang, D. and Lang, H. 2018b. Densities of FAMEs or FAEEs with ethanol at temperatures from 283.15 to 318.15 K. *Physics and Chemistry of Liquids*, 56 (1): 33-42.

[241] Wang, Y., Kim, K. H., Jeong, K., Kim, N.-K. and Yoo, C. G. 2020. Sustainable biorefinery processes using renewable deep eutectic solvents. *Current Opinion in Green and Sustainable Chemistry*: 100396.

[242] Washington, E. L. and Battino, R. 1968. Thermodynamics of binary solutions of nonelectrolytes with 2, 2, 4-trimethylpentane. III. Volumes of mixing with cyclohexane (10-80. deg.) and carbon tetrachloride (10-80. deg.). *The Journal of Physical Chemistry*, 72 (13): 4496-4502.

[243] Widegren, J. A. and Magee, J. W. 2007. Density, viscosity, speed of sound, and electrolytic conductivity for the ionic liquid 1-hexyl-3-methylimidazolium bis (trifluoromethylsulfonyl) imide and its mixtures with water. *Journal of Chemical & Engineering Data*, 52 (6): 2331-2338.

[244] Wilkes, J. S. and Zaworotko, M. J. 1992. Air and water stable 1-ethyl-3-methylimidazolium based ionic liquids. *Journal of the Chemical Society, Chemical Communications*, (13): 965-967.

[245] Wilson, G. and Deal, C. 1962. Activity coefficients and molecular structure. Activity coefficients in changing environments-solutions of groups. *Industrial & Engineering Chemistry Fundamentals*, 1 (1): 20-23.

[246] Wirth, H. E. and LoSurdo, A. 1968. Temperature dependence of volume changes on mixing electrolyte solutions. *Journal of Chemical & Engineering Data*, 13 (2): 226-231.

[247] Wishart, J. F. and Castner, E. W. 2007. The physical chemistry of ionic liquids. *The Journal of Physical Chemistry B*, 111 (18): 4639-4640.

[248] Wood, S. E. and Brusie, J. P. 1943. The Volume of Mixing and the Thermodynamic Functions of Benzene-Carbon Tetrachloride Mixture1. *Journal of the American Chemical Society*, 65 (10): 1891-1895.

[249] Xu, H., Kong, Y., Peng, J., Song, X., Liu, Y., Su, Z., Li, B., Gao, C. and Tian, W. 2021. Comprehensive analysis of important parameters of choline chloride-based deep eutectic solvent pretreatment of lignocellulosic biomass. *Bioresource Technology*, 319: 124209.

[250] Xue, J., Wang, J., Feng, D., Huang, H. and Wang, M. 2020. Processing of functional composite resins using deep eutectic solvent. *Crystals*, 10 (10): 864.

[251] Zaib, Q., Adeyemi, I., Warsinger, D. M. and AlNashef, I. M. 2020. Deep eutectic solvent assisted dispersion of carbon nanotubes in water. *Frontiers in Chemistry*, 8

[252] Zante, G., Braun, A., Masmoudi, A., Barillon, R., Trebouet, D. and Boltoeva, M. 2020. Solvent extraction fractionation of manganese, cobalt, nickel and lithium using ionic liquids and deep eutectic solvents. *Minerals Engineering*, 156: 106512.

[253] Zaoui-Djelloul-Daouadji, M., Mokbel, I., Bahadur, I., Negadi, A., Jose, J., Ramjugernath, D., Ebenso, E. E. and Negadi, L. 2016. Vapor-liquid equilibria, density and sound velocity measurements of (water or methanol or ethanol+ 1, 3-propanediol) binary systems at different temperatures. *Thermochimica Acta*, 642: 111-123.

[254] Zhang, S., Tsuboi, A., Nakata, H. and Ishikawa, T. 2003. Infinite dilution activity coefficients in ethylene glycol and ethylene carbonate. *Journal of Chemical & Engineering Data*, 48 (1): 167-170.

[255] Zhang, T., Bao, Y.-N., Zhang, L., Ren, R.-Z., Jiao, Y.-H. and Ge, M.-L. 2020a. Thermodynamics and selectivity of separation based on activity coefficients at infinite dilution of various solutes in ionic liquid [DMIM][Tf2N]. *The Journal of Chemical Thermodynamics*, 147: 106120.

[256] Zhang, W., Liu, X., He, B., Gong, Z., Zhu, J., Ding, Y., Chen, H. and Tang, Q. 2020b. Interface engineering of imidazolium ionic liquids toward efficient and stable CsPbBr3 perovskite solar cells. *ACS applied materials & interfaces*, 12 (4): 4540-4548.

[257] Zhao, H. and Baker, G. A. 2013. Ionic liquids and deep eutectic solvents for biodiesel synthesis: a review. *Journal of Chemical Technology & Biotechnology*, 88 (1): 3-12.

[258] Zhekenov, T., Toksanbayev, N., Kazakbayeva, Z., Shah, D. and Mjalli, F. S. 2017. Formation of type III Deep Eutectic Solvents and effect of water on their intermolecular interactions. *Fluid Phase Equilibria*, 441: 43-48.

[259] Zhou, T., Shi, H., Ding, X. and Zhou, Y. 2021. Thermodynamic modeling and rational design of ionic liquids for pre-combustion carbon capture. *Chemical Engineering Science*, 229: 116076.